ANALYSIS AND NUMERICAL METHODS FOR PARAMETERS IDENTIFICATION IN PARTIAL DIFFERENTIAL EQUATIONS

SIYU CEN

PhD

The Hong Kong Polytechnic University

2025

The Hong Kong Polytechnic University

Department of Applied Mathematics

Analysis and Numerical Methods for Parameters Identification in Partial Differential Equations

Siyu Cen

A thesis submitted in partial fulfilment of the requirements for the degree of Doctor of Philosophy

June 2025

CERTIFICATE OF ORIGINALITY

I hereby declare that this thesis is my own work and that, to the best of my knowledge and belief, it reproduces no material previously published or written, nor material that has been accepted for the award of any other degree or diploma, except where due acknowledgement has been made in the text.

_____ (Signed)

_____ Cen Siyu _____(Name of student)

Abstract

This thesis is devoted to design and analyze the numerical algorithm for parameter identification problem utlizing theoretical results.

In recent years, numerous numerical schemes for parameter identification problems were developed, analyzed and tested. Most of existing work emphasizes well-posedness, convergence (with respect to the noise level), and convergence rates under various source conditions. In practice, the inversion formulations are further discretized, traditionally via the Galerkin finite element methods (FEMs) or, more recently, neural networks (NNs). However, discretization introduces additional errors that affect reconstruction quality, and rigorous error bounds for numerical inversion algorithms remain underexplored.

After some background introduction and preliminaries in Chapters 1 and 2, we investigate the reconstruction of both the diffusion and reaction coefficients present in an elliptic/parabolic equation in Chapter 3. A decoupled algorithm is constructed to sequentially recover these two parameters. Our approach is stimulated by a constructive conditional stability, and we provide rigorous a priori error estimates in $L^2(\Omega)$ for the recovered diffusion and reaction coefficients. Next, in Chapter 4, we focus on the numerical analysis of quantitative photoacoustic tomography (QPAT). The stability of the inverse problem significantly depends on a non-zero condition in the internal observations, a condition that can be met using randomly chosen boundary excitation data. Utilizing these randomly generated boundary data, we provide a rigorous error estimate in $L^2(\Omega)$ norm for the numerical reconstruction. In Chapter 5, we propose a hybrid FEM-NN scheme, where the finite element method is employed to approximate the state and neural networks act as a smoothness prior to approximate the unknown parameter. We demonstrate that the hybrid approach enjoys both rigorous mathematical foundation of the FEM and inductive bias/approximation properties of NNs. In Chapter 6, we concern with numerically recovering multiple parameters simultaneously in the subdiffusion model from one single lateral measurement on a part of the boundary, while in an incompletely known medium. We prove a uniqueness result for special cases of diffusion coefficients and boundary excitations. The uniqueness analysis further inspires the development of a robust numerical algorithm for recovering the unknown parameters. Finally, in Chapter 7, we summarize our work and mention possible future research topics.

Throughout, extensive numerical experiments are provided to illustrate the efficiency and reliability of the proposed algorithms.

Acknowledgements

First and foremost, I would like to express my sincere gratitude to my supervisor, Dr. Zhi Zhou, for his invaluable guidance, unwavering support, and insightful suggestions throughout my research journey. I am also profoundly grateful to my co-supervisor Dr. Xun Li and longtime collaborator Dr. Bangti Jin for their constant support and encouragement. I feel truly fortunate to have met them during my time at the Hong Kong Polytechnic University. Beyond teaching me the fundamentals of scientific research, they have shaped my ability to think critically and approach problems with the rigor of a professional researcher. Their mentorship has been indispensable to the successful completion of this thesis.

Dr. Buyang Li taught me the numerical analysis for partial differential equations. Dr. Ting-kei Pong taught me nonlinear optimization methods. Dr. Xingqiu Zhao give me insights on methematical statistics. Dr. Xiaojun Chen taught me how to give a research presentation. I would like to thank them and all the professors who taught me at Hong Kong. I would also thank Dr. Defeng Sun, Dr. Yanping Lin, Dr. Zhonghua Qiao, Dr. Jianbo Cui, Miss. Teresa Ko Shuk-wai and all other staffs at the Department of applied mathematics for their appropriate support.

I also wish to thank my collaborators Dr. Giovanni S. Alberti, Dr. Erik Burman, Dr. Yavar Kian, Dr. Xiyao Li, Dr. Yikan Liu, Dr. Qimeng Quan, Dr. Kwancheol Shin, Dr. Eric Soccorsi, Dr. Rachid Zarouf. They provided me many great ideas and showed me many invaluable insights.

I am also grateful to Dr. Tengteng Cui, Dr. Kai Li, Dr. Xu Wu, Dr. Zhaoming Yuan, Dr. Zhengqi Zhang, Mr. Yongcheng Dai, Mr. Qingle Lin, Mr. Pinzhong Zheng and all my friends at our math department for their help and collaboration.

Finally, I have to express my deep gratitude to my parents and family for their love and patience.

Contents

List of Figures

List of Tables

CHAPTER 1.

Introduction

In this chapter, we will introduce the parameters identification problems associated with partial differential equations (PDEs). In Section 1.1, we present the an abstract framework for parameters identification problems governed by PDEs. This framework is further illustrated by the inverse diffusivity problem (IDP) in Section 1.2, where we show how theoretical results in parameter identification can inspire the development of numerical algorithms and analysis. In Section 1.3, we establish the subdiffusion model and introduce the parameters identification problem related to subdiffusion equations. This dissertation's contributions and organizational structure, are then described in Section 1.4.

1.1 Introduction to inverse problems

Estimating physical parameters in partial differential equations (PDEs), known as parameter identification, constitutes a critical class of inverse problems with broad applications. These include medical imaging (including electrical impedance tomography [28, 140] and diffuse optical tomography [75, 47] etc.), geophysical prospecting [154], and non-destructive testing [91]. Mathematically, these problems admit the following abstract operator equation:

$$Kx = y, \quad \text{with } x \in X,\, y \in Y, \tag{1.1}$$

where X and Y be two given Banach spaces, and $K : X \to Y$ be a densely defined, injective (but not necessary continuous or linear) mapping. Here K represents the forward mapping that relates the parameter $x^\dagger$ (e.g., a PDE coefficient) to the observable state $y^\dagger \equiv y(x^\dagger)$. The goal is to recover $x^\dagger$ from noisy measurements of $y^\dagger$.

This problem is ill-posed, namely their solutions can be highly susceptible to data noise. Thus specialized solution techniques known as regularization are needed for their stable and accurate numerical solution. This is often achieved using variational regularization (see, e.g., [73]), i.e., formulating the reconstruction task as solving a PDE constrained optimization problem that involves a data-fitting term and a regularization term

$$J_\gamma(x) := \|Kx - z^\delta\|_Y + \gamma\|x\|_Z^2. \tag{1.2}$$

Here, the first term measures fidelity of the model output with the noisy measurement data z^δ, whereas the second term (with regularization parameter γ) imposes stability via penalties like Sobolev smoothness, ℓ^1-sparsity or total variation.

Meanwhile, for many PDE inverse problems, there are conditional stability estimates that providing theoretical bounds on solution sensitivity within restricted parameter sets. They are conditional in the sense that the estimates are valid only on a suitable subset of admissible parameters, which often impose very strong regularity assumptions on the concerned parameters. In [34], Cheng et al formulate one delicate definition on the conditional stability

Definition 1.1. *Let $Z \subset X$ be a new Banach space with the embedding relation $Z \hookrightarrow X$ hold. Fix some $M > 0$, the admissible set is given by*

$$\mathcal{A}_M = \{x \in Z : \|x\|_Z \leq M\}$$

and choose $Q \subset Z$ suitably. Let ω be a non-negative monotone increasing function $\omega = \omega(\eta)$, $\eta \geqslant 0$, satisfying $\lim_{\eta \to 0} \omega(\eta) = 0$. The conditional stability holds in the operator equation $Kx = y$, if for a given $M > 0$, there exists a constant $c = c(M) > 0$ such that

$$\|x_1 - x_2\|_X \leq c(M)\omega\left(\|Kx_1 - Kx_2\|_Y\right) = c(M)\omega\left(\|y_1 - y_2\|_Y\right),$$

for every $x_1, x_2 \in \mathcal{A}_M \cap Q$. The function ω often indicates the modulus of the conditional stability under consideration.

Given the theoretical foundation of conditional stability estimates, it is a very natural question to combine them with numerical procedures. This idea first was suggested by Cheng and Yamamoto [34], who analyzed Tikhonov regularization using conditional stability, proposed a new rule for choosing the regularization parameter based on the stability estimates and exemplified the approach on multiple concrete PDE inverse problems. Since then the approach has been further studied in several works for both variational regularization [21, 49, 147] and iterative regularization [45].

In practical computation, one has to further discretize the governing equation and the objective functional. This can be achieved using finite difference, finite element and more recently also deep neural networks. From the perspective of numerical analysis, it would be desirable to also incorporate the discretization parameters in the error analysis. Indeed, a finer mesh leads to a more accurate approximation of the forward map, but at the cost of increased computational efforts, whereas a coarse mesh may significantly deteriorate the accuracy of the reconstruction (due to the discretization error). Therefore it is important to derive quantitative bounds on the approximation to guide the choice of various algorithmic parameters. Unfortunately, the rigorous numerical analysis of discrete variational regularization techniques lags far behind. This is due to the severe nonlinearity of the forward map for many PDE parameter identifications as well as the inherent ill-posedness of inverse problems. So far in the literature, there have only been a few studies prior to 2010s, prominently [54, 129].

In the thesis, we aim to employ conditional stability estimate to derive numerical error estimation for the parameters identification problems governed by PDEs. In particular, we investigate two inverse problems with finite element discretization in Chapter 3 and Chapter 4. We present the error analysis with neural network discretization in Chapter 5. In Chapter 6, we design a numerical algorithm for a highly ill-posed inverse problem motivating from the theoretical analysis.

1.2 Inverse diffusivity problem and error estimate

In this section, we provide a simple example, the inverse diffusivity problem. In particular, we demonstrate that the theoretical stability results motivate the numerical analysis of the reconstruction error. We consider the following elliptic equation

$$\begin{cases} -\mathrm{div}\big(q\nabla u\big) = f, & \text{in } \Omega, \\ u = g, & \text{on } \partial\Omega. \end{cases} \tag{1.3}$$

The elliptic problem (1.3) describes many important physical processes, and the related inverse problems are exemplary for parameter identifications for PDEs (see the monographs [6, 22] for overviews). For example, (1.3) is often used to model the steady state of diffusion process, where u represents the concentration of a substance (e.g., a chemical, pollutant, or particles) in the domain Ω, q represents the diffusion coefficient, which determines how easily the substance diffuses through the medium, f is the source and g is the concentration on boundary $\partial\Omega$. See also [56, 150] for parameter identifications in hydrology and [17] for related coupled-physics inverse problems arising in medical imaging.

Equation (1.3) admits a unique solution $u \in H^1(\Omega)$ when $f \in H^{-1}(\Omega)$, $g \in H^{\frac{1}{2}}(\partial\Omega)$ and $q \in L^\infty(\Omega)$ with positive lower and upper bounds. The inverse problem aims to identify the diffusion coefficient $q(x)$ with measurement data $z^\delta(x)$, $x \in \Omega$ with noise level δ, i.e.

$$\|z^\delta - u^\dagger\|_{L^2(\Omega)} \leq \delta,$$

where $u^\dagger = u(q^\dagger)$ is the solution of (1.3) corresponding to the exact diffusion coefficient $q^\dagger$.

The stability as well as error estimate of the inverse diffusion problem has been extensively studied in the literature. In [54], one of the earliest works, Falk consider the governing equation (1.3) with a Neumann boundary condition over a smooth domain $\Omega \subset \mathbb{R}^2$. They imposed a structural condition on the problem data:

$$\begin{aligned} &\text{There exists a constant unit vector } \boldsymbol{\nu} \in \mathbb{R}^2 \text{ and a} \\ &\text{constant } c_{\boldsymbol{\nu}} > 0, \text{such that } \nabla u^\dagger \cdot \boldsymbol{\nu} > c_{\boldsymbol{\nu}}, \text{ for all } x \in \Omega, \end{aligned} \tag{1.4}$$

and derive the conditional stability

$$\|q - q^\dagger\|_{L^2(\Omega)} \leq c\|\nabla(u - u^\dagger)\|^{\frac{1}{2}}_{L^2(\Omega)},$$

where c depends on the maximum of $\|q\|_{H^1(\Omega)}$, $\|q^\dagger\|_{H^1(\Omega)}$. The proof relies on the weak formulation of $u^\dagger$ and u with the test function $\varphi = e^{-2k\boldsymbol{x}\cdot\boldsymbol{\nu}}(q^\dagger - q)$, where $k > \|\Delta u^\dagger\|_{L^\infty(\Omega)}/(2c_{\boldsymbol{\nu}})$ is a given constant. Indeed, direct computation leads to following weighted stability

$$\int_\Omega (q^\dagger - q)^2 \big(k\nabla u^\dagger \cdot \boldsymbol{\nu} + \tfrac{1}{2}\Delta u^\dagger\big) e^{-2k\boldsymbol{x}\cdot\boldsymbol{\nu}} \,\mathrm{d}x \le c\|\nabla(u - u^\dagger)\|_{L^2(\Omega)}.$$

By the choice of k, one can remove the weight function and get the desired $L^2(\Omega)$ estimate. Motivated by the stability estimate, Falk [54] analyzed a Galerkin finite element method discretization of the standard output least-squares formulation, and derived a rate $O(h^r + h^{-2}\delta)$ in the $L^2(\Omega)$ norm, where r is the polynomial degree of the finite element space and h is the mesh size. The proof relies on the design of test function $\varphi = e^{-2k\boldsymbol{x}\cdot\boldsymbol{\nu}}(P_h q^\dagger - q_h^*)$ and applying energy argument. Here P_h denotes the projection onto finite element space, cf Section 2.1.1; and q_h^* denotes the minimizer of proposed least-squares formulation. However, this result requires sufficiently high regularity $u^\dagger \in C^{r+3}(\overline{\Omega})$ and $q^\dagger \in H^{r+1}(\Omega)$ and the restrictive structural condition (1.4).

Later, Wang and Zou [144] improved the error analysis of the inverse diffusion problem with a homogeneous Neumann boundary condition. To obtain a numerically stable reconstruction, they employed the output least-squares method with an $H^1(\Omega)$ seminorm penalty and discretizes both the diffusion coefficient q and the solution u using conforming piecewise linear finite elements. Their work relaxed the regularity assumption $q^\dagger, u^\dagger \in H^2(\Omega)\cap W^{1,\infty}(\Omega)$ and employed a mild structural condition:

$$\text{There exists a constant } c_0 > 0 \text{ such that } c_0|\nabla u^\dagger(x)|^2 \ge f(x) \text{ a.e. } x \in \Omega. \tag{1.5}$$

With these assumptions, they established the following weighted $L^2(\Omega)$ analysis

$$\|(q^\dagger - q_h^*)\nabla u^\dagger\|_{L^2(\Omega)} \le c\big(h^{\frac{1}{2}}\gamma^{-\frac{1}{2}} + h^{-\frac{1}{2}}\gamma^{-\frac{1}{4}}\big)\big(h^2 + \delta + \gamma^{\frac{1}{2}}\big),$$

where $\gamma > 0$ denotes the regularization parameter. The proof is similar to [54] by introducing the special test function $\varphi = (q^\dagger)^{-1}(q^\dagger - q)e^{-2c_0\underline{c}_q^{-1}u^\dagger}$. The following weighted stability holds

$$\int_\Omega \frac{(q^\dagger - q)^2}{(q^\dagger)^2}\big(2c_0\underline{c}_q^{-1}q^\dagger|\nabla u^\dagger|^2 - f\big)e^{-2c_0\underline{c}_q^{-1}u^\dagger}\mathrm{d}x \le c\|\nabla(u(q) - u^\dagger)\|_{L^2(\Omega)}.$$

The box constraint $0 < \underline{c}_q \le q(x) \le \overline{c}_q$ and the choice of c_0 imply the desired estimate.

The above reconstruction schemes are based on least-squares techniques. There are various approaches to reconstruct the diffusion coefficient and establish the error analysis. One approach relies on reformulating the inverse problem as a transport equation for the diffusivity q. Richter [128, 129] proved the uniqueness of the inverse problem (1.3) under the assumptions that q is given on the inflow boundary (the portion of the boundary where $\frac{\partial q}{\partial n} < 0$) and the condition

$$\inf_\Omega \max\{|\nabla u^\dagger|, \Delta u^\dagger\} > 0. \tag{1.6}$$

In addition, Richter [129] provided a modified upwind difference scheme for the transport problem and proved $O(h)$ convergence under restrictive regularity assumption $u^\dagger \in C^3(\overline{\Omega})$ and $q^\dagger \in C^2(\overline{\Omega})$. Another approach uses variational methods. Kohn and Lowe [101] proposed following unconstrained minimization problem to solve the inverse problem (1.3) with Neumann boundary condition:

$$\min_{\sigma_h, q_h} \|\sigma_h - q_h \nabla z^\delta\|^2_{L^2(\Omega)} + \|\nabla \cdot \sigma_h + f\|^2_{L^2(\Omega)} + \|\sigma_h \cdot n - g\|^2_{L^2(\partial\Omega)} + \gamma \|\nabla q_h\|^2_{L^2(\Omega)}.$$

The objective function matches equation error of the first order system with $u^\dagger$ replaced by noise measurement z^δ. Kohn and Lowe proved that assuming the regularity $u^\dagger \in H^3(\Omega)$, $\Delta u^\dagger \in C(\overline{\Omega})$, $q^\dagger \in H^2(\Omega)$ and $\|u^\dagger - z^\delta\|_{H^1(\Omega)} \leq \delta$, there holds

$$\|q_h^* - q^\dagger\|_{L^2(\Omega)} \leq c(h + \delta + \gamma^{\frac{1}{2}})^{\frac{1}{2}},$$

under the condition

$$\begin{aligned} &\text{For all } \psi \in H^1(\Omega), \text{ the equation } \nabla u^\dagger \cdot \nabla v_\psi = \psi \\ &\text{has a solution with } \|v_\psi\|_{H^1(\Omega)} \leq c\|\psi\|_{H^1(\Omega)}. \end{aligned} \tag{1.7}$$

They also showed the condition (1.7) is weaker than the condition (1.4) presented in Falk's result [101, Lemma 5].

It is important to highlight that the structural assumptions (1.4)-(1.7) are crucial for the stability and numerical analysis for the inverse diffusivity problem. These assumptions can be interpreted as variations of the following non-zero gradient condition:

$$|\nabla u(x)| \geq c_0 > 0 \quad \text{for all} \quad x \in \Omega. \tag{1.8}$$

In general, this non-zero condition does not holds. To achieve this condition, it is important to design some special input data (boundary excitation g or source f). In practical, these designs of input data may be restrictive. Below, we review and propose two strategies for designing the input data.

We first consider the case $f \neq 0$. Bonito et. al. [22] proposed a novel stability estimate with mild assumptions on problem data by considering (1.3) with zero Dirichlet boundary. Based on the energy argument and a special test function $\varphi = (q^\dagger)^{-1}(q^\dagger - q)u^\dagger \in H_0^1(\Omega)$, Bonito et al [22] established the following weighted stability estimate:

$$\int_\Omega \Big|\frac{q^\dagger - q}{q^\dagger}\Big|^2 \Big(q^\dagger |\nabla u^\dagger|^2 + f u^\dagger\Big)\, \mathrm{d}x \leq c\|\nabla(u^\dagger - u)\|_{L^2(\Omega)},$$

where c depends on the maximum of $\|q\|_{H^1(\Omega)}$, $\|q^\dagger\|_{H^1(\Omega)}$. We notice that since the source f does not vanish, there is flexibility to design the input data such that the weight function $q^\dagger|\nabla u^\dagger|^2 + f u^\dagger$ is positive. In [22], the authors consider the following positive condition:

$$q^\dagger |\nabla u^\dagger|^2 + f u^\dagger \geq c_0 \operatorname{dist}(x, \partial\Omega)^\beta, \quad \text{for a.e. } x \in \Omega. \tag{1.9}$$

The positive condition (1.9) describes the decay rate of the weight function near the boundary $\partial\Omega$. This condition has been shown for some certain cases with mild regularity assumptions on problem data. For example, (1.9) holds with $\beta = 2$ if Ω is a Lipschitz domain, $q^\dagger \in H^1(\Omega)$ with positive lower and upper bounds, and $f \in L^2(\Omega)$ with a strictly positive lower bound in Ω. Further, if Ω is a $C^{2,\mu}$ domain with $\mu \in (0,1)$, $q^\dagger \in C^{1,\mu}(\Omega)$ with positive lower and upper bounds, $f \in C^\mu(\Omega)$ with $f \geq c_f > 0$, then (1.9) holds with $\beta = 0$. The proofs follow from the maximum principle and Schauder estimates for second-order scalar elliptic equations, the decay rate of the Green function near the boundary $\partial\Omega$, see e.g., [22, Corollaries 3.4 and 3.8] for the related analysis. Inspired by the stability analysis in [22], the work in [84] develops a new error bound using a weighted energy estimate with a special test function $\varphi = (q^\dagger)^{-1}(q^\dagger - q_h^*)u^\dagger \in H_0^1(\Omega)$. They proved a weighted estimate under the regularity assumption $q^\dagger \in H^2(\Omega) \cap W^{1,\infty}(\Omega)$ and derived $L^2(\Omega)$ error analysis if in addition (1.9) holds:

$$\|q^\dagger - q_h^*\|_{L^2(\Omega)} \leq c((h\gamma^{-\frac{1}{2}}\eta + \min(h^{-1}\eta, 1))\gamma^{-\frac{1}{2}}\eta)^{\frac{1}{2(1+\beta)}},$$

where $\eta = h^2 + \delta + \gamma^{\frac{1}{2}}$. Later, Jin et al [84, 85, 83, 81, 87] extend this positive condition to inverse potential problem or non-stationary equations. In Chapter 3, we would extend this framework to an inverse problem with two unknown parameters. We provide rigorous a priori error estimates in $L^2(\Omega)$ for both parameters under similar positive conditions.

Now we focus the case $f = 0$ while $g \neq 0$. There are several approaches for constructing a boundary illumination g such that this condition holds. When $d = 2$, the works [8, 7] provide a simple criterion for choosing a special boundary illumination g that guarantees the non-zero condition. Roughly speaking, the graph of g should have a single maximum point, a single minimum point, and be monotone in between. For dimensions $d \geq 3$, ensuring the non-zero condition becomes more challenging [5]. In [16], the author uses the method of complex geometrical optics to construct boundary data g satisfying the nonzero condition. However, this construction is not very explicit and depends on the interior values of the unknown coefficient q. We note that it is possible to obtain θ-Hölder stability for the inverse problem even without requiring (1.8), provided the illuminations are suitably chosen [9]. However, the parameter θ is not explicit and the construction of the boundary values is not easily implementable numerically. Recently, [4, 6] considered using random boundary illuminations and proved that the corresponding solutions will satisfy the non-zero condition with overwhelming probability. This approach overcomes the drawbacks of the previous methods, as it imposes no restrictive constraints on the boundary illuminations and aligns well with practical situations. In Chapter 4, we present the numerical analysis for the inverse problem with nonzero condition provided in [4, 6].

1.3 Inverse problems for subdiffusion model

In recent decades, numerous experiments and studies have revealed that diffusion in complex systems often deviates from Brownian motion, instead following Lévy processes. This phenomenon, known as anomalous diffusion, is characterized by the mean square displacement of particles varying either superlinearly (superdiffusion) or sublinearly (subdiffusion) with time. Anomalous diffusion models are highly effective in describing experimental data across many significant practical applications. The list of successful applications is long and still fast growing, e.g., ion transport in column experiments [66], protein diffusion within cells [59] and contaminant transport in underground water [99]. See the reviews [117, 116] for the derivation of relevant mathematical models and diverse applications. In this thesis, we will only consider the subdiffusion diffusion in time, which can be represented by an equation of the form:

$$\begin{cases} \partial_t^\alpha u - \nabla \cdot (D\nabla u) + \sigma u = f & \text{in } \Omega \times (0,T], \\ u = g & \text{on } \partial\Omega \times (0,T], \\ u(0) = u_0 & \text{in } \Omega, \end{cases} \tag{1.10}$$

where $\partial_t^\alpha u$ is defined as

$$\partial_t^\alpha u(t) := \frac{1}{\Gamma(1-\alpha)} \int_0^t (t-s)^{-\alpha} u'(s)\,\mathrm{d}s. \tag{1.11}$$

The model (1.10) differs considerably from the normal diffusion model due to the presence of the nonlocal operator $\partial_t^\alpha u$: it has limited smoothing property in space and slow asymptotic decay at large time [102, 76].

The mathematical study on inverse problems for time-fractional models is of relatively recent origin, starting from the pioneering work [35] (see [82, 109, 114, 110] for overviews). One of the classical example of inverse problems for subdiffusion is the backward problem. This inverse problem aims to identify the initial data u_0 from the measurement $u(x,T)$, $x \in \Omega$. The existence, uniqueness and stability of the time-fractional backward problem were analyzed by Sakamoto and Yamamoto in [134]. A numerical method is proposed by Liu and Yamamoto [113] based on the quasi-reversibility method, and the approximation error is developed (in terms of noise level) under a priori smoothness assumption on u_0. In [153], Zhang and Zhou employ the finite element method and convolution quadrature to discretize the reconstruction scheme and provide a rigorous error analysis. Another classical identification problem is to recover the diffusivity term D or potential term σ from measurement data $u(x,T)$, $x \in \Omega$. In [71] Isakov showed the uniqueness and existence of the inverse potential problem for parabolic equations, by developing a unique continuation principle and a constructive fixed point iteration. Choulli and Yamamoto [36] proved a generic well-posedness result in a Hölder space, and then proved a conditional stability result in a Hilbert space setting [37] for sufficiently small T. More

recently, a series of works [85, 83, 81, 152, 86] derived conditional stability for diffusivity/potential identification problems and established error analysis based on the positive condition (1.9) mentioned in Section 1.2.

Instead of reconstructing space-dependent potential or diffusion coefficient from terminal measurement, it is more interesting to identifying space-dependent coefficients from lateral Cauchy data. In this scenario, the data and the unknown are misaligned in direction, leading to a severely ill-posed inverse problem. There are several existing works [131, 132, 145, 90, 86, 95]. Rundell and Yamamoto [131] showed that the lateral Cauchy data can uniquely determine the spectral data when $u_0 \equiv f \equiv 0$, and proved the unique determination of the potential using Gel'fand-Levitan theory. They also numerically studied the singular value spectrum of the linearized forward map, showing the severe ill-posed nature of the problem. Later, they [132] relaxed the regularity condition on the boundary excitation $g(t)$ in a suitable Sobolev space. Recently, Jing and Yamamoto [90] proved the identifiability of multiple parameters (including order, spatially dependent potential, initial value and Robin coefficients in the boundary condition) in a time-fractional subdiffusion model with a zero boundary condition and source, excited by a nontrivial initial condition from the lateral Cauchy data at both end points; see also [89]. Jin and Zhou [86] studied the unique recovery of the potential, fractional order and either initial data or source from the lateral Cauchy data, when the boundary excitation is judiciously chosen. All these interesting works are concerned with the one-dimensional setting due to their essential use of the inverse Sturm-Liouville theory. Wei et al [146] numerically investigated the recovery of the zeroth-order coefficient and fractional order in a time-fractional reaction-diffusion-wave equation from lateral boundary data. A direct extension of these theoretical works to the multi-dimensional case is challenging since the Gel'fand-Levitan theory is no longer applicable. Kian et al. [96] provided the first results for the multi-dimensional case, including the uniqueness for identifying two spatially distributed parameters in the subdiffusion model from one single lateral observation with a specially designed excitation Dirichlet input; see also [68] for a related study on determining the manifold from one measurement corresponding to a specialized source. Kian [95] studied also the issue of simultaneous recovery of these parameters along with the order and initial data using a similar choice of the boundary data. However, in the works [96, 95], the excitation data, which plays the role of infinity measurements, is numerically inconvenient to realize, if not impossible at all; see Remark 6.4 for further discussions. These considerations motivate one to design robust numerical algorithm for recovering multiple parameters from a single partial boundary measurement for multi-dimensional subdiffusion with a computable excitation Neumann data, in the presence of a partly unknown medium. The details are presented in Chapter 6.

1.4 Contributions and organizations of the thesis

In Chapter 2, we provide some necessary preliminaries needed for the numerical analysis of parameter identification problems. Firstly we list some standard results in Galerkin finite element method (FEM) approximation. Due to the excellent approximation property and recent algorithmic innovations of neural networks (NNs), we are interested in employing NNs in the parameter identification problems. In particular, we introduce the design and approximation theory of feedforward neural networks. We also introduce the subdiffusion model and provide solution representations based on the spectral expansion and the Mittag-Leffler functions (2.5). All these preliminaries form basis for the following mathematical analysis and numerical algorithms.

In Chapter 3, we extend the inverse diffusivity problem (1.3) by considering the following elliptic equation

$$\begin{cases} -\mathrm{div}\big(D\nabla u\big) + \sigma u = f, & \text{in } \Omega, \\ u = g, & \text{on } \partial\Omega. \end{cases} \tag{1.12}$$

This model extends (1.3) by adding the reaction term σu with σ denoting the reaction coefficient. The inverse problem target the simultaneous reconstruction of the diffusion coefficient D and the reaction coefficient σ in equation (1.12). This is done using two internal observations u_1 and u_2, which correspond to different source terms but share the same boundary data g. It is important to highlight that a similar problem, which involves reconstructing two parameters in equation (1.12) (with $f = 0$) from two internal observations σu_1 and σu_2 (corresponding to distinct boundary data), has been systematically investigated in previous studies [16, 15, 17]. This problem emerges in the context of quantitative photo-acoustic tomography in its diffusive regime. In the aforementioned studies, the two parameters were assumed to be known at the boundary, a prerequisite for constructing a reconstruction algorithm and proving uniqueness. Additionally, the measurements were assumed to satisfy the nonzero condition $|\nabla(u_1/u_2)| \geq \kappa > 0$ almost everywhere in Ω. Interestingly, these assumptions are not required in the current setting since we have a non-vanished source term. Our investigation will address several critical aspects of the inverse problem: the conditional stability of the reconstruction, the development of an efficient numerical algorithm, and a discrete numerical scheme with a provable error estimate. One of the key challenges in this coupled problem is the appropriate selection of function spaces for the analysis, such as for conditional stability estimates, due to the diverse degree of smoothing of the forward map. Our approach utilizes several technical tools, including the weighted stability estimate and energy technique with specific test functions [22]. Notably, the proposed approach differs significantly from existing ones, as the analysis naturally leads to the derivation of rigorous error bounds on the discrete approximations. We also extends the

argument to the parabolic equation

$$\begin{cases} \partial_t u - \nabla \cdot (D\nabla u) + \sigma u = f, & \text{in } \Omega \times (0,T] \\ u = g, & \text{on } \partial\Omega \times (0,T] \\ u(0) = u_0, & \text{in } \Omega. \end{cases} \tag{1.13}$$

We aim to identify the diffusion coefficient D and the reaction coefficient σ from the observation of $u(x,t)$ for $(x,t) \in (T_i - \theta, T_i] \times \Omega$ with $i = 1, 2$. Here T_1 and T_2 denote two distinct time levels, and θ is a fixed small constant. The error estimate for the numerical recovery of the single parameter has been extensively studied in different scenarios. See e.g., [84, 144] for inverse diffusivity problems and [92, 81, 152] for inverse potential problems. In [92], Kaltenbacher and Rundell analyzed the simultaneous recovery of σ and D in one dimensional diffusion equations using the spatial measurement $u(T)$ for two different sets of boundary conditions. The restriction on the one dimension is due to the use of the Sobolev embedding $W^{1,2}(\Omega) \hookrightarrow L^\infty(\Omega)$. In Chapter 3, we consider higher dimensional cases and use the interior observation of a single solution in $(T_i - \theta, T_i]$, $i = 1, 2$. Note that the coupled nonlinear inverse problem does not admits unique recovery in general, even for the one-dimensional case. See a simple counterexample in the beginning of Section 3.3. Therefore, such the recovery highly relies on the choice of the problem data. We will investigate the conditional stability of the reconstruction, develop a decoupled numerical algorithm to identify two parameters sequentially, and propose a completely discrete scheme with provable error bounds. The argument employs some technical arguments, including decoupling the original problem into two single-parameter identification problems [15, 92], exploring weighted $L^2(\Omega)$ stability estimates by an energy argument with special test functions [22, 81] and applying numerical analysis for the direct problems [139].

In Chapter 4, we consider parameter identification problems in photoacoustic tomography (PAT). Photoacoustic tomography is a biomedical imaging technique that combines the principles of optical imaging and ultrasound to produce high-resolution images of tissues within the body [107, 143]. It offers unique advantages by capturing the functional and structural characteristics of tissues, making it particularly useful for medical diagnostics, including cancer detection, monitoring of vascular diseases, and studying brain functions.

The quantitative photoacoustic tomography (QPAT) is a parameter identification problem of recovering the diffusion coefficient and the absorption coefficient from the deposited optical energy. Mathematically, it can be formulated as the following elliptic equation [31, 11]:

$$\begin{cases} -\mathrm{div}\big(D\nabla u\big) + \sigma u = 0, & \text{in } \Omega, \\ u = g, & \text{on } \partial\Omega. \end{cases} \tag{1.14}$$

We investigate the problem of QPAT raising in practical scenario, where the source term f vanishes and the measurement $H = \sigma u$ is generated by a boundary illumination g. The inverse problem aims

to simultaneously identify the diffusion coefficient D and the absorption coefficient σ from optical energy $H = \sigma u$. Compared with Chapter 3, the vanishing source term makes the required positivity condition fail in general, and the measurement, which is the product between the function u and the absorption coefficient σ, is more involved. In order to have a Hölder type stability, we employ specially designed random boundary illuminations [4, 6], and apply the weighted energy estimate with special test functions [22, 84]. We employ a decouple algorithm [16, 15]: first solve an inverse diffusivity problem and then solve a forward problem; cf Section 4.2. We then discuss the numerical inversion formula and analyze the approximation error for the reconstruction. One popular reconstruction approach is to reformulate the inverse diffusivity problem as a transport equation with variable q [16, 15]. This approach is non-iterative and hence efficient for computation. However, it requires the non-zero condition to hold on the whole domain Ω, while in our approach (see Proposition 4.1) the non-zero condition holds only locally for a specific boundary illumination. On the other hand, the least square formulation allows one to naturally incorporate the local non-zero property into the error analysis. Therefore, in this paper, we consider the least square fitting approach with a regularization term for the QPAT reconstruction. Motivated by the stability estimate, we employ weighted energy estimate with a special test function to analyze the approximation error in terms of the discretization mesh size h, the noise level δ, and the regularization parameter γ. Our approach employs several technical tools, including the decoupled procedure for QPAT, the weighted energy estimate, the non-vanishing gradient property, and *a priori* estimates for the finite element approximation.

In Chapter 5, we develop a hybrid scheme combining the neural networks and the finite element methods for the inverse diffusivity problem (1.3)

$$\begin{cases} -\operatorname{div}\big(q\nabla u\big) = f, & \text{in } \Omega, \\ u = 0, & \text{on } \partial\Omega. \end{cases}$$

Due to excellent approximation property of neural networks, many methods based on NNs have been devised and have demonstrated impressive empirical performance on a variety of PDE inverse problems (see [138] for a recent overview). One prominent approach within the class is physics-informed neural networks (PINNs) [126]. In the context of inverse problems, the idea is to minimize a PDE residual functional, and then to enforce both consistency with observational data via a suitable data-fitting functional and *a priori* regularity assumption on the unknown via a suitable penalty. The unknowns are then approximated via NNs, and the resulting loss is trained to yield an approximation. However, the theoretical analysis of neural PDE solvers for direct problems is still at an early stage, when compared with more conventional numerical methods, e.g., finite element methods. This has greatly hindered the mathematical analysis of relevant inverse solvers. To have the best of both approaches, one natural idea is to combine neural networks with FEMs. Therefore, in Chapter 5 we study the

hybrid NN-FEM approach for recovering the unknown coefficient q in problem (1.3) (and also the parabolic case), and provide an analysis on the numerical approximation. We contribute in the following three aspects. First, we develop a novel reconstruction formulation by incorporating the projection operator, which automatically guarantees the well-posedness of the discrete formulations. Second, we derive the $L^2(\Omega)$ error estimates on the NN approximation q_θ^* for both inverse elliptic and parabolic problems, under mild conditions on the problem data (u_0, f, q and Ω), cf. Theorems 5.2 and 5.6 for the elliptic and parabolic cases, respectively. The error bounds depend explicitly on the approximation accuracy ϵ of the NN, discretization parameters (h and τ), the noise level δ and the regularization parameter γ. The overall argument relies heavily on a suitable positivity condition. Third and last, in the context of hybrid solvers, quadrature errors are inevitable, due to the presence of the NN function in various integrals. We derive a useful $L^2(\Omega)$ bound depending on the NN architecture (e.g., width and maximum bound), cf. Theorems 5.4 and 5.8. The technical proofs rely on smoothness properties of NNs and the structure of the finite element space. To the best of our knowledge, these results are new and provide theoretical foundations for using the hybrid formulation for solving PDE inverse problems.

In Chapter 6, we investigate an inverse problem in subdiffusion model:

$$\begin{cases} \partial_t^\alpha u - \nabla \cdot (q \nabla u) = f & \text{in } \Omega \times (0, T], \\ q \partial_\nu u = g & \text{on } \partial\Omega \times (0, T], \\ u(0) = u_0 & \text{in } \Omega. \end{cases} \tag{1.15}$$

We study mathematical and numerical aspects of an inverse problem of recovering the diffusion coefficient q and fractional order α from a single lateral boundary measurement of the solution, without the knowledge of the initial data u_0 and source f. We note that this inverse problem is severely ill-posed: the model is partial known; and the data and the unknown are misaligned in direction. However, the theoretical uniqueness analysis could motivate the design of stably reconstruction algorithm. We make the following contributions to the mathematical analysis and numerics of the concerned inverse problem. First, we examine the feasibility to recover multiple parameters. We show that if the coefficient q is piecewise constant as defined in (6.2), then one single boundary measurement can uniquely determine the coefficient a and fractional order α, even though the initial data u_0 and source f are unknown. Note that the exciting Neumann data g given in (6.3) is easy to realize and hence allows the numerical recovery. The proof relies on the asymptotic behavior of Mittag-Leffler functions, analyticity in time of the solution, and the uniqueness of the inverse diffusivity problem (for elliptic problems) from one boundary measurement. In particular, the subdomain ω can be either a convex polygon / polyhedron or a disc / ball, cf. Theorem 6.2 and Remark 6.3. This analysis strategy follows a well-established procedure in the community, and roughly it consists of two steps. (1) Using the time-analyticity, the

uniqueness for the original inverse problem is reduced to the one for an inverse problem for the corresponding time-independent elliptic equation; (2) The reduction can be done by the Laplace transform or considering the asymptotics. Both strategies of reductions are well known. For example, the former way is used for an Dirichlet-to-Neumann map for the inverse coefficient problem for a multi-term time-fractional diffusion equation [108], while the latter way is used for the Dirichlet-to-Neumann map for the inverse parabolic problem [72, Section 4, Chapter 9]. Second, the uniqueness analysis lends itself to the development of a robust numerical algorithm: we develop a three-step recovery algorithm for identifying the piecewise constant coefficient a and the fractional order α: (i) use the asymptotic behavior of the solution of problem (1.15) near $t = 0$ to recover α; (ii) use analytic continuation to extract the solution of problem (1.15) with zero f and u_0; (iii) use the level set method to recover the shape of subdomain ω. To the best of our knowledge, this is the first work on the numerical recovery of a (piecewise constant) diffusion coefficient in the context of multi-dimensional subdiffusion model with missing initial and source data. Last, we present extensive numerical experiments to illustrate the feasibility of the approach. We refer interested readers to [133, 124] for some numerical studies for identifying a piecewise constant source from the boundary measurement.

Finally, we summarize the main results in the thesis and try to discuss possible future work in Chapter 7.

Throughout, we denote by $W^{s,p}(\Omega)$ the standard Sobolev spaces of order s for any integer $s \geq 0$ and real $p \geq 1$, equipped with the norm $\|\cdot\|_{W^{s,p}(\Omega)}$. Moreover, we write $H^s(\Omega)$ with the norm $\|\cdot\|_{H^s(\Omega)}$ if $p = 2$ we write $L^p(\Omega)$ with the norm $\|\cdot\|_{L^p(\Omega)}$ if $s = 0$. The space $C^{k,\mu}$ with integer $k \geq 0$ and $\mu \in (0, 1]$ denotes the set of Hölder continuous functions. For a Banach space X (with norm $\|\cdot\|_X$), we define $W^{m,p}(0, T; X) = \{v : v(t) \in X \text{ for a.e. } t \in (0, T) \text{ and } \|v\|_{W^{m,p}(0,T;X)} < \infty\}$ with $\|v\|_{W^{m,p}(0,T;X)} = (\sum_{j=0}^{m} \int_0^T \|u^{(j)}(t)\|_X^p)^{\frac{1}{p}}$, The space $L^\infty(0, T; X)$ is defined similarly. The space $C^\omega(T, \infty; X)$ denotes the set of functions valued in X and analytic in $t \in (T, \infty)$. The spaces on the boundary $\partial\Omega$ are defined similarly. The notation $(\cdot, \cdot)$ denotes the standard $L^2(\Omega)$ inner product and $(\cdot, \cdot)_{\partial\Omega}$ denotes the inner product on $L^2(\partial\Omega)$. We denote by c and C generic constants not necessarily the same at each occurrence but it is always independent of the concerned quantities.

CHAPTER 2.

Preliminary

2.1 Numerical algorithms

2.1.1 Finite element method

First, we briefly state some standard results in Galerkin FEM approximation. Let $\mathcal{T}_h$ be a shape regular quasi-uniform partitions of Ω that fit the boundary exactly with a mesh size h. We assume that $\partial\Omega'$ does not cross an element, that is, Ω' equals the union of some meshes. Let V_h denote the conforming finite element space with piecewise polynomials of degree 1 and $V_h^0 = V_h \cap H_0^1(\Omega)$. In particular the finite element space V_h can be characterized by curved element method [156, 157] when $d = 2$ or isoparametric element method [40, 104] when $d \geq 2$.

Following inverse inequality holds on the finite element space V_h^0 [24, Lemma 4.5.3]: for $0 \leq t \leq s \leq 1$, $1 \leq p, q \leq \infty$,

$$\|\varphi_h\|_{W^{s,p}(\Omega)} \leq Ch^{t-s+d/p-d/q}\|\varphi_h\|_{W^{t,q}(\Omega)}, \quad \forall \varphi_h \in V_h^0. \tag{2.1}$$

Let $\mathcal{I}_h \colon C(\overline{\Omega}) \to V_h$ be the Lagrange nodal interpolation operator. Following interpolation error holds [24, Corollary 4.4.20]: for $s = 1, 2$ and $1 \leq p \leq \infty$ (with $sp > d$ if $p > 1$ and $sp \geq d$ if $p = 1$)

$$\|v - \mathcal{I}_h v\|_{L^p(\Omega)} + \|\nabla(v - \mathcal{I}_h v)\|_{L^p(\Omega)} \leq Ch^s\|v\|_{W^{s,p}(\Omega)}, \quad \forall v \in W^{s,p}(\Omega). \tag{2.2}$$

Similarly, we use $\mathcal{I}_h^\partial$ to denote the Lagrange interpolation operator on the boundary. We define the $L^2(\Omega)$-projection $P_h \colon L^2(\Omega) \to V_h^0$ by

$$(P_h v, \varphi_h) = (v, \varphi_h), \quad \forall \varphi_h \in V_h^0.$$

The operator P_h satisfies the following error estimates [139, p. 32]: for any $s \in [1, 2]$

$$\|v - P_h v\|_{L^2(\Omega)} + \|\nabla(v - P_h v)\|_{L^2(\Omega)} \leq Ch^s\|v\|_{H^s(\Omega)}, \quad \forall v \in H^s(\Omega) \cap H_0^1(\Omega). \tag{2.3}$$

2.1.2 Neural networks

In this work, we employ fully connected feedforward neural networks. Let $L \in \mathbb{N}$ be the depth of a neural network (NN) and $\{d_\ell\}_{\ell=0}^L \subset \mathbb{N}$ be a sequence of integers, with $d_0 = d$ and $d_L = 1$, d_ℓ the number of neurons in the ℓth layer of the NN. Then the realization of the NN from $\Omega \subset \mathbb{R}^d$ to $\mathbb{R}$ is

defined by

$$\text{NN realization} \quad \begin{cases} v^{(0)} = x, \quad x \in \Omega, \\ v^{(\ell)} = \rho(A^{(\ell)} v^{(\ell-1)} + b^{(\ell)}), \quad \text{for } \ell = 1, 2, \cdots, L-1, \\ v := v^{(L)} = A^{(L)} v^{(L-1)} + b^{(L)}, \end{cases} \tag{2.4}$$

where $\rho : \mathbb{R} \to \mathbb{R}$ is a nonlinear activation function and applied componentwise to a vector. Throughout, we take $\rho \equiv \tanh$: $x \to \frac{e^x - e^{-x}}{e^x + e^{-x}}$. $A^{(\ell)} \in \mathbb{R}^{d_\ell \times d_{\ell-1}}$ and $b^{(\ell)} \in \mathbb{R}^{d_\ell}$ are weight matrices and bias vectors at the ℓ-th layer of the NN. The width W of the NN is defined by $W := \max_{\ell=0,\ldots,L} d_\ell$. We denote the NN parametrization by $\theta = \{(A^{(\ell)}, b^{(\ell)})\}_{\ell=1}^{L} \in \prod_{\ell=1}^{L} (\mathbb{R}^{d_\ell \times d_{\ell-1}} \times \mathbb{R}^{d_\ell})$. The following approximation property holds [61, Proposition 4.8].

Lemma 2.1. *Let $s \in \mathbb{N}_0$ and $p \in [1, \infty]$ be fixed, and $v \in W^{k,p}(\Omega)$ with $k \geq s+1$. Then for any $\epsilon > 0$, there exists at least one $\theta \in \Theta$ with depth $\mathcal{O}\big(\log(d+k)\big)$ and total number of nonzero parameters $\mathcal{O}\big(\epsilon^{-\frac{d}{k-s-\mu(s=2)}}\big)$, where $\mu > 0$ is arbitrarily small, such that the NN realization v_θ of θ satisfies*

$$\|v - v_\theta\|_{W^{s,p}(\Omega)} \leq \epsilon.$$

Moreover, the maximum norm of the weights in the NN is bounded by $\mathcal{O}(\epsilon^{-2-\frac{2(d/p+d+s+\mu(s=2))+d/p+d}{k-s-\mu(s=2)}})$.

Remark 2.1. *On the domain $\Omega = (0,1)^d$, Guhring and Raslan [64] proved Lemma 2.1 using three steps. They first divide the domain $(0,1)^d$ into $(N+1)^d$ equal patches with gridsize $1/N$ and construct approximation of partitions of unity by neural networks [64, Lemma 4.5]. Next, they approximate a function $v \in W^{k,p}(\Omega)$ by a localized Taylor polynomial v_{poly}: $\|v - v_{\text{poly}}\|_{W^{s,p}(\Omega)} \leq c_{\text{poly}} N^{-(k-s-\mu(s=2))}$, where the construction of v_{poly} relies on the approximated partition of unity and the constant $c_{\text{poly}} = c_{\text{poly}}(d,p,k,s) > 0$. Finally, they show that there exists a DNN parameter θ, satisfying the conditions in Lemma 2.1, such that [64, Lemma D.5]:*

$$\|v_{\text{poly}} - v_\theta\|_{W^{s,p}(\Omega)} \leq c_{\text{NN}} \|v\|_{W^{k,p}(\Omega)} \tilde{\epsilon},$$

where the constant $c_{\text{NN}} = c_{\text{NN}}(d,p,k,s) > 0$ and $\tilde{\epsilon} \in (0, \frac{1}{2})$. Now for small $\epsilon > 0$, the desired estimate follows directly from the choice below $N = (\frac{\epsilon}{2c_{\text{poly}}})^{-\frac{1}{k-s-\mu(s=2)}}$ and $\tilde{\epsilon} = \frac{\epsilon}{2c_{\text{NN}}\|v\|_{W^{k,p}(\Omega)}}$.

Remark 2.2. *The study of approximation capabilities of neural networks begins with the universal approximation theorem [44, 70], i.e., every continuous function defined on a compact domain can be uniformly approximated by shallow neural networks, under certain mild conditions on the activation function. Later, the works [18, 118] examined the approximation capability of sigmoid neural networks for (piecewise) smooth functions. These studies employed neural networks to approximate globally defined polynomials, with the polynomial degree increasing concurrently with the desired approximation accuracy. For the popular rectified linear unit (ReLU) neural network, Yarotsky [149] constructed*

neural networks to approximate localized Taylor polynomials and provided an analysis of the approximation error. However, the approach in [149] heavily relies on the ReLU activation function, which facilitates the construction of an exact partition of unity. The work [64] extended the approach to a wide class of smooth activation functions by constructing an approximate partition of unity.

We denote the set of NNs of depth L, the number of nonzero entries N_θ, and maximum bound R on the parameter vector θ by

$$\mathcal{N}(L, N_\theta, R) =: \{v_\theta \text{ is an NN with depth } L : \|\theta\|_{\ell^0} \le N_\theta, \|\theta\|_{\ell^\infty} \le R\},$$

where $\|\cdot\|_{\ell^0}$ and $\|\cdot\|_{\ell^\infty}$ denote the number of nonzero entries in and the maximum norm of, respectively, a vector. Further, for any $\epsilon > 0$ and $p \ge 1$, we denote by $\mathfrak{P}_{p,\epsilon}$ the NN parameter set for the NN function class

$$\mathcal{N}\Big(C\log(d+1), C\epsilon^{-\frac{d}{1-\mu}}, C\epsilon^{-2-\frac{2p+3d+3pd+2\mu}{p(1-\mu)}}\Big),$$

which will be used to approximate the coefficient q. We focus on two cases: $p = \max(2, d+\mu)$ (with small $\mu > 0$) and $p = \infty$ for the cases without and with the quadrature error, respectively.

The next result bounds the tanh activation function ρ.

Lemma 2.2. *The following estimates hold*

$$\|\rho\|_{L^\infty(\mathbb{R})} \le 1, \quad \|\rho'\|_{L^\infty(\mathbb{R})} \le 1, \quad \|\rho''\|_{L^\infty(\mathbb{R})} \le 1, \quad \|\rho'''\|_{L^\infty(\mathbb{R})} \le 2.$$

Proof. Clearly $\|\rho\|_{L^\infty(\mathbb{R})} \le 1$. Next, using the definition of ρ, direct computation gives

$$\rho'(x) = 1 - \rho^2(x), \quad \rho''(x) = -2\rho(x)(1-\rho^2(x)), \quad \rho'''(x) = (6\rho^2(x) - 2)(1-\rho^2(x)).$$

Thus the desired assertions follow directly. □

2.2 Subdiffusion model

For $\alpha \in (0,1)$, we define the Djrbashian-Caputo fractional derivative $\partial_t^\alpha u$ by ([97, p. 92] or [76, Section 2.3])

$$\partial_t^\alpha u(t) := \frac{1}{\Gamma(1-\alpha)} \int_0^t (t-s)^{-\alpha} u'(s)\,\mathrm{d}s,$$

where Γ denotes the Gamma function. In the following, we introduce the Mittag-Leffler function, which is a basis for fractional differential equations. The two parameter Mittag-Leffler function $E_{\alpha,\beta}(z)$ is defined by ([97, pp. 40-45], [76, Section 3.1])

$$E_{\alpha,\beta}(z) = \sum_{k=0}^{\infty} \frac{z^k}{\Gamma(k\alpha+\beta)}, \quad \forall z \in \mathbb{C}. \tag{2.5}$$

The function $E_{\alpha,\beta}(z)$ generalizes the exponential function e^z. For example,

$$E_{1,1}(z) = \mathrm{e}^z, \quad E_{2,1}(z^2) = \cosh(z), \quad E_{2,2}(z^2) = \frac{\sinh(z)}{z}.$$

The following decay estimate of $E_{\alpha,\beta}(z)$ is crucial; See e.g., [97, eq. (1.8.28), p. 43] and [76, Theorem 3.2] for the proof.

Lemma 2.3. *Let $\alpha \in (0,2)$, $\beta \in \mathbb{R}$, $\varphi \in (\frac{\alpha}{2}\pi, \min(\pi, \alpha\pi))$ and $N \in \mathbb{N}$. Then for $\varphi \le |\arg z| \le \pi$ with $|z| \to \infty$, there holds*

$$E_{\alpha,\beta}(z) = -\sum_{k=1}^{N} \frac{z^{-k}}{\Gamma(\beta - \alpha k)} + O(|z|^{-N-1}).$$

Now, we introduce the representation of the solution to the (sub)diffusion problem:

$$\begin{cases} \partial_t^\alpha u + \mathcal{L}u = f & \text{in } \Omega \times (0,T], \\ u = g & \text{on } \partial\Omega \times (0,T], \\ u(0) = u_0 & \text{in } \Omega. \end{cases} \tag{2.6}$$

Here $\alpha \in (0,1]$, this model coincides with classical diffusion with $\alpha = 1$. The elliptic operator is defined as $\mathcal{L}u := -\nabla \cdot (D\nabla u) + \sigma u$, with $D, \sigma \in L^\infty(\Omega)$ satisfying $0 < \underline{c}_D \le D \le \overline{c}_D$ and $0 \le \sigma \le \overline{c}_\sigma$. Let $A : H^2(\Omega) \cap H_0^1(\Omega) \to L^2(\Omega)$ be the realization of the operator $\mathcal{L}$ with zero Dirichlet boundary condition and its domain $\mathrm{Dom}(A) := \{u \in H_0^1(\Omega) : \mathcal{L}u \in L^2(\Omega)\}$. It is unbounded, closed and, by elliptic regularity [58, Theorem 8.12] and Sobolev embedding theorem [58, Theorem 7.26], its inverse $A^{-1} : L^2(\Omega) \to L^2(\Omega)$ is compact. Thus, by spectral theory of compact operators, A admits eigenvalues (with finite multiplicity): $0 < \lambda_1 < \lambda_2 \le \cdots \le \lambda_j \le \cdots \to \infty$, as $j \to \infty$. The corresponding eigenfunctions $\varphi_j \in H^2(\Omega) \cap H_0^1(\Omega)$ and $\{\varphi_j\}_{j=1}^\infty$ can be taken to form an orthonormal basis of $L^2(\Omega)$.

Then the solution of the forward problem (2.6) could be written as [76]

$$u(t) = Bu(t) + F(t)(u_0 - Bu_0) + \int_0^t E(t-s)(f(s) - \partial_t^\alpha Bu(s))\mathrm{d}s, \tag{2.7}$$

where $Bu(t)$ solves the elliptic equation

$$\begin{cases} \mathcal{L}Bu = f & \text{in } \Omega, \\ Bu = g & \text{on } \partial\Omega, \end{cases}$$

and the solution operators $F(t)$ and $E(t)$ are given by

$$F(t)v = \sum_{j=1}^{\infty} E_{\alpha,1}(-\lambda_j t^\alpha)(v, \varphi_j)\varphi_j, \quad E(t)v = \sum_{j=1}^{\infty} t^{\alpha-1} E_{\alpha,\alpha}(-\lambda_j t^\alpha)(v, \varphi_j)\varphi_j.$$

Another strategy for deriving the solution representation is (vector-valued) Laplace transform. Note that the operator A satisfies the following resolvent estimate [139, p. 92]

$$\|(z + A)^{-1}\|_{L^2(\Omega) \to L^2(\Omega)} \le c(1 + |z|)^{-1}, \quad \forall z \in \Sigma_\rho, \tag{2.8}$$

where $\Sigma_\rho = \{0 \neq z \in \mathbb{C} : |\arg(z)| \leq \rho\}$ with a fixed $\rho \in (\pi/2, \pi)$. Then the solution representation (2.7) holds with the solution operators given by

$$F(t) = \frac{1}{2\pi i} \int_{\Gamma_{\rho,\kappa}} e^{zt} z^{\alpha-1} (z + A)^{-1} \mathrm{d}z, \quad E(t) = \frac{1}{2\pi i} \int_{\Gamma_{\rho,\kappa}} e^{zt} (z + A)^{-1} \mathrm{d}z,$$

where $\Gamma_{\rho,\kappa} = \{z \in \mathbb{C} : |z| = \kappa, |\arg(z)| \leq \rho\} \cup \{z \in \mathbb{C} : z = \rho e^{i\rho}, \rho \geq \kappa\}$ with fixed constants $\kappa \in (0, \infty)$ and $\rho \in (\pi/2, \pi)$.

We end this section with following remarks. Note that in both approaches, when $\alpha = 1$, there holds $F(t) = E(t) = e^{-At}$. In addition, the boundary condition in (2.6) can be taken as Neumann or Robin type.

CHAPTER 3.

Numerical Reconstruction of Diffusion and Reaction Coefficients from Two Observations: Decoupled Recovery and Error Estimates

This chapter is concerned with the identification problem for numerically recovering spatially dependent diffusion coefficient $D(x)$ and reaction coefficient $\sigma(x)$ for elliptic problems. Let $\Omega \subset \mathbb{R}^d (d = 1, 2, 3)$ be a convex polyhedral domain with a boundary $\partial\Omega$. We consider the following elliptic boundary value problem:

$$\begin{cases} -\nabla \cdot (D\nabla u) + \sigma u = f, & \text{in } \Omega, \\ u = g, & \text{on } \partial\Omega, \end{cases} \tag{3.1}$$

where f denotes a given source term and g denotes the boundary data. The solution to problem (3.1) is denoted by $u(D, \sigma)$, to indicate its dependence on the coefficients D and σ. The inverse problem under consideration is to recover exact coefficients $D^\dagger(x)$ and $\sigma^\dagger(x)$ from two interior measurements of solutions, denoted by $u_1(D^\dagger, \sigma^\dagger)$ and $u_2(D^\dagger, \sigma^\dagger)$. Here, $u_i(a^\dagger, q^\dagger)$ be the solution of the elliptic problem (3.1) with source function f_i and boundary data g. Besides, we assume that the empirical observation z_i^δ is noisy with level δ, i.e.,

$$\|u_i(D^\dagger, \sigma^\dagger) - z_i^\delta\|_{L^2(\Omega)} \leq \delta \quad \text{for} \quad i = 1, 2. \tag{3.2}$$

Throughout, the diffusion coefficient and reaction coefficient are respectively sought within the following admissible sets

$$\begin{aligned} &\mathcal{A}_D = \{D \in H^1(\Omega) : 0 < \underline{c}_D \leq D \leq \bar{c}_D \text{ a.e. in } \Omega\} \quad \text{and} \\ &\mathcal{A}_\sigma = \{\sigma \in L^\infty(\Omega) : 0 \leq \sigma \leq \bar{c}_\sigma \text{ a.e. in } \Omega\}, \end{aligned} \tag{3.3}$$

for some positive constants $\underline{c}_D, \bar{c}_D, \bar{c}_\sigma > 0$.

We also extends the argument to the parabolic equation

$$\begin{cases} \partial_t u - \nabla \cdot (D\nabla u) + \sigma u = f, & \text{in } \Omega \times (0, T] \\ u = g, & \text{on } \partial\Omega \times (0, T] \\ u(0) = u_0, & \text{in } \Omega. \end{cases} \tag{3.4}$$

We aim to identify the exact diffusion coefficient $D^\dagger$ and the exact reaction coefficient $\sigma^\dagger$ from the observation of $u(x, t)$ for $(x, t) \in (T_i - \theta, T_i] \times \Omega$ with $i = 1, 2$. Here T_1 and T_2 denote two distinct

[1]Chapter 3 is reprinted with permission from "Numerical Reconstruction of Diffusion and Potential Coefficients from Two Observations: Decoupled Recovery and Error Estimates", Siyu Cen and Zhi Zhou, SIAM J. Numer. Anal., 62 (5) (2024) 2276–2307. The candidate mainly works on the research methodology discussion, the proof details and the coding and data collection in numerical experiments.

time levels, and θ is a fixed small constant. We assume that $D^\dagger$ and $\sigma^\dagger$ belong to the admissible sets $\mathcal{A}_D$ and $\mathcal{A}_\sigma$ respectively, defined in (3.3) and the empirical observation z^δ is noisy with level δ, i.e.,

$$\|u(D^\dagger, \sigma^\dagger) - z^\delta\|_{L^\infty(T_i-\theta,T_i;L^2(\Omega))} \leq \delta, \qquad i = 1, 2. \tag{3.5}$$

The rest of this Chapter is organized as follows. In Section 3.1, we show the Hölder type stability of the inverse problem for the elliptic equations, under several positivity conditions which could be fulfilled. Then the stability estimate further motivates a decoupled recovery algorithm and the error analysis of the discrete approximation, that will be presented in Section 3.2. In Section 3.3, we extend our argument to the parabolic equation. Numerical experiments will be presented in Section 3.4.

3.1 Conditional stability of inversion for elliptic equation

In this section, we aim to derive a conditional stability estimate for the inverse problem, which involves identifying both the diffusion and reaction coefficients in an elliptic equation using two internal observations.

To accomplish this, we must first establish an assumption related to the problem data.

Assumption 3.1. *The source and boundary terms satisfy following properties*

(i) The source terms $f_1, f_2 \in L^\infty(\Omega)$ and the boundary data $g \in H^{\frac{3}{2}}(\partial\Omega) \cap W^{1,\infty}(\partial\Omega)$.

(ii) The source terms $f_1, f_2 \geq 0$ and the boundary data $g \geq c_g > 0$.

(iii) The exact diffusion coefficient $D^\dagger \in \mathcal{A}_D \cap W^{1,\infty}(\Omega) \cap H^2(\Omega)$ and the exact reaction coefficient $\sigma^\dagger \in \mathcal{A}_\sigma$.

Under Assumption 3.1, the elliptic equation (3.1) with source term f_i $(i = 1, 2)$ and boundary data g admits a unique solution $u_i = u_i(D^\dagger, \sigma^\dagger)$ such that

$$u_1, u_2 \in H^2(\Omega) \cap W^{1,\infty}(\Omega). \tag{3.6}$$

Moreover, by the strong maximum principle of the elliptic equation [53, Section 6.4], we conclude that there exists a constant $\underline{c}_u$ depending on $D^\dagger$, $\sigma^\dagger$, g and Ω, but independent of f_1, f_2 such that

$$u_1, u_2 \geq \underline{c}_u > 0. \tag{3.7}$$

3.1.1 Stability estimate for the recovery of diffusion coefficient

To begin with, we eliminate the reaction coefficient σ and recover the diffusion coefficient D from a reformulated elliptic problem. Motivated by the idea in [15], we multiply the equation for u_1 by u_2,

and the equation for u_2 by u_1, and subtract these two relations. As a result, we eliminate the reaction coefficient σ and obtain

$$\begin{cases} -\nabla \cdot \left(D u_1^2 \nabla \left(\dfrac{u_2}{u_1} - 1 \right) \right) = f_2 u_1 - f_1 u_2, & \text{in } \Omega, \\ \dfrac{u_2}{u_1} - 1 = 0, & \text{on } \partial\Omega. \end{cases} \tag{3.8}$$

Let $w := \frac{u_2}{u_1} - 1$, $q := D u_1^2$ and $F := f_2 u_1 - f_1 u_2$, hence the elliptic problem (3.8) can be written as

$$\begin{cases} -\nabla \cdot (q \nabla w) = F, & \text{in } \Omega, \\ w = 0, & \text{on } \partial\Omega. \end{cases} \tag{3.9}$$

Let the diffusion coefficient D, the reaction coefficient σ, the source terms f_i $(i = 1, 2)$ and the boundary data g satisfy Assumption 3.1. Then $q = D u_1^2$ is uniformly bounded and strictly positive, and hence we define the following admissible set

$$\mathcal{A}_q = \{ q \in H^1(\Omega) : 0 < \underline{c}_q \leq q \leq \bar{c}_q \text{ a.e. in } \Omega \}. \tag{3.10}$$

Note that the lower bound $\underline{c}_q \geq \underline{c}_D \underline{c}_u^2$ and the upper bound $\bar{c}_q$ depends on D, σ, f_1 and g. Meanwhile, note that $D u_1^2 \in H^2(\Omega) \cap W^{1,\infty}(\Omega)$ and $f_2 u_1 - f_1 u_2 \in L^\infty(\Omega)$. Consequently, we make the following assumption.

Assumption 3.2. *The exact diffusion coefficient $q^\dagger = D^\dagger |u_1(D^\dagger, \sigma^\dagger)|^2 \in H^2(\Omega) \cap W^{1,\infty}(\Omega) \cap \mathcal{A}_q$ and source term $F = f_2 u_1(D^\dagger, \sigma^\dagger) - f_1 u_2(D^\dagger, \sigma^\dagger) \in L^\infty(\Omega)$.*

Under Assumption 3.2, we deduce that $w \in W_0^{1,2}(\Omega) \cap H^2(\Omega) \cap W^{1,\infty}(\Omega)$. This allows us to present the following conditional stability results in both weighted and standard $L^2(\Omega)$ norms, which play a pivotal role in the numerical analysis in Section 3.2. The proof of these results modifies the proof of [22, Theorem 2.2], incorporating a perturbed source term.

Theorem 3.3. *Suppose that $F, \widetilde{F} \in L^\infty(\Omega)$, $q, \widetilde{q} \in \mathcal{A}_q$, and q satisfies Assumption 3.2. Also, suppose the $H^1(\Omega)$-norm of q and $\widetilde{q}$ are bounded by a generic constant c. Let w be the solution of (3.9) with the diffusion coefficient q and source F, and $\widetilde{w}$ as the solution with the diffusion coefficient $\widetilde{q}$ and source $\widetilde{F}$. Under these conditions, the following holds:*

$$\int_\Omega \frac{(q - \widetilde{q})^2}{q^2} \left(q |\nabla w|^2 + F w \right) \mathrm{d}x \leq c \left(\|w - \widetilde{w}\|_{H^1(\Omega)} + \|F - \widetilde{F}\|_{L^2(\Omega)} \right).$$

Moreover, if the following positive condition holds

$$(q |\nabla w|^2 + F w)(x) \geq c \, \mathrm{dist}(x, \partial\Omega)^\beta \quad \text{a.e. on } \Omega \tag{3.11}$$

for some generic constants $\beta \geq 0$ and $c > 0$. Then the following estimate holds

$$\|q - \widetilde{q}\|_{L^2(\Omega)} \leq c \left(\|w - \widetilde{w}\|_{H^1(\Omega)} + \|F - \widetilde{F}\|_{L^2(\Omega)} \right)^{\frac{1}{2(1+\beta)}}. \tag{3.12}$$

Proof. Define $\xi = q - \widetilde{q}$. For any $v \in H_0^1(\Omega)$, integration by parts in (3.8) yields

$$\int_\Omega \xi \nabla w \cdot \nabla v \mathrm{d}x = \int_\Omega \widetilde{q} \nabla (\widetilde{w} - w) \cdot \nabla v + (F - \widetilde{F}) v \mathrm{d}x. \tag{3.13}$$

Besides, multiplying $\xi v/q$ on both sides of (3.8) and applying integration by parts, we derive

$$\int_\Omega \frac{\xi v}{q} F \mathrm{d}x = \int_\Omega q \nabla w \cdot \nabla \frac{\xi v}{q} \mathrm{d}x = \int_\Omega q v \nabla w \cdot \nabla \frac{\xi}{q} \mathrm{d}x + \int_\Omega q \frac{\xi}{q} \nabla w \cdot \nabla v \mathrm{d}x,$$

and hence

$$\int_\Omega \xi \nabla w \cdot \nabla v \mathrm{d}x = \frac{1}{2} \int_\Omega q \frac{\xi}{q} \nabla w \cdot \nabla v \mathrm{d}x - \frac{1}{2} \int_\Omega q v \nabla w \cdot \nabla \frac{\xi}{q} \mathrm{d}x + \frac{1}{2} \int_\Omega \frac{\xi v}{q} F \mathrm{d}x. \tag{3.14}$$

Now we choose the test function $v = \xi w/q$. Note that q satisfies Assumption 3.1, $\widetilde{q} \in \mathcal{A}_q$ and $F, \widetilde{F} \in L^\infty(\Omega)$. As a result, we conclude that $v \in H_0^1(\Omega)$ with

$$\|v\|_{L^2(\Omega)} \le \|(q - \widetilde{q}) w/q\|_{L^2(\Omega)} \le \frac{2\bar{c}_q}{\underline{c}_q} \|w\|_{L^2(\Omega)}$$

and

$$\begin{aligned}
\|\nabla v\|_{L^2(\Omega)}^2 &\le \Big\| \frac{q \nabla [(q - \widetilde{q}) w] - (q - \widetilde{q}) w \nabla q}{q^2} \Big\|_{L^2(\Omega)} \\
&\le \frac{1}{\underline{c}_q^2} \Big(\bar{c}_q \|w \nabla (q - \widetilde{q})\|_{L^2} + \bar{c}_q \|(q - \widetilde{q}) \nabla w\|_{L^2(\Omega)} + 2\bar{c}_q \|w\|_{L^\infty(\Omega)} \|\nabla q\|_{L^2(\Omega)} \Big) \\
&\le \frac{1}{\underline{c}_q^2} \Big(\bar{c}_q \|w\|_{L^\infty(\Omega)} (\|\nabla q\|_{L^2(\Omega)} + \|\nabla \widetilde{q}\|_{L^2(\Omega)}) + 2\bar{c}_q^2 \|\nabla w\|_{L^2(\Omega)} + 2\bar{c}_q \|w\|_{L^\infty(\Omega)} \|\nabla q\|_{L^2(\Omega)} \Big).
\end{aligned}$$

With this test function v, a direct computation yields that the first two terms on the right hand side of (3.14) is equal to $\frac{1}{2} \int_\Omega \frac{\xi^2}{q} |\nabla w|^2 \mathrm{d}x$. Hence, The relation (3.13) and (3.14) yields

$$\begin{aligned}
\frac{1}{2} \int_\Omega \frac{\xi^2}{q^2} \left(q |\nabla w|^2 + F w \right) \mathrm{d}x &= \int_\Omega \widetilde{q} \nabla (\widetilde{w} - w) \cdot \nabla v + \left(F - \widetilde{F} \right) v \mathrm{d}x \\
&\le c \left(\|w - \widetilde{w}\|_{H^1(\Omega)} + \|F - \widetilde{F}\|_{L^2(\Omega)} \right).
\end{aligned}$$

With the positive condition (3.11), we divide the domain Ω into two parts, $\Omega_\rho = \{x \in \Omega : \mathrm{dist}(x, \partial\Omega) \ge \rho\}$, $\Omega_\rho^c = \Omega \setminus \Omega_\rho$. Thus we have

$$\begin{aligned}
\frac{1}{\underline{c}_q^2} \int_{\Omega_\rho} |\xi|^2 \mathrm{d}x &\le \int_{\Omega_\rho} \left(\frac{\xi}{q} \right)^2 \mathrm{d}x \le c\rho^{-\beta} \int_{\Omega_\rho} \left(\frac{\xi}{q} \right)^2 \rho^\beta \mathrm{d}x \le c\rho^{-\beta} \int_{\Omega_\rho} \left(\frac{\xi}{q} \right)^2 \mathrm{dist}(x, \partial\Omega)^\beta \mathrm{d}x \\
&\le c\rho^{-\beta} \int_{\Omega_\rho} \left(\frac{\xi}{q} \right)^2 \left(q |\nabla w|^2 + F w \right) \mathrm{d}x \le c\rho^{-\beta} \left(\|w - \widetilde{w}\|_{H^1(\Omega)} + \|F - \widetilde{F}\|_{L^2(\Omega)} \right).
\end{aligned}$$

On the other hand, $\int_{\Omega_\rho^c} \xi^2 \mathrm{d}x \le c|\Omega_\rho^c| \le c\rho$. Then the desired result follows by balancing the above two estimates with ρ. □

Remark 3.1. *The positivity condition* (3.11) *is introduced in Section 1.2. It looks artificial, as its physical interpretation is not immediately apparent. However, the condition becomes more intuitive when considering the special case $\beta = 0$ and $F \ge 0$. Then by maximum principle of the elliptic equation, we conclude that the solution $w \ge 0$ and hence $Fw \ge 0$. Consequently, Condition (2.6) requires that the gradient $|\nabla w|$ and the solution w cannot vanish concurrently.*

Let u_i ($\widetilde{u}_i$) be the solution to the elliptic equation (3.1) with diffusion coefficient D ($\widetilde{D}$), reaction coefficient σ ($\widetilde{\sigma}$), the boundary data g and source functions f_i. Using the strict positivity of u_i and $\widetilde{u}_i$ in (3.7) and the uniform boundedness of u_i and $\widetilde{u}_i$, we obtain

$$\begin{aligned}\|D-\widetilde{D}\|_{L^2(\Omega)} &= \Big\|\frac{q}{u_1^2}-\frac{\widetilde{q}}{\widetilde{u}_1^2}\Big\|_{L^2(\Omega)} \le c\|q\widetilde{u}_1^2-\widetilde{q}u_1^2\|_{L^2(\Omega)}\\ &\le c\Big(\|q\widetilde{u}_1^2-qu_1^2\|_{L^2(\Omega)}+\|qu_1^2-\widetilde{q}u_1^2\|_{L^2(\Omega)}\Big)\\ &\le c\Big(\|\widetilde{u}_1-u_1\|_{L^2(\Omega)}+\|q-\widetilde{q}\|_{L^2(\Omega)}\Big).\end{aligned}$$

Using Theorem 3.3, the positivity (3.7) and solution regularity (3.6) , we obtain

$$\begin{aligned}\|D-\widetilde{D}\|_{L^2(\Omega)} &\le c\Big(\|\widetilde{u}_1-u_1\|_{L^2(\Omega)}+\big(\|w-\widetilde{w}\|_{H^1(\Omega)}+\|F-\widetilde{F}\|_{L^2(\Omega)}\big)^{\frac{1}{2(1+\beta)}}\Big)\\ &\le c\Big(\|\widetilde{u}_1-u_1\|_{L^2(\Omega)}+\big(\|u_1-\widetilde{u}_1\|_{H^1(\Omega)}+\|u_2-\widetilde{u}_2\|_{H^1(\Omega)}\big)^{\frac{1}{2(1+\beta)}}\Big)\\ &\le c\big(\|u_1-\widetilde{u}_1\|_{H^1(\Omega)}+\|u_2-\widetilde{u}_2\|_{H^1(\Omega)}\big)^{\frac{1}{2(1+\beta)}}.\end{aligned} \tag{3.15}$$

3.1.2 Stability estimate for the recovery of reaction coefficient

In the preceding section, we derived the stability for the recovery of the diffusion coefficient D. Now, we will shift our focus to the stability analysis for the reaction coefficient σ. We introduce $\zeta := u_2 - u_1$, which satisfies the following elliptic problem:

$$\begin{cases}-\nabla\cdot(D\nabla\zeta)+\sigma\zeta = f_2-f_1, & \text{in } \Omega,\\ \zeta = 0, & \text{on } \partial\Omega.\end{cases} \tag{3.16}$$

Then the next theorem provide a conditional stability for the identification of σ.

Theorem 3.4. *Assume that Assumptions 3.1 and 3.2 are valid. Let $\sigma,\widetilde{\sigma}\in\mathcal{A}_\sigma$, with their $H^1(\Omega)$-norm being bounded by a generic constant c. Under these conditions, the following weighted estimate holds:*

$$\|(\sigma-\widetilde{\sigma})\zeta\|_{L^2(\Omega)}\le c\Big(\sum_{i=1}^{2}\|u_i-\widetilde{u}_i\|_{H^1(\Omega)}+\|\widetilde{D}-D\|_{L^2(\Omega)}\Big)^{\frac{1}{2}}.$$

Moreover, if $f_2-f_1\ge c>0$ a.e. in Ω, then for any compact subset $\Omega'\Subset\Omega$ with $\operatorname{dist}(\overline{\Omega'},\partial\Omega)>0$, there exists a positive constant c, depending on $\operatorname{dist}(\overline{\Omega'},\partial\Omega)$ and D,σ, such that

$$\|\sigma-\widetilde{\sigma}\|_{L^2(\Omega')}\le c\Big(\sum_{i=1}^{2}\|u_i-\widetilde{u}_i\|_{H^1(\Omega)}+\|\widetilde{D}-D\|_{L^2(\Omega)}\Big)^{\frac{1}{2}}.$$

Proof. Denote $\widetilde{\zeta}$ be the solution of (3.16) with coefficients $\widetilde{D},\widetilde{\sigma}$. For a test function $v\in H_0^1(\Omega)$, we consider the $L^2(\Omega)$-inner product $((\sigma-\widetilde{\sigma})z,v)$. By integration by parts, we have

$$\begin{aligned}((\sigma-\widetilde{\sigma})\zeta,v) &= (\sigma\zeta,v)-(\widetilde{\sigma}\zeta,v)+(\widetilde{\sigma}\widetilde{\zeta},v)-(\widetilde{\sigma}\widetilde{\zeta},v)\\ &= (\widetilde{D}\nabla\widetilde{\zeta}-D\nabla\zeta,\nabla v)+(\widetilde{\sigma}(\widetilde{\zeta}-\zeta),v).\end{aligned}$$

Now we take $v = (\sigma - \widetilde{\sigma})\zeta$. Recall that $\zeta \in W^{1,\infty}(\Omega)$, $\sigma, \widetilde{\sigma} \in \mathcal{A}_\sigma$, and $\|\nabla\sigma\|_{L^2(\Omega)}, \|\nabla\widetilde{\sigma}\|_{L^2(\Omega)} \leq c$. Hence

$$\|\nabla v\|_{L^2(\Omega)} \leq (\|\nabla\sigma\|_{L^2(\Omega)} + \|\nabla\widetilde{\sigma}\|_{L^2(\Omega)})\|\zeta\|_{L^\infty(\Omega)} + 2\bar{c}_\sigma\|\nabla\zeta\|_{L^\infty(\Omega)} \leq c.$$

As a result, noting that $D, \widetilde{D} \in \mathcal{A}_D$, we obtain

$$\begin{aligned}
|(\widetilde{D}\nabla\widetilde{\zeta} - D\nabla\zeta, \nabla v)| &\leq \Big(\|\widetilde{D}(\nabla\widetilde{\zeta} - \nabla\zeta)\|_{L^2(\Omega)} + \|(\widetilde{D} - D)\nabla\zeta\|_{L^2(\Omega)}\Big)\|\nabla v\|_{L^2(\Omega)} \\
&\leq c\Big(\bar{c}_D\|\nabla(\widetilde{\zeta} - \zeta)\|_{L^2(\Omega)} + \|\widetilde{D} - D\|_{L^2(\Omega)}\|\nabla\zeta\|_{L^\infty(\Omega)}\Big) \\
&\leq c\Big(\sum_{i=1}^{2}\|u_i - \widetilde{u}_i\|_{H^1(\Omega)} + \|\widetilde{D} - D\|_{L^2(\Omega)}\Big)
\end{aligned}$$

and

$$|(\widetilde{\sigma}(\widetilde{\zeta} - \zeta), v)| \leq \bar{c}_\sigma\|\widetilde{\zeta} - \zeta\|_{L^2(\Omega)}\|v\|_{L^2(\Omega)} \leq c\sum_{i=1}^{2}\|u_i - \widetilde{u}_i\|^2_{L^2(\Omega)} + \frac{1}{2}\|v\|^2_{L^2(\Omega)}.$$

Then we complete the proof of the first assertion.

Since the source term in (3.16) satisfying $f_2 - f_1 \geq c > 0$ in Ω, then the strong maximum principle [141, Theorem 1] implies that for any $\Omega' \Subset \Omega$, there exists a positive constant c depending on $\mathrm{dist}(\Omega', \partial\Omega)$ such that $\zeta(\sigma^\dagger) \geq c > 0$ in Ω' , and consequently, the second assertion holds. □

By combining Theorem 3.4 with the estimate (3.15), we can reformulate the stability estimate for σ in terms of u_1 and u_2. It is important to note that, in comparison with (3.15), the reaction σ exhibits weaker stability than the diffusion coefficient D. This observation is in alignment with the numerical findings discussed in Section 3.4.

Corollary 3.1. *Under the same conditions as in Theorem 3.3 and Theorem 3.4, suppose the positive condition* (3.11) *holds and* $f_2 - f_1 \geq c > 0$ *a.e. in* Ω*, then for any compact subset* $\Omega' \Subset \Omega$ *with* $\mathrm{dist}(\overline{\Omega'}, \partial\Omega) > 0$*, there exists a positive constant* c*, depending on* $\mathrm{dist}(\overline{\Omega'}, \partial\Omega)$ *and* D, σ*, such that*

$$\|\sigma - \widetilde{\sigma}\|_{L^2(\Omega')} \leq c\Big(\sum_{i=1}^{2}\|u_i - \widetilde{u}_i\|_{H^1(\Omega)}\Big)^{\frac{1}{4(1+\beta)}}.$$

3.2 Finite element approximation and error analysis

In this section, we will introduce a numerical scheme aimed at reconstructing the diffusion coefficient $D^\dagger$ and the reaction coefficient $\sigma^\dagger$. This is achieved using the output least-squares formulation. Taking inspiration from the stability estimate, we propose a decoupled algorithm that first recovers the diffusion coefficient $D^\dagger$, followed by the reconstruction of the reaction coefficient $\sigma^\dagger$.

3.2.1 Step one: Numerically recover the diffusion coefficient

Recall that the elliptic problem (3.9) enables to recover the diffusion coefficient without the knowledge of reaction. Note that the exact solution $u_i^\dagger := u_i(D^\dagger, \sigma^\dagger)$, with $i = 1, 2$, is strictly positive with a fixed lower bound (cf. (3.7)). For ease of simplicity, we assume that the empirical observation z_i^δ satisfies the same positive lower bound. We define

$$w^\delta(x) = \frac{z_2^\delta(x)}{z_1^\delta(x)} - 1 \quad \text{and} \quad w^\dagger(x) = \frac{u_2^\dagger(x)}{u_1^\dagger(x)} - 1.$$

Using (3.2), (3.6) and (3.7), we derive

$$\begin{aligned}\|w^\delta - w^\dagger\|_{L^2(\Omega)} = \Big\|\frac{z_1^\delta u_2^\dagger - z_2^\delta u_1^\dagger}{u_1^\dagger z_1^\delta}\Big\|_{L^2(\Omega)} &\leq \Big\|\frac{z_1^\delta u_2^\dagger - u_1^\dagger u_2^\dagger}{u_1^\dagger z_1^\delta}\Big\|_{L^2(\Omega)} + \Big\|\frac{u_1^\dagger u_2^\dagger - z_2^\delta u_1^\dagger}{u_1^\dagger z_1^\delta}\Big\|_{L^2(\Omega)} \\ &\leq \frac{1}{\underline{c}_u^2}\Big(\|z_1^\delta u_2^\dagger - u_1^\dagger u_2^\dagger\|_{L^2(\Omega)} + \|u_1^\dagger u_2^\dagger - z_2^\delta u_1^\dagger\|_{L^2(\Omega)}\Big) \leq c\delta.\end{aligned}$$

Moreover, we should also take care of the source term F in (3.9) where the exact solutions u_1 and u_2 should be replaced with noisy observations. Hence we define $F^\delta := f_2 z_1^\delta - f_1 z_2^\delta$ with

$$\|F - F^\delta\|_{L^2(\Omega)} \leq \|(u_1 - z_1^\delta) f_2\|_{L^2(\Omega)} + \|(u_2 - z_2^\delta) f_1\|_{L^2(\Omega)} \leq c\delta. \tag{3.17}$$

We look for the numerical reconstruction of diffusion coefficient of the system (3.9) in the admissible set $\mathcal{A}_{q,h_1} = \mathcal{A}_q \cap V_{h_1}$, where V_{h_1} is the finite element space generated by mesh size h_1; cf Section 2.1.1. The finite element scheme reads

$$\min_{q_{h_1} \in \mathcal{A}_{q,h_1}} J_{\gamma_1}(q_{h_1}) = \frac{1}{2}\|w_{h_1}(q_{h_1}) - w^\delta\|_{L^2(\Omega)}^2 + \frac{\gamma_1}{2}\|\nabla q_{h_1}\|_{L^2(\Omega)}^2 \tag{3.18}$$

where $w_{h_1}(q_{h_1}) \in V_{h_1}^0$ is a weak solution of

$$(q_{h_1}\nabla w_{h_1}, \nabla \varphi_{h_1}) = (F^\delta, \varphi_{h_1}) \quad \forall\, \varphi_{h_1} \in V_{h_1}^0. \tag{3.19}$$

For any $\gamma_1, h_1 > 0$, there exists at least one minimizer $q_{h_1}^*$ to problem (3.18)-(3.19); see [69, 158] for related analysis for the well-posedness and convergence. Then our objective is to bound the error $q^\dagger - q_{h_1}^*$, where $q^\dagger = D^\dagger u_1^2$ is the exact coefficient satisfying $q^\dagger \in H^2(\Omega) \cap W^{1,\infty}(\Omega)$ provided that Assumption 3.2 holds valid. To this end, we state the following a *priori* estimate for $\|w_{h_1}(q_{h_1}^*) - w(q^\dagger)\|_{L^2(\Omega)}$ and $\|\nabla q_{h_1}^*\|_{L^2(\Omega)}$.

Lemma 3.1. *Suppose that $q^\dagger$ and F satisfy Assumption 3.2. Let $q_{h_1}^* \in \mathcal{A}_{q,h}$ be a minimizer of problem* (3.18)-(3.19)*. Then there holds*

$$\|w_{h_1}(q_{h_1}^*) - w^\delta\|_{L^2(\Omega)}^2 + \gamma_1\|\nabla q_{h_1}^*\|_{L^2(\Omega)}^2 \leq c(h_1^4 + \delta^2 + \gamma_1).$$

Proof. First of all, we notice the following estimate

$$\|w_{h_1}(\mathcal{I}_{h_1}q^\dagger) - w(q^\dagger)\|_{L^2(\Omega)} \le c(h_1^2 + \delta). \tag{3.20}$$

The proof follows from the Lax–Milgram lemma and the standard duality argument, similar to that of [84, Lemma A.1]. The only difference is that the source term F^δ in (3.19) is noisy with level δ, cf. (3.17). Since $q_{h_1}^*$ is a minimizer of J_{γ_1,h_1}, we have $J_{\gamma_1,h_1}(q_{h_1}^*) \le J_{\gamma_1,h_1}(\mathcal{I}_{h_1}q^\dagger)$. This combined with the estimate (3.20) leads to

$$\begin{aligned}
&\|w_{h_1}(q_{h_1}^*) - w^\delta\|_{L^2(\Omega)}^2 + \gamma_1\|\nabla q_{h_1}^*\|_{L^2(\Omega)}^2\\
\le&\|w_{h_1}(\mathcal{I}_{h_1}q^\dagger) - w^\delta\|_{L^2(\Omega)}^2 + \gamma_1\|\nabla\mathcal{I}_{h_1}q^\dagger\|_{L^2(\Omega)}^2\\
\le&\|w_{h_1}(\mathcal{I}_{h_1}q^\dagger) - w(q^\dagger)\|_{L^2(\Omega)}^2 + \|w(q^\dagger) - w^\delta\|_{L^2(\Omega)}^2 + \gamma_1\|\nabla\mathcal{I}_{h_1}q^\dagger\|_{L^2(\Omega)}^2\\
\le&c(h_1^4 + \delta^2 + \gamma_1).
\end{aligned}$$

Then the proof is complete. □

The following theorem establishes a bound for the error $q^\dagger - q_{h_1}^*$. The approach is inspired by the stability estimate provided in Theorem 3.3.

Theorem 3.5. *Suppose Assumptions 3.1 and 3.2 hold valid. Let $q^\dagger = D^\dagger|u_1(D^\dagger,\sigma^\dagger)|^2 \in \mathcal{A}_q$ be the exact parameter in (3.9), $w^\dagger = w(q^\dagger)$ be the solution of (3.9), and $q_{h_1}^* \in \mathcal{A}_{q,h_1}$ be a minimizer of problem (3.18)-(3.19). Then with $\eta = h_1^2 + \delta + \gamma_1^{\frac{1}{2}}$, there holds*

$$\int_\Omega \left(\frac{q^\dagger - q_{h_1}^*}{q^\dagger}\right)^2 \Big(q^\dagger|\nabla w^\dagger|^2 + Fw(q^\dagger)\Big)\,\mathrm{d}x \le c\big((h_1\eta\gamma_1^{-\frac{1}{2}} + \min(h_1 + h_1^{-1}\eta, 1))\eta\gamma_1^{-\frac{1}{2}} + \delta\big).$$

Moreover, let $D_{h_1}^* = q_{h_1}^*/|z_1^\delta|^2$. If the positive condition (3.11) holds with some $\beta \ge 0$, then

$$\|D_{h_1}^* - D^\dagger\|_{L^2(\Omega)} \le c\big((h_1\eta\gamma_1^{-\frac{1}{2}} + h_1^{-1}\eta)\eta\gamma_1^{-\frac{1}{2}} + \delta\big)^{\frac{1}{2(1+\beta)}}.$$

Proof. For any test function $\varphi \in H_0^1(\Omega)$, then the weak formulation of $w(q^\dagger)$ and $w_{h_1}(q_{h_1}^*)$ imply

$$\begin{aligned}
\Big((q^\dagger - q_{h_1}^*)\nabla w^\dagger, \nabla\varphi\Big) &= \Big((q^\dagger - q_{h_1}^*)\nabla w^\dagger, \nabla(\varphi - P_{h_1}\varphi)\Big) + \Big((q^\dagger - q_{h_1}^*)\nabla w^\dagger, \nabla P_{h_1}\varphi\Big)\\
&= -\Big(\nabla\cdot\Big((q^\dagger - q_{h_1}^*)\nabla w^\dagger\Big), \varphi - P_{h_1}\varphi\Big)\\
&\quad + \Big(q_{h_1}^*(\nabla w_{h_1}(q_{h_1}^*) - \nabla w^\dagger), \nabla P_{h_1}\varphi\Big) + \Big(F - F^\delta, P_{h_1}\varphi\Big).
\end{aligned}$$

Motivated by the proof of Theorem 3.3, we choose $\varphi = \frac{q^\dagger - q_{h_1}^*}{q^\dagger}w^\dagger$. A direct computation leads to

$$\nabla\varphi = \left(\frac{q^\dagger\nabla(q^\dagger - q_{h_1}^*) - (q^\dagger - q_{h_1}^*)\nabla q^\dagger}{q^{\dagger 2}}\right)w + \frac{q^\dagger - q_{h_1}^*}{q^\dagger}\nabla w^\dagger.$$

By the box constraint of the admissible sets $\mathcal{A}_q$ and $\mathcal{A}_{q,h}$ as well as the regularity of $w^\dagger$, we derive

$$\begin{aligned}\|\nabla\varphi\|_{L^2(\Omega)} &\le c\|q^\dagger\nabla(q^\dagger - q^*_{h_1}) - (q^\dagger - q^*_{h_1})\nabla q^\dagger\|_{L^2(\Omega)}\|w^\dagger\|_{L^\infty(\Omega)} + c\|q^\dagger - q^*_{h_1}\|_{L^\infty(\Omega)}\|\nabla w^\dagger\|_{L^2(\Omega)}\\ &\le c\|q^\dagger\|_{L^\infty(\Omega)}(\|\nabla q^\dagger\|_{L^2(\Omega)} + \|\nabla q^*_{h_1}\|_{L^2(\Omega)}) + c(\|q^\dagger\|_{L^\infty(\Omega)} + \|q^*_{h_1}\|_{L^\infty(\Omega)})\|\nabla q^\dagger\|_{L^2(\Omega)}) + c\\ &\le c(1 + \|\nabla q^*_{h_1}\|_{L^2(\Omega)}).\end{aligned}$$

Next, according to the box constraint of $q^\dagger$ and $q^*_{h_1}$, the regularity of $q^\dagger$ and $w^\dagger$, the approximation property of P_{h_1} in (2.3), as well as Lemma 3.1, we have

$$\begin{aligned}&|\big(\nabla\cdot\big((q^\dagger - q^*_{h_1})\nabla w^\dagger\big), \varphi - P_{h_1}\varphi\big)|\\ &\le \big(\|\nabla q^\dagger\|_{L^\infty(\Omega)}\|\nabla w^\dagger\|_{L^2(\Omega)} + \|q^\dagger - q^*_{h_1}\|_{L^\infty(\Omega)}\|\Delta w^\dagger\|_{L^2(\Omega)} + \|\nabla q^*_{h_1}\|_{L^2(\Omega)}\|\nabla w^\dagger\|_{L^\infty(\Omega)}\big)\|\varphi - P_{h_1}\varphi\|_{L^2(\Omega)}\\ &\le c\big(1 + \|\nabla q^*_{h_1}\|_{L^2(\Omega)}\big)\|\varphi - P_{h_1}\varphi\|_{L^2(\Omega)} \le ch_1\big(1 + \|\nabla q^*_{h_1}\|_{L^2(\Omega)}\big)\|\nabla\varphi\|_{L^2(\Omega)}\\ &\le ch_1\big(1 + \|\nabla q^*_{h_1}\|_{L^2(\Omega)}\big)^2 \le ch_1(1 + \gamma_1^{-1}\eta^2).\end{aligned}$$

For the remaining terms, by the triangle inequality, the inverse inequality (2.1), the stability and approximation of P_{h_1}, and Lemma 3.1, we have

$$\begin{aligned}&\|\nabla(w_{h_1}(q^*_{h_1}) - w^\dagger)\|_{L^2(\Omega)}\\ \le&\|\nabla(w_{h_1}(q^*_{h_1}) - P_{h_1}w^\dagger)\|_{L^2(\Omega)} + \|\nabla(P_{h_1}w^\dagger - w^\dagger)\|_{L^2(\Omega)}\\ \le&ch_1^{-1}\|w_{h_1}(q^*_{h_1}) - P_{h_1}w^\dagger\|_{L^2(\Omega)} + ch_1\|w^\dagger\|_{H^2(\Omega)}\\ \le&ch_1^{-1}\Big(\|w_{h_1}(q^*_{h_1}) - P_{h_1}w_{h_1}(q^*_{h_1})\|_{L^2(\Omega)} + \|P_{h_1}w_{h_1}(q^*_{h_1}) - P_{h_1}w^\dagger\|_{L^2(\Omega)}\Big) + ch_1\|w^\dagger\|_{H^2(\Omega)}\\ \le&c\Big(h_1 + h_1^{-1}\|w_{h_1}(q^*_{h_1}) - w(q^\dagger)\|_{L^2(\Omega)}\Big) \le c\left(h_1 + h_1^{-1}\eta\right).\end{aligned}$$

Meanwhile, the Lax–Milgram lemma implies

$$\|\nabla(w_{h_1}(q^*_{h_1}) - w^\dagger)\|_{L^2(\Omega)} \le \|\nabla w_{h_1}(q^*_{h_1})\|_{L^2(\Omega)} + \|\nabla w^\dagger\|_{L^2(\Omega)} \le c.$$

As a result, we derive

$$\begin{aligned}&|(q^*_{h_1}(\nabla w_{h_1}(q^*_{h_1}) - \nabla w^\dagger), \nabla P_{h_1}\varphi) + (F - F^\delta, P_{h_1}\varphi)|\\ \le&c\|\nabla(w_{h_1}(q^*_{h_1}) - w^\dagger)\|_{L^2(\Omega)}\|\nabla\varphi\|_{L^2(\Omega)} + \delta\|\varphi\|_{L^2(\Omega)}\\ \le&c\Big(\min(h_1 + h_1^{-1}\eta, 1)\gamma_1^{-1/2}\eta + \delta\Big).\end{aligned}$$

Then using integration by parts and $F = -\nabla\cdot(q^\dagger\nabla w(q^\dagger))$, we have

$$\Big((q^\dagger - q^*_{h_1})\nabla w(q^\dagger), \nabla\varphi\Big) = \frac{1}{2}\int_\Omega\left(\frac{q^\dagger - q^*_{h_1}}{q^\dagger}\right)^2\Big(q^\dagger|\nabla w(q^\dagger)|^2 + Fw(q^\dagger)\Big)\,\mathrm{d}x.$$

Consequently, under positivity condition (3.11), the same argument of (3.12) yields

$$\|q^*_{h_1} - q^\dagger\|_{L^2(\Omega)} \le c\big((h_1\eta\gamma_1^{-\frac{1}{2}} + \min(h_1 + h_1^{-1}\eta, 1))\eta\gamma_1^{-\frac{1}{2}} + \delta\big)^{\frac{1}{2(1+\beta)}}.$$

Finally, we let $D_{h_1}^* = q_{h_1}^*/|z_1^\delta|^2$ and recall that $D^\dagger = q^\dagger/|u_1^\dagger|^2$ with $u_1^\dagger = u_1(D^\dagger, \sigma^\dagger)$. Using the box constraint of $q_{h_1}^*$, the estimate (3.2), the regularity of $u_1^\dagger$ (provided that Assumption 3.1 holds valid), and the fact that $u_1^\dagger, z_1^\delta \geq c_u$, we derive

$$\begin{aligned}\|D_{h_1}^* - D^\dagger\|_{L^2(\Omega)} &\leq c(\|q_{h_1}^*\|_{L^\infty(\Omega)}\|(z_1^\delta)^2 - (u_1^\dagger)^2\|_{L^2(\Omega)} + \|q_{h_1}^* - q^\dagger\|_{L^2(\Omega)}\|u_1^\dagger\|_{L^\infty(\Omega)}) \\ &\leq c(\delta + \|q_{h_1}^* - q^\dagger\|_{L^2(\Omega)}) \leq c\big((h_1\eta\gamma_1^{-\frac{1}{2}} + \min(h_1 + h_1^{-1}\eta, 1))\eta\gamma_1^{-\frac{1}{2}} + \delta\big)^{\frac{1}{2(1+\beta)}}.\end{aligned}$$

This completes the proof of the theorem. □

Remark 3.2. *Theorem 3.5 serves as a guideline for the a priori selection of algorithmic parameters, suggesting $\gamma_1 \sim \delta^2$ and $h_1 \sim \sqrt{\delta}$. Given the positivity condition* (3.11) *with $\beta \geq 0$, the following estimate is valid:*

$$\|D^\dagger - D_{h_1}^*\|_{L^2(\Omega)} \leq c\delta^{\frac{1}{4(1+\beta)}}.$$

This estimate is optimal with respect to the conditional stability estimate (3.15)*.*

3.2.2 Step two: Numerically recover the reaction

In this section, we give the reconstruction formula of reaction σ and corresponding error analysis. We make following regularity assumption for true reaction coefficient $\sigma^\dagger$.

Assumption 3.6. *The reaction coefficient $\sigma^\dagger$ satisfies $\sigma^\dagger \in H^2(\Omega) \cap \mathcal{A}_\sigma$.*

Recall $\zeta = u_2 - u_1$ satisfies following elliptic equation

$$\begin{cases} -\nabla \cdot \left(D^\dagger \nabla \zeta\right) + \sigma^\dagger \zeta = f_2 - f_1, & \text{in } \Omega, \\ \zeta = 0, & \text{on } \partial\Omega. \end{cases}$$

The noisy observational data for equation (3.16) is $\zeta^\delta = z_2^\delta - z_1^\delta$ and $\|\zeta - \zeta^\delta\|_{L^2(\Omega)} \leq c\delta$.

From now on, let h_2 represent the spatial mesh size, which may differ from h_1 used in the previous section. Utilizing the output least-squares formulation, we can approximate the recovery of the reaction as follows:

$$\min_{\sigma_{h_2} \in \mathcal{A}_{\sigma,h_2}} \mathcal{J}_{\gamma_2,h_2}(\sigma_{h_2}) = \frac{1}{2}\|\zeta_{h_2}(\sigma_{h_2}) - \zeta^\delta\|_{L^2(\Omega)}^2 + \frac{\gamma_2}{2}\|\nabla\sigma_{h_2}\|_{L^2(\Omega)}^2 \tag{3.21}$$

where $\mathcal{A}_{\sigma,h_2} = \mathcal{A}_\sigma \cap V_{h_2}$ and $\zeta_{h_2}(\sigma_{h_2}) \in V_{h_2}^0$ is the solution to the finite dimensional problem

$$(D_{h_1}^* \nabla\zeta_{h_2}, \nabla v_{h_2}) + (\sigma_{h_2}\zeta_{h_2}, v_{h_2}) = (f_2 - f_1, v_{h_2}) \qquad \forall\ v_{h_2} \in V_{h_2}^0. \tag{3.22}$$

Here $D_{h_1}^*$ is the diffusion coefficient we reconstructed in Theorem 3.5. As stated in Remark 3.2, we have the *a priori* error estimate

$$\|D_{h_1}^* - D^\dagger\|_{L^2(\Omega)} \leq \epsilon \qquad \text{with } \ \epsilon = c\delta^{\frac{1}{(4(1+\beta))}}.$$

The discrete problem (3.21)-(3.22) is well-posed: there exists at least one global minimizer $\sigma_{h_2}^*$ to problem (3.21)-(3.22) and it depends continuously on the data perturbation. Then we aim to establish an *a priori* error bound between $\sigma_{h_2}^*$ and $\sigma^\dagger$.

To accomplish this, we initially derive a bound for $\zeta_{h_2}(\mathcal{I}_{h_2}\sigma^\dagger) - \zeta(\sigma^\dagger)$. This is achieved using the standard estimates applicable to the finite element method.

Lemma 3.2. *Suppose Assumption 3.6 holds, $D^\dagger \in \mathcal{A}_D \cap W^{1,\infty}(\Omega)$ and $\|D_{h_1}^* - D^\dagger\|_{L^2(\Omega)} \leq \epsilon$. Let $\zeta(\sigma^\dagger)$ be the solution to the elliptic problem* (3.16)*, while $\zeta_{h_2}(\mathcal{I}_{h_2}\sigma^\dagger)$ be the solution to the finite dimensional problem* (3.22) *where σ_{h_2} is replaced with $\mathcal{I}_{h_2}\sigma^\dagger$. Then*

$$\|\zeta_{h_2}(\mathcal{I}_{h_2}\sigma^\dagger) - \zeta(\sigma^\dagger)\|_{L^2(\Omega)} \leq c(h_2^2 + \epsilon).$$

Proof. We apply the following splitting

$$\zeta_{h_2}(\mathcal{I}_{h_2}\sigma^\dagger) - \zeta(\sigma^\dagger) = (\zeta_{h_2}(\mathcal{I}_{h_2}\sigma^\dagger) - \overline{\zeta}_{h_2}) + (\overline{\zeta}_{h_2} - \widetilde{\zeta}_{h_2}) + (\widetilde{\zeta}_{h_2} - \zeta(\sigma^\dagger)) =: \sum_{j=1}^{3} e_j,$$

where $\overline{\zeta}_{h_2}$ and $\widetilde{\zeta}_{h_2}$ respectively satisfy

$$\begin{aligned}(D^\dagger \nabla \overline{\zeta}_{h_2}, \nabla v_{h_2}) + (\mathcal{I}_{h_2}\sigma^\dagger \overline{\zeta}_{h_2}, v_{h_2}) &= (f_2 - f_1, v_{h_2}) \qquad \forall\ v_{h_2} \in V_{h_2}^0, \quad \text{and}\\ (D^\dagger \nabla \widetilde{\zeta}_{h_2}, \nabla v_{h_2}) + (\sigma^\dagger \widetilde{\zeta}_{h_2}, v_{h_2}) &= (f_2 - f_1, v_{h_2}) \qquad \forall\ v_{h_2} \in V_{h_2}^0.\end{aligned}$$

We begin with the $L^2(\Omega)$ bound of e_1, which satisfies

$$(D_{h_1}^* \nabla e_1, \nabla v_{h_2}) + ((\mathcal{I}_{h_2}\sigma^\dagger)e_1, v_{h_2}) = ((D^\dagger - D_{h_1}^*)\nabla \overline{\zeta}_{h_2}, \nabla v_{h_2}) \qquad \forall\ v_{h_2} \in V_{h_2}^0.$$

Now we choose $v_{h_2} = e_1$ in the above relation. By the regularity $\|D^\dagger\|_{W^{1,\infty}(\Omega)} + \|(\mathcal{I}_{h_2})\sigma^\dagger\|_{L^\infty(\Omega)} \leq c$, we conclude that $\|\nabla \overline{\zeta}_{h_2}\|_{L^\infty(\Omega)} \leq c$ (cf. [127] and [63, Theorem 2]). This together with the fact that $D_{h_1}^* \in \mathcal{A}_D$ and Poincaré's inequality implies

$$\|e_1\|_{H^1(\Omega)} \leq \|D^\dagger - D_{h_1}^*\|_{L^2(\Omega)} \|\nabla \overline{\zeta}_{h_2}\|_{L^\infty(\Omega)} \leq c\epsilon.$$

Now we turn to the second term e_2 which satisfies

$$(D^\dagger \nabla e_2, \nabla v_{h_2}) + ((\mathcal{I}_{h_2}\sigma^\dagger)e_2, v_{h_2}) = ((\sigma^\dagger - \mathcal{I}_{h_2}\sigma^\dagger)\widetilde{\zeta}_{h_2}, v_{h_2}) \qquad \forall\ v_{h_2} \in V_{h_2}^0.$$

Letting $v_{h_2} = e_2$ and using the fact that $\|\widetilde{\zeta}_{h_2}\|_{L^\infty(\Omega)} \leq C$, we arrive at

$$\|\nabla e_2\|_{L^2(\Omega)} \leq c\|\sigma^\dagger - \mathcal{I}_{h_2}\sigma^\dagger\|_{L^2} \|\widetilde{\zeta}_{h_2}\|_{L^\infty(\Omega)} \leq ch_2^2,$$

where we use the estimate (2.2) and the assumption that $\sigma^\dagger \in H^2(\Omega)$. Finally, the estimate for the third term, $\|e_3\|_{L^2(\Omega)} \leq Ch_2^2$, can be estimated directly by applying the standard argument. □

The subsequent lemma offers useful bounds for the state $\zeta_{h_2}(\sigma^*_{h_2})$ and the $H^1(\Omega)$ seminorm of $\sigma^*_{h_2}$.

Lemma 3.3. *Suppose Assumption 3.6 holds, $D^\dagger \in \mathcal{A}_D \cap W^{1,\infty}(\Omega)$ and $\|D^*_{h_1} - D^\dagger\|_{L^2(\Omega)} \le \epsilon$. Then there is*

$$\|\zeta(\sigma^\dagger) - \zeta_{h_2}(\sigma^*_{h_2})\|_{L^2(\Omega)} + \gamma_2^{\frac{1}{2}} \|\nabla \sigma^*_{h_2}\|_{L^2(\Omega)} \le c(h_2^2 + \epsilon + \delta + \gamma_2^{\frac{1}{2}}).$$

Proof. Since $\sigma^*_{h_2}$ is a minimizer of $\mathcal{J}_{\gamma_2,h_2}$, we have $\mathcal{J}_{\gamma_2,h_2}(\sigma^*_{h_2}) \le \mathcal{J}_{\gamma_2,h_2}(\mathcal{I}_{h_2}\sigma^\dagger)$. Then we derive

$$\begin{aligned}
&\|\zeta_{h_2}(\sigma^*_{h_2}) - \zeta^\delta\|^2_{L^2(\Omega)} + \gamma_2 \|\nabla \sigma^*_{h_2}\|^2_{L^2(\Omega)} \\
\le &\|\zeta_{h_2}(\mathcal{I}_{h_2}\sigma^\dagger) - \zeta^\delta\|^2_{L^2(\Omega)} + \gamma_2 \|\nabla \mathcal{I}_{h_2}\sigma^\dagger\|^2_{L^2(\Omega)} \\
\le &\|\zeta_{h_2}(\mathcal{I}_{h_2}\sigma^\dagger) - \zeta(\sigma^\dagger)\|^2_{L^2(\Omega)} + \|\zeta(\sigma^\dagger) - \zeta^\delta\|^2_{L^2(\Omega)} + \gamma_2 \|\nabla \mathcal{I}_{h_2}\sigma^\dagger\|^2_{L^2(\Omega)} \\
\le &c\left((h_2^2 + \epsilon)^2 + \delta^2 + \gamma_2\right),
\end{aligned}$$

where in the last inequality we use the result in Lemma 3.2. □

Then we are ready to show the error bound of numerically recovered reaction.

Theorem 3.7. *Suppose that Assumption 3.6 holds valid, $D^\dagger \in \mathcal{A}_D \cap W^{1,\infty}(\Omega)$ and $\|D^*_{h_1} - D^\dagger\|_{L^2(\Omega)} \le \epsilon$. Let $\sigma^*_{h_2}$ be the numerical reconstruction of the reaction given in (3.21)-(3.22). Then with $\eta = h_2^2 + \epsilon + \delta + \gamma_2^{\frac{1}{2}}$, there holds*

$$\|(\sigma^\dagger - \sigma^*_{h_2})\zeta(\sigma^\dagger)\|_{L^2(\Omega)} \le c\big(h_2 \gamma_2^{-\frac{1}{2}} \eta + \eta + \big(\gamma_2^{-\frac{1}{2}} \eta (\min\{h_2 + h_2^{-1}\eta, 1\} + \epsilon)\big)^{\frac{1}{2}}\big).$$

Finally, if $f_2 - f_1 \ge c > 0$ a.e. in Ω, then for any $\Omega' \Subset \Omega$, there exists a constant c depending on $\mathrm{dist}(\Omega', \partial\Omega)$ and $D^\dagger, \sigma^\dagger$ such that

$$\|\sigma^*_{h_2} - \sigma^\dagger\|_{L^2(\Omega')} \le c\big(h_2 \gamma_2^{-\frac{1}{2}} \eta + \eta + \big(\gamma_2^{-\frac{1}{2}}(h_2 + \epsilon)\big)^{\frac{1}{2}}\big).$$

Proof. For any test function $\varphi \in H^1_0(\Omega)$, by weak formulation of $\zeta_{h_2}(\sigma^*_{h_2})$ and $\zeta(\sigma^\dagger)$, we have

$$\begin{aligned}
&\big((\sigma^\dagger - \sigma^*_{h_2})\zeta(\sigma^\dagger), \varphi\big) \\
=&\big((\sigma^\dagger - \sigma^*_{h_2})\zeta(\sigma^\dagger), \varphi - P_{h_2}\varphi\big) + \big((\sigma^\dagger - \sigma^*_{h_2})\zeta(\sigma^\dagger), P_{h_2}\varphi\big) \\
=&\big((\sigma^\dagger - \sigma^*_{h_2})\zeta(\sigma^\dagger), \varphi - P_{h_2}\varphi\big) + \big(D^*_{h_1}\nabla\zeta_{h_2}(\sigma^*_{h_2}) - D^\dagger \nabla\zeta(\sigma^\dagger), \nabla P_{h_2}\varphi\big) + \big(\sigma^*_{h_2}(\zeta_{h_2}(\sigma^*_{h_2}) - \zeta(\sigma^\dagger)), P_{h_2}\varphi\big) \\
=:&\sum_{j=1}^n \mathrm{I}_j.
\end{aligned}$$

Now, we take $\varphi = (\sigma^\dagger - \sigma^*_{h_2})\zeta(\sigma^\dagger)$. A direct computation implies $\varphi \in H^1_0(\Omega)$ and

$$\|\varphi\|_{L^2(\Omega)} \le c \quad \text{and} \quad \|\nabla\varphi\|_{L^2(\Omega)} \le c(1 + \|\nabla\sigma^*_{h_2}\|_{L^2(\Omega)}).$$

By the box constraint of $\mathcal{A}_{\sigma,h_2}$, the error estimate of P_{h_2} in (2.3) and Lemma 3.3, we have

$$\begin{aligned}|\mathrm{I}_1| \leq & \|(\sigma^\dagger - \sigma^*_{h_2})\zeta(\sigma^\dagger)\|_{L^2(\Omega)}\|\varphi - P_{h_2}\varphi\|_{L^2(\Omega)} \leq ch_2\|(\sigma^\dagger - \sigma^*_{h_2})\zeta(\sigma^\dagger)\|_{L^2(\Omega)}\|\nabla\varphi\|_{L^2(\Omega)} \\ \leq & ch_2\|(\sigma^\dagger - \sigma^*_{h_2})\zeta(\sigma^\dagger)\|_{L^2(\Omega)}(1 + \|\nabla\sigma^*_{h_2}\|_{L^2(\Omega)}) \leq ch_2^2\gamma_2^{-1}\eta^2 + \frac{1}{3}\|(\sigma^\dagger - \sigma^*_{h_2})\zeta(\sigma^\dagger)\|^2_{L^2(\Omega)}.\end{aligned} \tag{3.23}$$

By the stability of P_{h_2} and Lemma 3.3 we conclude

$$\begin{aligned}|\mathrm{I}_3| \leq & \|\sigma^*_{h_2}\|_{L^\infty(\Omega)}\|\zeta_{h_2}(\sigma^*_{h_2}) - \zeta(\sigma^\dagger)\|_{L^2(\Omega)}\|P_{h_2}\varphi\|_{L^2(\Omega)} \\ \leq & c\|\zeta_{h_2}(\sigma^*_{h_2}) - \zeta(\sigma^\dagger)\|^2_{L^2(\Omega)} + \frac{1}{3}\|\varphi\|^2_{L^2(\Omega)} \leq c\eta^2 + \frac{1}{3}\|\varphi\|^2_{L^2(\Omega)}.\end{aligned} \tag{3.24}$$

Finally, we turn to the term I_2 and use the splitting

$$\mathrm{I}_2 = \Big(D^*_{h_1}\nabla\zeta_{h_2}(\sigma^*_{h_2}) - D^*_{h_1}\nabla\zeta(\sigma^\dagger), \nabla P_{h_2}\varphi\Big) + \Big(D^*_{h_1}\nabla\zeta(\sigma^\dagger) - D^\dagger\nabla\zeta(\sigma^\dagger), \nabla P_{h_2}\varphi\Big) =: \mathrm{I}_{2,1} + \mathrm{I}_{2,2}.$$

It is easy to observe

$$|\mathrm{I}_{2,2}| \leq \|D^*_{h_1} - D^\dagger\|_{L^2(\Omega)}\|\nabla\zeta(\sigma^\dagger)\|_{L^\infty(\Omega)}\|\nabla P_{h_2}\varphi\|_{L^2(\Omega)} \leq c\gamma_2^{-\frac{1}{2}}\eta\epsilon,$$

where we use the *a priori* estimate that $\|\nabla\zeta(\sigma^\dagger)\|_{L^\infty(\Omega)} \leq c$ and the assumption that $\|D^*_{h_1} - D^\dagger\|_{L^2(\Omega)} \leq \epsilon$. Moreover, by Lemma 3.3, we have

$$|\mathrm{I}_{2,1}| \leq \|D^*_{h_1}\|_{L^\infty(\Omega)}\|\nabla\zeta_{h_2}(\sigma^*_{h_2}) - \nabla\zeta(\sigma^\dagger)\|_{L^2(\Omega)}\|\nabla P_{h_2}\varphi\|_{L^2(\Omega)} \leq c\gamma_2^{-\frac{1}{2}}\eta\|\nabla\zeta_{h_2}(\sigma^*_{h_2}) - \nabla\zeta(\sigma^\dagger)\|_{L^2(\Omega)}.$$

By the inverse inequality (2.1) and the approximation property (2.3), we have

$$\begin{aligned}\|\nabla\zeta_{h_2}(\sigma^*_{h_2}) - \nabla\zeta(\sigma^\dagger)\|_{L^2(\Omega)} \leq & \|\nabla(\zeta_{h_2}(\sigma^*_{h_2}) - P_{h_2}\zeta(\sigma^\dagger))\|_{L^2(\Omega)} + \|\nabla(P_{h_2}\zeta(\sigma^\dagger) - \zeta(\sigma^\dagger))\|_{L^2(\Omega)} \\ \leq & c\Big(h_2^{-1}\|\zeta_{h_2}(\sigma^*_{h_2}) - P_{h_2}\zeta(\sigma^\dagger)\|_{L^2(\Omega)} + h_2\|\zeta(\sigma^\dagger)\|_{H^2(\Omega)}\Big) \\ \leq & c\big(h_2^{-1}\eta + h_2\big).\end{aligned}$$

Meanwhile, using the stability estimate $\|\nabla\zeta_{h_2}(\sigma^*_{h_2})\|_{L^2(\Omega)} + \|\nabla\zeta(\sigma^\dagger)\|_{L^2(\Omega)} \leq c$, we conclude that

$$|\mathrm{I}_{2,1}| \leq c\gamma_2^{-\frac{1}{2}}\eta\min\big(h_2^{-1}\eta + h_2, 1\big).$$

Thus we arrive at the estimate

$$|\mathrm{I}_2| \leq c\gamma_2^{-\frac{1}{2}}\eta\big(\min\big(h_2^{-1}\eta + h_2, 1\big) + \epsilon\big). \tag{3.25}$$

Then the desired estimate follows immediately by combining the estimates (3.23), (3.24) and (3.25). Finally, if $f_2 - f_1 \geq c > 0$, with the same argument as that of Theorem 3.4, we have the second assertion. □

Remark 3.3. *According to Theorem 3.5 and Remark 3.2, we have*

$$\|D^*_{h_1} - D^\dagger\| \leq \epsilon = c\delta^{\frac{1}{4(1+\beta)}},$$

provided that $h_1 \sim \sqrt{\delta}$, $\gamma_1 \sim \delta^2$ *and the positivity condition* (3.11) *is valid. As a result, with the choice of parameters* $h_2 \sim \epsilon^{\frac{1}{2}}$ *and* $\gamma_2 \sim \epsilon^2$, *there holds the estimate*

$$\|(\sigma^\dagger - \sigma_{h_2}^*)\zeta(\sigma^\dagger)\|_{L^2(\Omega)} \leq c\delta^{\frac{1}{8(1+\beta)}}.$$

Moreover, if we choose source terms such that $f_2 - f_1 \geq c > 0$ *in* Ω, *then similar argument as that of Theorem 3.4 implies that*

$$\|\sigma^\dagger - \sigma_{h_2}^*\|_{L^2(\Omega')} \leq c\delta^{\frac{1}{8(1+\beta)}},$$

where $\Omega' \Subset \Omega$ *and the constant* c *depending on* $\operatorname{dist}(\Omega', \partial\Omega)$ *and* $D^\dagger, \sigma^\dagger$.

Remark 3.4. *Instead of adopting the aforementioned decoupled approach, alternative reconstruction formulas exist to address the inverse problem. One intuitive method involves the following least-squares formulation:*

$$\min_{D_h \in \mathcal{A}_{D,h}, \sigma_h \in \mathcal{A}_{\sigma,h}} \mathcal{J}(D_h, \sigma_h) = \frac{1}{2}\sum_{i=1}^{2} \|u_{i,h} - z_i^\delta\|_{L^2(\Omega)}^2 + \frac{\gamma_1}{2}\|\nabla D_h\|_{L^2(\Omega)}^2 + \frac{\gamma_2}{2}\|\nabla \sigma_h\|_{L^2(\Omega)}^2, \tag{3.26}$$

where $u_{i,h} = u_{i,h}(D_h, \sigma_h) \in V_h$ *satisfies* $u_{i,h}(D_h, \sigma_h)|_{\partial\Omega} = \mathcal{I}_h g$ *and*

$$(D_h \nabla u_{i,h}, \nabla v_h) + (\sigma_h u_{i,h}, v_h) = (f_i, v_h) \quad \forall\ v_h \in V_h^0. \tag{3.27}$$

Due to the non-homogeneous boundary condition, deriving an error estimate similar to Theorem 3.5 and 3.7 for the coupled reconstruction formula (3.26)-(3.27) *and its numerical discretization is not feasible. Furthermore, a numerical comparison between the decoupled approach and the coupled approach is presented in Section 3.4.*

Remark 3.5. *We assume that* Ω *is a convex polyhedral domain to ensure the solution* u *is in the Sobolev space* $H^2(\Omega)$, *which is a prerequisite for obtaining an optimal approximation rate with the finite element method on quasi-uniform meshes. Note that the proof of Theorems 3.5 and 3.7 rely on the application of the inverse inequality* (2.1), *which necessitates the quasi-uniformity of the mesh partition. In contrast, if* Ω *is a nonconvex polygon, attaining the aforementioned optimal rates requires a geometrically graded mesh, which is inherently non-quasi-uniform. Under such circumstances, the inverse inequality is not applicable, thus the error estimate in this paper does not hold in general. Nevertheless, the argument in this paper could be easily adapted to arbitrary domains with smooth boundary conditions.*

3.3 Inverse problem for parabolic equation

In this section, we extend the argument to the following non-stationary parabolic problem with exact conductivity $D^\dagger$ and reaction coefficient $\sigma^\dagger$

$$\begin{cases} \partial_t u - \nabla \cdot (D^\dagger \nabla u) + \sigma^\dagger u = f, & \text{in } \Omega \times (0,T], \\ u = g, & \text{on } \partial\Omega \times (0,T], \\ u(0) = u_0, & \text{in } \Omega. \end{cases} \tag{3.28}$$

We aim to reconstruct the conductivity $D^\dagger$ and the reaction coefficient $\sigma^\dagger$ by observing $u(x,t)$ for $(x,t) \in (T_i - \theta, T_i] \times \Omega$, where $i = 1, 2$. Here, $\theta > 0$ represents a small positive constant.

The inverse problem under consideration generally does not allow for unique recovery. To illustrate this, let's examine a one-dimensional example within the unit interval $\Omega = (0,1)$, where $g = 0$ and $f = 0$. Suppose $u_0(x) = \sin(\pi x)$. In this case, both of the following parameter sets yield identical solutions $u(x,t)$ for all $(x,t) \in \Omega \times [0,\infty)$:

(1) $D(x) = 1$ and $\sigma(x) = \pi^2$;

(2) $D(x) = 2$ and $\sigma(x) = 0$.

As a result, the recovery process is highly sensitive to the choice of problem data. Therefore, it is necessary to impose certain assumptions on the problem data in the parabolic problem given by equation (3.28).

Assumption 3.8. *The problem data in* (3.28) *satisfy following properties.*

(i) The initial data $u_0 \in H^2(\Omega) \cap W^{1,\infty}(\Omega)$ *and* $u_0 \geq c_0 > 0$.

(ii) The source data $f \in C^k(0,T; L^\infty(\Omega)) \cap C^{k+1}(0,T; L^2(\Omega))$ *with* $k \in \mathbb{N}^*$ *and* $f \geq 0$. *Moreover, there exists* $T_0 > 0$ *such that*

$$f(x,t) = \begin{cases} f_1(x), & 0 < t \leq T_0, \\ f_2(x), & t \geq 2T_0. \end{cases} \tag{3.29}$$

(iii) The boundary data $g \in H^{\frac{3}{2}}(\partial\Omega) \cap W^{1,\infty}(\partial\Omega)$ *and* $g \geq c_g > 0$.

(iv) The exact diffusion coefficient $D^\dagger \in \mathcal{A}_D \cap W^{1,\infty}(\Omega)$ *and the exact reaction coefficient* $\sigma^\dagger \in \mathcal{A}_\sigma$.

Under regularity Assumption 3.8, the parabolic equation (3.28) admits a unique solution $u \in L^\infty(0,T; W^{1,\infty}(\Omega))$. Moreover, the parabolic maximum principle [53, Section 7.1.4] implies that there exists a constant $\underline{c}_u$ depending on $D^\dagger$, $\sigma^\dagger$, g and Ω, but independent of f such that

$$u(x,t) \geq \underline{c}_u > 0, \quad \forall\, x,t \in \overline{\Omega} \times [0,T]. \tag{3.30}$$

3.3.1 Stability estimate

We first give *a priori* estimate which will be frequently used in the stability analysis. We denote $A = A(D^\dagger, \sigma^\dagger)$ be the realization of $-\nabla \cdot D^\dagger \nabla + \sigma^\dagger$ with a zero Dirichlet boundary condition. Note that the operator A satisfies the following resolvent estimate

$$\|(z + A)^{-1}\|_{L^p(\Omega)\to L^p(\Omega)} \le c(1 + |z|)^{-1}, \quad \forall z \in \Sigma_\phi, \tag{3.31}$$

where $\Sigma_\phi = \{0 \neq z \in \mathbb{C} : |\arg(z)| \le \phi\}$ with a fixed $\phi \in (\pi/2, \pi)$. If $D^\dagger \in \mathcal{A}_D$ and $\sigma^\dagger \in \mathcal{A}_\sigma$, then the resolvent estimate (3.31) with $p = 2$ holds for a constant c independent of $D^\dagger$ and $\sigma^\dagger$ (but depending on $\underline{c}_D$, $\bar{c}_D$ and $\bar{c}_\sigma$ in (3.3)). This could be easily proved by using a standard energy argument; see e.g., [139, p. 92]. Moreover, if $D^\dagger \in W^{1,\infty}(\Omega)$, then the resolvent estimate (3.31) holds for $p = \infty$ (cf. [137, Theorem 1], [14, Theorem 2.1] and [105, Appendix A]).

Then we introduce the solution operator

$$E(t) = \frac{1}{2\pi i} \int_{\Gamma_{\phi,\kappa}} e^{zt}(z + A)^{-1} \mathrm{d}z. \tag{3.32}$$

Here $\Gamma_{\phi,\kappa} = \{z \in \mathbb{C} : |z| = \kappa, |\arg(z)| \le \phi\} \cup \{z \in \mathbb{C} : z = \rho e^{i\phi}, \rho \ge \kappa\}$ with fixed constants $\kappa \in (0, \infty)$ and $\phi \in (\pi/2, \pi)$. Then the solution u to the parabolic problem (3.28) could be written as

$$u(t) = E(t)(u_0 - \bar{g}) + \int_0^t E(s) f(t - s) \mathrm{d}s, \tag{3.33}$$

where $\bar{g}$ satisfies elliptic equation $A\bar{g} = 0$ with Dirichlet boundary condition $\bar{g}|_{\partial\Omega} = g$. Under Assumption 3.8, by the elliptic regularity theory and maximum principle, $\bar{g} \in W^{1,\infty}(\Omega) \cap H^2(\Omega)$ and has a strictly positive lower bound.

Next, we provide a selection of valuable smoothing properties associated with the solution operator $E(t)$.

Lemma 3.4. *Let $E(t)$ be the solution opetator defined in* (3.32)*. Suppose that $D^\dagger \in \mathcal{A}_D$ and $\sigma^\dagger \in \mathcal{A}_\sigma$. Then there exists a constant c independent of $D^\dagger$ and $\sigma^\dagger$ (but depending on $\underline{c}_D$, $\bar{c}_D$ and $\bar{c}_\sigma$ in* (3.3)*) such that for any nonnegative integer ℓ,*

$$\|E^{(\ell)}(t)\|_{L^2(\Omega)\to L^2(\Omega)} \le c \min(t^{-\ell-1}, t^{-\ell}).$$

Moreover, if $D^\dagger \in W^{1,\infty}(\Omega)$, then there holds

$$\|E^{(\ell)}(t)\|_{L^\infty(\Omega)\to L^\infty(\Omega)} \le c \min(t^{-\ell-1}, t^{-\ell}).$$

Proof. The proof of the lemma follows by the contour integral (3.32) and the resolvent estimate (3.31). If $D^\dagger \in \mathcal{A}_D$ and $\sigma^\dagger \in \mathcal{A}_\sigma$, then the resolvent estimate (3.31) with $p = 2$ holds for a constant c depending

on $\underline{c}_D$, $\bar{c}_D$ and $\bar{c}_\sigma$ in (3.3). Then for $\ell \geq 0$ we have

$$\begin{aligned}\|E^{(\ell)}(t)\|_{L^2(\Omega)\to L^2(\Omega)} &\leq c\int_{\Gamma_{\phi,\kappa}} |z|^\ell |e^{zt}| \|(z+A)^{-1}\|_{L^2(\Omega)\to L^2(\Omega)} |\mathrm{d}z| \leq C\int_{\Gamma_{\phi,\kappa}} |e^{zt}||z|^\ell (1+|z|)^{-1}|\mathrm{d}z| \\ &\leq c\Big(\int_\kappa^\infty e^{-st\cos\phi}\frac{s^\ell}{s+1}\,\mathrm{d}s + \int_{-\phi}^{\phi} e^{-\kappa t\cos\psi}\frac{\kappa^{\ell+1}}{1+\kappa}\,\mathrm{d}\psi\Big) \leq c\min(t^{-\ell-1}, t^{-\ell}),\end{aligned}$$

where we take $\kappa = t^{-1}$ in the last inequality. The estimate in maximum-norm could be derived similarly using the resolvent estimate (3.31) with $p = \infty$. □

Lemma 3.4 immediately leads to the next lemma showing the decay properties of the solution.

Lemma 3.5. *Suppose that Assumption 3.8 (i)-(iii) holds valid. Let u be the solution of the parabolic problem* (3.28)*. If $D^\dagger \in \mathcal{A}_D$ and $\sigma^\dagger \in \mathcal{A}_\sigma$, then for $\ell = 1, \cdots, k+1$, there holds*

$$\|\partial_t^\ell u(t)\|_{L^2(\Omega)} \leq c\max(t^{-\ell}, 1), \quad \forall\ t \in (0,\infty).$$

Moreover, if $D^\dagger \in W^{1,\infty}(\Omega)$, then there holds

$$\|\partial_t u(t)\|_{L^\infty(\Omega)} \leq \begin{cases} ct^{-1}, & \forall\ t \in (0, T_0], \\ c(t-2T_0)^{-1}, & \forall\ t \in (2T_0, \infty). \end{cases}$$

Proof. By solution representation (3.33), we may write

$$\partial_t^\ell u(t) = E^{(\ell)}(t)(u_0 - \bar{g}) + \sum_{i=0}^{\ell-1} E^{(i)}(t) f^{(\ell-1-i)}(0) + \int_0^t E(s) f^{(\ell)}(t-s)\mathrm{d}s.$$

According to Assumption 3.8 (iii), we have $f^{(i)}(0) = 0$, $i = 1, \cdots, \ell-1$. Then Lemma 3.4 implies

$$\begin{aligned}\|\partial_t^\ell u(t)\|_{L^2(\Omega)} \leq& \|E^{(\ell)}(t)\|_{L^2(\Omega)\to L^2(\Omega)}\|u_0 - \bar{g}\|_{L^2(\Omega)} + \|E^{(\ell-1)}(t)\|_{L^2(\Omega)\to L^2(\Omega)}\|f(0)\|_{L^2(\Omega)} \\ &+ \int_0^t \|E(s)\|_{L^2(\Omega)\to L^2(\Omega)}\|f^{(\ell)}(t-s)\|_{L^2(\Omega)}\mathrm{d}s \\ \leq& ct^{-\ell} + ct^{-\ell+1} + c \leq c\max(t^{-\ell}, 1).\end{aligned}$$

Now we assume that $D^\dagger \in W^{1,\infty}(\Omega)$. Similarly, with solution representation (3.33), $\partial_t u$ could be written as

$$\partial_t u(t) = E'(t)(u_0 - \bar{g}) + E(t)f(0) + \int_0^t E(s)\partial_t f(t-s)\mathrm{d}s.$$

For any $t \in (0, T_0]$, we recall that $\partial_t f = 0$ according to Assumption 3.8. Then the regularity of problem data in Assumption 3.8 and Lemma 3.4 lead to

$$\|\partial_t u(t)\|_{L^\infty(\Omega)} \leq \|E'(t)\|_{L^\infty(\Omega)\to L^\infty(\Omega)}\|u_0 - \bar{g}\|_{L^\infty(\Omega)} + \|E(t)\|_{L^\infty(\Omega)\to L^\infty(\Omega)}\|f(0)\|_{L^\infty(\Omega)} \leq ct^{-1}.$$

Next, we turn to the case that $t \in (2T_0, \infty)$. Assumption 3.8 leads to $\partial_t f \neq 0$ for $t \in (T_0, 2T_0)$ and $\partial_t f \equiv 0$ otherwise. Then Lemma 3.4 yields

$$\begin{aligned}\|\partial_t u(t)\|_{L^\infty(\Omega)} \leq & \|E'(t)\|_{L^\infty(\Omega)\to L^\infty(\Omega)}\|u_0 - \bar{g}\|_{L^\infty(\Omega)} + \|E(t)\|_{L^\infty(\Omega)\to L^\infty(\Omega)}\|f(0)\|_{L^\infty(\Omega)} \\ & + \int_0^t \|E(s)\|_{L^\infty(\Omega)\to L^\infty(\Omega)}\|\partial_t f(t-s)\|_{L^\infty(\Omega)}\mathrm{d}s \\ \leq & Ct^{-1} + C\int_{t-2T_0}^{t-T_0} s^{-1}\mathrm{d}s \leq C(t-2T_0)^{-1}.\end{aligned}$$

This completes the proof of the lemma. □

The stability estimation follows a similar approach to that of the elliptic case. First, we decouple the parameters, and then sequentially determine the stability for the diffusion coefficient D and the reaction coefficient σ. To achieve this, we select time intervals such that $0 < T_1 \leq T_0$ and $T_2 \geq 2T_0$. Multiplying the equation at time T_1 by $u(T_2)$ and at time T_2 by $u(T_1)$, after subtracting the two equations, we can eliminate the reaction coefficient σ and obtain

$$\begin{cases} -\nabla\cdot\left(Du^2(T_1)\nabla\left(\dfrac{u(T_2)}{u(T_1)} - 1\right)\right) = (f(T_2) - \partial_t u(T_2))u(T_1) - (f(T_1) - \partial_t u(T_1))u(T_2), & \text{in } \Omega, \\ \dfrac{u(T_2)}{u(T_1)} - 1 = 0, \quad \text{on } \partial\Omega. \end{cases} \tag{3.34}$$

For ease of reference, let's introduce the following notation:

$$w := \frac{u(T_2)}{u(T_1)} - 1, \quad q := D|u(T_1)|^2 \quad \text{and} \quad F := (f(T_2) - \partial_t u(T_2))u(T_1) - (f(T_1) - \partial_t u(T_1))u(T_2). \tag{3.35}$$

Then the system (3.34) could be written as the form (3.9). Therefore, the following result is an immediate application of Theorem 3.3 and we omit the proof.

Assumption 3.9. *The exact diffusion coefficient $q^\dagger = D^\dagger|u(T_1)|^2 \in H^2(\Omega)\cap W^{1,\infty}(\Omega)\cap\mathcal{A}_q$ and source term $F = (f(T_2) - \partial_t u(T_2))u(T_1) - (f(T_1) - \partial_t u(T_1))u(T_2) \in L^\infty(\Omega)$.*

Theorem 3.10. *Suppose that F, $\widetilde{F} \in L^\infty(\Omega)$, q satisfy Assumption 3.9 and $\widetilde{q} \in \mathcal{A}_q$. Also, suppose the $H^1(\Omega)$-norm of q and $\widetilde{q}$ are bounded by a generic constant c. Let w be the solution of (3.34) with diffusion coefficient q and source F, while $\widetilde{w}$ be the solution with diffusion coefficient $\widetilde{q}$ and source $\widetilde{F}$. Then there holds*

$$\int_\Omega \frac{(q-\widetilde{q})^2}{q^2}\left(q\,|\nabla w|^2 + Fw\right)\mathrm{d}x \leq c\left(\|w - \widetilde{w}\|_{H^1(\Omega)} + \|F - \widetilde{F}\|_{L^2(\Omega)}\right).$$

Moreover, if the following positive condition holds

$$q\,|\nabla w|^2 + Fw \geq c\,\mathrm{dist}(x, \partial\Omega)^\beta \quad \textit{a.e. on } \Omega \tag{3.36}$$

for some $\beta \geq 0$ and $c > 0$. Then the following estimate holds

$$\|q - \widetilde{q}\|_{L^2(\Omega)} \leq c\left(\|w - \widetilde{w}\|_{H^1(\Omega)} + \|F - \widetilde{F}\|_{L^2(\Omega)}\right)^{\frac{1}{2(1+\beta)}}.$$

Remark 3.6. *As suggested in Section 1.2, the crucial aspect to ensure the positivity condition in* (3.36) *is to establish the strict positivity of the function F. It is worth noting that F contains the time derivative term $\partial_t u$, making the positive condition more intricate than that presented in Section 1.2. Therefore, a careful examination is required. Next, we demonstrate that the positive condition holds valid under certain specific excitations f and g.*

We claim that the function F in (3.35) *could be strictly positive provided some restrictions on excitation f and g. For example, with Assumption 3.8, we take a time dependent source term*

$$f(x,t) = \begin{cases} 0, & 0 < t \le T_0, \\ c_f, & t > 2T_0, \end{cases}$$

for some T_0. Here we assume that T_0 is sufficient large, $T_1 = T_0$, and $T_2 = 3T_0$. As a result, according to Lemma 3.5, $\|\partial_t u(T_1)\|_{L^\infty(\Omega)} + \|\partial_t u(T_2)\|_{L^\infty(\Omega)} \le CT_0^{-1}$. Since u has a strict positive lower bound (3.30) *and $\|u(t)\|_{L^\infty(\Omega)} \le c$ uniform in t, we conclude that for sufficiently large T_0,*

$$F \ge c_f \underline{c}_u - T_0^{-1}(\underline{c}_u + \|u(T_2)\|_{L^\infty(\Omega)}) > c_F > 0.$$

Then the positivity condition (3.36) *holds valid for some $\beta \in [0,2]$.*

The following corollary gives the estimate of $\|F - \widetilde{F}\|_{L^2(\Omega)}$ and hence the estimate of $\|D - \widetilde{D}\|_{L^2(\Omega)}$.

Corollary 3.2. *Suppose that Assumption 3.8 holds valid, $\widetilde{D} \in \mathcal{A}_D$ and $\sigma \in \mathcal{A}_\sigma$. Let u ($\widetilde{u}$) be the solution to the parabolic equation* (3.4) *with diffusion coefficient D ($\widetilde{D}$), reaction coefficient σ ($\widetilde{\sigma}$), the boundary data g and source f. Let $D \in W^{1,\infty}(\Omega) \cap \mathcal{A}_D$, $\sigma \in L^\infty(\Omega) \cap \mathcal{A}_\sigma$. Assume that $\|\widetilde{u}(T_i)\|_{L^2(\Omega)} \le c$ for $i = 1, 2$. Then there holds*

$$\|F - \widetilde{F}\|_{L^2(\Omega)} \le c\Big(\sum_{i=1}^{2} \|u - \widetilde{u}\|_{L^\infty(T_i - \theta, T_i; L^2(\Omega))} \Big)^{\frac{k}{k+1}},$$

where k is the regularity of source f given in Assumption 3.8 (ii). If in addition, the positive condition (3.36) *holds for some $\beta \ge 0$, then*

$$\|D - \widetilde{D}\|_{L^2(\Omega)} \le c \left(\sum_{i=1}^{2} \|(u - \widetilde{u})(T_i)\|_{H^1(\Omega)} + \Big(\sum_{i=1}^{2} \|u - \widetilde{u}\|_{L^\infty(T_i - \theta, T_i; L^2(\Omega))} \Big)^{\frac{k}{k+1}} \right)^{\frac{1}{2(1+\beta)}}.$$

Proof. By definition in (3.35), $F - \widetilde{F}$ can be written as

$$\begin{aligned} F - \widetilde{F} = {} & f(T_2)\,(u(T_1) - \widetilde{u}(T_1)) + f(T_1)\,(\widetilde{u}(T_2) - u(T_2)) \\ & + u(T_2)\partial_t u(T_1) - \widetilde{u}(T_2)\partial_t \widetilde{u}(T_1) + \widetilde{u}(T_1)\partial_t \widetilde{u}(T_2) - u(T_1)\partial_t u(T_2). \end{aligned}$$

The first two terms can be easily bounded by

$$\|f(T_2)\,(u(T_1) - \widetilde{u}(T_1)) + f(T_1)\,(\widetilde{u}(T_2) - u(T_2))\,\|_{L^2(\Omega)} \le c \sum_{i=1}^{2} \|(u - \widetilde{u})(T_i)\|_{L^2(\Omega)}.$$

Inserting an intermediate term $\widetilde{u}(T_2)\partial_t u(T_1)$, we have

$$\begin{aligned}\|u(T_2)\partial_t u(T_1) - \widetilde{u}(T_2)\partial_t\widetilde{u}(T_1)\|_{L^2(\Omega)} \leq \|\widetilde{u}(T_2)\|_{L^\infty(\Omega)}\|\partial_t u(T_1) - \partial_t\widetilde{u}(T_1)\|_{L^2(\Omega)} \\ + \|\partial_t u(T_1)\|_{L^\infty(\Omega)}\|u(T_2) - \widetilde{u}(T_2)\|_{L^2(\Omega)}.\end{aligned}$$

By assumption, we have $\|\widetilde{u}(T_2)\|_{L^\infty(\Omega)} \leq c$. Meanwhile, Lemma 3.5 implies $\|\partial_t u(T_1)\|_{L^\infty(\Omega)} \leq cT_1^{-1} \leq c$. These together imply

$$\|u(T_2)\partial_t u(T_1) - \widetilde{u}(T_2)\partial_t\widetilde{u}(T_1)\|_{L^2(\Omega)} \leq c\left(\|\partial_t u(T_1) - \partial_t\widetilde{u}(T_1)\|_{L^2(\Omega)} + \|u(T_2) - \widetilde{u}(T_2)\|_{L^2(\Omega)}\right).$$

To analyze the term $\|\partial_t u(T_1) - \partial_t\widetilde{u}(T_1)\|_{L^2(\Omega)}$, we insert the backward difference quotient of order k,

$$\partial_\tau u(T_1) = \tau^{-1}\sum_{j=0}^{k} a_j u(T_1 - j\tau) \quad \text{and} \quad \partial_\tau\widetilde{u}(T_1) = \tau^{-1}\sum_{j=0}^{k} a_j\widetilde{u}(T_1 - j\tau),$$

for some $0 < \tau < \theta/k$, where $\{a_j\}_{j=1}^k$ are backward difference quotient coefficients. By Lemma 3.5, we have $\|\partial_t^{k+1}u\|_{L^\infty(T_1-\theta,T_1;L^2(\Omega))} \leq c$, and hence by Taylor's expansion we obtain

$$\|\partial_t u(T_1) - \partial_\tau u(T_1)\|_{L^2(\Omega)} \leq c\tau^k\|\partial_t^{k+1}u\|_{L^\infty(T_1-\theta,T_1;L^2(\Omega))} \leq c\tau^k. \tag{3.37}$$

Then we obtain

$$\|u(T_2)\partial_t u(T_1) - \widetilde{u}(T_2)\partial_t\widetilde{u}(T_1)\|_{L^2(\Omega)} \leq c\left(\tau^k + \tau^{-1}\|u - \widetilde{u}\|_{L^\infty(T_1-\theta,T_1;L^2(\Omega))} + \|(u-\widetilde{u})(T_2)\|_{L^2(\Omega)}\right).$$

The bound for $\|u(T_1)\partial_t u(T_2) - \widetilde{u}(T_1)\partial_t\widetilde{u}(T_2)\|_{L^2(\Omega)}$ can be obtained similarly. Consequently, we arrive at

$$\|F - \widetilde{F}\|_{L^2(\Omega)} \leq c\Big(\tau^k + \tau^{-1}\sum_{i=1}^{2}\|u - \widetilde{u}\|_{L^\infty(T_i-\theta,T_i;L^2(\Omega))}\Big).$$

If $\sum_{i=1}^2\|u - \widetilde{u}\|_{L^\infty(T_i-\theta,T_i;L^2(\Omega))} \leq (\theta/k)^{k+1}$, then the choice $\tau = \left(\sum_{i=1}^2\|u - \widetilde{u}\|_{L^\infty(T_i-\theta,T_i;L^2(\Omega))}\right)^{\frac{1}{k+1}}$ leads to the desired estimate. Otherwise, it suffices to take $\tau = \theta/(2k)$ and derive

$$\begin{aligned}\|F - \widetilde{F}\|_{L^2(\Omega)} \leq & c\Big(\theta^k + \theta^{-1}\sum_{i=1}^{2}\|u - \widetilde{u}\|_{L^\infty(T_i-\theta,T_i;L^2(\Omega))}\Big) \leq c\theta^{-1}\Big(\theta^{k+1} + \sum_{i=1}^{2}\|u - \widetilde{u}\|_{L^\infty(T_i-\theta,T_i;L^2(\Omega))}\Big) \\ \leq & c\sum_{i=1}^{2}\|u - \widetilde{u}\|_{L^\infty(T_i-\theta,T_i;L^2(\Omega))} \leq c\Big(\sum_{i=1}^{2}\|u - \widetilde{u}\|_{L^\infty(T_i-\theta,T_i;L^2(\Omega))}\Big)^{\frac{k}{k+1}},\end{aligned}$$

where we use the fact that θ and k are constants and the *a priori* bound $\|u - \widetilde{u}\|_{L^\infty(T_i-\theta,T_i;L^2(\Omega))} \leq c$.

The second assertion of the corollary is a direct consequence of applying Theorem 3.10. □

Having obtained the reconstructed conductivity, we can now proceed to recover the reaction coefficient. The subsequent theorem offers conditional stability for the parameter's recovery.

Theorem 3.11. *Let the assumptions in Corollary 3.2 hold true. Then there holds*

$$\|(\sigma-\widetilde{\sigma})(u(T_2)-u(T_1))\|_{L^2(\Omega)}$$
$$\leq c\left(\Big(\sum_{i=1}^{2}\|u-\widetilde{u}\|_{L^\infty(T_i-\theta,T_i;L^2(\Omega))}\Big)^{\frac{2k}{k+1}}+\sum_{i=1}^{2}\|(u-\widetilde{u})(T_i)\|_{H^1(\Omega)}+\|D-\widetilde{D}\|_{L^2(\Omega)}\right)^{\frac{1}{2}}.$$

Proof. Letting $\zeta=u(T_2)-u(T_1)$ and choosing a test function $v\in H_0^1(\Omega)$, we have

$$((\sigma-\widetilde{\sigma})\zeta,v)=(\widetilde{D}\nabla\widetilde{\zeta}-D\nabla\zeta,\nabla v)+(\widetilde{\sigma}(\widetilde{\zeta}-\zeta),v)+\sum_{i=1}^{2}(\partial_t(\widetilde{u}-u)(T_1),v).$$

Now we take $v=(\sigma-\widetilde{\sigma})\zeta$ and note that $\|\nabla v\|_{L^2(\Omega)}\leq c$. Then we obtain

$$\begin{aligned}\|v\|_{L^2(\Omega)}^2\leq& c\Big(\|\zeta-\widetilde{\zeta}\|_{H^1(\Omega)}+\|D-\widetilde{D}\|_{L^2(\Omega)}+\|\widetilde{\zeta}-\zeta\|_{L^2(\Omega)}\|v\|_{L^2(\Omega)}\\&+\sum_{i=1}^{2}\|\partial_t(\widetilde{u}-u)(T_i)\|_{L^2(\Omega)}\|v\|_{L^2(\Omega)}\Big).\end{aligned}$$

Using the argument in the proof of Corollary 3.2, we use backward difference quotient to estimate $\|\partial_t(\widetilde{u}-u)(T_i)\|_{L^2(\Omega)}$ and obtain

$$\sum_{i=1}^{2}\|\partial_t(\widetilde{u}-u)(T_i)\|_{L^2(\Omega)}\leq\Big(\sum_{i=1}^{2}\|u-\widetilde{u}\|_{L^\infty(T_i-\theta,T_i;L^2(\Omega))}\Big)^{\frac{k}{k+1}}.$$

As a result, we conclude that

$$\|v\|_{L^2(\Omega)}^2\leq c\Big(\sum_{i=1}^{2}\|(u-\widetilde{u})(T_i)\|_{H^1(\Omega)}+\|D-\widetilde{D}\|_{L^2(\Omega)}+\Big(\sum_{i=1}^{2}\|u-\widetilde{u}\|_{L^\infty(T_i-\theta,T_i;L^2(\Omega))}\Big)^{\frac{2k}{k+1}}\Big).$$

This completes the proof of the theorem. □

Remark 3.7. *Similar as in Theorem 3.4, for any compact subset $\Omega'\Subset\Omega$ with $\operatorname{dist}(\overline{\Omega'},\partial\Omega)>0$, we can obtain the bound for $\|\sigma-\widetilde{\sigma}\|_{L^2(\Omega')}$, if $\zeta=u(T_2)-u(T_1)\geq C>0$ in Ω'. This condition can be achieved by following choice of data: we take $f_2-f_1\geq c_f>0$ in (3.29), $T_1=T_0$, $T_2=3T_0$, with T_0 sufficiently large. Then ζ satisfies the elliptic equation with source $F=f_2-f_1+\partial_t u(T_1)-\partial_t u(T_2)$. According to Lemma 3.5, there holds $\|\partial_t u(T_1)\|_{L^\infty(\Omega)}+\|\partial_t u(T_2)\|_{L^\infty(\Omega)}\leq cT_0^{-1}$, we conclude that $F\geq c_f-cT_0^{-1}$ is strictly positive when T_0 is sufficiently large. Consequently, the strong maximum principle [141, Theorem 1] implies $\zeta\geq c>0$ in Ω' and hence*

$$\|\sigma-\widetilde{\sigma}\|_{L^2(\Omega')}\leq c\Big(\big(\sum_{i=1}^{2}\|u-\widetilde{u}\|_{L^\infty(T_i-\theta,T_i;L^2(\Omega))}\big)^{\frac{2k}{k+1}}+\sum_{i=1}^{2}\|(u-\widetilde{u})(T_i)\|_{H^1(\Omega)}+\|D-\widetilde{D}\|_{L^2(\Omega)}\Big)^{\frac{1}{2}}.$$

Remark 3.8. *Throughout we assume that g is time-independent in order to have the relation that*

$$w(x)=\frac{u(T_2,x)}{u(T_1,x)}-1=0\quad\text{for all}\ \ x\in\partial\Omega.$$

The zero boundary condition of w is very crucial in the stability analysis and the error analysis of numerical recovery. For boundary data $g(x,t)$ that varies with time, we would need to impose the condition that $D=\widetilde{D}$ and $\sigma=\widetilde{\sigma}$ on $\partial\Omega$ to ensure the applicability of our current argument.

3.3.2 Numerical scheme and error analysis

In this part, we present the numerical scheme for the reconstruction of diffusion coefficient and reaction coefficient. First of all, we use the system (3.34) to recover the diffusion coefficient without the knowledge of reaction coefficient. Denote the exact solution $u^\dagger(x,t) := u(x,t;D^\dagger,\sigma^\dagger)$ and define

$$w^\dagger = \frac{u(T_1)}{u(T_2)} - 1 \quad \text{and} \quad w^\delta = \frac{z^\delta(T_1)}{z^\delta(T_2)} - 1.$$

Recall that the exact solution $u^\dagger$ is strictly positive, cf. (3.30). Then for ease of simplicity, we assume that z^δ are strictly positive in $\overline{\Omega}$. Moreover, we assume that

$$\|z^\delta\|_{C((T_i-\theta_i,T];L^\infty(\Omega))} \le c, \tag{3.38}$$

with some generic constant c. Then it is easy to observe

$$\|w^\delta - w^\dagger\| \le c\delta.$$

Moreover, we take

$$F^\delta = \Big(f(T_2) - \partial_\tau z^\delta(T_2)\Big)\, z^\delta(T_1) - \Big(f(T_1) - \partial_\tau z^\delta(T_1)\Big)\, z^\delta(T_2),$$

where ∂_τ denote backward difference quotient of orde k for some $0 < \tau < \theta/k$. We apply the following output least squares formulation

$$\min_{q_{h_1}\in\mathcal{A}_{q,h_1}} J_{\gamma_1,h_1}(q_{h_1}) = \frac{1}{2}\|w_{h_1}(q_{h_1}) - w^\delta\|^2_{L^2(\Omega)} + \frac{\gamma_1}{2}\|\nabla q_{h_1}\|^2_{L^2(\Omega)} \tag{3.39}$$

where $w_{h_1}(q_{h_1}) \in V^0_{h_1}$ is a weak solution of

$$(q_{h_1}\nabla w_{h_1}, \nabla v_{h_1}) = (F^\delta, v_{h_1}), \quad \forall v_{h_1} \in V^0_{h_1}. \tag{3.40}$$

The following theorem is a direct consequence of Theorem 3.5.

Theorem 3.12. *Suppose Assumptions 3.8 and 3.9 hold. Let $q^\dagger = D^\dagger|u^\dagger(T_1)|^2 \in \mathcal{A}_q$ be the exact parameter in the elliptic equation (3.34), $w(q^\dagger)$ be the exact solution, and $q^*_{h_1} \in \mathcal{A}_{q,h}$ be a minimizer of problem (3.39)-(3.40). Then with $\eta = h_1^2 + \delta + \tau^k + \delta\tau^{-1} + \gamma_1^{\frac{1}{2}}$, there holds*

$$\int_\Omega \Big(\frac{q^\dagger - q^*_{h_1}}{q^\dagger}\Big)^2 \big(q^\dagger|\nabla w(q^\dagger)|^2 + Fw(q^\dagger)\big)\mathrm{d}x \le c\Big(\big(h_1\eta\gamma_1^{-\frac{1}{2}} + \min(h_1 + h_1^{-1}\eta, 1)\big)\eta\gamma_1^{-\frac{1}{2}} + \delta + \tau^k + \delta\tau^{-1}\Big).$$

Moreover, if the following positive condition (3.36) holds for $\beta \ge 0$, we have

$$\|q^\dagger - q^*_{h_1}\|_{L^2(\Omega)} \le c\left(\left(h_1\eta\gamma_1^{-\frac{1}{2}} + \min(h_1 + h_1^{-1}\eta, 1)\right)\eta\gamma_1^{-\frac{1}{2}} + \delta + \tau^k + \delta\tau^{-1}\right)^{\frac{1}{2(1+\beta)}}.$$

Proof. The proof closely resembles that of Theorem 3.5, with the primary distinction being the estimation of $F - F^\delta$. More specifically, we obtain

$$\begin{aligned}\|F - F^\delta\|_{L^2(\Omega)} &= \|f(T_2)\big(u(T_1) - z^\delta(T_1)\big)\|_{L^2(\Omega)} + \|f(T_1)\big(u(T_2) - z^\delta(T_2)\big)\|_{L^2(\Omega)} \\ &\quad + \|\partial_t u(T_1)u(T_2) - \partial_\tau z^\delta(T_1)z^\delta(T_2)\|_{L^2(\Omega)} + \|\partial_t u(T_2)u(T_1) - \partial_\tau z^\delta(T_2)z^\delta(T_1)\|_{L^2(\Omega)} \\ &\le c\delta + \|\partial_t u(T_1)u(T_2) - \partial_\tau z^\delta(T_1)z^\delta(T_2)\|_{L^2(\Omega)} + \|\partial_t u(T_2)u(T_1) - \partial_\tau z^\delta(T_2)z^\delta(T_1)\|_{L^2(\Omega)}.\end{aligned}$$

Then it suffices to bound the second term, and then the third term follows analogously. Inserting the terms $\partial_\tau u(T_1)u(T_2)$ and $\partial_\tau u(T_1)z^\delta(T_2)$, we have

$$\begin{aligned}&\|\partial_t u(T_1)u(T_2) - \partial_\tau z^\delta(T_1)z^\delta(T_2)\|_{L^2(\Omega)} \\ &\le \|\partial_t u(T_1)u(T_2) - \partial_\tau u(T_1)u(T_2)\|_{L^2(\Omega)} + \|\partial_\tau u(T_1)u(T_2) - \partial_\tau u(T_1)z^\delta(T_2)\|_{L^2(\Omega)} \\ &+ \|\partial_\tau u(T_1)z^\delta(T_2) - \partial_\tau z^\delta(T_1)z^\delta(T_2)\|_{L^2(\Omega)} = \sum_{j=1}^3 \mathrm{I}_j.\end{aligned}$$

By Lemma 3.5, we observe that $\|\partial_t^{k+1}u\|_{L^\infty(T_i-\theta,T_i;L^2(\Omega))} + \|u(T_i)\|_{L^\infty(\Omega)} \le c$ and hence we apply the estimate (3.37) to obtain

$$\mathrm{I}_1 \le \|\partial_t u(T_1) - \partial_\tau u(T_1)\|_{L^2(\Omega)}\|u(T_2)\|_{L^\infty(\Omega)} \le c\tau^k \|\partial_t^{k+1}u\|_{L^\infty(T_1-\theta,T_1;L^2(\Omega))}\|u(T_2)\|_{L^\infty(\Omega)} \le c\tau^k.$$

For the second term, we apply Lemma 3.5 and the assumption (3.5) to obtain

$$\mathrm{I}_2 \le \|\partial_\tau u(T_1)\|_{L^\infty(\Omega)}\|u(T_2) - z^\delta\|_{L^2(\Omega)} \le c\delta\tau^{-1}\int_{T_1-\theta}^{T_1} \|u_t(t)\|_{L^\infty(\Omega)}\,\mathrm{d}t \le c\delta\tau^{-1}.$$

Finally, for the term I_3, we use the assumption (3.5) and (3.38) to derive

$$\begin{aligned}\mathrm{I}_3 &\le \|\partial_\tau u(T_1)z^\delta(T_2) - \partial_\tau z^\delta(T_1)z^\delta(T_2)\|_{L^2(\Omega)} \\ &\le c\|\partial_\tau(u(T_1) - z^\delta(T_1))\|_{L^2(\Omega)}\|z^\delta(T_2)\|_{L^\infty(\Omega)} \le c\delta\tau^{-1}.\end{aligned}$$

Consequently, we arrive at

$$\|F - F^\delta\|_{L^2(\Omega)} \le c(\delta + \tau^k + \delta\tau^{-1}).$$

The proof that follows simply involves substituting $\|F - F^\delta\|_{L^2(\Omega)}$ in Theorem 3.5 with the newly established error bound. As such, we omit this largely redundant proof. □

Remark 3.9. *In Theorem 3.12, the choice $\tau \sim \delta^{\frac{1}{k+1}}$ implies that $\|F - F^\delta\|_{L^2(\Omega)} \le c\delta^{\frac{k}{k+1}}$. With a priori choice of the algorithmic parameters: $h_1 \sim \delta^{\frac{k}{2(k+1)}}$, $\gamma_1 \sim \delta^{\frac{2k}{k+1}}$. Under the positivity condition* (3.36) *with $\beta \ge 0$, there holds the estimate*

$$\|D^\dagger - D_{h_1}^*\|_{L^2(\Omega)} \le c\,\delta^{\frac{k}{4(1+\beta)(k+1)}}.$$

When f is smooth over time, the optimal order is nearly $(4(1+\beta))^{-1}$. This estimation aligns with the one given in the elliptic case, as detailed in Remark 3.2.

Now we turn to the reconstruction formula of reaction coefficient $\sigma^\dagger$ and study the approximation error. Let $\zeta = u(T_1) - u(T_2)$ which is a solution to the elliptic problem

$$\begin{cases} -\nabla \cdot (D\nabla\zeta) + \sigma\zeta = f(T_1) - f(T_2) + \partial_t u(T_2) - \partial_t u(T_1), & \text{in } \Omega, \\ \zeta = 0, & \text{on } \partial\Omega. \end{cases} \tag{3.41}$$

The noisy observational data for equation (3.41) is $\zeta^\delta = z^\delta(T_2) - z^\delta(T_1)$ satisfying $\|\zeta - \zeta^\delta\|_{L^2(\Omega)} \le c\delta$. We consider following least-squares formulation

$$\min_{\sigma_{h_2}\in\mathcal{A}_{\sigma,h_2}} \mathcal{J}_{\gamma_2,h_2}(\sigma_{h_2}) = \frac{1}{2}\|\zeta_{h_2}(\sigma_{h_2}) - \zeta^\delta\|^2_{L^2(\Omega)} + \frac{\gamma_2}{2}\|\nabla\sigma_{h_2}\|^2_{L^2(\Omega)} \tag{3.42}$$

where $\mathcal{A}_{\sigma,h_2} = \mathcal{A}_\sigma \cap V_{h_2}$ and $\zeta_{h_2}(\sigma_{h_2}) \in V^0_{h_2}$ is the solution to the finite dimensional problem

$$(D^*_{h_1}\nabla\zeta_{h_2}, \nabla v_{h_2}) + (\sigma_{h_2}\zeta_{h_2}, v_{h_2}) = (f(T_1) - f(T_2) + \partial_\tau z^\delta(T_2) - \partial_\tau z^\delta(T_1), v_{h_2}), \quad \forall v_{h_2} \in V^0_{h_2}, \tag{3.43}$$

where ∂_τ denote backward difference quotient of orde k for some $0 < \tau < \theta/k$. Similar as Section 3.2, we use h_2 to denote the different spatial mesh size. Here ∂_τ denotes the difference quotient as the discretized scheme (3.40) and $D^*_{h_1}$ is the diffusion coefficient we reconstructed in previous step with *a priori* estimate

$$\|D^*_{h_1} - D^\dagger\|_{L^2(\Omega)} \le \epsilon \qquad \text{with } \epsilon = c\delta^{\frac{k}{4(1+\beta)(k+1)}}.$$

The subsequent result offers an error estimation for $\sigma_{h_2} - \sigma^\dagger$. Given that the proof parallels that of Theorem 3.7, we have decided not to reproduce it here.

Theorem 3.13. *Suppose Assumptions 3.8 and 3.6 holds, $D^\dagger \in \mathcal{A}_D \cap W^{1,\infty}(\Omega)$ and $\|D^*_{h_1} - D^\dagger\|_{L^2(\Omega)} \le \epsilon$. Let $\zeta(\sigma^\dagger)$ be the solution to equation* (3.41)*, while $\sigma^*_{h_2}$ be the minimizer of* (3.42)-(3.43)*. Then with $\eta = h_2^2 + \epsilon + (\tau^k + \delta\tau^{-1})^2 + \sqrt{\gamma_2}$, there holds*

$$\|(\sigma^\dagger - \sigma^*_{h_2})\zeta(\sigma^\dagger)\|_{L^2(\Omega)} \le c\left(h_2\gamma_2^{-\frac{1}{2}}\eta + \eta + \tau^k + \delta\tau^{-1} + \left(\gamma_2^{-\frac{1}{2}}\eta(\min\{h_2 + h_2^{-1}\eta, 1\} + \epsilon)\right)^{\frac{1}{2}}\right).$$

Moreover, if $f_2 - f_1 \ge c > 0$ a.e. in Ω, $T_1 = T_0$ and $T_2 = 3T_0$ with T_0 being sufficiently large, then for any $\Omega' \Subset \Omega$, there exists a constant c depending on $\operatorname{dist}(\Omega', \partial\Omega)$*, f, g, u_0, $D^\dagger$ and $\sigma^\dagger$, such that*

$$\|(\sigma^\dagger - \sigma^*_{h_2}\|_{L^2(\Omega')} \le c\left(h_2\gamma_2^{-\frac{1}{2}}\eta + \eta + \tau^k + \delta\tau^{-1} + \left(\gamma_2^{-\frac{1}{2}}\eta(\min\{h_2 + h_2^{-1}\eta, 1\} + \epsilon)\right)^{\frac{1}{2}}\right).$$

Remark 3.10. *According to Theorem 3.5 and Remark 3.2, we have*

$$\|D^*_{h_1} - D^\dagger\| \le \epsilon = c\,\delta^{\frac{k}{4(1+\beta)(k+1)}},$$

provided that $h \sim \delta^{\frac{k}{2(k+1)}}$, $\gamma_1 \sim \delta^{\frac{2k}{k+1}}$ and the positivity condition (3.11) *is valid with $\beta \in [0, 2]$. As a result, with the choice of parameters $h_2 \sim \epsilon^{\frac{1}{2}}, \gamma_2 \sim \epsilon^2, \tau \sim \delta^{\frac{1}{k+1}}$, there holds the estimate*

$$\|(\sigma^\dagger - \sigma^*_{h_2})\zeta(\sigma^\dagger)\|_{L^2(\Omega)} \le c\,\delta^{\frac{k}{8(1+\beta)(k+1)}}.$$

Finally, if $f_2 - f_1 \geq c > 0$ *a.e. in* Ω, $T_1 = T_0$ *and* $T_2 = 3T_0$ *with* T_0 *being sufficiently large, then*

$$\|\sigma^\dagger - \sigma^*_{h_2}\|_{L^2(\Omega')} \leq c\,\delta^{\frac{k}{8(1+\beta)(k+1)}},$$

where $\Omega' \Subset \Omega$ *and the constant* c *depending on* $\mathrm{dist}(\Omega', \partial\Omega)$, f, g, u_0, $D^\dagger$ *and* $\sigma^\dagger$.

3.4 Numerical results

In this section, we present empirical results that demonstrate the precision of our proposed decoupled numerical algorithm. The reconstruction accuracy is measured in relatively $L^2(\Omega)$ error:

$$e_D = \|D^*_{h_1} - D^\dagger\|_{L^2(\Omega)}/\|D^\dagger\|_{L^2(\Omega)} \quad \text{and} \quad e_\sigma = \|\sigma^*_{h_2} - \sigma^\dagger\|_{L^2(\Omega)}/\|\sigma^\dagger\|_{L^2(\Omega)}.$$

To begin with, we present numerical results for one- and two-dimensional elliptic equations.

Example 3.1. $\Omega = (0,1)$, $D^\dagger(x) = 2 + \sin(2\pi x)$, $\sigma^\dagger(x) = 1 + x(1-x)$. *The boundary is* $g \equiv 1$ *and the two sources are given by* $f_1 \equiv 1$ *and* $f_2 \equiv 10$.

Table 3.1: Examples 3.1 and 3.2: convergence with respect to δ.

	(a) Example 3.1					(b) Example 3.2				
δ	1e-2	5e-3	1e-3	5e-4	1e-4	1e-2	5e-3	1e-3	5e-4	1e-4
e_D	4.87e-2	3.51e-2	1.73e-2	7.12e-3	4.67e-3	1.29e-1	6.34e-2	3.20e-2	1.95e-2	1.14e-2
e_σ	1.78e-2	1.73e-2	1.61e-2	1.00e-2	9.24e-3	7.70e-2	3.55e-2	3.12e-2	2.23e-2	2.13e-2

The results of the reconstruction at different noise levels can be seen in Figure 3.1, while the relative errors are displayed in Table 3.1. For different noise level δ, we adopt the regularization parameter γ_1 and mesh size h as $\gamma_1 = C_{\gamma_1}\delta^2$ and $h_1 = C_{h_1}\delta^{\frac{1}{2}}$ respectively. This choice is guided by the recommendations made in Remark 3.2 for the reconstruction of $D^\dagger$. Next, in the process of reconstructing $\sigma^\dagger$, we follow the guidelines provided in Remark 3.3. Specifically, we assign values to γ_2 and h_2 as $\gamma_2 = C_{\gamma_2}\epsilon^2$ and $h_2 = C_{h_2}\epsilon^{\frac{1}{2}}$ respectively. Here, ϵ represents the empirical convergence rates observed in our experiments. The constant C_{γ_1}, C_{h_1}, C_{γ_2} and C_{h_2} are determined by a trial and error way. For reconstruction of $D^\dagger$, we initially take $\gamma_1 =$ 1e-6 and $h_1 = 1/16$. The numerical results indicate that the error e_D decays to zero as the noise level tends to zero, with rate $O(\delta^{0.52})$. For reconstruction of reaction coefficient $\sigma^\dagger$, we initially take $\gamma_2 =$ 1e-5 and $h_2 = 1/16$ and observe a convergence rate $O(\delta^{0.18})$. It's important to note, as discussed in Remark 3.1, that the predicted rate for $D^\dagger$ is $O(\delta^{1/4})$, which is significantly lower than the empirically observed rate. Moreover, with the empirical rate $\gamma = 0.52$, the predicted rate for $\sigma^\dagger$ is expected to be $O(\delta^{0.26})$ as noted in Remark 3.2.

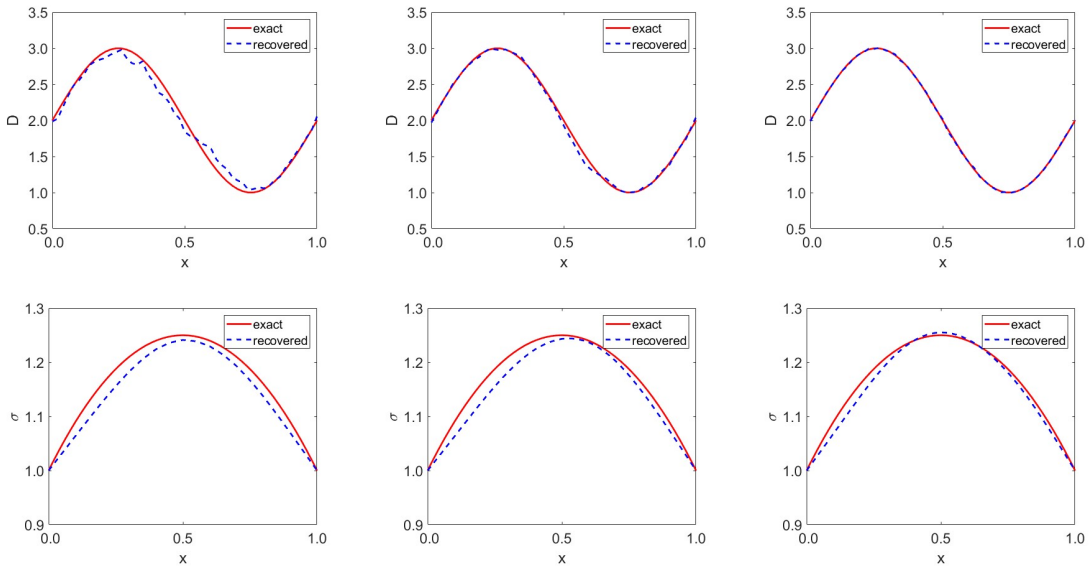

(a) $\delta =$ 1e-2 (b) $\delta =$ 1e-3 (c) $\delta =$ 1e-4

Figure 3.1: Example 3.1. First row: reconstructions of $D^\dagger$. Second row: reconstructions of $\sigma^\dagger$.

However, this rate is seldom observed in practical applications. The discrepancy between numerical experiments and theoretical predictions can be attributed to optimization error. In the decoupled algorithm, two optimization problems must be solved to obtain D_h^* and σ_h^*. The loss functions are non-convex and contain local minima, which making it challenging to achieve the theoretical convergence rates.

Example 3.2. $\Omega = (0,1)^2$, $D^\dagger(x,y) = 2 + \sin(2\pi x)\sin(2\pi y)$ *and* $\sigma^\dagger(x,y) = 1 + y(1-y)\sin(\pi x)$. *The boundary is* $g \equiv 1$ *and the two sources are given by* $f_1 \equiv 1$, $f_2 \equiv 10$.

The numerical results for Example 3.2 are presented in Table 3.1 and Fig. 3.2. The mesh sizes and regularization parameters are initialized to $h_1 = 1/16$, $\gamma_1 =$ 1e-8, $h_2 = 1/12$ and $\gamma_2 =$ 5e-6. The empirical convergence rates for e_D and e_σ with respect to δ are about $O(\delta^{0.51})$ and $O(\delta^{0.25})$, respectively, which are comparable with that for Example 3.1

Next we compare our decoupled reconstruction process with the scheme (3.26)-(3.27) where we compute D_h^* and σ_h^* simultaneously. We address the optimization problem defined in (3.26)-(3.27), using the conjugate gradient method. The solution process alternates between two directions. We initially set σ_h as fixed and employ the conjugate gradient descent to optimize D_h. Subsequently, we fix D_h and utilize the conjugate gradient descent to optimize σ_h. We continue this alternating process until convergence is reached. In the computation, we select a mesh size of $h = 1/50$. The regularization parameters are determined through a process of trial and error. The reconstruction results, carried out with a noise level of $\delta = 2\%$, are presented in Figure 3.3. The first column illustrates the convergence of the conjugate gradient iteration. In both methods, the errors first decays and then increase or

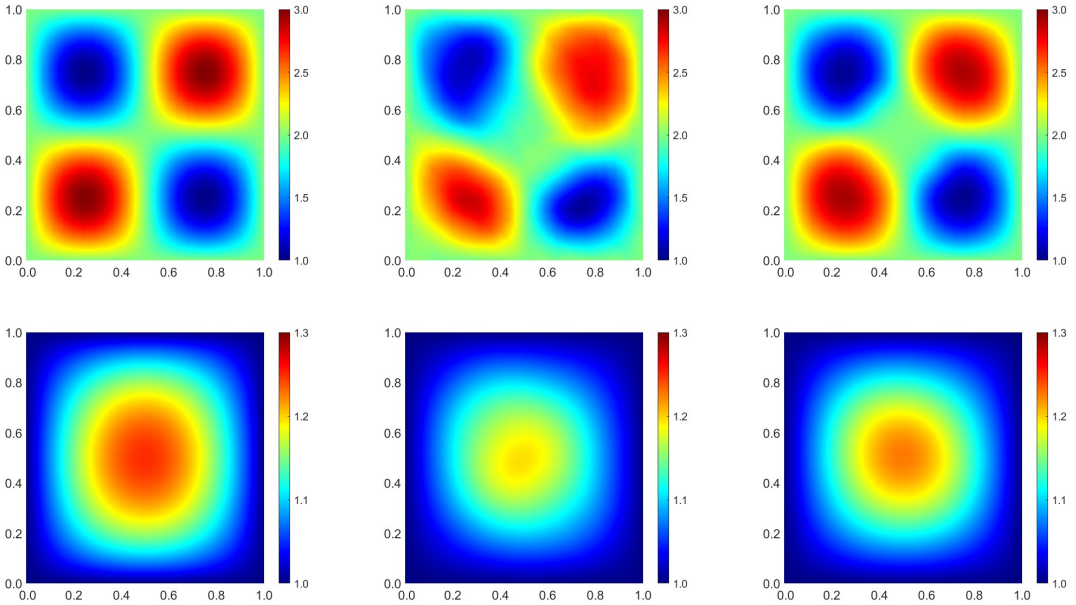

(a) exact (b) $\delta = 5\text{e-}3$ (c) $\delta = 5\text{e-}4$

Figure 3.2: Example 3.2. First row: reconstructions of $D^\dagger$. Second row: reconstructions of $\sigma^\dagger$.

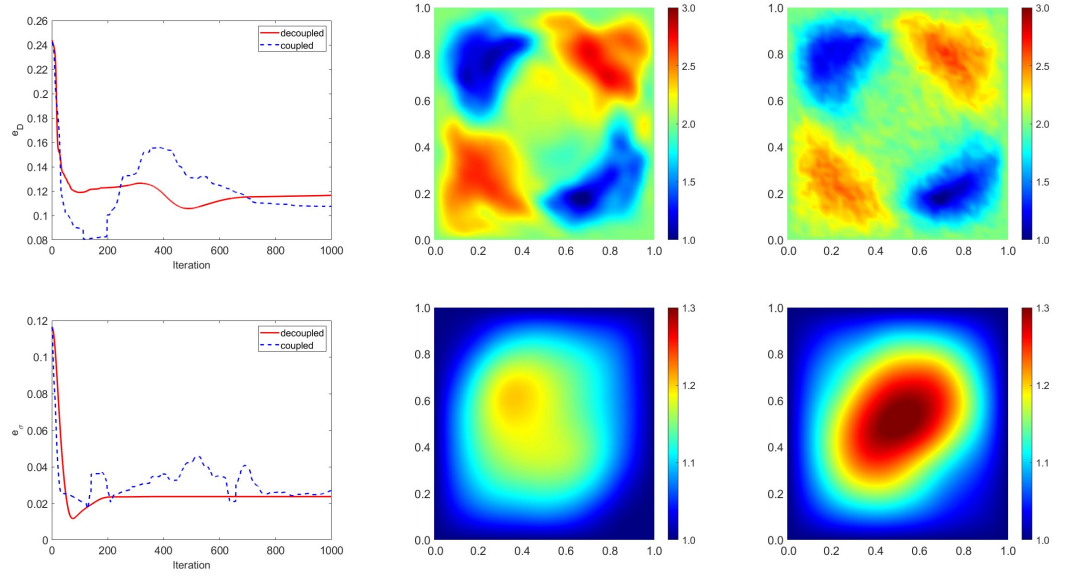

(a) error (b) coupled scheme (c) decoupled scheme

Figure 3.3: Comparison between the proposed decoupled algorithm and the coupled scheme (3.26)-(3.26). First row: diffusion coefficient D. Second row: reaction coefficient σ.

oscillate and finally become steady. This phenomenon indicates that it is essential to choose a good regularization parameter or apply early stopping strategy. Notably, the errors for the decoupled scheme demonstrate a rapid and steady decay. However, for the coupled scheme as defined in (3.26)-(3.27), the optimization problem is considerably more complicated. As a result, the errors exhibit a period of oscillation and require a significantly longer time to converge.

Next, we present numerical results for the parabolic equation. Throughout, we use backward Euler scheme, i.e. $k = 1$, to discretize in time variable.

Example 3.3. $\Omega = (0,1)$, $D^\dagger(x) = 2 + \sin(2\pi x)$, $\sigma^\dagger(x) = 1 - |x - \frac{1}{2}|^{1.1}$, $u_0(x) = 1 + \frac{1}{2}\sin(\pi x)$ *and* $g \equiv 1$. *We take the source term as*

$$f(x,t) = \begin{cases} 1, & \text{for } t \in [0, 1.5]; \\ \frac{9}{2}\sin(\frac{\pi}{2}(t - \frac{5}{2})) + \frac{11}{2}, & \text{for } t \in (1.5, 3.5); \\ 10, & \text{for } t \in [3.5, \infty). \end{cases} \tag{3.44}$$

The measurement is taken in the time-space domain $(t,x) \in [0.9, 1] \times \Omega$ *and* $(t,x) \in [4.9, 5] \times \Omega$.

Table 3.2: Examples 3.3 and 3.4: convergence with respect to δ.

	(a) Example 3.3					(b) Example 3.4				
δ	1e-2	5e-3	1e-3	5e-4	1e-4	1e-2	5e-3	1e-3	5e-4	1e-4
e_D	5.49e-2	3.78e-2	1.37e-2	7.45e-3	6.69e-3	1.59e-1	1.00e-1	3.15e-2	1.98e-3	8.78e-3
e_σ	5.23e-2	5.14e-2	3.32e-2	2.29e-2	2.13e-2	4.41e-2	2.43e-2	2.24e-2	1.98e-2	1.53e-2

The reconstruction results are listed in Table 3.2 and Figure 3.4. For reconstructing diffusion coefficient $D^\dagger$, the parameters are taken to be $h_1 = C_{h_1}\delta^{\frac{1}{4}}$, $\tau = C_\tau \delta^{\frac{1}{2}}$ and $\gamma_1 = C_{\gamma_1}\delta$, according to Theorem 3.12. We observe e_D decays in a rate $O(\delta^{0.49})$ with initial mesh size $h_1 = 1/16$, time step $\tau = 0.1$ and regularization parameter $\gamma_1 =$ 1e-6. As shown in Theorem 3.13, for reconstructing $\sigma^\dagger$, we take parameters $h_2 = C_{h_2}\epsilon^{\frac{1}{2}}$, $\tau = C_\tau \delta^{\frac{1}{2}}$ and $\gamma_2 = C_{\gamma_2}\epsilon^2$. Here, ϵ represents the empirical convergence rates for recovering $D^\dagger$ observed in our experiments. We initialize the mesh size $h_2 = 1/16$, time step $\tau = 0.1$ and regularization parameter $\gamma_2 =$ 1e-5. The numerical results show that the error e_σ have decay rates $O(\delta^{0.22})$. These results are comparable with that for Examples 3.1 and 3.2.

Example 3.4. $\Omega = (0,1)^2$, $D^\dagger = 2 + D_1 - D_2$ *with* $D_1(x,y) = e^{-20(x-0.5)^2-20(y-0.7)^2}$, $D_2(x,y) = e^{-20(x-0.5)^2-20(y-0.3)^2}$, $\sigma^\dagger(x,y) = 1 + 0.5e^{-20(x-0.6)^2-20(y-0.6)^2}$, $u_0(x) = 1 + \frac{1}{2}\sin(\pi x)\sin(\pi y)$ *and* $g \equiv 1$. *The source term is given by* (3.44). *The measurement data is observed in the time-space domain* $(t,x,y) \in [0.9, 1] \times \Omega$ *and* $(t,x,y) \in [4.9, 5] \times \Omega$.

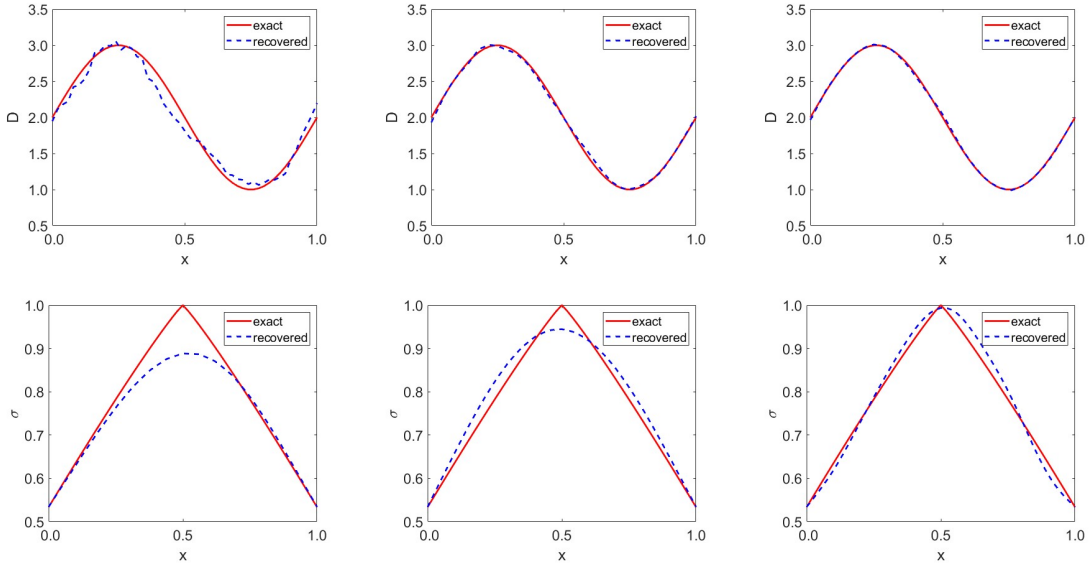

(a) δ = 1e-2 (b) δ = 1e-3 (c) δ = 1e-4

Figure 3.4: Example 3.3. First row: reconstructions of $D^\dagger$. Second row: reconstructions of $\sigma^\dagger$.

The numerical results for Example 3.4 are shown in Table 3.2 and Figure 3.5. The computational parameters are initialized to $h_1 = 1/16$, $\tau = 0.1$, γ_1 = 1e-6 and $h_2 = 1/16$, $\tau = 0.1$, γ_2 = 1e-6. It was discovered that the empirical convergence rate for e_D in relation to δ was approximately $O(\delta^{0.48})$. This rate is higher than the theoretical one. Moreover, the empirical rate for e_σ was found to be about $O(\delta^{0.22})$, which aligns with the theoretical estimate.

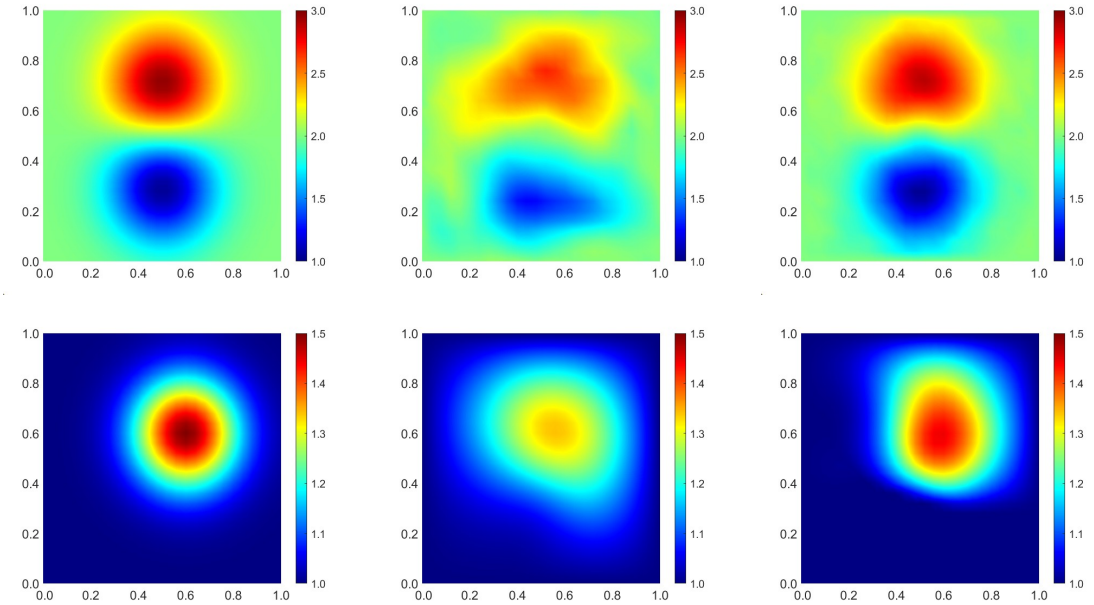

(a) exact (b) $\delta = 5\text{e-}3$ (c) $\delta = 5\text{e-}4$

Figure 3.5: Example 3.4. First row: reconstructions of $D^\dagger$. Second row: reconstructions of $\sigma^\dagger$.

CHAPTER 4.

Finite element approximation for quantitative photoacoustic tomography in a diffusive regime

In this chapter, we investigate the inverse problem raising in the quantitative photoacoustic tomography (QPAT):

$$\begin{cases} -\nabla \cdot (D(x)\nabla u) + \sigma(x)u = 0 & \text{in } \Omega, \\ u = g & \text{on } \partial\Omega. \end{cases} \tag{4.1}$$

Here, Ω is a bounded Lipschitz domain in $\mathbb{R}^d$ $(d = 2, 3)$ with boundary $\partial\Omega$. The optical coefficients $(D(x), \sigma(x))$, with $D(x)$ being the diffusion coefficient and $\sigma(x)$ the absorption coefficient, are assumed to be bounded and positive. The QPAT inverse problem consists of recovering $D(x)$ and $\sigma(x)$ from the internal observation of the optical energy

$$H(x) = \sigma(x)u(x) \quad \text{for all } x \in \Omega.$$

The problem of QPAT has been extensively studied in the literature. Since the inverse problem involves multiple parameters (D and σ), a common method uses multiple illuminations g to generate various optical energies H and reconstruct the unknown parameters. In [16, 15], the authors propose a decoupled procedure and prove the uniqueness and Hölder stability for the inverse problem. The decoupled scheme relies on the following observation: if u_1, u_2 are two solutions to equation (4.1) corresponding to illuminations g_1, g_2 respectively, then the quotient $u = u_2/u_1 = H_2/H_1$ satisfies the following elliptic equation with one parameter:

$$\begin{cases} -\nabla \cdot (q\nabla u) = 0 & \text{in } \Omega, \\ u = g & \text{on } \partial\Omega, \end{cases} \tag{4.2}$$

where $q = Du_1^2$ and $g = g_2/g_1$. Thus, the problem of QPAT is solved by a two-step procedure. The first step is to solve an inverse diffusivity problem (IDP) of recovering q given u and the boundary value $q|_{\partial\Omega}$. After obtaining $q = Du_1^2$, the second step is solving a direct problem:

$$\begin{cases} -\nabla \cdot (Du_1^2\nabla(1/u_1)) = H_1 & \text{in } \Omega, \\ 1/u_1 = 1/g_1 & \text{on } \partial\Omega, \end{cases} \tag{4.3}$$

to find u_1 and hence determine D and σ.

The rest of this chapter is organized as follows. In Section 4.1, we discuss the choice of random boundary illuminations and show the Hölder type stability of the inverse diffusivity problem under

the non-zero condition. We also propose an iterative reconstruction algorithm and study the finite element approximation error. In Section 4.2, we establish the numerical inversion scheme for QPAT and analyze the discrete approximation error. Numerical experiments are presented in Section 4.3 to validate the theoretical results.

4.1 Inverse diffusivity problem

In this section, we consider the inverse diffusivity problem of the second-order elliptic equation (4.2):

$$\begin{cases} -\nabla \cdot (q \nabla w) = 0 & \text{in } \Omega, \\ w = g & \text{on } \partial\Omega. \end{cases} \tag{4.2}$$

Let $\Omega' \Subset \Omega$ be a given Lipschitz subdomain and suppose that the exact diffusion coefficient $q^\dagger(x)$ is known for all $x \in \Omega \setminus \Omega'$. The diffusion coefficient is assumed to be in the following admissible set:

$$\mathcal{A}_q = \{q \in H^1(\Omega) : 0 < \underline{c}_q \leq q \leq \overline{c}_q \text{ a.e. in } \Omega,\ q = q^\dagger \text{ in } \Omega \setminus \Omega'\}, \tag{4.4}$$

with a priori known positive constants $\underline{c}_q$, $\overline{c}_q$. Moreover, we assume that the coefficient and boundary data satisfy the following assumption.

Assumption 4.1. *Let Ω be a bounded Lipschitz domain in $\mathbb{R}^d$ and $\Omega' \Subset \Omega$ be a given Lipschitz subdomain. We assume that the exact diffusivity coefficient $q^\dagger \in C^{0,1}(\overline{\Omega}) \cap \mathcal{A}_q$. Further, we let $g^{(\ell)}$ (with $\ell = 1, \ldots, L$) denote boundary data, which are taken as independent and identically distributed random variables in $H^{\frac{1}{2}}(\partial\Omega)$ satisfying the expansion*

$$g^{(\ell)} = \sum_{k=1}^{M} a_k^{(\ell)} e_k, \qquad \ell = 1, \ldots, L, \tag{4.5}$$

where M is a given positive integer, $\{e_k\}_{k=1}^{\infty}$ is a fixed orthonormal basis of $H^{\frac{1}{2}}(\partial\Omega)$ and $a_k^{(\ell)} \sim N(0, \theta_k^2)$ are independent real Gaussian variables, with $\theta_k > 0$ for every k and $\sum_{k\geq 1} \theta_k < \infty$.

Remark 4.1. *Let $w^{(\ell)}(q^\dagger)$ denote the solution to the elliptic problem (4.2) associated with the diffusion coefficient $q^\dagger$ and the boundary excitation $g^{(\ell)}$. Under the regularity assumption, classical elliptic regularity theory ([57, Theorem 5.20] and [58, Theorem 8.8]) implies that the corresponding solution to the elliptic equation (4.2) satisfies $w^{(\ell)}(q^\dagger) \in C^{1,\kappa}_{loc}(\Omega) \cap H^1(\Omega)$ for all $\kappa \in (0, 1)$.*

The inverse diffusivity problem (IDP) consists of recovering the diffusion coefficient in Ω' from the multiple internal observations $w^{(\ell)}(x; q^\dagger)$ for all $x \in \Omega'$, where $\ell = 1, 2, \ldots, L$. With the above choice of $g^{(\ell)}$, by using the result of [4] we have the following non-zero condition, which is crucial for stability and error estimates.

Proposition 4.1. *Suppose that Assumption 4.1 holds. Take $\nu \in \mathbb{R}^d$ with $|\nu| = 1$. Then, with a probability greater than*

$$1 - L^d \exp(-C_1 L) - L \exp(-C_2 M), \tag{4.6}$$

the following non-zero condition holds

$$\max_{\ell=1,\dots,L} |\nabla w^{(\ell)}(x) \cdot \nu| \geq C_0, \quad x \in \Omega', \tag{4.7}$$

and the random boundary data has upper bound

$$\max_{\ell=1,\dots,L} \|g^{(\ell)}\|_{H^{\frac{1}{2}}(\partial\Omega)} \leq L^{\frac{1}{2}}. \tag{4.8}$$

Here $w^{(\ell)}$ (with $\ell = 1, \dots, L$) is the solution to (4.2) corresponding to the boundary illumination $g^{(\ell)}$. The positive constants C_0, C_1 and C_2 depend only on Ω, Ω', $\{\theta_k\}$, $\{e_k\}$, $\underline{c}_q$, $\overline{c}_q$ and $\|q\|_{C^{0,1}(\overline{\Omega})}$.

Proof. All the constants appearing in the proof will depend only on Ω, Ω', $\{\theta_k\}$, $\{e_k\}$, $\underline{c}_q$, $\overline{c}_q$ and $\|q\|_{C^{0,1}(\overline{\Omega})}$. Let $\overline{w}^{(\ell)}$ be the solution to (4.2) with boundary data

$$\overline{g}^{(\ell)} = \sum_{k=1}^{\infty} a_k^{(\ell)} e_k, \quad \ell = 1, \dots, L,$$

where $\{e_k\}_{k=1}^{\infty}$ and $a_k^{(\ell)}$ are as in Assumption 4.1. By [4, Theorem 1] (with the choice $\zeta(u) = \nabla w \cdot \nu$, as a minor variation of [4, Example 2]) and [4, Lemma 5]), with probability greater than $1 - L^d \exp(-C_1 L)$, we have the following non-zero condition

$$\max_{\ell=1,\dots,L} |\nabla \overline{w}^{(\ell)}(x) \cdot \nu| \geq 2C_0, \quad x \in \Omega'$$

and

$$\max_{\ell=1,\dots,L} \|\overline{g}^{(\ell)}\|_{H^{\frac{1}{2}}(\partial\Omega)} \leq L^{\frac{1}{2}}/2.$$

Now we estimate the difference between $\overline{g}^{(\ell)}$ and the truncated boundary values $g^{(\ell)}$. We view $\|\overline{g}^{(\ell)} - g^{(\ell)}\|_{H^{\frac{1}{2}}(\partial\Omega)}$ as a random variable. Since $a_k^{(\ell)} \sim N(0, \theta_k^2)$ and e_k are orthonormal in $H^{\frac{1}{2}}(\partial\Omega)$, the moment generating function satisfies for all $\lambda \in \mathbb{R}$:

$$\mathbb{E} \exp\left(\lambda^2 \|\overline{g}^{(\ell)} - g^{(\ell)}\|^2_{H^{\frac{1}{2}}(\partial\Omega)}\right) = \mathbb{E} \exp\left(\lambda^2 \sum_{k=M+1}^{\infty} (a_k^{(\ell)})^2\right) = \exp\left(\lambda^2 \sum_{k=M+1}^{\infty} \theta_k^2\right).$$

The condition $\sum_{k=1}^{\infty} \theta_k < \infty$ implies that $\sum_{k=M+1}^{\infty} \theta_k^2 \leq CM^{-1}$. By [142, Proposition 2.5.2], we have

$$\mathbb{P}\left(\|\overline{g}^{(\ell)} - g^{(\ell)}\|_{H^{\frac{1}{2}}(\partial\Omega)} \geq t\right) \leq 2 \exp\left(-C^2 t^2 M\right), \quad \forall t \geq 0,\ \ell = 1, \dots, L.$$

Thus, with probability greater than $1 - 2L \exp\left(-C^2 t^2 M\right)$, we have

$$\|\overline{g}^{(\ell)} - g^{(\ell)}\|_{H^{\frac{1}{2}}(\partial\Omega)} \leq t, \qquad \ell = 1, \dots, L.$$

Hence, elliptic regularity yields

$$\|\overline{w}^{(\ell)} - w^{(\ell)}\|_{C^1(\overline{\Omega'})} \leq \widetilde{C}t, \qquad \ell = 1, \dots, L.$$

With the choice $t = \min\{C_0/\widetilde{C}, L^{\frac{1}{2}}/2\}$, we have $\|\overline{w}^{(\ell)} - w^{(\ell)}\|_{C^1(\overline{\Omega'})} \leq C_0$ and $\|g^{(\ell)}\|_{H^{\frac{1}{2}}(\partial\Omega)} \leq L^{\frac{1}{2}}$. Let $C_2 = C^2t^2$, with a probability greater than

$$1 - L^d \exp\left(-C_1 L\right) - 2L \exp\left(-C_2 M\right),$$

the non-zero condition (4.7) and the upper bound on the boundary values (4.8) hold. □

4.1.1 Conditional stability

In this part, we derive a useful conditional stability estimate in Sobolev spaces for the inverse diffusivity problem. According to the non-zero condition (4.7) and the smoothness of the solutions $w^{(\ell)} \in C^{1,\kappa}_{loc}(\Omega) \cap H^1(\Omega)$, there exist open sets Ω_ℓ, $\ell = 1, \dots, L$, covering Ω' such that

$$\Omega' \subset \bigcup_{\ell=1}^{L} \overline{\Omega}_\ell \quad \text{where} \quad |\nabla w^{(\ell)} \cdot \nu| > C_0/2 \text{ for all } x \in \Omega_\ell. \tag{4.9}$$

Theorem 4.2. *Suppose the diffusion coefficient q and the boundary terms $g^{(\ell)}$ (with $\ell = 1, \dots, L$) satisfy Assumption 4.1, and let $\widetilde{q} \in \mathcal{A}_q$ be a perturbation. Let $w^{(\ell)}$ and $\widetilde{w}^{(\ell)}$ be the corresponding solutions to* (4.2) *with parameters q and $\widetilde{q}$, respectively. Then, with a probability greater than* (4.6)*, the following stability estimate holds:*

$$\|q - \widetilde{q}\|_{L^2(\Omega)} \leq cC_0^{-1}L^{\frac{1}{4}}\Big(\sum_{\ell=1}^{L} \|w^{(\ell)} - \widetilde{w}^{(\ell)}\|_{H^1(\Omega')}\Big)^{\frac{1}{2}}. \tag{4.10}$$

Here $c > 0$ is a constant depending only on Ω, Ω', $\overline{c}_q$ and $\|q\|_{C^{0,1}(\overline{\Omega})}$, and C_0 is the lower bound of the non-zero condition given in (4.7)*.*

Proof. With an abuse of notation, several positive constants depending only on Ω, Ω', $\underline{c}_q$, $\overline{c}_q$ and $\|q\|_{C^{0,1}(\overline{\Omega})}$ will be denoted by the same letter c. By Proposition 4.1, with overwhelming probability (4.6), both the non-zero condition (4.7) and the uniform bound (4.8) are satisfied. Then for a given $\ell \in \{1, \dots, L\}$, for any test function $\varphi^{(\ell)} \in H^1_0(\Omega)$, integration by parts in (4.2) yields

$$\big((q - \widetilde{q})\nabla w^{(\ell)}, \nabla\varphi^{(\ell)}\big) = \big(\widetilde{q}\nabla(\widetilde{w}^{(\ell)} - w^{(\ell)}), \nabla\varphi^{(\ell)}\big). \tag{4.11}$$

Furthermore, multiplying both sides of (4.2) by $\frac{q-\widetilde{q}}{q}\varphi^{(\ell)}$ and applying integration by parts, we obtain

$$0 = \big(q\nabla w^{(\ell)}, \nabla\frac{(q-\widetilde{q})\varphi^{(\ell)}}{q}\big) = \big(q\varphi^{(\ell)}\nabla w^{(\ell)}, \nabla\frac{(q-\widetilde{q})}{q}\big) + \big(q\frac{(q-\widetilde{q})}{q}\nabla w^{(\ell)}, \nabla\varphi^{(\ell)}\big),$$

and hence

$$\big((q - \widetilde{q})\nabla w^{(\ell)}, \nabla\varphi^{(\ell)}\big) = \frac{1}{2}\big((q - \widetilde{q})\nabla w^{(\ell)}, \nabla\varphi^{(\ell)}\big) - \frac{1}{2}\big(q\varphi^{(\ell)}\nabla w^{(\ell)}, \nabla\frac{(q-\widetilde{q})}{q}\big). \tag{4.12}$$

Now, we choose the test function $\varphi^{(\ell)} = (q - \widetilde{q})w^{(\ell)}/q$. Since $q = \widetilde{q}$ on $\Omega \setminus \Omega'$, $\varphi^{(\ell)}$ vanishes on $\partial\Omega$. Noting that $q, \widetilde{q} \in \mathcal{A}_q$ and $w^{(\ell)} \in C^{1,\kappa}(\overline{\Omega'})$, we conclude that $\varphi^{(\ell)} \in H_0^1(\Omega)$, with

$$\|\varphi^{(\ell)}\|_{L^2(\Omega)} = \|(q - \widetilde{q})w^{(\ell)}/q\|_{L^2(\Omega)} \leq 2\underline{c}_q^{-1}\overline{c}_q\|w^{(\ell)}\|_{L^2(\Omega)} \leq cL^{\frac{1}{2}}$$

and

$$\begin{aligned}\|\nabla\varphi^{(\ell)}\|_{L^2(\Omega)} =& \left\| \frac{q\nabla[(q - \widetilde{q})w^{(\ell)}] - (q - \tilde{q})w^{(\ell)}\nabla q}{q^2} \right\|_{L^2(\Omega')} \\ \leq& \underline{c}_q^{-2}\Big(\overline{c}_q\|w^{(\ell)}\|_{L^\infty(\Omega')}(\|\nabla q\|_{L^2(\Omega')} + \|\nabla\widetilde{q}\|_{L^2(\Omega')}) + 2\overline{c}_q^2\|\nabla w^{(\ell)}\|_{L^2(\Omega')}\Big) \\ &+ 2\underline{c}_q^{-2}\overline{c}_q\|w^{(\ell)}\|_{L^\infty(\Omega')}\|\nabla q\|_{L^2(\Omega')} \leq cL^{\frac{1}{2}}.\end{aligned}$$

With the test function $\varphi^{(\ell)}$, the right hand side of (4.12) equals to $\frac{1}{2}\int_\Omega \frac{(q-\widetilde{q})^2}{q}|\nabla w^{(\ell)}|^2\mathrm{d}x$. Therefore, by the relations (4.11), (4.12) and the assumption $q = \tilde{q}$ in $\Omega \setminus \Omega'$, we achieve

$$\frac{1}{2}\int_{\Omega'} \frac{(q - \widetilde{q})^2}{q}|\nabla w^{(\ell)}|^2\mathrm{d}x = \int_{\Omega'} \widetilde{q}\nabla(\widetilde{w}^{(\ell)} - w^{(\ell)}) \cdot \nabla\varphi^{(\ell)}\mathrm{d}x \leq cL^{\frac{1}{2}}\|\widetilde{w}^{(\ell)} - w^{(\ell)}\|_{H^1(\Omega')}.$$

Taking summation with respect to ℓ, we obtain

$$\int_{\Omega'} \frac{(q - \widetilde{q})^2}{q^2}\sum_{\ell=1}^{L}|\nabla w^{(\ell)}|^2\mathrm{d}x \leq cL^{\frac{1}{2}}\sum_{\ell=1}^{L}\|\widetilde{w}^{(\ell)} - w^{(\ell)}\|_{H^1(\Omega')}.$$

The non-zero condition (4.7) indicates $\sum_{\ell=1}^{L}|\nabla w^{(\ell)}(x)|^2 \geq C_0^2$, for all $x \in \Omega'$. Hence, we conclude

$$\|q - \tilde{q}\|_{L^2(\Omega')}^2 \leq cC_0^{-2}L^{\frac{1}{2}}\sum_{\ell=1}^{L}\|\widetilde{w}^{(\ell)} - w^{(\ell)}\|_{H^1(\Omega')}.$$

Since $q = \widetilde{q}$ in $\Omega \setminus \Omega'$, the proof is completed. □

Remark 4.2. *The proof of Theorem 4.2 depends on the non-zero condition* (4.7) *and the boundedness of* $\|w^{(\ell)}\|_{L^\infty(\Omega')} \leq c\|g^{(\ell)}\|_{H^{\frac{1}{2}}(\partial\Omega)} \leq cL^{\frac{1}{2}}$*, which is satisfied under an overwhelming probability. It is important to emphasize that the constant* c *in* (4.10) *is influenced by the distance between* Ω' *and* $\partial\Omega$*. As the subdomain* Ω' *approaches the boundary of* Ω*, controlling the regularity of solutions and maintaining the stability of the inverse problem becomes increasingly challenging. In the limiting case, where* $\Omega' = \Omega$ *and* $q = \widetilde{q}$ *on* $\partial\Omega$*, the domain* Ω *and the boundary conditions* $g^{(\ell)}$ *must exhibit higher regularity to ensure that* $w^{(\ell)} \in C^{1,\kappa}(\overline{\Omega})$*.*

4.1.2 Error estimate

In this section, we introduce a numerical algorithm for the IDP and derive the reconstruction error estimation. We employ the FEM discretization specified in Section 2.1.1. In addition, we assume that $\partial\Omega'$ does not cross an element, that is , Ω equals the union of some meshes.

Now, we present the reconstruction algorithm. Slightly different from the stability analysis, we aim to reconstruct the diffusion coefficient in the whole domain Ω using the measurement in the entire domain. Throughout this section, we let $z_\delta^{(\ell)}$ denote the practical noisy observations corresponding to $w^{(\ell)}(q^\dagger)$ with noise level δ, i.e.

$$\|w^{(\ell)}(q^\dagger) - z_\delta^{(\ell)}\|_{L^2(\Omega)} \le \delta, \quad \forall \ell = 1, \ldots, L. \tag{4.13}$$

The reconstruction is based on standard regularized least-squares with further discretization using finite element methods. More precisely, the minimization problem is

$$\min_{q \in \mathcal{A}_q} J_\gamma(q) = \frac{1}{2} \sum_{\ell=1}^{L} \|w^{(\ell)}(q) - z_\delta^{(\ell)}\|_{L^2(\Omega)}^2 + \frac{\gamma L}{2} \|\nabla q\|_{L^2(\Omega)}^2, \tag{4.14}$$

where $\gamma > 0$ is the regularization parameter, and $w^{(\ell)}(q) \in H^1(\Omega)$ is the weak solution of

$$\begin{cases} -\nabla \cdot (q \nabla w^{(\ell)}) = 0, & \text{in } \Omega, \\ w^{(\ell)} = g^{(\ell)}, & \text{on } \partial\Omega. \end{cases} \tag{4.15}$$

We formulate the finite element approximation of problem (4.14)-(4.15):

$$\min_{q_h \in \mathcal{A}_{q,h}} J_{\gamma,h}(q_h) = \frac{1}{2} \sum_{\ell=1}^{L} \|w_h^{(\ell)}(q_h) - z_\delta^{(\ell)}\|_{L^2(\Omega)}^2 + \frac{\gamma L}{2} \|\nabla q_h\|_{L^2(\Omega)}^2, \tag{4.16}$$

where $w_h^{(\ell)}(q_h) \in V_h$ is the weak solution of

$$\begin{cases} (q_h \nabla w_h^{(\ell)}, \nabla v_h) = 0, & \forall v_h \in V_h^0, \\ w_h^{(\ell)} = \mathcal{I}_h^\partial g^{(\ell)}, & \text{on } \partial\Omega. \end{cases} \tag{4.17}$$

Here, the admissible set is defined as

$$\mathcal{A}_{q,h} = \{q_h \in V_h : 0 < \underline{c}_q \le q_h \le \overline{c}_q \text{ a.e. in } \Omega,\ q_h = \mathcal{I}_h q^\dagger \text{ on } \partial\Omega\}. \tag{4.18}$$

The discrete problem (4.16)-(4.17) is well-posed: there exists at least one global minimizer q_h^* and it depends continuously on the data perturbation. The main objective in this section is to bound the approximation error $\|q^\dagger - q_h^*\|_{L^2(\Omega)}$. The strategy is based upon the stability analysis in the preceding section. Furthermore, we need the following higher regularity assumption on the exact diffusivity coefficient and boundary data.

Assumption 4.3. *Let $\Omega \subset \mathbb{R}^d$ $(d = 2, 3)$ be a bounded domain with $C^{1,1}$ boundary $\partial\Omega$. Assume that the exact diffusivity coefficient $q^\dagger \in W^{2,p}(\Omega) \cap \mathcal{A}_q$ with $p > d$. Assume the boundary data $g^{(\ell)}$ (with $\ell = 1, \ldots, L$) are taken as independent and identically distributed satisfying the expansion* (4.5)*, where $\{e_k\}_{k=1}^\infty$ are assumed to be in $H^2(\partial\Omega)$ and $a_k^{(\ell)} \sim N(0, k^{-2s}\theta_k^2)$, with $s > \frac{3}{2(d-1)} + \frac{1}{2}$.*

Remark 4.3. *Assumption 4.3 requires higher regularity for the domain Ω as well as the parameter $q^\dagger$ and $g^{(\ell)}$ to ensure that the finite element approximation achieves an optimal convergence rate. Indeed, under the regularity assumption, elliptic regularity theory ([57, Theorem 7.2] and [58, Theorem 8.12]) implies that the solution satisfies $w^{(\ell)}(q^\dagger) \in H^2(\Omega) \cap W^{1,p}(\Omega)$ for all $p > 2$. The non-zero condition* (4.7) *still hold with overwhelming probability under Assumption 4.3. Under Assumption 4.3, with a probability greater than*

$$1 - L^d \exp\left(-C_1 L\right) - L \exp\left(-C_2 M\right),$$

the non-zero condition (4.7) *holds and the random boundary data has upper bound*

$$\max_{\ell=1,\dots,L} \|g^{(\ell)}\|_{H^2(\partial\Omega)} \leq L^{\frac{1}{2}}, \tag{4.19}$$

where the positive constants C_0, C_1 and C_2 depend only on s, Ω, Ω', $\{\theta_k\}$, $\{e_k\}$, $\underline{c}_q$, $\overline{c}_q$ and $\|q\|_{C^{0,1}(\overline{\Omega})}$. The nonzero condition is a direct consequence of Proposition 4.1. It suffices to investigate the upper bound of $\|g^{(\ell)}\|_{H^2(\partial\Omega)}$. Note that the Laplace–Beltrami operator $-\Delta$ on $\partial\Omega$ admits a positive sequence $\{\lambda_k\}_{k=1}^\infty$ of eigenvalues and the corresponding eigenfunctions $\{\varphi_k\}_{k=1}^\infty$ form an orthonormal basis of $L^2(\partial\Omega)$. Here we use the equivalent norm in space $H^s(\partial\Omega)$, with $s > 0$, defined by [111, Remark 7.6]

$$\|g\|_{H^s(\partial\Omega)}^2 = \|g\|_{L^2(\partial\Omega)}^2 + \sum_{k=1}^\infty \lambda_k^s (g, \varphi_k)_{\partial\Omega}^2.$$

Therefore, the orthonormal basis of $H^{\frac{1}{2}}(\partial\Omega)$ can be chosen as $e_k = (1 + \lambda_k^{\frac{1}{4}})^{-1}\varphi_k$ which satisfies

$$\|e_k\|_{H^2(\partial\Omega)} = (1 + \lambda_k^2)^{\frac{1}{2}}(1 + \lambda_k^{\frac{1}{4}})^{-1}.$$

By Cauchy-Schwarz inequality and the asymptotic behavior of eigenvalues $\lambda_k \sim k^{2/d}$ [119], the moment generating function of $\|g^{(\ell)}\|_{H^2(\partial\Omega)}$ satisfies for all $\lambda \in \mathbb{R}$:

$$\begin{aligned}
\mathbb{E}\exp\left(\lambda^2 \|g^{(\ell)}\|_{H^2(\partial\Omega)}^2\right) &\leq \mathbb{E}\exp\left(\lambda^2 \Big(\sum_{k=1}^M (a_k^{(\ell)} k^s)^2\Big)\Big(\sum_{k=1}^M k^{-2s} \|e_k\|_{H^2(\partial\Omega)}^2\Big)\right) \\
&\leq c\mathbb{E}\exp\left(\lambda^2 \Big(\sum_{k=1}^M (a_k^{(\ell)} k^s)^2\Big)\Big(\sum_{k=1}^M k^{-2s+3/d}\Big)\right) \\
&\leq c\mathbb{E}\exp\left(\lambda^2 \sum_{k=1}^M \theta_k^2\right).
\end{aligned}$$

Then, by [142, Proposition 2.5.2], with probability greater than $1 - L\exp(-C_1 L)$, we have

$$\max_{\ell=1,\dots,L} \|g^{(\ell)}\|_{H^2(\partial\Omega)} \leq L^{\frac{1}{2}}.$$

We have the following $L^2(\Omega)$ error estimate for $w_h(q^\dagger) - w_h(\mathcal{I}_h q^\dagger)$.

Lemma 4.1. *Let Assumption 4.3 hold and the boundary data satisfy* $\|g\|_{H^2(\partial\Omega)} \leq L^{\frac{1}{2}}$. *We denote the solutions of equation* (4.17) *with coefficients* $q^\dagger$ *and* $\mathcal{I}_h q^\dagger$ *by* $w_h(q^\dagger)$ *and* $w_h(\mathcal{I}_h q^\dagger)$, *respectively. Then*

$$\|w_h(q^\dagger) - w_h(\mathcal{I}_h q^\dagger)\|_{L^2(\Omega)} \leq ch^2 L^{\frac{1}{2}},$$

where c *is a positive constant depending only on* Ω *and* $q^\dagger$.

Proof. With an abuse of notation, several positive constants depending only on Ω and $q^\dagger$ will be denoted by the same letter c. We start with the estimate in energy norm. By subtracting the weak formulations of $w_h(q^\dagger)$ and $w_h(\mathcal{I}_h q^\dagger)$, we derive

$$\big(\mathcal{I}_h q^\dagger(\nabla w_h(\mathcal{I}_h q^\dagger) - \nabla w_h(q^\dagger)), \nabla v_h\big) = \big((q^\dagger - \mathcal{I}_h q^\dagger)\nabla w_h(q^\dagger), \nabla v_h\big), \quad \text{for all } \ v_h \in V_h^0.$$

Select the test function $v_h = w_h(\mathcal{I}_h q^\dagger) - w_h(q^\dagger)$. Note that it belongs to V_h^0 since $u_h(\mathcal{I}_h q^\dagger)$ and $u_h(q^\dagger)$ share the same boundary value. Using the box constraint on $q^\dagger$ and the Cauchy–Schwarz inequality, we obtain

$$\begin{aligned}
&\|\nabla w_h(\mathcal{I}_h q^\dagger) - \nabla w_h(q^\dagger)\|_{L^2(\Omega)}^2 \\
&\leq c\|q^\dagger - \mathcal{I}_h q^\dagger\|_{L^\infty(\Omega)} \|\nabla w_h(q^\dagger)\|_{L^2(\Omega)} \|\nabla w_h(\mathcal{I}_h q^\dagger) - \nabla w_h(q^\dagger)\|_{L^2(\Omega)}.
\end{aligned}$$

Then the approximation estimate (2.2) implies

$$\|\nabla w_h(\mathcal{I}_h q^\dagger) - \nabla w_h(q^\dagger)\|_{L^2(\Omega)} \leq ch \|\nabla w_h(q^\dagger)\|_{L^2(\Omega)} \leq chL^{\frac{1}{2}}. \tag{4.20}$$

Next, we apply the duality argument to get the estimate in $L^2(\Omega)$ norm. Let ψ satisfy

$$\begin{cases}
-\nabla \cdot (q^\dagger \nabla \psi) = w_h(\mathcal{I}_h q^\dagger) - w_h(q^\dagger), & \text{in } \Omega, \\
\psi = 0, & \text{on } \partial\Omega.
\end{cases}$$

Then we have

$$\begin{aligned}
\|w_h(\mathcal{I}_h q^\dagger) - w_h(q^\dagger)\|_{L^2(\Omega)}^2 =& \big(-\nabla \cdot (q^\dagger \nabla \psi), w_h(\mathcal{I}_h q^\dagger) - w_h(q^\dagger)\big) \\
=& \big(q^\dagger \nabla \psi, \nabla(w_h(\mathcal{I}_h q^\dagger) - w_h(q^\dagger))\big) \\
=& \big((q^\dagger - \mathcal{I}_h q^\dagger)\nabla \psi, \nabla(w_h(\mathcal{I}_h q^\dagger) - w_h(q^\dagger))\big) \\
&+ \big(\mathcal{I}_h q^\dagger \nabla(\psi - P_h\psi), \nabla(w_h(\mathcal{I}_h q^\dagger) - w_h(q^\dagger))\big) \\
&+ \big((q^\dagger - \mathcal{I}_h q^\dagger)\nabla P_h\psi, \nabla w_h(q^\dagger)\big),
\end{aligned}$$

where we used the weak formulation of $w_h(q^\dagger)$ and $w_h(\mathcal{I}_h q^\dagger)$ in the last equality. Therefore, by Hölder inequality, error estimate (2.2), (2.3) and (4.20) yield that

$$\begin{aligned}
\|u_h(\mathcal{I}_h q^\dagger) - u_h(q^\dagger)\|_{L^2(\Omega)}^2 \leq& ch^2 \|q^\dagger\|_{W^{1,\infty}(\Omega)} \|\nabla\psi\|_{L^2(\Omega)} \|\nabla w_h(q^\dagger)\|_{L^2(\Omega)} \\
&+ ch^2 \|\mathcal{I}_h q^\dagger\|_{L^\infty(\Omega)} \|\psi\|_{H^2(\Omega)} \|\nabla w_h(q^\dagger)\|_{L^2(\Omega)} \\
&+ ch^2 \|q^\dagger\|_{W^{2,p}(\Omega)} \|\nabla P_h\psi\|_{L^q(\Omega)} \|\nabla w_h(q^\dagger)\|_{L^2(\Omega)}.
\end{aligned}$$

Here $\frac{1}{p}+\frac{1}{q}+\frac{1}{2}=1$ and, by Assumption 4.3, $q=\frac{2p}{p-2}<\frac{2d}{d-2}$. Thus the stability of the $L^2(\Omega)$ projection (see [43, Theorem 4] and [13, Lemma 2.1]) and the Sobolev embedding imply $\|\nabla P_h\psi\|_{L^q(\Omega)}\leq c\|\nabla\psi\|_{L^q(\Omega)}\leq c\|\psi\|_{H^2(\Omega)}$. By using standard elliptic regularity estimates, according to which $\|\psi\|_{H^2(\Omega)}\leq c\|u_h(\mathcal{I}_h q^\dagger)-u_h(q^\dagger)\|_{L^2(\Omega)}$, we obtain

$$\|w_h(\mathcal{I}_h q^\dagger)-w_h(q^\dagger)\|_{L^2(\Omega)}\leq ch^2\|\nabla w_h(q^\dagger)\|_{L^2(\Omega)}\leq ch^2L^{\frac{1}{2}}.$$

This completes the proof of the lemma. □

Corollary 4.1. *Let Assumption 4.3 hold and the boundary data satisfy $\|g\|_{H^2(\partial\Omega)}\leq L^{\frac{1}{2}}$. Let $w(q^\dagger)$ be the solution of equation (4.15) and $w_h(\mathcal{I}_h q^\dagger)$ be the solution of equation (4.17). Then*

$$\|w_h(\mathcal{I}_h q^\dagger)-w(q^\dagger)\|_{L^2(\Omega)}\leq ch^2L^{\frac{1}{2}},$$

where c is a positive constant depending only on Ω and $q^\dagger$.

Proof. We use the following splitting

$$\|w_h(\mathcal{I}_h q^\dagger)-w(q^\dagger)\|_{L^2(\Omega)}\leq\|w_h(\mathcal{I}_h q^\dagger)-w_h(q^\dagger)\|_{L^2(\Omega)}+\|w_h(q^\dagger)-w(q^\dagger)\|_{L^2(\Omega)}.$$

For the first term, we apply Lemma 4.1 and obtain

$$\|w_h(\mathcal{I}_h q^\dagger)-w_h(q^\dagger)\|_{L^2(\Omega)}\leq ch^2L^{\frac{1}{2}}.$$

The second term can be estimated by utilizing the standard duality argument with the interpolation estimate $\|g-\mathcal{I}_h^\partial g\|_{L^2(\partial\Omega)}\leq ch^2L^{\frac{1}{2}}$. □

The next lemma gives an *a priori* estimate.

Lemma 4.2. *Let Assumption 4.3 hold and boundary data satisfy $\|g^{(\ell)}\|_{H^2(\partial\Omega)}\leq L^{\frac{1}{2}}$, $\ell=1,\dots,L$. Let $q_h^*\in\mathcal{A}_{q,h}$ be a minimizer of problem (4.16)-(4.17). Then we have*

$$\sum_{\ell=1}^{L}\|w_h^{(\ell)}(q_h^*)-w^{(\ell)}(q^\dagger)\|_{L^2(\Omega)}+L\gamma^{\frac{1}{2}}\|\nabla q_h^*\|_{L^2(\Omega)}\leq cL(h^2L^{\frac{1}{2}}+\delta+\gamma^{\frac{1}{2}}),$$

where c is a positive constant depending only on Ω and $q^\dagger$.

Proof. With an abuse of notation, several positive constants depending only on Ω and $q^\dagger$ will be denoted by the same letter c. Since q_h^* is a minimizer of $J_{\gamma,h}$, we have $J_{\gamma,h}(q_h^*)\leq J_{\gamma,h}(\mathcal{I}_h q^\dagger)$. As a result,

$$\begin{aligned}
&\frac{1}{2}\sum_{\ell=1}^{L}\|w_h^{(\ell)}(q_h^*)-z_\delta^{(\ell)}\|_{L^2(\Omega)}^2+\frac{\gamma L}{2}\|\nabla q_h^*\|_{L^2(\Omega)}^2\\
&\leq\frac{1}{2}\sum_{\ell=1}^{L}\|w_h^{(\ell)}(\mathcal{I}_h q^\dagger)-z_\delta^{(\ell)}\|_{L^2(\Omega)}^2+\frac{\gamma L}{2}\|\nabla\mathcal{I}_h q^\dagger\|_{L^2(\Omega)}^2\\
&\leq\sum_{\ell=1}^{L}\Big(\|w_h^{(\ell)}(\mathcal{I}_h q^\dagger)-w^{(\ell)}(q^\dagger)\|_{L^2(\Omega)}^2+\|u^{(\ell)}(q^\dagger)-z_\delta^{(\ell)}\|_{L^2(\Omega)}^2\Big)+\frac{\gamma L}{2}\|\nabla\mathcal{I}_h q^\dagger\|_{L^2(\Omega)}^2.
\end{aligned}$$

By the interpolation property (2.2) and regularity of $q^\dagger$, the term $\|\nabla \mathcal{I}_h q^\dagger\|_{L^2(\Omega)}$ can be bounded by

$$\begin{aligned}\|\nabla \mathcal{I}_h q^\dagger\|_{L^2(\Omega)} \leq & \|\nabla \mathcal{I}_h q^\dagger - \nabla q^\dagger\|_{L^2(\Omega)} + \|\nabla q^\dagger\|_{L^2(\Omega)} \\ \leq & ch\|q^\dagger\|_{H^2(\Omega)} + \|q^\dagger\|_{H^1(\Omega)} \leq c.\end{aligned}$$

This, together with Corollary 4.1 and the bound for the noise level in (4.13), implies that

$$\frac{1}{2}\sum_{\ell=1}^{L} \|w_h^{(\ell)}(q_h^*) - z_\delta^{(\ell)}\|_{L^2(\Omega)}^2 + \frac{\gamma L}{2}\|\nabla q_h^*\|_{L^2(\Omega)}^2 \leq cL(h^4 L + \delta^2 + \gamma).$$

Hence, we derive $\gamma^{\frac{1}{2}}\|\nabla q_h^*\|_{L^2(\Omega)} \leq c(h^2 L^{\frac{1}{2}} + \delta + \gamma^{\frac{1}{2}})$. Then the triangle inequality and the Cauchy-Schwarz inequality lead to

$$\begin{aligned}\sum_{\ell=1}^{L} \|w_h^{(\ell)}(q_h^*) - w^{(\ell)}(q^\dagger)\|_{L^2(\Omega)} \leq & \sum_{\ell=1}^{L} \|w_h^{(\ell)}(q_h^*) - z_\delta^{(\ell)}\|_{L^2(\Omega)} + \sum_{\ell=1}^{L} \|z_\delta^{(\ell)} - w^{(\ell)}(q^\dagger)\|_{L^2(\Omega)} \\ \leq & L^{\frac{1}{2}}\Big(\sum_{\ell=1}^{L} \|w_h^{(\ell)}(q_h^*) - z_\delta^{(\ell)}\|_{L^2(\Omega)}^2\Big)^{\frac{1}{2}} + L\delta \\ \leq & cL(h^2 L^{\frac{1}{2}} + \delta + \gamma^{\frac{1}{2}}).\end{aligned}$$

□

Next, we state our main theorem, estimating the error between the exact diffusivity coefficient $q^\dagger$ and the numerical reconstruction q_h^*.

Theorem 4.4. *Suppose the exact diffusivity coefficient $q^\dagger$ and the random boundary illuminations $g^{(\ell)}$ (with $\ell = 1, \ldots, L$) satisfy Assumption 4.3. Let $q_h^* \in \mathcal{A}_{q,h}$ be a minimizer of problem (4.16)-(4.17). Set $\eta = h^2 L^{\frac{1}{2}} + \delta + \gamma^{\frac{1}{2}}$. Then, with probability greater than (4.6), we have*

$$\|q^\dagger - q_h^*\|_{L^2(\Omega')}^2 \leq cC_0^{-2}L^2(1+\gamma^{-\frac{1}{2}}\eta)\left(h + h^{1-\epsilon}(1+\gamma^{-\frac{1}{2}}\eta) + \min\left(1, h + h^{-1}L^{-\frac{1}{2}}\eta\right)\right),$$

where $\epsilon > 0$ is arbitrary small, c is a positive constant depending only on Ω and $q^\dagger$, and C_0 is given in (4.7).

Proof. With an abuse of notation, several positive constants depending only on Ω and $q^\dagger$ will be denoted by the same letter c. Let $u^{(\ell)} = u^{(\ell)}(q^\dagger)$ be the solution to (4.15) with boundary value $g^{(\ell)}$. For a test function $\varphi^{(\ell)} \in H_0^1(\Omega)$, we multiply both sides of (4.15) by $(\mathcal{I}_h q^\dagger - q_h^*)\varphi^{(\ell)}/q^\dagger$, and apply integration by parts:

$$0 = \big(q^\dagger \nabla w^{(\ell)}, \nabla \frac{(\mathcal{I}_h q^\dagger - q_h^*)\varphi^{(\ell)}}{q^\dagger}\big) = \big(q^\dagger \varphi^{(\ell)} \nabla w^{(\ell)}, \nabla \frac{(\mathcal{I}_h q^\dagger - q_h^*)}{q^\dagger}\big) + \big((\mathcal{I}_h q^\dagger - q_h^*)\nabla w^{(\ell)}, \nabla \varphi^{(\ell)}\big).$$

Thus, we obtain

$$\big((\mathcal{I}_h q^\dagger - q_h^*)\nabla w^{(\ell)}, \nabla \varphi^{(\ell)}\big) = \frac{1}{2}\big((\mathcal{I}_h q^\dagger - q_h^*)\nabla w^{(\ell)}, \nabla \varphi^{(\ell)}\big) - \frac{1}{2}\big(q^\dagger \varphi^{(\ell)} \nabla w^{(\ell)}, \nabla \frac{(\mathcal{I}_h q^\dagger - q_h^*)}{q^\dagger}\big). \quad (4.21)$$

Set the test function $\varphi^{(\ell)} = (\mathcal{I}_h q^\dagger - q_h^*)u^{(\ell)}/q^\dagger$. We first verify $\varphi^{(\ell)} \in H_0^1(\Omega)$. Since $q_h^* \in \mathcal{A}_{q,h}$, $\varphi^{(\ell)}$ vanishes on $\partial\Omega$. Recall that, under the current assumptions, we have $\|g^{(\ell)}\|_{H^2(\partial\Omega)} \leq L^{\frac{1}{2}}$ for every $\ell = 1, \ldots, L$, cf. Remark 4.3. By the regularity of $q^\dagger$ and $u^{(\ell)}$, and in view of Lemma 4.2, we conclude that $\varphi^{(\ell)} \in H_0^1(\Omega)$, with

$$\|\varphi^{(\ell)}\|_{L^2(\Omega)} = \|(\mathcal{I}_h q^\dagger - q_h^*)w^{(\ell)}/q^\dagger\|_{L^2(\Omega)} \leq 2\underline{c}_q^{-1}\overline{c}_q\|w^{(\ell)}\|_{L^2(\Omega)} \leq cL^{\frac{1}{2}}$$

and

$$\begin{aligned}
\|\nabla\varphi^{(\ell)}\|_{L^2(\Omega)} &= \left\| \frac{q^\dagger\nabla[(\mathcal{I}_h q^\dagger - q_h^*)w^{(\ell)}] - (\mathcal{I}_h q^\dagger - q_h^*)w^{(\ell)}\nabla q^\dagger}{(q^\dagger)^2} \right\|_{L^2(\Omega)} \\
&\leq \underline{c}_q^{-2}\overline{c}_q\|w^{(\ell)}\|_{L^\infty(\Omega)}(\|\nabla\mathcal{I}_h q^\dagger\|_{L^2(\Omega)} + \|\nabla q_h^*\|_{L^2(\Omega)}) \\
&\quad + \underline{c}_q^{-2}\left(2\overline{c}_q^2\|\nabla w^{(\ell)}\|_{L^2(\Omega)} + 2\overline{c}_q\|w^{(\ell)}\|_{L^\infty(\Omega)}\|\nabla q^\dagger\|_{L^2(\Omega)}\right) \\
&\leq cL^{\frac{1}{2}}(1 + \|\nabla q_h^*\|_{L^2(\Omega)}) \leq cL^{\frac{1}{2}}(1 + \gamma^{-\frac{1}{2}}\eta).
\end{aligned} \tag{4.22}$$

With this test function $\varphi^{(\ell)}$, by direct computation, we can further write the left hand side of (4.21) as

$$\big((\mathcal{I}_h q^\dagger - q_h^*)\nabla w^{(\ell)}, \nabla\varphi^{(\ell)}\big) = \frac{1}{2}\int_\Omega \frac{(\mathcal{I}_h q^\dagger - q_h^*)^2}{q^\dagger}|\nabla w^{(\ell)}|^2 \mathrm{d}x. \tag{4.23}$$

On the other hand, by the weak formulation of (4.15) and (4.17), we have

$$\begin{aligned}
\big((\mathcal{I}_h q^\dagger - q_h^*)\nabla w^{(\ell)}, \nabla\varphi^{(\ell)}\big) &= \big((\mathcal{I}_h q^\dagger - q^\dagger)\nabla w^{(\ell)}, \nabla\varphi^{(\ell)}\big) + \big((q^\dagger - q_h^*)\nabla w^{(\ell)}, \nabla\varphi^{(\ell)}\big) \\
&= \big((\mathcal{I}_h q^\dagger - q^\dagger)\nabla w^{(\ell)}, \nabla\varphi^{(\ell)}\big) + \big((q^\dagger - q_h^*)\nabla w^{(\ell)}, \nabla(\varphi^{(\ell)} - P_h\varphi^{(\ell)})\big) \\
&\qquad + \big(q_h^*\nabla(w_h^{(\ell)}(q_h^*) - w^{(\ell)}), \nabla P_h\varphi^{(\ell)}\big) \\
&= \mathrm{I}_1^{(\ell)} + \mathrm{I}_2^{(\ell)} + \mathrm{I}_3^{(\ell)}.
\end{aligned}$$

For $\mathrm{I}_1^{(\ell)}$, the interpolation error (2.2) and the estimate (4.22) yield that

$$|\mathrm{I}_1^{(\ell)}| \leq c\|\mathcal{I}_h q^\dagger - q^\dagger\|_{L^\infty(\Omega)}\|\nabla w^{(\ell)}\|_{L^2(\Omega)}\|\nabla\varphi^{(\ell)}\|_{L^2(\Omega)} \leq chL(1 + \gamma^{-\frac{1}{2}}\eta).$$

Now, we consider $\mathrm{I}_2^{(\ell)}$. Applying integration by parts, the regularity of $q^\dagger$ and $w^{(\ell)}$, the inverse inequality (2.1), the projection error (2.3) and estimate (4.22) imply that

$$\begin{aligned}
|\mathrm{I}_2^{(\ell)}| &= |\big(\nabla\cdot((q^\dagger - q_h^*)\nabla w^{(\ell)}), \varphi^{(\ell)} - P_h\varphi^{(\ell)}\big)| \\
&\leq \big(\|\nabla(q^\dagger - q_h^*)\|_{L^q(\Omega)}\|\nabla u^{(\ell)}\|_{L^p(\Omega)} + \|q^\dagger - q_h^*\|_{L^\infty(\Omega)}\|\Delta w^{(\ell)}\|_{L^2(\Omega)}\big)\|\varphi^{(\ell)} - P_h\varphi^{(\ell)}\|_{L^2(\Omega)} \\
&\leq ch\left(L^{\frac{1}{2}} + L^{\frac{1}{2}}h^{d/q-d/2}\|\nabla q_h^*\|_{L^2(\Omega)})\right)\|\varphi^{(\ell)}\|_{H^1(\Omega)} \\
&\leq ch^{1+d/q-d/2}L(1 + \gamma^{-\frac{1}{2}}\eta)^2 = ch^{1-\epsilon}L(1 + \gamma^{-\frac{1}{2}}\eta)^2.
\end{aligned}$$

Here $\frac{1}{p} + \frac{1}{q} + \frac{1}{2} = 1$ with $q = \frac{2d}{d-2\epsilon}$. To estimate $\mathrm{I}_3^{(\ell)}$, by the inverse inequality (2.1) and the projection

error (2.3), we first derive that

$$\begin{aligned}\|\nabla w^{(\ell)} - \nabla w_h^{(\ell)}(q_h^*)\|_{L^2(\Omega)} \leq & \|\nabla w^{(\ell)} - \nabla P_h w^{(\ell)}\|_{L^2(\Omega)} + \|\nabla P_h w^{(\ell)} - \nabla w_h^{(\ell)}(q_h^*)\|_{L^2(\Omega)} \\ \leq & c\big(h\|w^{(\ell)}\|_{H^2(\Omega)} + h^{-1}\|P_h w^{(\ell)} - w_h^{(\ell)}(q_h^*)\|_{L^2(\Omega)}\big) \\ \leq & c\big(hL^{\frac{1}{2}} + h^{-1}\|u^{(\ell)} - w_h^{(\ell)}(q_h^*)\|_{L^2(\Omega)}\big).\end{aligned}$$

There obviously holds that $\|\nabla w^{(\ell)} - \nabla w_h^{(\ell)}(q_h^*)\|_{L^2(\Omega)} \leq cL^{\frac{1}{2}}$. Therefore, by using these two inequalities, (4.22) and Lemma 4.2, we obtain

$$\begin{aligned}\sum_{\ell=1}^{L} |\mathrm{I}_3^{(\ell)}| &\leq \sum_{\ell=1}^{L} \|q_h^*\|_{L^\infty(\Omega)} \|\nabla w_h^{(\ell)}(q_h^*) - \nabla w^{(\ell)}\|_{L^2(\Omega)} \|\nabla P_h \varphi^{(\ell)}\|_{L^2(\Omega)} \\ &\leq cL^{\frac{1}{2}}(1+\gamma^{-\frac{1}{2}}\eta) \sum_{\ell=1}^{L} \|\nabla w_h^{(\ell)}(q_h^*) - \nabla u^{(\ell)}\|_{L^2(\Omega)} \\ &\leq cL^{\frac{1}{2}}(1+\gamma^{-\frac{1}{2}}\eta) \min\Big(L^{\frac{3}{2}}, L^{\frac{3}{2}}h + h^{-1}\sum_{\ell=1}^{L} \|w_h^{(\ell)}(q_h^*) - w^{(\ell)}\|_{L^2(\Omega)}\Big) \\ &\leq cL^2(1+\gamma^{-\frac{1}{2}}\eta) \min\Big(1, h + h^{-1}L^{-\frac{1}{2}}\eta\Big).\end{aligned}$$

Taking summation with respect to $\ell = 1, \ldots, L$ in (4.23), the estimates of $\mathrm{I}_1^{(\ell)}, \mathrm{I}_2^{(\ell)}, \mathrm{I}_3^{(\ell)}$ yield that

$$\begin{aligned}&\frac{1}{2}\int_\Omega \frac{(\mathcal{I}_h q^\dagger - q_h^*)^2}{q^\dagger} \sum_{\ell=1}^{L} |\nabla w^{(\ell)}|^2 \mathrm{d}x \\ &\qquad \leq cL^2(1+\gamma^{-\frac{1}{2}}\eta)\left(h + h^{1-\epsilon}(1+\gamma^{-\frac{1}{2}}\eta) + \min\left(1, h + h^{-1}L^{-\frac{1}{2}}\eta\right)\right).\end{aligned}$$

Applying the interpolation error bound $\|q^\dagger - \mathcal{I}_h q^\dagger\|_{L^2(\Omega)} \leq Ch^2\|q^\dagger\|_{H^2(\Omega)}$ (see (2.2)), we arrive at the weighted estimate

$$\begin{aligned}&\frac{1}{2}\int_\Omega \frac{(q^\dagger - q_h^*)^2}{q^\dagger} \sum_{\ell=1}^{L} |\nabla w^{(\ell)}|^2 \mathrm{d}x \\ &\qquad \leq cL^2h^4 + cL^2(1+\gamma^{-\frac{1}{2}}\eta)\left(h + h^{1-\epsilon}(1+\gamma^{-\frac{1}{2}}\eta) + \min\left(1, h + h^{-1}L^{-\frac{1}{2}}\eta\right)\right).\end{aligned}$$

By Proposition 4.1, we have the non-zero condition (4.7):

$$\sum_{\ell=1}^{L} |\nabla w^{(\ell)}(x)|^2 \geq C_0^2, \quad \text{for all } x \in \Omega'.$$

Hence, we conclude

$$\|q^\dagger - q_h^*\|_{L^2(\Omega')}^2 \leq cC_0^{-2}L^2h^4 + cC_0^{-2}L^2(1+\gamma^{-\frac{1}{2}}\eta)\left(h + h^{1-\epsilon}(1+\gamma^{-\frac{1}{2}}\eta) + \min\left(1, h + h^{-1}L^{-\frac{1}{2}}\eta\right)\right).$$

□

Remark 4.4. *Theorem 4.4 provides a guideline for the a priori choice of the algorithmic parameters h and γ, in relation to δ. The choice $h^2L^{\frac{1}{2}} \sim \delta$ and $\gamma \sim \delta^2$ yields a convergence rate*

$$\|q^\dagger - q_h^*\|_{L^2(\Omega)} \leq cL^{\frac{7}{8}}\delta^{\frac{1}{4}-\epsilon},$$

with $\epsilon > 0$ arbitrary small. This rate is consistent with the stability in Theorem 4.2, that shows

$$\|q^\dagger - q\|_{L^2(\Omega)} \leq cL^{\frac{1}{4}} \Big(\sum_{\ell=1}^{L} \|w^{(\ell)}(q^\dagger) - w^{(\ell)}(q)\|_{H^1(\Omega)} \Big)^{\frac{1}{2}}.$$

Thus, the Gagliardo-Nirenberg interpolation inequality [25]

$$\|w^{(\ell)}\|_{H^1(\Omega)} \leq \|w^{(\ell)}\|^{\frac{1}{2}}_{L^2(\Omega)} \|w^{(\ell)}\|^{\frac{1}{2}}_{H^2(\Omega)},$$

and the regularity $\|w^{(\ell)}(q^\dagger)\|_{H^2(\Omega)} + \|w^{(\ell)}(q)\|_{H^2(\Omega)} \leq c\|g^{(\ell)}\|_{H^2(\partial\Omega)} \leq cL^{\frac{1}{2}}$ directly yields

$$\begin{aligned} \|q^\dagger - q\|_{L^2(\Omega)} &\leq cL^{\frac{1}{4}} \Big(\sum_{\ell=1}^{L} (\|w^{(\ell)}(q^\dagger)\|_{H^2(\Omega)} + \|w^{(\ell)}(q^\dagger)\|_{H^2(\Omega)})^{\frac{1}{2}} \|w^{(\ell)}(q^\dagger) - w^{(\ell)}(q)\|^{\frac{1}{2}}_{L^2(\Omega)} \Big)^{\frac{1}{2}} \\ &\leq cL^{\frac{7}{8}} \delta^{\frac{1}{4}}. \end{aligned}$$

Remark 4.5. *In two dimensions, the above analysis can be extended to the case where Ω is a convex polygon. We parameterize $\partial\Omega$ by arc length and generate $H^{\frac{1}{2}}(\partial\Omega)$ orthonormal basis using the eigenvalues and eigenfunctions of Laplace–Beltrami operator on $\partial\Omega$. Indeed, the eigenfunctions are trigonometric functions on each edge which are continuous at each vertex. Therefore, with appropriate normalization, we obtain the $H^{\frac{1}{2}}(\partial\Omega)$ orthonormal basis. With the same argument as in Remark 4.3, the following upper bound holds with high probability*

$$\sum_{i=1}^{N} \|g^{(\ell)}\|_{H^2(\Gamma_i)} \leq CL^{\frac{1}{2}}, \quad \ell = 1, \ldots, L,$$

where Γ_i, $i = 1, \ldots, N$ are the edges of the polygon Ω. As a consequence, the forward problem (4.15) *admits $H^2(\Omega)$ solutions [60, Theorem 5.1.2.4] and the $L^2(\Omega)$ error estimate $\|w^{(\ell)}(q^\dagger) - w^{(\ell)}_h(q^\dagger)\|_{L^2(\Omega)} \leq ch^2 L^{\frac{1}{2}}$ holds as a consequence of [52, Corollary 3.29].*

4.2 Quantitative Photoacoustic Tomography

In this section, we study the numerical inversion scheme for quantitative photoacoustic tomography. We consider the case where radiation propagation is approximated by a second-order elliptic equation (4.1). Our objective is to numerically reconstruct the true diffusion coefficient $D^\dagger$ and absorption coefficient $\sigma^\dagger$ from multiple internal observations

$$H^{(\ell)}(x) = \sigma^\dagger u^{(\ell)}(x; D^\dagger, \sigma^\dagger) \quad \text{for all} \quad x \in \Omega,$$

where $u^{(\ell)} := u^{(\ell)}(D^\dagger, \sigma^\dagger)$ denotes the solution to the elliptic equation (4.1) with parameters $D^\dagger$ and $\sigma^\dagger$, and associated with the Dirichlet boundary illuminations $g^{(\ell)}$, $\ell = 1, 2, \ldots, L+1$:

$$\begin{cases} -\nabla \cdot (D^\dagger \nabla u^{(\ell)}) + \sigma^\dagger u^{(\ell)} = 0 & \text{in } \Omega, \\ u^{(\ell)} = g^{(\ell)} & \text{on } \partial\Omega. \end{cases} \tag{4.24}$$

We need the following assumptions on the parameters and boundary data. In particular, as in the previous section, we assume the parameters to be known in $\Omega \setminus \Omega'$.

Assumption 4.5. *We assume that the parameters and boundary data satisfy the following assumptions.*

(i) Let $\Omega \subset \mathbb{R}^d$ ($d = 2, 3$) be a bounded domain with $C^{1,1}$ boundary $\partial\Omega$. The exact diffusion coefficient $D^\dagger \in W^{2,p}(\Omega) \cap \mathcal{A}_D$ with $p > d$ and the exact absorption coefficient $\sigma^\dagger \in \mathcal{A}_\sigma$, where

$$\mathcal{A}_D = \{D \in W^{1,\infty}(\Omega) :\ 0 < \underline{c}_D \le D \le \overline{c}_D \text{ a.e. in } \Omega,\ D = D^\dagger \text{ a.e. in } \Omega \setminus \Omega'\} \text{ and}$$
$$\mathcal{A}_\sigma = \{\sigma \in L^\infty(\Omega) :\ 0 < \underline{c}_\sigma \le \sigma \le \overline{c}_\sigma \text{ a.e. in } \Omega,\ \sigma = \sigma^\dagger \text{ a.e. in } \Omega \setminus \Omega'\},$$

with some a priori known positive constants $\overline{c}_D$ and $\overline{c}_\sigma$.

(ii) Let $g^{(1)} \equiv 1$, and $g^{(\ell)}$ (with $\ell = 2, \dots, L+1$) be independent and identically distributed random boundary data given by the expansion (4.5) satisfying Assumption 4.3.

We assume that the empirical observational data, denoted by $Z_\delta^{(\ell)}$ is noisy in the sense that

$$\|Z_\delta^{(\ell)} - H^{(\ell)}\|_{L^2(\Omega)} \le \delta, \quad \text{for all } \ \ell = 1, 2, \dots, L+1. \tag{4.25}$$

Assumption 4.5 together with the elliptic maximum principle implies that $0 < \underline{c}_0 \le H^{(1)} \le 1$ for some positive constant $\underline{c}_0$. Without loss of generality, we assume that the empirical observation $Z_\delta^{(1)}$ satisfies the same bound $0 < \underline{c}_0 \le Z_\delta^{(1)} \le 1$. Indeed, otherwise, it is enough to project $Z_\delta^{(1)}$ pointwise onto $[\underline{c}_0, 1]$, which preserves (4.25).

For $\ell = 1, 2, \dots, L$, we define

$$q^\dagger = D^\dagger |u^{(1)}|^2, \ \ w_\delta^{(\ell)} = \frac{Z_\delta^{(\ell+1)}}{Z_\delta^{(1)}}, \ \ w^{(\ell)} = \frac{H^{(\ell+1)}}{H^{(1)}} = \frac{u^{(\ell+1)}}{u^{(1)}} \text{ in } \Omega,$$

and

$$f^{(\ell)} = \frac{g^{(\ell+1)}}{g^{(1)}} = g^{(\ell+1)} \text{ on } \partial\Omega.$$

It is straightforward to observe that

$$\begin{aligned}
\|w_\delta^{(\ell)} - w^{(\ell)}\|_{L^2(\Omega)} &\le \Big\| \frac{Z_\delta^{(\ell+1)} H^{(1)} - H^{(1)} H^{(\ell+1)}}{H^{(1)} Z_\delta^{(1)}} \Big\|_{L^2(\Omega)} + \Big\| \frac{H^{(1)} H^{(\ell+1)} - Z_\delta^{(1)} H^{(\ell+1)}}{H^{(1)} Z_\delta^{(1)}} \Big\|_{L^2(\Omega)} \\
&\le \frac{1}{\underline{c}_0^2} \Big(\|H^{(1)}(Z_\delta^{(\ell+1)} - H^{(\ell+1)})\|_{L^2(\Omega)} + \|H^{(\ell+1)}(H^{(1)} - Z_\delta^{(1)})\|_{L^2(\Omega)} \Big) \\
&\le c\delta.
\end{aligned}$$

A direct calculation ([16, 15]) shows that $w^{(\ell)}$ is the solution of the following elliptic equation

$$\begin{cases} -\nabla \cdot (q^\dagger \nabla w^{(\ell)}) = 0, & \text{in } \Omega, \\ w^{(\ell)} = f^{(\ell)}, & \text{on } \partial\Omega. \end{cases} \tag{4.26}$$

Thus, the first step of the reconstruction algorithm consists of the recovery of $q^\dagger$ from the practical observation $w_\delta^{(\ell)}$. This is the inverse diffusivity problem discussed in Section 4.1. Indeed, Assumption 4.5 and elliptic regularity [58, Theorem 9.15] imply $u^{(1)} \in W^{2,p}(\Omega)$ and hence $q^\dagger \in W^{2,p}(\Omega)$. By the bounds of $D^\dagger$ and maximum principle, we may assume that the diffusivity coefficient $q^\dagger$ has positive lower and upper bound $0 < \underline{c}_q \le q \le \overline{c}_q$. Moreover, since $g^{(1)} \equiv 1$, the boundary data $f^{(\ell)} = g^{(\ell+1)}$ still satisfy Assumption 4.3 and the non-zero condition given in Proposition 4.1 holds for equation (4.26). Therefore, as in Section 4.1.2 we propose to consider the following least-squares formula with $H^1(\Omega)$-seminorm penalty:

$$\min_{q_h \in \mathcal{A}_{q,h}} J_{\gamma,h}(q_h) = \frac{1}{2}\sum_{\ell=1}^{L} \|w_h^{(\ell)}(q_h) - w_\delta^{(\ell)}\|_{L^2(\Omega)}^2 + \frac{\gamma L}{2}\|\nabla q_h\|_{L^2(\Omega)}^2, \tag{4.27}$$

where the admissible set $\mathcal{A}_{q,h}$ is defined in (4.18) and $w_h^{(\ell)}(q_h) \in V_h$ is the weak solution of

$$\begin{cases} (q_h \nabla w_h^{(\ell)}, \nabla v_h) = 0, & \forall v_h \in V_h^0, \\ w_h^{(\ell)} = \mathcal{I}_h^\partial f^{(\ell)}, & \text{on } \partial\Omega. \end{cases} \tag{4.28}$$

The following error analysis is a direct consequence of Theorem 4.4.

Proposition 4.2. *Suppose Assumption 4.5 holds valid and set $q^\dagger = D^\dagger |u^{(1)}|^2$. Let $q_h^* \in \mathcal{A}_{q,h}$ be a minimizer of problem (4.27)-(4.28). Set $\eta = h^2 L^{\frac{1}{2}} + \delta + \gamma^{\frac{1}{2}}$. Then, with probability greater than (4.6), we have*

$$\|q^\dagger - q_h^*\|_{L^2(\Omega')}^2 \le CL^2(1+\gamma^{-\frac{1}{2}}\eta)\left(h + h^{1-\epsilon}(1+\gamma^{-\frac{1}{2}}\eta) + \min\left(1, h + h^{-1}L^{-\frac{1}{2}}\eta\right)\right),$$

where c is a constant independent of h, δ, γ and L.

The second step of the inverse algorithm is to recover $u^{(1)}$. The reconstruction of $D^\dagger$ and $\sigma^\dagger$ will follow immediately by using the relations $D^\dagger = q^\dagger/|u^{(1)}|^2$ and $\sigma^\dagger = H^{(1)}/u^{(1)}$. Since $u^{(1)}|_{\partial\Omega} = g^{(1)} \equiv 1$, by (4.24) we have that $v = 1/u^{(1)} - 1$ satisfies the following boundary value problem

$$\begin{cases} -\nabla \cdot (q^\dagger \nabla v) = H^{(1)}, & \text{in } \Omega, \\ v = 0, & \text{on } \partial\Omega. \end{cases} \tag{4.29}$$

We are now ready to show the error bound of the numerically recovered parameters.

Theorem 4.6. *Suppose that Assumption 4.5 holds valid and set $q^\dagger = D^\dagger |u^{(1)}|^2$. Let $q_h^* \in \mathcal{A}_{q,h}$ be such that $\|q^\dagger - q_h^*\|_{L^2(\Omega')} \le \xi$ for some $\xi \ge 0$ and set the reconstructed coefficient q^* as*

$$q^* = \begin{cases} q_h^* & \text{in } \Omega', \\ D^\dagger (Z_\delta^{(1)}/\sigma^\dagger)^2 & \text{in } \Omega \setminus \Omega'. \end{cases}$$

Let $v_h \in V_h^0$ solve

$$(q^* \nabla v_h, \nabla \varphi_h) = (Z_\delta^{(1)}, \varphi_h), \quad \forall \varphi_h \in V_h^0. \tag{4.30}$$

Then there holds

$$\|v - v_h\|_{L^2(\Omega)} \leq C(h + \xi + \delta).$$

Moreover, set $D^* = q^*|v_h + 1|^2$ and $\sigma^* = Z_\delta^{(1)}(v_h + 1)$, we have

$$\|D^\dagger - D^*\|_{L^2(\Omega)} \leq C(h + \xi + \delta) \quad \textit{and} \quad \|\sigma^\dagger - \sigma^*\|_{L^2(\Omega)} \leq C(h + \xi + \delta),$$

where c is a constant independent of h, δ and ξ.

Proof. We observe that

$$\begin{aligned}
\|q^\dagger - q^*\|_{L^2(\Omega\setminus\Omega')} &= \Big\| D^\dagger \frac{(H^{(1)})^2}{(\sigma^\dagger)^2} - D^\dagger \frac{(Z_\delta^{(1)})^2}{(\sigma^\dagger)^2} \Big\|_{L^2(\Omega\setminus\Omega')} \\
&\leq \underline{c}_\sigma^{-2} \overline{c}_D \|H^{(1)} + Z_\delta^{(1)}\|_{L^\infty(\Omega\setminus\Omega')} \|H^{(1)} - Z_\delta^{(1)}\|_{L^2(\Omega\setminus\Omega')} \\
&\leq c\delta.
\end{aligned}$$

By equation (4.29) and (4.30), we have

$$\begin{aligned}
(q^*(\nabla P_h v - \nabla v_h), \nabla \varphi_h) &= (q^*(\nabla P_h v - \nabla v), \nabla \varphi_h) + (q^*(\nabla v - \nabla v_h), \nabla \varphi_h) \\
&= (q^*(\nabla P_h v - \nabla v), \nabla \varphi_h) + ((q^* - q^\dagger)\nabla v, \nabla \varphi_h) + (H^{(1)} - Z_\delta^{(1)}, \varphi_h).
\end{aligned}$$

Taking $\varphi_h = P_h v - v_h$, Cauchy-Schwarz inequality and Poincáre's inequality yield

$$\begin{aligned}
\|\nabla \varphi_h\|_{L^2(\Omega)}^2 \leq & c\|\nabla(P_h v - v)\|_{L^2(\Omega)} \|\nabla \varphi_h\|_{L^2(\Omega)} + c\|\nabla v\|_{L^\infty(\Omega)} \|q^* - q^\dagger\|_{L^2(\Omega)} \|\nabla \varphi_h\|_{L^2(\Omega)} \\
& + c\|H^{(1)} - Z_\delta^{(1)}\|_{L^2(\Omega)} \|\nabla \varphi_h\|_{L^2(\Omega)}.
\end{aligned}$$

By elliptic regularity theory, we have $v \in H^2(\Omega) \cap W^{1,\infty}(\Omega)$. Hence, by the projection error (2.3), estimate of q^* and the noise level (4.25), we derive that

$$\|\nabla P_h v - \nabla v_h\|_{L^2(\Omega)} = \|\nabla \varphi_h\|_{L^2(\Omega)} \leq c(h + \xi + \delta).$$

Thus, by Poincáre's inequality and the error bound (2.3), we conclude

$$\|v - v_h\|_{L^2(\Omega)} \leq \|P_h v - v_h\|_{L^2(\Omega)} + \|P_h v - v\|_{L^2(\Omega)} \leq c(h + \xi + \delta).$$

Moreover, direct computation yields

$$\begin{aligned}
\|D^\dagger - D^*\|_{L^2(\Omega)} &= \Big\| \frac{q^\dagger}{|u^{(1)}|^2} - q^*|v_h + 1|^2 \Big\|_{L^2(\Omega)} = \Big\| q^\dagger |v + 1|^2 - q^*|v_h + 1|^2 \Big\|_{L^2(\Omega)} \\
&\leq \Big\| (q^\dagger - q^*)|v + 1|^2 \Big\|_{L^2(\Omega)} + \Big\| q^*(|v + 1|^2 - |v_h + 1|^2) \Big\|_{L^2(\Omega)} \\
&\leq c(\xi + \delta) + c(h + \xi + \delta) \leq c(h + \xi + \delta),
\end{aligned}$$

and

$$\|\sigma^\dagger - \sigma^*\|_{L^2(\Omega)} = \left\| \frac{H^{(1)}}{u^{(1)}} - Z_\delta^{(1)}(v_h+1) \right\|_{L^2(\Omega)} = \left\| H^{(1)}(v+1) - Z_\delta^{(1)}(v_h+1) \right\|_{L^2(\Omega)}$$
$$\leq \|(H^{(1)} - Z_\delta^{(1)})(v+1)\|_{L^2(\Omega)} + \|Z_\delta^{(1)}(v - v_h)\|_{L^2(\Omega)}$$
$$\leq c\delta + c(h+\xi+\delta) \leq c(h+\xi+\delta).$$

□

Remark 4.6. *The error analysis in Proposition 4.2 and Theorem 4.6 provide a guideline for choosing the mesh size h and regularization parameter γ, see also Remark 4.4. Indeed, by choosing $h^2 L^{\frac{1}{2}} \sim \delta$ and $\gamma \sim \delta^2$, with probability greater than* (4.6)*, there holds*

$$\|D^\dagger - D_h^*\|_{L^2(\Omega)} + \|\sigma^\dagger - \sigma_h^*\|_{L^2(\Omega)} \leq cL^{\frac{7}{8}} \delta^{\frac{1}{4}-\epsilon}.$$

4.3 Numerical results

In this section, we provide numerical reconstructions of the diffusion coefficient $D^\dagger$ and the absorption coefficient $\sigma^\dagger$ based on the two stage algorithm discussed in Section 4.2. We first solve the optimization problem (4.27)-(4.28) and then solve the direct problem (4.30). We consider the two-dimensional setting ($d = 2$).

4.3.1 Numerical implementation

In this part, we introduce the numerical implementation for the reconstruction algorithm. We first describe the generation of the boundary illuminations $g^{(\ell)}$, $\ell = 1, \ldots, L+1$. Recall in Assumption 4.5(iii), $g^{(1)} \equiv 1$ is fixed and $g^{(\ell)}$ (with $\ell = 2, \ldots, L+1$) are taken as

$$g^{(\ell)} = \sum_{k=1}^{M} a_k^{(\ell)} e_k,$$

where $\{e_k\}_{k=1}^\infty$ is a fixed orthonormal basis of $H^{\frac{1}{2}}(\partial\Omega)$ generated by the eigenfunctions of Laplace–Beltrami operator. The coefficients $a_k^{(\ell)} \sim N(0, \theta_k^2)$ are independent and identically distributed random variables satisfying Assumption 4.3 with $\theta_k = k^{-2}$ and $s = \frac{5}{2}$.

In all the examples, we take the first five terms in the series, i.e. $M = 5$. With the truncated boundary illuminations, we generate noisy measurements as follows:

$$Z_\delta^{(\ell)}(x) = H^{(\ell)}(x) + \delta \sup_{z\in\Omega} |H^{(\ell)}(z)| \xi(x), \quad \ell = 1, \ldots, L+1,$$

where ξ follows standard Gaussian distribution, while δ denotes the level of noise. The exact data $H^{(\ell)} = \sigma^\dagger u^{(\ell)}(D^\dagger, \sigma^\dagger)$ correspond to the precise values of $D^\dagger$ and $\sigma^\dagger$, calculated using a highly refined mesh with $h = \frac{1}{500}$.

4.3.2 Numerical experiments

In this part, we provide numerical verification of the non-zero condition in Proposition 4.1 and the numerical reconstructions of the diffusion coefficient $D^\dagger$ and the absorption coefficient $\sigma^\dagger$. To verify the non-zero condition, we plot the region in which

$$\max_{\ell=1,\dots,L} |\nabla w^{(\ell)}(x) \cdot \nu| \geq C_0, \quad x \in \Omega,$$

where $w^{(\ell)}(x) = H^{(\ell+1)}/H^{(1)}$. In the following numerical experiments, we fix the direction $\nu = (1, 0)$ and the threshold $C_0 = 0.1$. To quantify the performance of the numerical reconstruction, we introduce the following relative $L^2(\Omega)$ error:

$$e_D = \|D_h^* - D^\dagger\|_{L^2(\Omega)}/\|D^\dagger\|_{L^2(\Omega)} \quad \text{and} \quad e_\sigma = \|\sigma_h^* - \sigma^\dagger\|_{L^2(\Omega)}/\|\sigma^\dagger\|_{L^2(\Omega)}.$$

We start with the following examples with smooth coefficients.

Example 4.1. $\Omega = (0, 1)^2$, $D^\dagger(x, y) = 2 + \sin(2\pi x)\sin(2\pi y)$ *and* $\sigma^\dagger = 6 + 4\sigma_1 + 4\sigma_2$ *with* $\sigma_1(x, y) = e^{-20(x-0.3)^2-20(y-0.7)^2}$ *and* $\sigma_2(x, y) = e^{-20(x-0.7)^2-20(y-0.3)^2}$.

Table 4.1: The convergence rates for Example 4.1 with respect to δ.

δ	1e-2	5e-3	2e-3	1e-3	5e-4	2e-4	1e-4	rate
e_D	6.53e-2	4.17e-2	2.98e-2	2.61e-2	2.33e-2	2.30e-2	2.12e-2	$O(\delta^{0.22})$
e_σ	1.45e-2	7.90e-3	5.23e-3	4.77e-3	4.13e-3	4.06e-3	3.76e-3	$O(\delta^{0.26})$

In Figure 4.1(a), we plot the random boundary data $f^{(\ell)} = g^{(\ell+1)}/g^{(1)} = g^{(\ell+1)}$. We show the region in which the non-zero condition is satisfied with different L in Figures 4.1(b)-(f). We observe that the region where the non-zero condition is satisfied expands as the number of random boundary data increases. For $L = 1$, the non-zero condition is satisfied only in a small region, while for $L = 3$, the non-zero condition is satisfied in most parts of the domain Ω. We also notice that as L increases, the lower bound C_0 increases, indicating better stability of the inverse problem.

Table 4.1 displays the convergence rate of the reconstruction errors. The mesh size and the regularization parameter are chosen by following the guidelines in Remark 4.6 with fixed number of illuminations $L = 5$: $h \sim \delta^{\frac{1}{2}}$ and $\gamma \sim \delta^2$. We initialize the mesh size $h = 1/12$ and the regularization parameter $\gamma = 3e\text{-}7$. The numerical results indicate that the error e_D and e_σ decay to zero as the noise level tends to zero, with rate $O(\delta^{0.22})$ and $O(\delta^{0.26})$, respectively. These convergence rates are consistent with the rate predicted in Remark 4.6, which is $O(\delta^{0.25})$. Figure 4.2 shows the recovered diffusion coefficient and absorption coefficient in 5% and 1% noise. Here we take $h = 1/20$, $\gamma = 1e\text{-}6$ for noise level $\delta = 5e\text{-}2$ and $h = 1/45$, $\gamma = 4e\text{-}8$ for $\delta = 1e\text{-}2$.

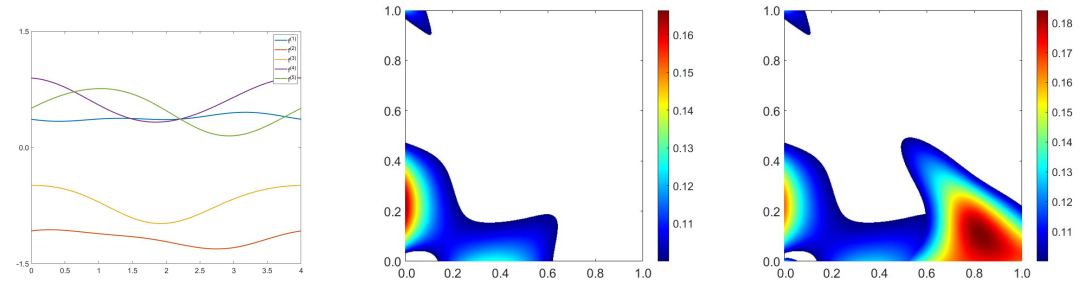

(a) Boundary $f^{(\ell)}$ (b) $L = 1$ (c) $L = 2$

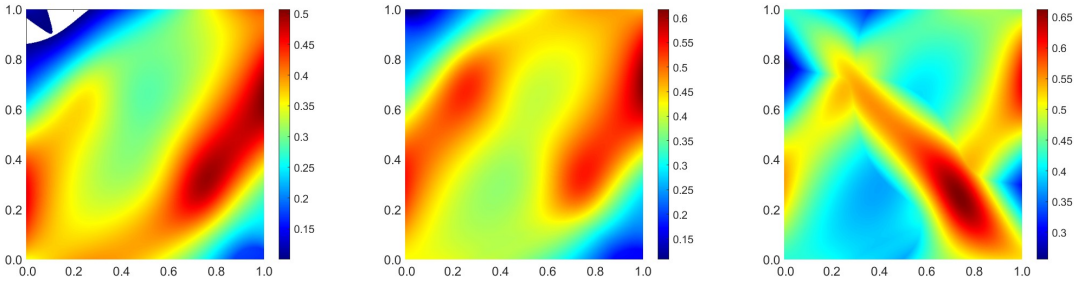

(d) $L = 3$ (e) $L = 4$ (f) $L = 5$

Figure 4.1: Boundary illuminations and the non-zero region of Example 4.1. Top left: plot of boundary data $f^{(\ell)} = g^{(\ell+1)}$. Top middle to bottom right: region where the non-zero condition is satisfied as the number of boundary inputs increases.

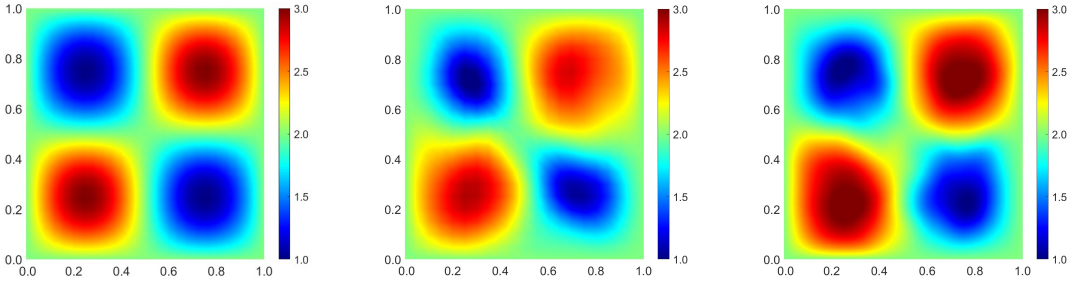

(a) $D^\dagger$ (b) $\delta = 5e\text{-}2$ (c) $\delta = 1e\text{-}2$

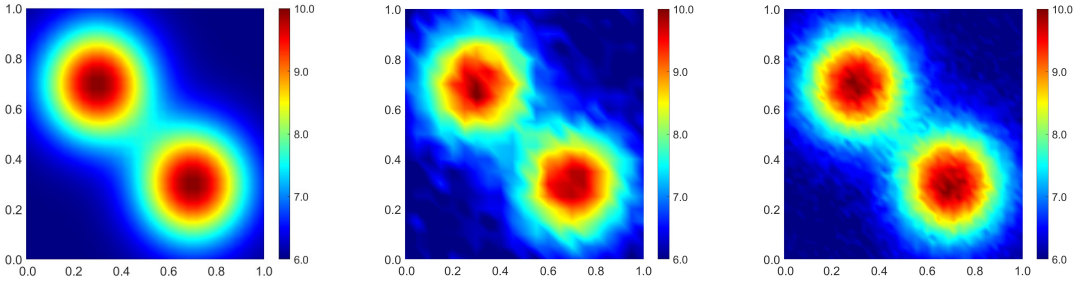

(d) $\sigma^\dagger$ (e) $\delta = 5e\text{-}2$ (f) $\delta = 1e\text{-}2$

Figure 4.2: Example 4.1. First row: reconstructions of $D^\dagger$. Second row: reconstructions of $\sigma^\dagger$.

Example 4.2. $\Omega = (0,1)^2$, $D^\dagger = 1 + D_1 - \frac{1}{2}D_2 - \frac{1}{2}D_3$ *with* $D_1(x,y) = e^{-40(x-0.5)^2-40(y-0.7)^2}$, $D_2(x,y) = e^{-15(x-0.3)^2-15(y-0.3)^2}$, $D_3(x,y) = e^{-15(x-0.7)^2-15(y-0.3)^2}$ *and the absorption coefficient* $\sigma^\dagger(x,y) = 1 + 0.5\sin(\pi x)\sin(\pi y)e^{-4(1-x)y}$.

Table 4.2: The convergence rates for Example 4.2 with respect to δ.

δ	1e-2	5e-3	2e-3	1e-3	5e-4	2e-4	1e-4	rate
e_D	6.34e-2	5.72e-2	3.47e-2	2.65e-2	2.40e-2	1.85e-2	1.24e-2	$O(\delta^{0.35})$
e_σ	1.04e-2	5.67e-3	4.08e-3	2.95e-3	2.70e-3	1.84e-3	1.24e-3	$O(\delta^{0.42})$

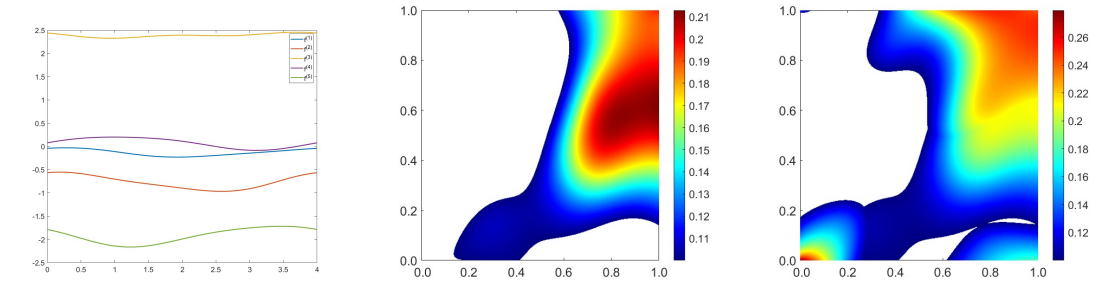

(a) Boundary $f^{(\ell)}$ (b) $L = 1$ (c) $L = 2$

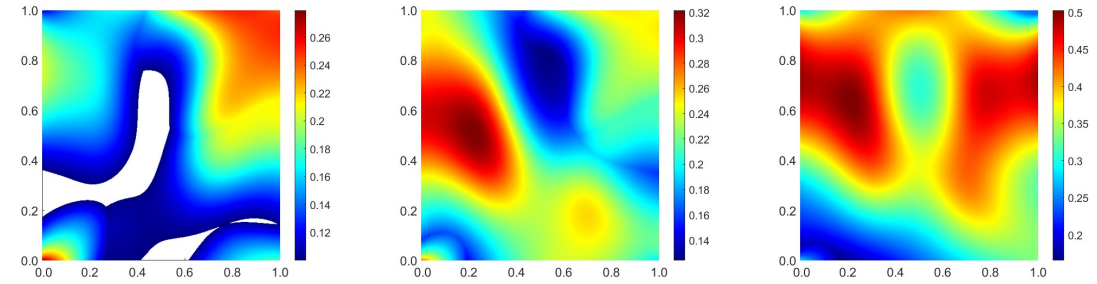

(d) $L = 3$ (e) $L = 4$ (f) $L = 5$

Figure 4.3: Boundary illuminations and the non-zero region of Example 4.2. Top left: plot of boundary data $f^{(\ell)} = g^{(\ell+1)}$. Top middle to bottom right: region which satisfying the non-zero condition as number of boundary input increasing.

The region representing the non-zero condition and the numerical reconstructions of Example 4.2 are shown in Figures 4.3-4.4 and Table 4.2. For the non-zero condition region, we observe a similar behavior as in Example 4.1, the region enlarges with the addition of boundary illuminations. For testing the convergence rates of reconstruction errors, we initially choose the mesh size $h = 1/12$ and the regularization parameter $\gamma = 5e\text{-}7$. We observe the convergence rate $O(\delta^{0.35})$ for e_D and $O(\delta^{0.42})$ for e_σ. The experimental convergence rates are slightly higher than the theoretical rate $O(\delta^{0.25})$. Since in the first step of the reconstruction algorithm we need to solve an optimization problem to get q_h^*,

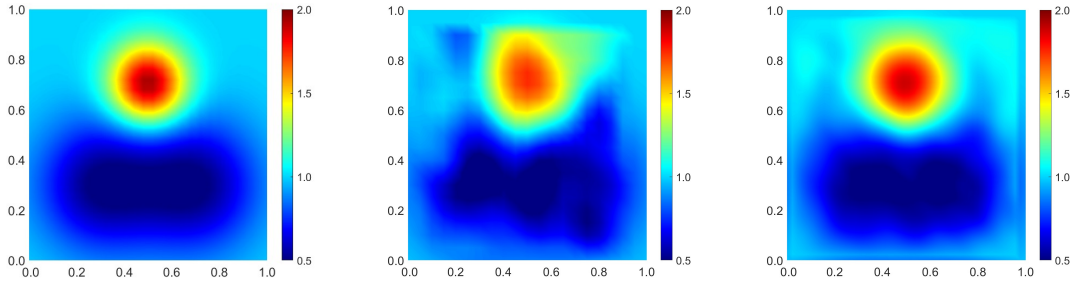

(a) $D^\dagger$ (b) $\delta = 5e\text{-}2$ (c) $\delta = 1e\text{-}2$

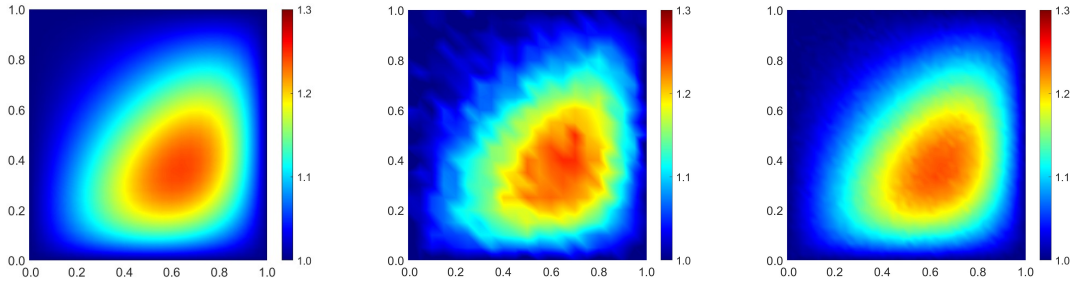

(d) $\sigma^\dagger$ (e) $\delta = 5e\text{-}2$ (f) $\delta = 1e\text{-}2$

Figure 4.4: Example 4.2. First row: reconstructions of $D^\dagger$. Second row: reconstructions of $\sigma^\dagger$.

the non-convexity of the loss function may lead to local minima, making it challenging to verify the theoretical convergence rates. Figure 4.4 shows the reconstructions in 5% and 1% noise level, with $h = 1/20$, $\gamma = 5e\text{-}7$ and $h = 1/45$, $\gamma = 2e\text{-}8$, respectively.

Example 4.3. $\Omega = (0,1)^2$, $D^\dagger(x,y) = 1 + \frac{1}{2}\sin(2\pi x)\sin(2\pi y)e^{xy}$ *and* $\sigma^\dagger(x,y) = 3 + \sin(3\pi x)\sin(3\pi y)$.

Table 4.3: The convergence rates for Example 4.3 with respect to δ.

δ	1e-2	5e-3	2e-3	1e-3	5e-4	2e-4	1e-4	rate
e_D	7.80e-2	5.78e-2	3.53e-2	3.13e-2	2.82e-2	2.78e-2	2.15e-2	$O(\delta^{0.26})$
e_σ	1.36e-2	7.73e-3	3.24e-3	3.06e-3	2.54e-3	2.42e-3	1.89e-3	$O(\delta^{0.39})$

In this example, we consider a more challenging setting. The absorption coefficient $\sigma^\dagger$ has high oscillations. Figure 4.5 shows the behavior of the non-zero condition. The non-zero condition is satisfied in the whole domain when sufficiently many random boundary illuminations are used. Table 4.3 present the convergence rates. Here, we choose the initial mesh size $h = 1/16$ and the regularization parameter $\gamma = 2e\text{-}6$. The convergence rate for e_D is $O(\delta^{0.26})$, which aligns with the predicted rate $O(\delta^{0.25})$. However, we observe a much faster decay for e_σ, with convergence rate $O(\delta^{0.39})$. Figure 4.6 demonstrates that even for this challenging absorption coefficient, the reconstruction is accurate for

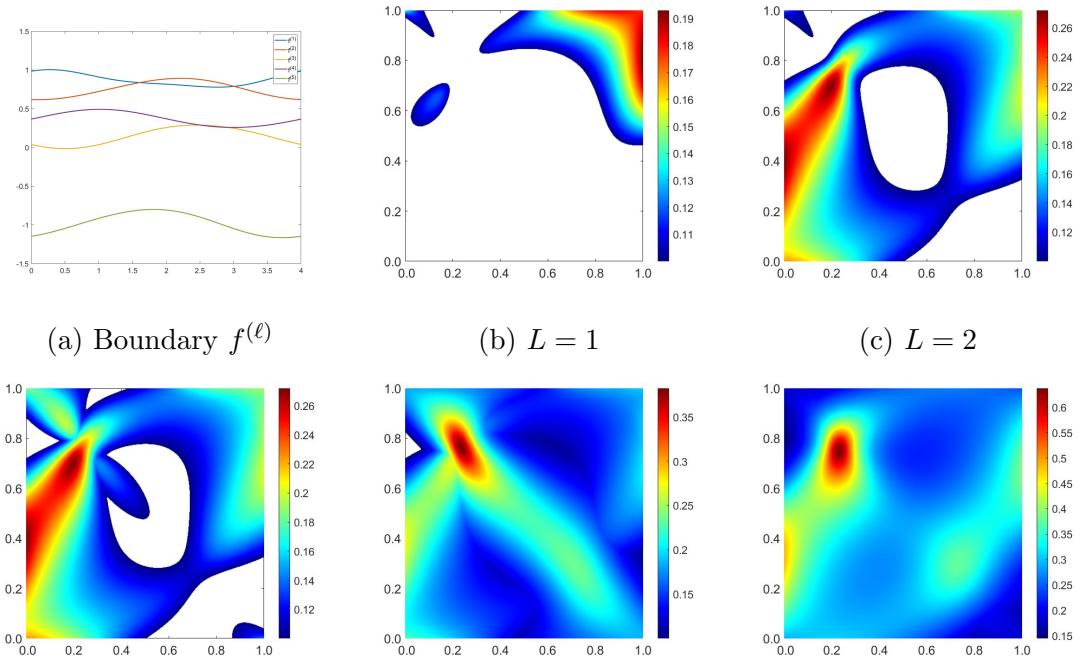

(a) Boundary $f^{(\ell)}$ (b) $L = 1$ (c) $L = 2$

(d) $L = 3$ (e) $L = 4$ (f) $L = 5$

Figure 4.5: Boundary illuminations and the non-zero region of Example 4.3. Top left: plot of boundary data $f^{(\ell)} = g^{(\ell+1)}$. Top middle to bottom right: region which satisfying the non-zero condition as number of boundary input increasing.

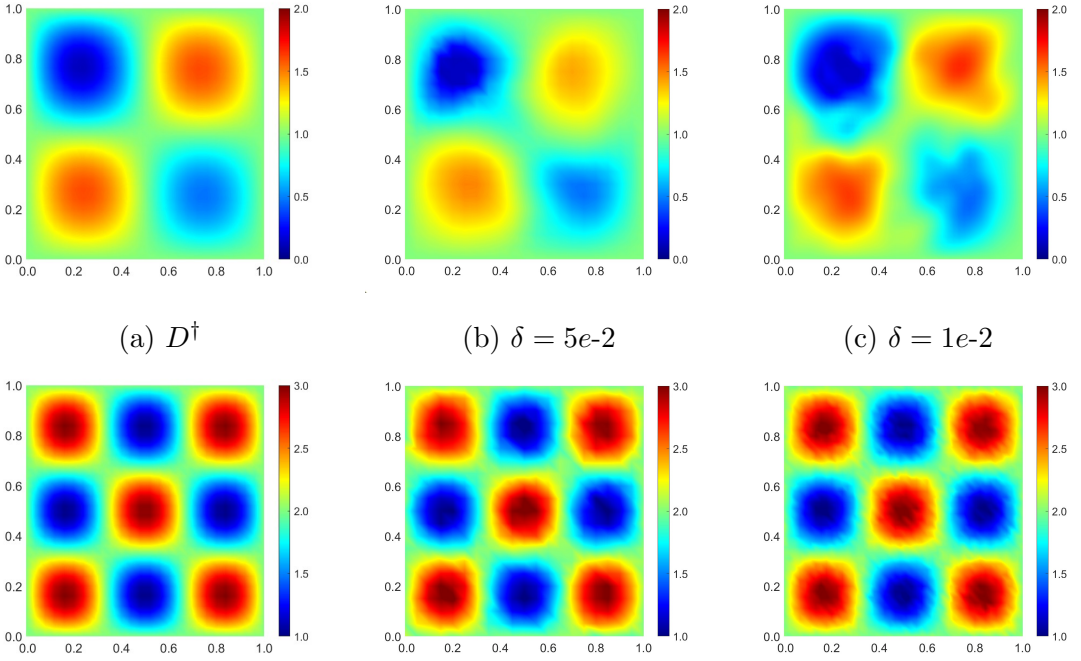

(a) $D^\dagger$ (b) $\delta = 5e\text{-}2$ (c) $\delta = 1e\text{-}2$

(d) $\sigma^\dagger$ (e) $\delta = 5e\text{-}2$ (f) $\delta = 1e\text{-}2$

Figure 4.6: Example 4.3. First row: reconstructions of $D^\dagger$. Second row: reconstructions of $\sigma^\dagger$.

high noise levels. Here we take $h = 1/20$, $\gamma = 2e\text{-}6$ for noise level $\delta = 5e\text{-}2$ and $h = 1/45$, $\gamma = 8e\text{-}8$ for $\delta = 1e\text{-}2$.

Next, we present numerical results for nonsmooth coefficients.

Example 4.4. $\Omega = (0,1)^2$, $D^\dagger(x,y) = \min(1.4, 1+2x(1-x)\sin(\pi y))$ *and* $\sigma^\dagger(x,y) = 6+2\tanh(20x-10)$.

Table 4.4: The convergence rates for Example 4.4 with respect to δ.

δ	1e-2	5e-3	2e-3	1e-3	5e-4	2e-4	1e-4	rate
e_D	4.89e-2	4.72e-2	3.39e-2	2.68e-2	2.14e-2	1.86e-2	1.31e-2	$O(\delta^{0.29})$
e_σ	1.65e-2	1.25e-2	7.89e-3	6.23e-3	5.17e-3	4.61e-3	3.33e-3	$O(\delta^{0.33})$

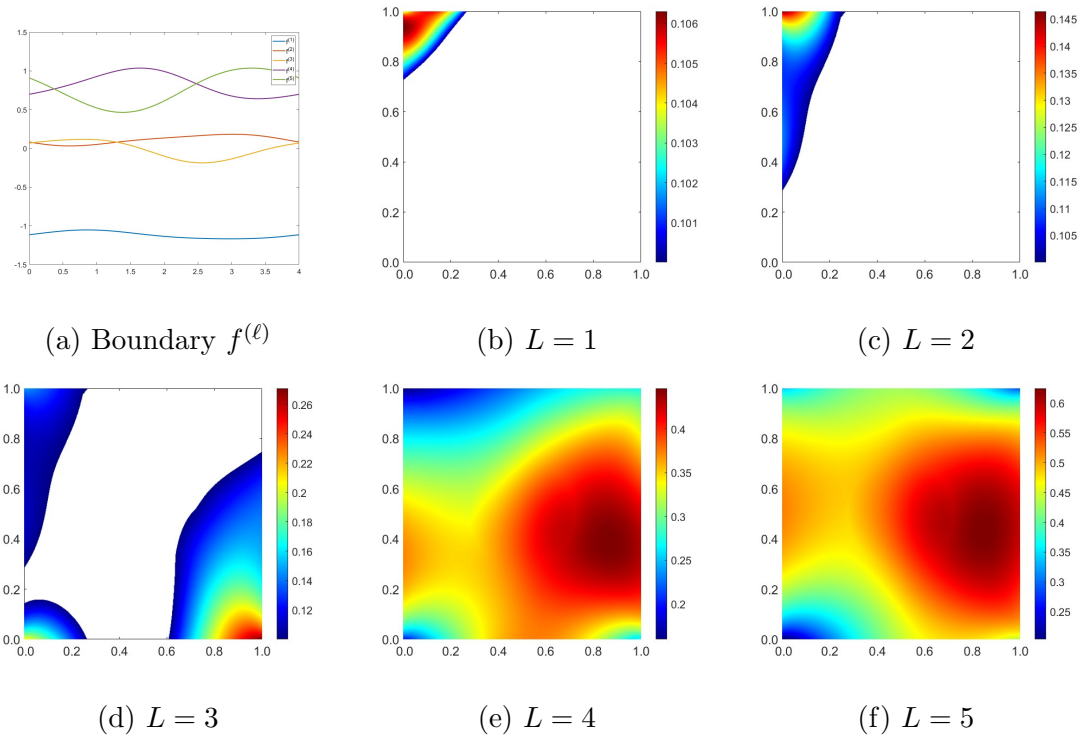

(a) Boundary $f^{(\ell)}$ (b) $L = 1$ (c) $L = 2$

(d) $L = 3$ (e) $L = 4$ (f) $L = 5$

Figure 4.7: Boundary illuminations and the non-zero region of Example 4.4. Top left: plot of boundary data $f^{(\ell)} = g^{(\ell+1)}$. Top middle to bottom right: region which satisfying the non-zero condition as number of boundary input increasing.

Here, we cut off the diffusion coefficient $D^\dagger$ in order to have discontinuous derivatives. Additionally, the absorption coefficient $\sigma^\dagger$ includes a sharp interface where the magnitudes of the derivatives are large. The non-zero condition and the numerical reconstructions are presented in Figures 4.7-4.8 and Table 4.4. The mesh size and the regularization parameter are initialized as $h = 1/12$ and $\gamma = 1e\text{-}5$.

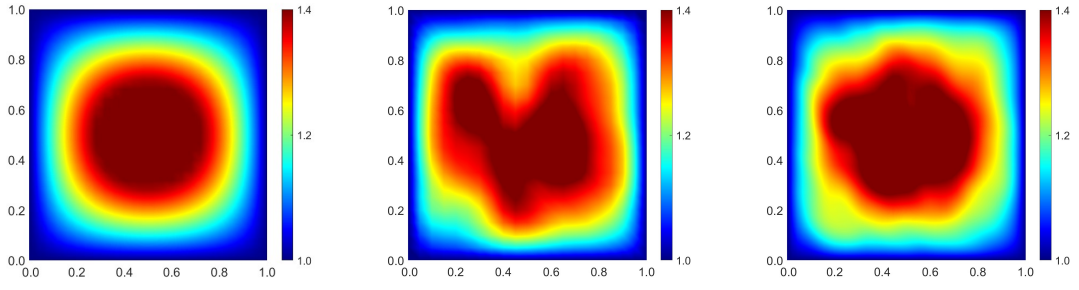

(a) $D^\dagger$ (b) $\delta = 5e\text{-}2$ (c) $\delta = 1e\text{-}2$

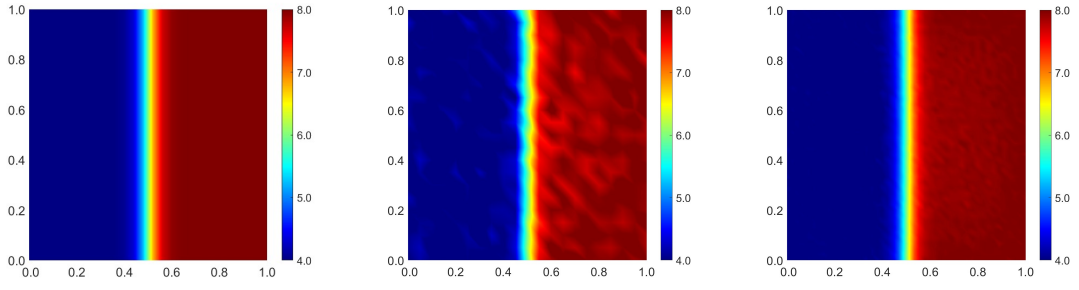

(d) $\sigma^\dagger$ (e) $\delta = 5e\text{-}2$ (f) $\delta = 1e\text{-}2$

Figure 4.8: Example 4.4. First row: reconstructions of $D^\dagger$. Second row: reconstructions of $\sigma^\dagger$.

For this nonsmooth case, we still observe the convergence rates $O(\delta^{0.29})$ and $O(\delta^{0.33})$ for e_D and e_σ, respectively. The convergence rate for the diffusion coefficient $D^\dagger$ matches the predicted rate, whereas the convergence rate for absorption coefficient $\sigma^\dagger$ is slightly higher. In the numerical reconstructions Figure 4.8, we take $h = 1/20$, $\gamma = 5e\text{-}6$ and $h = 1/45$, $\gamma = 2e\text{-}7$ for noise level δ =5e-2 and δ =1e-2, respectively.

Example 4.5. $\Omega = (0,1)^2$, $D^\dagger(x,y) = 1 + 0.2\chi_{\{|x-0.3|^2+|y-0.3|^2<0.1^2\}}$ *and the absorbtion coefficient* $\sigma^\dagger(x,y) = 1 + 0.2\chi_{[0.6,0.8]\times[0.2,0.6]}$.

In this case, both the diffusion coefficient $D^\dagger$ and the absorption coefficient $\sigma^\dagger$ are piecewise constant, which is out the scope of our theoretical framework. Figures 4.9-4.10 show the non-zero condition and the numerical reconstructions. The results indicate that the non-zero condition remains valid numerically even if the coefficients do not satisfy Assumption 4.5. Meanwhile, the reconstructions are satisfactory for these piecewise constant coefficients. Here we take $h = 1/20$, $\gamma = 1e\text{-}6$ for noise level $\delta = 5e\text{-}2$ and $h = 1/45$, $\gamma = 4e\text{-}8$ for $\delta = 1e\text{-}2$.

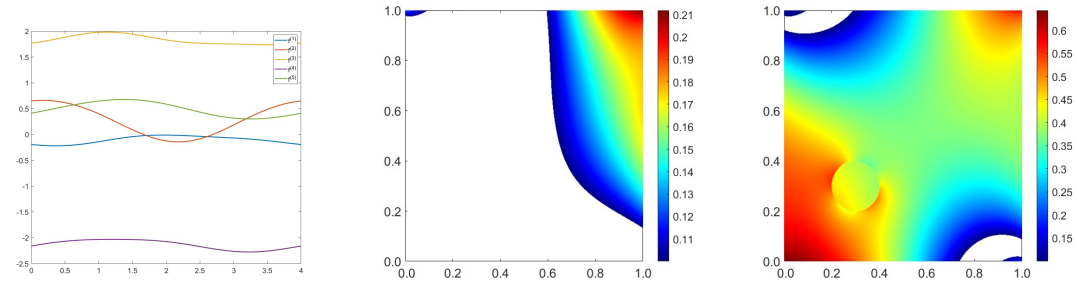

(a) Boundary $f^{(\ell)}$ (b) $L = 1$ (c) $L = 2$

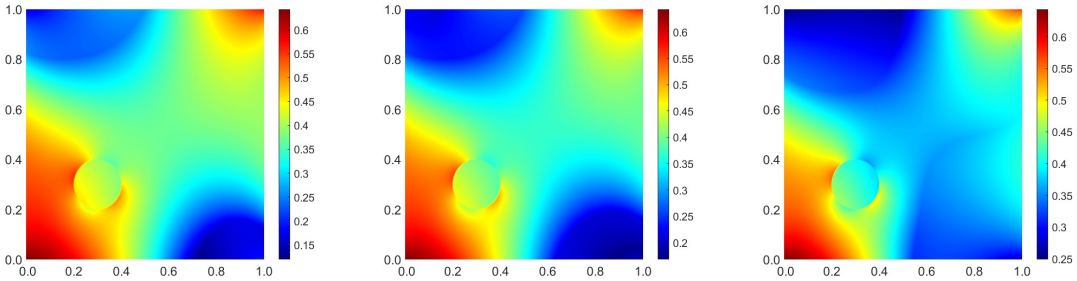

(d)$L = 3$ (e) $L = 4$ (f) $L = 5$

Figure 4.9: Boundary illuminations and the non-zero region of Example 4.5. Top left: plot of boundary data $f^{(\ell)} = g^{(\ell+1)}$. Top middle to bottom right: region which satisfying the non-zero condition as number of boundary input increasing.

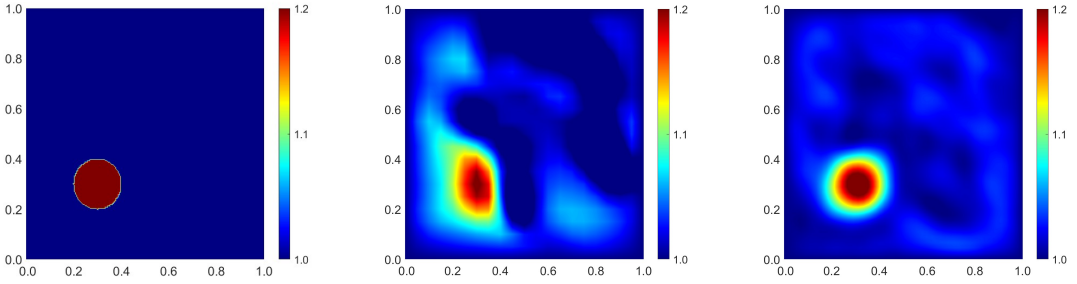

(a) exact D (b) $\delta = 5e\text{-}2$ (c) $\delta = 1e\text{-}2$

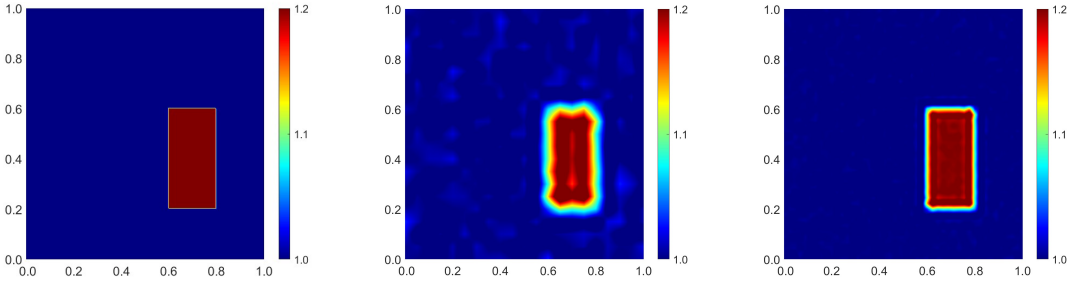

(d) exact σ (e) $\delta = 5e\text{-}2$ (f) $\delta = 1e\text{-}2$

Figure 4.10: Example 4.5. First row: reconstructions of $D^{\dagger}$. Second row: reconstructions of $\sigma^{\dagger}$.

CHAPTER 5.

Hybrid Neural-Network FEM Approximation of Diffusion Coefficient in Elliptic and Parabolic Problems

In this chapter, we study the inverse problem of recovering a space-dependent diffusion coefficient in elliptic and parabolic problems from one internal measurement using neural networks. Let $\Omega \subset \mathbb{R}^d\,(d = 1, 2, 3)$ be a convex polyhedral domain with a boundary $\partial\Omega$. Consider the following elliptic problem

$$\begin{cases} -\nabla \cdot (q\nabla u) = f, & \text{in } \Omega, \\ u = 0, & \text{on } \partial\Omega, \end{cases} \tag{5.1}$$

where f is a known source. The diffusion coefficient q belongs to the admissible set

$$\mathcal{A} = \{q \in H^1(\Omega) : \underline{c}_q \leq q(x) \leq \overline{c}_q \text{ a.e. in } \Omega\},$$

with the constants $0 < \underline{c}_q < \overline{c}_q < \infty$ being the lower and upper bounds on the diffusivity. Below we use the notation $u(q)$ to indicate the dependence of the solution u to problem (5.1) on the coefficient q. Further, we are given the noisy observational data z^δ in the domain Ω:

$$\|u(q^\dagger)(x) - z^\delta(x)\|_{L^2(\Omega)} \leq \delta,$$

where $u(q^\dagger)$ denotes the exact data (for the exact coefficient $q^\dagger$), and δ denotes the noise. The inverse problem is to identify the diffusion coefficient $q^\dagger$ from z^δ. We investigate the hybrid NN-FEM approach for recovering the unknown coefficient q in problem (5.1) (and also the parabolic case in (5.24)), and provide an analysis on the numerical approximation.

The rest of the chapter is organized as follows. In Sections 5.1 and 5.2, we establish the $L^2(\Omega)$ error bounds of the hybrid NN-FEM approximation for elliptic and parabolic cases with or without numerical quadrature. In Section 5.3, we describe the algorithmic details of the approaches and present several numerical experiments to complement the theoretical results.

5.1 Elliptic inverse problem

In this section, we develop and analyze a novel hybrid NN-FEM approximation for the elliptic inverse problem.

[1]Chapter 5 is reprinted with permission from "Hybrid Neural-Network FEM Approximation of Diffusion Coefficient in Elliptic and Parabolic Problems", Siyu Cen, Bangti Jin, Qimeng Quan, Zhi Zhou, IMA J. Numer. Anal., 44 (5) (2024) 3059-3093. The candidate mainly works on the research methodology discussion and the coding and data collection in numerical experiments.

5.1.1 The regularized problem and its hybrid approximation

To recover the diffusion coefficient q, we employ the standard regularized output least-squares formulation with an $H^1(\Omega)$ seminorm penalty, which amounts to minimizing the following objective:

$$\min_{q\in\mathcal{A}} J_\gamma(q) = \frac{1}{2}\|u(q) - z^\delta\|^2_{L^2(\Omega)} + \frac{\gamma}{2}\|\nabla q\|^2_{L^2(\Omega)}, \tag{5.2}$$

with $u \equiv u(q) \in H^1_0(\Omega)$ subject to the following PDE constraint

$$(q\nabla u, \nabla\varphi) = (f, \varphi), \quad \forall\varphi \in H^1_0(\Omega). \tag{5.3}$$

A standard argument in calculus of variation shows the well-posedness of the regularized problem (5.2)-(5.3): for any fixed $\gamma > 0$, it has at least one global minimizer, which depends continuously on the data [51, 73]. In practice, the regularized problem has to be properly discretized, and this is often achieved using finite element / finite difference methods [129, 54, 158, 65].

We employ an alternative discretization strategy: we approximate the coefficient q using NNs, and the state u using the Galerkin FEM. Note that NNs are globally defined, unlike compactly supported FEM basis functions. Hence, it is challenging to impose the box constraint of the admissible set $\mathcal{A}$ directly. In order to preserve the box constraint of $\mathcal{A}$, we apply to the NN output a cutoff operation $P_{\mathcal{A}} : H^1(\Omega) \to \mathcal{A}$ defined by

$$P_{\mathcal{A}}(v) = \min(\max(\underline{c}_q, v), \overline{c}_q). \tag{5.4}$$

The operator $P_{\mathcal{A}}$ is stable in the following sense [155, Corollary 2.1.8]

$$\|\nabla P_{\mathcal{A}}(v)\|_{L^p(\Omega)} \le \|\nabla v\|_{L^p(\Omega)}, \quad \forall v \in W^{1,p}(\Omega), p \in [1,\infty], \tag{5.5}$$

and moreover, for all $v \in \mathcal{A}$, there holds

$$\|P_{\mathcal{A}}(w) - v\|_{L^p(\Omega)} \le \|w - v\|_{L^p(\Omega)}, \quad \forall w \in L^p(\Omega),\ p \in [1,\infty]. \tag{5.6}$$

Now we can formulate the hybrid NN-FEM approximation scheme as

$$\min_{\theta\in\mathfrak{P}_{p,\epsilon}} J_{\gamma,h}(q_\theta) = \frac{1}{2}\|u_h\big(P_{\mathcal{A}}(q_\theta)\big) - z^\delta\|^2_{L^2(\Omega)} + \frac{\gamma}{2}\|\nabla q_\theta\|^2_{L^2(\Omega)}, \tag{5.7}$$

where $\mathfrak{P}_{p,\epsilon}$ is the NN parameter set defined in Section 2.1.2, the discrete state $u_h \equiv u_h(P_{\mathcal{A}}(q_\theta)) \in V_h^0$ satisfies the following discrete variational problem

$$(P_{\mathcal{A}}(q_\theta)\nabla u_h, \nabla\varphi_h) = (f, \varphi_h), \quad \forall\varphi_h \in V_h^0. \tag{5.8}$$

The well-posedness of problem (5.7)-(5.8) holds trivially true. Indeed, the uniform boundedness of the admissible set $\mathfrak{P}_{p,\epsilon}$ in a finite-dimension space implies the compactness of the parametrization set.

Together with the continuity of the discrete forward map, the existence of a minimizer θ^* to problem (5.7)–(5.8) follows by a standard argument. We denote its NN realization by q_θ^*.

The hybrid formulation (5.7)-(5.8) enjoys the following distinct features. First, the construction naturally preserves the box constraint, which is highly nontrivial to impose on the NN functions directly; Second, the resulting objective $J_{\gamma,h}(q_\theta)$ is differentiable with respect to the NN parameters θ, which facilitates the training process by gradient type methods; Third, it is amenable with rigorous convergence analysis, i.e., *a priori* error estimates. In sum, it enjoys both rigorous mathematical foundation of the FEM and excellent inductive bias / approximation properties of NNs.

Remark 5.1. *The formulation* (5.7)–(5.8) *includes the operator $P_{\mathcal{A}}$, and uses $P_{\mathcal{A}}(q_\theta)$ to approximate the exact one $q^\dagger$. It differs from the existing ones. Berg and Nyström [19] suggested the objective*

$$\min_{\theta\in\mathfrak{P}_\epsilon} J_{\gamma,h}(q_\theta) = \frac{1}{2}\|u_h\big(q_\theta\big) - z^\delta\|_{L^2(\Omega)}^2 + \frac{\gamma}{2}\|q_\theta\|_{L^2(\Omega)}^2,$$

where $\gamma \geq 0$ is the regularization parameter. Their numerical evaluation focuses on $\gamma = 0$, i.e., unregularized case, which necessitates the use of tiny NNs for approximating q, in order to avoid overfitting. The well-posedness of this formulation remains unclear, due to a lack of the box constraint. In addition, even assuming the box constraint, the $L^2(\Omega)$ penalty induces only very weak compactness and greatly complicates the mathematical analysis: the existence of a minimizer is only ensured in the sense of H-convergence and the minimizer might be matrix-valued [46, 112]. Mitusch et al [120] suggested including an $H^1(\Omega)$ penalty to stabilize the training process. Note that one should not apply the projection $P_{\mathcal{A}}$ in the penalty term, in order to preserve the differentiability of the objective.

5.1.2 Error analysis

Now we derive (weighted) $L^2(\Omega)$ error estimates of the approximation $P_{\mathcal{A}}(q_\theta^*)$. Under Assumption 5.1, the solution $u^\dagger \equiv u(q^\dagger)$ to (5.1) satisfies $u^\dagger \in H^2(\Omega)\cap H_0^1(\Omega)\cap W^{1,\infty}(\Omega)$ [106, Lemma 2.1].

Assumption 5.1. *$f \in L^\infty(\Omega)$, and $q^\dagger \in W^{2,p}(\Omega)\cap\mathcal{A}$ for some $p \geq \max(2, d+\mu)$ with $\mu > 0$.*

The next lemma gives the existence of an approximant in the admissible set $\mathfrak{P}_{p,\epsilon}$.

Lemma 5.1. *Let Assumption 5.1 hold. Then for any $\epsilon > 0$, there exists $\theta_\epsilon \in \mathfrak{P}_{p,\epsilon}$ such that*

$$\|u^\dagger - u_h\big(P_{\mathcal{A}}(q_{\theta_\epsilon})\big)\|_{L^2(\Omega)} \leq c(h^2+\epsilon).$$

Proof. By the choice of p, $W^{1,p}(\Omega)$ continuously embeds into $L^\infty(\Omega)$ [2, Theorem 4.12, p. 85]. Since $q^\dagger \in W^{2,p}(\Omega)$, by Lemma 2.1, there exists $\theta_\epsilon \in \mathfrak{P}_{p,\epsilon}$ such that its NN realization q_{θ_ϵ} satisfies

$$\|q^\dagger - q_{\theta_\epsilon}\|_{H^1(\Omega)} + \|q^\dagger - q_{\theta_\epsilon}\|_{L^\infty(\Omega)} \leq c\|q^\dagger - q_{\theta_\epsilon}\|_{W^{1,p}(\Omega)} \leq c\epsilon. \tag{5.9}$$

Then by the stability estimate (5.6) of the operator $P_{\mathcal{A}}$, we deduce

$$\|q^\dagger - P_{\mathcal{A}}(q_{\theta_\epsilon})\|_{L^\infty(\Omega)} \le c\epsilon. \tag{5.10}$$

Next we bound $\varrho_h := u_h(P_{\mathcal{A}}(q_{\theta_\epsilon})) - u_h(q^\dagger) \in V_h^0$. It follows from the weak formulations of $u_h(P_{\mathcal{A}}(q_{\theta_\epsilon}))$ and $u_h(q^\dagger)$, cf. (5.8), and Hölder's inequality that for any $\varphi_h \in V_h^0$,

$$\begin{aligned}(P_{\mathcal{A}}(q_{\theta_\epsilon})\nabla\varrho_h, \nabla\varphi_h) &= \big((q^\dagger - P_{\mathcal{A}}(q_{\theta_\epsilon}))\nabla u_h(q^\dagger), \nabla\varphi_h\big)\\ &\le \|q^\dagger - P_{\mathcal{A}}(q_{\theta_\epsilon})\|_{L^\infty(\Omega)}\|\nabla u_h(q^\dagger)\|_{L^2(\Omega)}\|\nabla\varphi_h\|_{L^2(\Omega)}.\end{aligned}$$

Next we set $\varphi_h = \varrho_h$ in the inequality. Upon noting $P_{\mathcal{A}}(q_{\theta_\epsilon}) \in \mathcal{A}$, by the approximation property (5.10), Poincaré inequality, Hölder's inequality and the estimate $\|\nabla u_h(q^\dagger)\|_{L^2(\Omega)} \le c\|f\|_{L^2(\Omega)}$, we obtain

$$\|\varrho_h\|_{L^2(\Omega)} \le c\|\nabla\varrho_h\|_{L^2(\Omega)} \le c\|q^\dagger - P_{\mathcal{A}}(q_{\theta_\epsilon})\|_{L^\infty(\Omega)}\|\nabla u_h(q^\dagger)\|_{L^2(\Omega)} \le c\epsilon.$$

This and the standard *a priori* error estimate $\|u^\dagger - u_h(q^\dagger)\|_{L^2(\Omega)} \le ch^2$ yield the desired estimate. □

The next lemma gives crucial *a priori* bounds on $\|u^\dagger - u_h(P_{\mathcal{A}}(q_\theta^*))\|_{L^2(\Omega)}$ and $\|\nabla P_{\mathcal{A}}(q_\theta^*)\|_{L^2(\Omega)}$.

Lemma 5.2. *Let Assumption 5.1 hold. For any $\epsilon > 0$, let $\theta^* \in \mathfrak{P}_{p,\epsilon}$ be a minimizer to problem* (5.7)-(5.8)*. Then the following estimate holds*

$$\|u^\dagger - u_h(P_{\mathcal{A}}(q_\theta^*))\|_{L^2(\Omega)}^2 + \gamma\|\nabla P_{\mathcal{A}}(q_\theta^*)\|_{L^2(\Omega)}^2 \le c(h^4 + \epsilon^2 + \delta^2 + \gamma).$$

Proof. Let q_{θ_ϵ} be the NN realization of $\theta_\epsilon \in \mathfrak{P}_{p,\epsilon}$ satisfying the estimate (5.9), which also implies $\|q_{\theta_\epsilon}\|_{H^1(\Omega)} \le c$. Then Lemma 5.1 and the minimizing property of q_θ^*, i.e., $J_{\gamma,h}(q_\theta^*) \le J_{\gamma,h}(q_{\theta_\epsilon})$, yield

$$\begin{aligned}&\|u_h(P_{\mathcal{A}}(q_\theta^*)) - z^\delta\|_{L^2(\Omega)}^2 + \gamma\|\nabla q_\theta^*\|_{L^2(\Omega)}^2 \le \|u_h(P_{\mathcal{A}}(q_{\theta_\epsilon})) - z^\delta\|_{L^2(\Omega)}^2 + \gamma\|\nabla q_{\theta_\epsilon}\|_{L^2(\Omega)}^2\\ \le& c\big(\|u_h(P_{\mathcal{A}}(q_{\theta_\epsilon})) - u^\dagger\|_{L^2(\Omega)}^2 + \|u^\dagger - z^\delta\|_{L^2(\Omega)}^2 + \gamma\big) \le c(h^4 + \epsilon^2 + \delta^2 + \gamma).\end{aligned}$$

Applying the triangle inequality leads to

$$\begin{aligned}\|u^\dagger - u_h(P_{\mathcal{A}}(q_\theta^*))\|_{L^2(\Omega)}^2 + \gamma\|\nabla q_\theta^*\|_{L^2(\Omega)}^2 &\le c\|u^\dagger - z^\delta\|_{L^2(\Omega)}^2\\ + c\|z^\delta - u_h(P_{\mathcal{A}}(q_\theta^*))\|_{L^2(\Omega)}^2 + \gamma\|\nabla q_\theta^*\|_{L^2(\Omega)}^2 &\le c(h^4 + \epsilon^2 + \delta^2 + \gamma).\end{aligned}$$

Finally, the bound on $\|\nabla P_{\mathcal{A}}(q_\theta^*)\|_{L^2(\Omega)}$ follows from (5.5) and the constraint $P_{\mathcal{A}}(q_\theta^*) \in \mathcal{A}$. □

To derive an *a priori* estimate for $P_{\mathcal{A}}(q_\theta^*)$, we use the following positivity condition introduced in (1.9): for some $\beta \ge 0$,

$$q^\dagger|\nabla u^\dagger|^2 + fu^\dagger \ge c\ \mathrm{dist}(x, \partial\Omega)^\beta. \tag{5.11}$$

Theorem 5.2. *Let Assumption 5.1 hold. For any $\epsilon > 0$, let $\theta^* \in \mathfrak{P}_{p,\epsilon}$ be a minimizer to problem (5.7)-(5.8), with q_θ^* its NN realization. Then with $\eta^2 := h^4 + \epsilon^2 + \delta^2 + \gamma$, there holds*

$$\int_\Omega \Big(\frac{q^\dagger - P_{\mathcal{A}}(q_\theta^*)}{q^\dagger}\Big)^2 \big(q^\dagger |\nabla u^\dagger|^2 + f u^\dagger\big)\, \mathrm{d}x \le c(\min(h^{-1}\eta + h, 1) + h\gamma^{-\frac{1}{2}}\eta)\gamma^{-\frac{1}{2}}\eta.$$

Moreover, if condition (5.11) holds, then

$$\|q^\dagger - P_{\mathcal{A}}(q_\theta^*)\|_{L^2(\Omega)} \le c\big[(\min(h^{-1}\eta + h, 1) + h\gamma^{-\frac{1}{2}}\eta)\gamma^{-\frac{1}{2}}\eta\big]^{\frac{1}{2(1+\beta)}}.$$

Proof. By the weak formulations of $u^\dagger$ and $u_h(P_{\mathcal{A}}(q_\theta^*))$, cf. (5.3) and (5.8), for any $\varphi \in H_0^1(\Omega)$, we have

$$\begin{aligned}\big((q^\dagger - P_{\mathcal{A}}(q_\theta^*))\nabla u^\dagger, \nabla\varphi\big) &= \big((q^\dagger - P_{\mathcal{A}}(q_\theta^*))\nabla u^\dagger, \nabla(\varphi - P_h\varphi)\big) + \big((q^\dagger - P_{\mathcal{A}}(q_\theta^*))\nabla u^\dagger, \nabla P_h\varphi\big)\\ = -\big(\nabla\cdot((q^\dagger - P_{\mathcal{A}}(q_\theta^*))\nabla u^\dagger), \varphi - P_h\varphi\big) &+ \big(P_{\mathcal{A}}(q_\theta^*)\nabla(u_h(P_{\mathcal{A}}(q_\theta^*)) - u^\dagger), \nabla P_h\varphi\big) =: \mathrm{I} + \mathrm{II}.\end{aligned}$$

Let $\varphi \equiv \frac{q^\dagger - P_{\mathcal{A}}(q_\theta^*)}{q^\dagger} u^\dagger$. Next we bound the terms I and II separately. Direct computation gives

$$\nabla\varphi = (q^\dagger)^{-1}(u^\dagger\nabla(q^\dagger - P_{\mathcal{A}}(q_\theta^*)) + (q^\dagger - P_{\mathcal{A}}(q_\theta^*))\nabla u^\dagger) - (q^\dagger)^{-2}(q^\dagger - P_{\mathcal{A}}(q_\theta^*))(\nabla q^\dagger)u^\dagger.$$

This identity and Assumption 5.1 imply $\varphi \in H_0^1(\Omega)$, and further

$$\|\nabla\varphi\|_{L^2(\Omega)} \le c(1 + \|\nabla P_{\mathcal{A}}(q_\theta^*)\|_{L^2(\Omega)}). \tag{5.12}$$

Using Assumption 5.1 again and Lemma 5.2, we obtain

$$\begin{aligned}\|\nabla\cdot\big((q^\dagger - P_{\mathcal{A}}(q_\theta^*))\nabla u^\dagger\big)\|_{L^2(\Omega)} &\le \|q^\dagger - P_{\mathcal{A}}(q_\theta^*)\|_{L^\infty(\Omega)}\|\Delta u^\dagger\|_{L^2(\Omega)}\\ &+ \|\nabla q^\dagger - \nabla P_{\mathcal{A}}(q_\theta^*)\|_{L^2(\Omega)}\|\nabla u^\dagger\|_{L^\infty(\Omega)} \le c(1 + \|\nabla P_{\mathcal{A}}(q_\theta^*)\|_{L^2(\Omega)}) \le c\gamma^{-\frac{1}{2}}\eta.\end{aligned}$$

Hence, we can bound the term I by

$$|\mathrm{I}| \le ch(1 + \|\nabla P_{\mathcal{A}}(q_\theta^*)\|_{L^2(\Omega)})\|\nabla\varphi\|_{L^2(\Omega)} \le ch(1 + \|\nabla P_{\mathcal{A}}(q_\theta^*)\|_{L^2(\Omega)}^2) \le ch\gamma^{-1}\eta^2.$$

By the Cauchy–Schwarz inequality and the estimate (5.12), we can bound the term II by

$$\begin{aligned}|\mathrm{II}| &\le \|P_{\mathcal{A}}(q_\theta^*)\|_{L^\infty(\Omega)}\|\nabla(u_h(P_{\mathcal{A}}(q_\theta^*)) - u^\dagger)\|_{L^2(\Omega)}\|\nabla\varphi\|_{L^2(\Omega)}\\ &\le c\|\nabla(u_h(P_{\mathcal{A}}(q_\theta^*)) - u^\dagger)\|_{L^2(\Omega)}\|\nabla\varphi\|_{L^2(\Omega)}\\ &\le c\big(1 + \|\nabla P_{\mathcal{A}}(q_\theta^*)\|_{L^2(\Omega)}\big)\|\nabla(u_h(P_{\mathcal{A}}(q_\theta^*)) - u^\dagger)\|_{L^2(\Omega)}.\end{aligned}$$

Then by Lemma 5.2, the inverse inequality in the space V_h^0 (2.1), the approximation property (2.3) and the $L^2(\Omega)$-stability of P_h and the regularity $u^\dagger \in H^2(\Omega)$, we can bound the term II by

$$\begin{aligned}|\mathrm{II}| &\le c\gamma^{-\frac{1}{2}}\eta\left(\|\nabla(u_h(P_{\mathcal{A}}(q_\theta^*)) - P_h u^\dagger)\|_{L^2(\Omega)} + \|\nabla(P_h u^\dagger - u^\dagger)\|_{L^2(\Omega)}\right)\\ &\le c\gamma^{-\frac{1}{2}}\eta\left(h^{-1}\|u_h(P_{\mathcal{A}}(q_\theta^*)) - P_h u^\dagger\|_{L^2(\Omega)} + h\|u^\dagger\|_{H^2(\Omega)}\right)\\ &\le c\gamma^{-\frac{1}{2}}\eta\left(h^{-1}\|u_h(P_{\mathcal{A}}(q_\theta^*)) - u^\dagger\|_{L^2(\Omega)} + h\|u^\dagger\|_{H^2(\Omega)}\right) \le c\gamma^{-\frac{1}{2}}\eta\,(h^{-1}\eta + h).\end{aligned}$$

Further, the estimate $\|\nabla u_h(P_{\mathcal{A}}(q_\theta^*))\|_{L^2(\Omega)} \leq c\|f\|_{L^2(\Omega)}$ and the regularity $u^\dagger \in H^2(\Omega)$ imply $\|\nabla(u_h(P_{\mathcal{A}}(q_\theta^*)) - u^\dagger)\|_{L^2(\Omega)} \leq c$. Hence, $|\mathrm{II}| \leq c\gamma^{-\frac{1}{2}}\eta$. Combining these estimates on II yields

$$|\mathrm{II}| \leq c\gamma^{-\frac{1}{2}}\eta \min(h^{-1}\eta + h, 1).$$

Moreover, direct computation gives [22, Theorem 2.2]

$$\big((q^\dagger - P_{\mathcal{A}}(q_\theta^*))\nabla u^\dagger, \nabla\varphi\big) = \frac{1}{2}\int_\Omega \Big(\frac{q^\dagger - P_{\mathcal{A}}(q_\theta^*)}{q^\dagger}\Big)^2 \big(q^\dagger|\nabla u^\dagger|^2 + fu^\dagger\big)\,\mathrm{d}x.$$

This and the preceding bounds together show the first assertion. The second assertion follows the same argument as Theorem 3.3. □

Remark 5.2. *Theorem 5.2 provides useful guidelines for choosing the algorithmic parameters: $\gamma = \mathcal{O}(\delta^2)$, $h = \mathcal{O}(\delta^{\frac{1}{2}})$ and $\epsilon = \mathcal{O}(\delta)$. Then under condition* (5.11)*, we obtain $\|q^\dagger - P_{\mathcal{A}}(q_\theta^*)\|_{L^2(\Omega)} \leq c\delta^{\frac{1}{4(1+\beta)}}$. This result is comparable with that for the purely FEM approximation [84, Corollary 3.3].*

5.1.3 Quadrature error analysis

The weak formulation and objective require evaluating various integrals. This is commonly done via a quadrature scheme. While this issue is direct for the standard FEM [41], it is nontrivial when NNs are involved: NNs are globally supported and no longer polynomials within each finite element. Thus, the use of quadrature schemes is required, and there is an inevitable quadrature error, which may influence the accuracy of the NN approximation [20, 130]. We aim to provide a quadrature error analysis.

There are many possible quadrature rules [139, Chapter 15]. We focus on one simple scheme to shed useful insights. On each element $K \in \mathcal{T}_h$, we uniformly divide it into 2^{dn} sub-simplexes, denoted by $\{K_i\}_{i=1}^{2^{dn}}$, with the uniform diameter $h_K/2^n$. The division for $d = 1, 2$ is trivial, and for $d = 3$, it is also feasible [122]. Then consider the following quadrature rule over the element K (with P_j^i denoting the jth node of the ith sub-simplex K_i):

$$Q_K(v) = \sum_{i=1}^{2^{dn}} \frac{|K_i|}{d+1} \sum_{j=1}^{d+1} v(P_j^i), \quad \forall v \in C(\overline{K}).$$

The embedding $H^2(\Omega) \hookrightarrow L^\infty(\Omega)$ (for $d = 1, 2, 3$) and Bramble–Hilbert lemma [41, Theorem 4.1.3] lead to

$$\Big|\int_K v\,\mathrm{d}x - Q_K(v)\Big| \leq c|K|^{\frac{1}{2}}2^{-2n}h_K^2|v|_{H^2(K)}, \quad \forall v \in H^2(K). \tag{5.13}$$

Then we can define a global quadrature rule:

$$Q_h(v) = \sum_{K\in\mathcal{T}_h} Q_K(v), \quad \forall v \in C(\overline{\Omega}), \tag{5.14}$$

which satisfies the following error estimate

$$\Big| \int_\Omega v \, \mathrm{d}x - Q_h(v) \Big| \leq c 2^{-2n} h^2 |v|_{H^2(\Omega)}, \quad \forall v \in H^2(\Omega). \tag{5.15}$$

Similarly, we define a discrete / broken $L^2(\Omega)$ inner product $(\cdot,\cdot)_h$ by

$$(w, v)_h := Q_h(wv) = \sum_{K \in \mathcal{T}_h} Q_K(wv), \quad \forall w, v \in C(\overline{\Omega}).$$

Lemma 5.3. *The following error estimate holds for any $v_h, w_h \in V_h^0$, and $n \in \mathbb{N}$:*

$$|(q\nabla v_h, \nabla w_h) - (q\nabla v_h, \nabla w_h)_h| \leq c(2^{-n}h)^p \|q\|_{W^{p,\infty}(\Omega)} \|\nabla v_h\|_{L^2(\Omega)} \|\nabla w_h\|_{L^2(\Omega)}, \quad \textit{with } p = 1, 2;$$

Proof. Let $\Pi_{K_j} : C(K_j) \to P_1(K_j)$ be the Lagrange nodal interpolation operator on the sub-simplex K_j. Since the quadrature rule on K_j is exact for $P_1(K_j)$, we have

$$(q\nabla v_h, \nabla w_h) - (q\nabla v_h, \nabla w_h)_h = \sum_{K \in \mathcal{T}_h} \sum_{j=1}^{2^{dn}} \int_{K_j} (q - \Pi_{K_j} q) \nabla v_h \cdot \nabla w_h \, \mathrm{d}x.$$

Then the local estimate for Lagrange interpolation leads to

$$\begin{aligned} |(q\nabla v_h, \nabla w_h) - (q\nabla v_h, \nabla w_h)_h| &\leq \sum_{K \in \mathcal{T}_h} \sum_{j=1}^{2^{dn}} \int_{K_j} \Big| (q - \Pi_{K_j} q) \nabla v_h \cdot \nabla w_h \Big| \, \mathrm{d}x \\ \leq c \sum_{K \in \mathcal{T}_h} \sum_{j=1}^{2^{dn}} (2^{-n}h)^p \|q\|_{W^{p,\infty}(K_j)} \|\nabla v_h\|_{L^2(K_j)} \|\nabla w_h\|_{L^2(K_j)} &\leq c(2^{-n}h)^p \|q\|_{W^{p,\infty}(\Omega)} \|\nabla v_h\|_{L^2(\Omega)} \|\nabla w_h\|_{L^2(\Omega)}. \end{aligned}$$

This proves the desired estimate. □

Then the hybrid NN-FEM approximation of problem (5.2)-(5.3) (with numerical integration) reads

$$\min_{\theta \in \mathfrak{P}_{\infty,\epsilon}} \widetilde{J}_{\gamma,h}(q_\theta) = \frac{1}{2} \|\widetilde{u}_h(P_{\mathcal{A}}(q_\theta)) - z^\delta\|_{L^2(\Omega)}^2 + \frac{\gamma}{2} Q_h(|\nabla q_\theta|^2), \tag{5.16}$$

where $\widetilde{u}_h \equiv \widetilde{u}_h(P_{\mathcal{A}}(q_\theta)) \in V_h^0$ satisfies the following discrete variational problem

$$(P_{\mathcal{A}}(q_\theta)\nabla \widetilde{u}_h, \nabla \varphi_h)_h = (f, \varphi_h), \quad \forall \varphi_h \in V_h^0. \tag{5.17}$$

We focus on approximating the integrals involving NNs only. The variational problem (5.17) involves also the quadrature approximation, which necessitates quantifying the associated error. The presence of $P_{\mathcal{A}}$ in the weak formulation ensures the V_h^0-ellipticity of the broken $L^2(\Omega)$ semi-inner product, and hence the unique existence of the discrete forward map is ensured [39, 1]. Then repeating the argument for problem (5.7)-(5.8) yields the well-posedness of problem (5.16)-(5.17). The analysis of the quadrature error requires the following condition on the problem data.

Assumption 5.3. *$q^\dagger \in W^{2,\infty}(\Omega) \cap \mathcal{A}$ and $f \in L^\infty(\Omega)$.*

Next we state an analogue of Lemma 5.1 in the presence of numerical integration.

Lemma 5.4. *Let Assumption 5.3 hold. Then for any $\epsilon > 0$, there exists $\theta_\epsilon \in \mathfrak{P}_{\infty,\epsilon}$ such that*

$$\|u^\dagger - \widetilde{u}_h(P_{\mathcal{A}}(q_{\theta_\epsilon}))\|_{L^2(\Omega)} \leq c(h^2 + \epsilon).$$

Proof. The proof is similar to Lemma 5.1. First, under Assumption 5.3, there holds $\|u^\dagger - \widetilde{u}_h(q^\dagger)\|_{L^2(\Omega)} \leq ch^2$ [1, Theorem 5]. Next by Lemma 2.1, there exists $\theta_\epsilon \in \mathfrak{P}_{\infty,\epsilon}$ such that its NN realization q_{θ_ϵ} satisfies

$$\|q^\dagger - q_{\theta_\epsilon}\|_{W^{1,\infty}(\Omega)} \leq \epsilon. \tag{5.18}$$

Then by the stability estimate (5.6) of the operator $P_{\mathcal{A}}$, we deduce

$$\|q^\dagger - P_{\mathcal{A}}(q_{\theta_\epsilon})\|_{L^\infty(\Omega)} \leq \epsilon. \tag{5.19}$$

Let $\widetilde{w}_h := \widetilde{u}_h(P_{\mathcal{A}}(q_{\theta_\epsilon})) - \widetilde{u}_h(q^\dagger) \in V_h^0$. Repeating the argument of Lemma 5.1 yields

$$\begin{aligned}\underline{c}_q\|\nabla\widetilde{w}_h\|_{L^2(\Omega)}^2 &\leq (P_{\mathcal{A}}(q_{\theta_\epsilon})\nabla\widetilde{w}_h, \nabla\widetilde{w}_h)_h = \big((q^\dagger - P_{\mathcal{A}}(q_{\theta_\epsilon}))\nabla\widetilde{u}_h(q^\dagger), \nabla\widetilde{w}_h\big)_h \\ &\leq \|q^\dagger - P_{\mathcal{A}}(q_{\theta_\epsilon})\|_{L^\infty(\Omega)}\|\nabla\widetilde{u}_h(q^\dagger)\|_{L^2(\Omega)}\|\nabla\widetilde{w}_h\|_{L^2(\Omega)},\end{aligned}$$

since $|(q\nabla u_h, \nabla v_h)_h| \leq c\|q\|_{L^\infty(\Omega)}\|\nabla u_h\|_{L^2(\Omega)}\|\nabla v_h\|_{L^2(\Omega)}$. Using the estimate (5.19), the stability of Lagrange interpolation and the *a priori* estimate $\|\nabla\widetilde{u}_h(q^\dagger)\|_{L^2(\Omega)} \leq c$ and Poincaré inequality, we deduce

$$\|\widetilde{w}_h\|_{L^2(\Omega)} \leq c\|\nabla\widetilde{w}_h\|_{L^2(\Omega)} \leq c\|q^\dagger - P_{\mathcal{A}}(q_{\theta_\epsilon})\|_{L^\infty(\Omega)}\|\nabla\widetilde{u}_h(q^\dagger)\|_{L^2(\Omega)} \leq c\|q^\dagger - P_{\mathcal{A}}(q_{\theta_\epsilon})\|_{L^\infty(\Omega)} \leq c\epsilon.$$

This completes the proof of the lemma. □

The next lemma provides an *a priori* bound on $\|u^\dagger - \widetilde{u}_h(P_{\mathcal{A}}(q_\theta^*))\|_{L^2(\Omega)}$ and $\nabla P_{\mathcal{A}}(q_\theta^*)$.

Lemma 5.5. *Let Assumption 5.3 hold. Fix $\epsilon > 0$, and let $\theta^* \in \mathfrak{P}_{\infty,\epsilon}$ be a minimizer to problem* (5.16)-(5.17) *and q_θ^* its NN realization. Then the following estimate holds*

$$\|u^\dagger - \widetilde{u}_h(P_{\mathcal{A}}(q_\theta^*))\|_{L^2(\Omega)}^2 + \gamma Q_h(|\nabla P_{\mathcal{A}}(q_\theta^*)|^2) \leq c(h^4 + \epsilon^2 + \delta^2 + \gamma).$$

Proof. The proof relies on the minimizing property of θ^*, Lemma 5.4 and the existence of an element $q_{\theta_\epsilon} \in W^{1,\infty}(\Omega)$ satisfying (5.18). The estimate (5.18) and the regularity $q^\dagger \in W^{2,\infty}(\Omega)$ implies $\|q_\epsilon\|_{W^{1,\infty}(\Omega)} \leq c$. This yields $Q_h(|\nabla q_\epsilon|^2) \leq c$, since the quadrature operator Q_h is stable on $C(\overline{\Omega})$. The rest of the proof is identical with that for Lemma 5.2, and hence, we omit the details. □

Next we show an *a priori* bound on quadrature error of the penalty term.

Lemma 5.6. *Let $\theta \in \mathfrak{P}_{\infty,\epsilon}$, of depth L, width W and bound R, and v_θ be its NN realization, with $RW > 2$. Then the following quadrature error estimate holds*

$$\|\nabla v_\theta\|^2_{L^2(\Omega)} - Q_h(\|\nabla v_\theta\|^2_{\ell^2}) \le c2^{-2n}h^2 |\sum_{i=1}^{d} (\partial_{x_i} v_\theta)^2|_{W^{2,\infty}(\Omega)} \le c2^{-2n}h^2 R^{4L} W^{4L-4}.$$

Proof. By the NN realization (2.4), we have for every layer $\ell = 1, \dots, L-1$ and each $i = 1, \dots, d_\ell$, $v_i^{(\ell)} = \rho\Big(\sum_{j=1}^{d_{\ell-1}} A_{ij}^{(\ell)} v_j^{(\ell-1)} + b_i^{(\ell)}\Big)$. Then for all $1 \le k, m \le d$, direct computation with the chain rule gives

$$\begin{aligned}\partial^2_{x_k,x_m} v_i^{(\ell)} =& \rho''\Big(\sum_{j=1}^{d_{\ell-1}} A_{ij}^{(\ell)} v_j^{(\ell-1)} + b_i^{(\ell)}\Big)\Big(\sum_{j=1}^{d_{\ell-1}} A_{ij}^{(\ell)} \partial_{x_k} v_j^{(\ell-1)}\Big)\Big(\sum_{j=1}^{d_{\ell-1}} A_{ij}^{(\ell)} \partial_{x_m} v_j^{(\ell-1)}\Big) \\ &+ \rho'\Big(\sum_{j=1}^{d_{\ell-1}} A_{ij}^{(\ell)} v_j^{(\ell-1)} + b_i^{(\ell)}\Big)\Big(\sum_{j=1}^{d_{\ell-1}} A_{ij}^{(\ell)} \partial^2_{x_k,x_m} v_j^{(\ell-1)}\Big).\end{aligned}$$

Note that for the tanh activation function ρ, $\|\rho'\|_{L^\infty(\mathbb{R})} \le 1, \|\rho''\|_{L^\infty(\mathbb{R})} \le 1$, cf. Lemma 2.2, and further [80, Lemma 3.4, eq. (3.6)]

$$\|\partial_{x_k} v_j^{(\ell)}\|_{L^\infty(\Omega)} \le R^\ell W^{\ell-1}, \quad \forall \ell = 1, \dots, L-1, j = 1, \dots, d_\ell. \tag{5.20}$$

Then we arrive at

$$\begin{aligned}\|\partial^2_{x_k,x_m} v_i^{(\ell)}\|_{L^\infty(\Omega)} &\le R^2 W^2 \max_{j=1,\dots,d_{\ell-1}} \|\partial_{x_k} v_j^{(\ell-1)}\|_{L^\infty(\Omega)} \max_{j=1,\dots,d_{\ell-1}} \|\partial_{x_m} v_j^{(\ell-1)}\|_{L^\infty(\Omega)} \\ &\quad + RW \max_{j=1,\dots,d_{\ell-1}} \|\partial^2_{x_k,x_m} v_j^{(\ell-1)}\|_{L^\infty(\Omega)} \\ &\le R^{2\ell} W^{2\ell-2} + RW \max_{j=1,\dots,d_{\ell-1}} \|\partial^2_{x_k,x_m} v_j^{(\ell-1)}\|_{L^\infty(\Omega)}.\end{aligned}$$

Note also the trivial estimate

$$\|\partial^2_{x_k,x_m} v_i^{(1)}\|_{L^\infty(\Omega)} \le \Big\|\rho''\Big(\sum_{j=1}^{d} A_{ij}^{(1)} x_j + b_i^{(1)}\Big) A_{ik}^{(1)} A_{im}^{(1)}\Big\|_{L^\infty(\Omega)} \le R^2.$$

Taking maximum in $i = 1, \dots, d_\ell$ and then applying the inequality recursively lead to

$$\begin{aligned}\max_{i=1,\dots,d_\ell} \|\partial_{x_k,x_m} v_i^{(\ell)}\|_{L^\infty(\Omega)} &\le R^2 \sum_{j=1}^{\ell-1} (RW)^{2j} (RW)^{\ell-1-j} + (RW)^{\ell-1} \max_{i=1,\dots,d_{\ell-1}} \|\partial_{x_k,x_m} v_i^{(1)}\|_{L^\infty(\Omega)} \\ &= R^{2\ell} W^{2\ell-2} \sum_{j=0}^{\ell-1} (RW)^{-j} \le \frac{R^{2\ell} W^{2\ell-2}}{1 - (RW)^{-1}}.\end{aligned}$$

Hence, under the condition $RW \ge 2$, we may bound

$$\|\partial^2_{x_k,x_s} v_i^{(\ell)}\|_{L^\infty(\Omega)} \le 2R^{2\ell} W^{2\ell-2}, \quad \forall \ell = 1, \dots, L, i = 1, \dots, d_\ell. \tag{5.21}$$

By direct computation, we obtain for $1 \le k, m, n \le d$

$$\begin{aligned}
\partial^3_{x_k,x_m,x_n} v_i^{(\ell)} =& \rho'''\Big(\sum_{j=1}^{d_{\ell-1}} A_{ij}^{(\ell)} v_j^{(\ell-1)} + b_i^{(\ell)}\Big)\Big(\sum_{j=1}^{d_{\ell-1}} A_{ij}^{(\ell)} \partial_{x_k} v_j^{(\ell-1)}\Big)\Big(\sum_{j=1}^{d_{\ell-1}} A_{ij}^{(\ell)} \partial_{x_m} v_j^{(\ell-1)}\Big)\Big(\sum_{j=1}^{d_{\ell-1}} A_{ij}^{(\ell)} \partial_{x_n} v_j^{(\ell-1)}\Big) \\
&+ \rho''\Big(\sum_{j=1}^{d_{\ell-1}} A_{ij}^{(\ell)} v_j^{(\ell-1)} + b_i^{(\ell)}\Big)\Big(\sum_{j=1}^{d_{\ell-1}} A_{ij}^{(\ell)} \partial^2_{x_k,x_n} v_j^{(\ell-1)}\Big)\Big(\sum_{j=1}^{d_{\ell-1}} A_{ij}^{(\ell)} \partial_{x_m} v_j^{(\ell-1)}\Big) \\
&+ \rho''\Big(\sum_{j=1}^{d_{\ell-1}} A_{ij}^{(\ell)} v_j^{(\ell-1)} + b_i^{(\ell)}\Big)\Big(\sum_{j=1}^{d_{\ell-1}} A_{ij}^{(\ell)} \partial^2_{x_m,x_n} v_j^{(\ell-1)}\Big)\Big(\sum_{j=1}^{d_{\ell-1}} A_{ij}^{(\ell)} \partial_{x_k} v_j^{(\ell-1)}\Big) \\
&+ \rho''\Big(\sum_{j=1}^{d_{\ell-1}} A_{ij}^{(\ell)} v_j^{(\ell-1)} + b_i^{(\ell)}\Big)\Big(\sum_{j=1}^{d_{\ell-1}} A_{ij}^{(\ell)} \partial^2_{x_k,x_m} v_j^{(\ell-1)}\Big)\Big(\sum_{j=1}^{d_{\ell-1}} A_{ij}^{(\ell)} \partial_{x_n} v_j^{(\ell-1)}\Big) \\
&+ \rho'\Big(\sum_{j=1}^{d_{\ell-1}} A_{ij}^{(\ell)} v_j^{(\ell-1)} + b_i^{(\ell)}\Big)\Big(\sum_{j=1}^{d_{\ell-1}} A_{ij}^{(\ell)} \partial^3_{x_k,x_m,x_n} v_j^{(\ell-1)}\Big).
\end{aligned}$$

This, along with the bound $\|\rho'''\|_{L^\infty(\mathbb{R})} \le 2$ from Lemma 2.2, implies

$$\begin{aligned}
\|\partial^3_{x_k,x_m,x_n} v_i^{(\ell)}\|_{L^\infty(\Omega)} \le\ & RW \max_{j=1,\ldots,d_{\ell-1}} \|\partial^3_{x_k,x_m,x_n} v_j^{(\ell-1)}\|_{L^\infty(\Omega)} \\
&+ 2R^3W^3 \max_{j=1,\ldots,d_{\ell-1}} \|\partial_{x_k} v_j^{(\ell-1)}\|_{L^\infty(\Omega)} \max_{j=1,\ldots,d_{\ell-1}} \|\partial_{x_m} v_j^{(\ell-1)}\|_{L^\infty(\Omega)} \max_{j=1,\ldots,d_{\ell-1}} \|\partial_{x_n} v_j^{(\ell-1)}\|_{L^\infty(\Omega)} \\
&+ R^2W^2\Big(\max_{j=1,\ldots,d_{\ell-1}} \|\partial^2_{x_k,x_n} v_j^{(\ell-1)}\|_{L^\infty(\Omega)} \max_{j=1,\ldots,d_{\ell-1}} \|\partial_{x_m} v_j^{(\ell-1)}\|_{L^\infty(\Omega)} \\
&+ \max_{j=1,\ldots,d_{\ell-1}} \|\partial^2_{x_m,x_n} v_j^{(\ell-1)}\|_{L^\infty(\Omega)} \max_{j=1,\ldots,d_{\ell-1}} \|\partial_{x_k} v_j^{(\ell-1)}\|_{L^\infty(\Omega)} \\
&+ \max_{j=1,\ldots,d_{\ell-1}} \|\partial^2_{x_k,x_m} v_j^{(\ell-1)}\|_{L^\infty(\Omega)} \max_{j=1,\ldots,d_{\ell-1}} \|\partial_{x_n} v_j^{(\ell-1)}\|_{L^\infty(\Omega)}\Big).
\end{aligned}$$

Then it follows from the estimates (5.20) and (5.21) and the condition $RW \ge 2$ that

$$\begin{aligned}
\|\partial^3_{x_k,x_m,x_n} v_i^{(\ell)}\|_{L^\infty(\Omega)} &\le 2R^{3\ell}W^{3\ell-3} + 6R^{3\ell-1}W^{3\ell-4} + RW \max_{j=1,\ldots,d_{\ell-1}} \|\partial^3_{x_k,x_m,x_n} v_j^{(\ell-1)}\|_{L^\infty(\Omega)} \\
&\le 5R^{3\ell}W^{3\ell-3} + RW \max_{j=1,\ldots,d_{\ell-1}} \|\partial^3_{x_k,x_m,x_n} v_j^{(\ell-1)}\|_{L^\infty(\Omega)}.
\end{aligned}$$

Meanwhile, direct computation gives the estimate

$$\|\partial^3_{x_k,x_m,x_n} v_i^{(1)}\|_{L^\infty(\Omega)} \le \Big\|\rho'''\Big(\sum_{j=1}^{d} A_{ij}^{(1)} x_j + b_i^{(1)}\Big) A_{ik}^{(1)} A_{im}^{(1)} A_{in}^{(1)}\Big\|_{L^\infty(\Omega)} \le 2R^3.$$

The last two estimates together and the condition $RW \ge 2$ yield

$$\|\partial^3_{x_k,x_s,x_t} v_i^{(\ell)}\|_{L^\infty(\Omega)} \le 10R^{3\ell}W^{3\ell-3}, \quad \forall \ell = 1, \ldots, L. \tag{5.22}$$

Substituting this estimate into (5.14) completes the proof of the lemma. □

Now we can state the error estimate on the approximation $\widetilde{q}_\theta^*$.

Theorem 5.4. *Let Assumption 5.3 hold. Fix $\epsilon > 0$, and let $\widetilde{\theta}^* \in \mathfrak{P}_{\infty,\epsilon}$ be a minimizer to problem (5.16)-(5.17) and $\widetilde{q}_\theta^*$ be its NN realization. Then with $\eta^2 := h^4 + \epsilon^2 + \delta^2 + \gamma$ and $\zeta := 1 + \gamma^{-1}\eta^2 + 2^{-2n}h^2R^{4L}W^{4L-4}$, we have*

$$\int_\Omega \Big(\frac{q^\dagger - P_{\mathcal{A}}(\widetilde{q}_\theta^*)}{q^\dagger}\Big)^2 \big(q^\dagger|\nabla u^\dagger|^2 + fu^\dagger\big)\,\mathrm{d}x \le c\big(h\zeta^{\frac{1}{2}} + (\min(h^{-1}\eta + h, 1) + 2^{-n}hR^LW^L)\zeta^{\frac{1}{2}}.$$

Moreover, if condition (5.11) holds, then

$$\|q^\dagger - P_{\mathcal{A}}(\widetilde{q}_\theta^*)\|_{L^2(\Omega)} \le c\big(h\zeta^{\frac{1}{2}} + (\min(h^{-1}\eta + h, 1) + 2^{-n}hR^LW^L)\zeta^{\frac{1}{2}}\big)^{\frac{1}{2(\beta+1)}}.$$

Proof. By the weak formulations of $u^\dagger$ and $\widetilde{u}_h(P_{\mathcal{A}}(\widetilde{q}_\theta^*)$, cf. (5.3) and (5.17), we have for any $\varphi \in H_0^1(\Omega)$,

$$\begin{aligned}
\big((q^\dagger - P_{\mathcal{A}}(\widetilde{q}_\theta^*))\nabla u^\dagger, \nabla\varphi\big) &= \big((q^\dagger - P_{\mathcal{A}}(\widetilde{q}_\theta^*))\nabla u^\dagger, \nabla(\varphi - P_h\varphi)\big) + \big((q^\dagger - P_{\mathcal{A}}(\widetilde{q}_\theta^*))\nabla u^\dagger, \nabla P_h\varphi\big)\\
&= -\big(\nabla\cdot((q^\dagger - P_{\mathcal{A}}(\widetilde{q}_\theta^*))\nabla u^\dagger), \varphi - P_h\varphi\big) + \big(P_{\mathcal{A}}(\widetilde{q}_\theta^*)\nabla(\widetilde{u}_h(P_{\mathcal{A}}(\widetilde{q}_\theta^*)) - u^\dagger), \nabla P_h\varphi\big)\\
&\quad + [\big(P_{\mathcal{A}}(\widetilde{q}_\theta^*)\nabla\widetilde{u}_h(P_{\mathcal{A}}(\widetilde{q}_\theta^*)), \nabla P_h\varphi\big)_h - \big(P_{\mathcal{A}}(\widetilde{q}_\theta^*)\nabla\widetilde{u}_h(P_{\mathcal{A}}(\widetilde{q}_\theta^*)), \nabla P_h\varphi\big)] =: \mathrm{I} + \mathrm{II} + \mathrm{III}.
\end{aligned}$$

Next we set $\varphi \equiv \frac{q^\dagger - P_{\mathcal{A}}(\widetilde{q}_\theta^*)}{q^\dagger}u^\dagger$ in the identity and bound the three terms separately. By the stability estimate (5.5) of the operator $P_{\mathcal{A}}$ and Lemmas 5.5 and 5.6, we have

$$\begin{aligned}
\|\nabla P_{\mathcal{A}}(\widetilde{q}_\theta^*)\|_{L^2(\Omega)}^2 &\le \|\nabla\widetilde{q}_\theta^*\|_{L^2(\Omega)}^2 = Q_h(|\nabla\widetilde{q}_\theta^*|^2) + [\|\nabla\widetilde{q}_\theta^*\|_{L^2(\Omega)}^2 - Q_h(|\nabla\widetilde{q}_\theta^*|^2)]\\
&\le c(\gamma^{-1}\eta^2 + 2^{-2n}h^2R^{4L}W^{4L-4}).
\end{aligned}$$

Thus we can bound $\|\nabla\varphi\|_{L^2(\Omega)}$ by

$$\|\nabla\varphi\|_{L^2(\Omega)} \le c(1 + \|\nabla P_{\mathcal{A}}(\widetilde{q}_\theta^*)\|_{L^2(\Omega)}) \le c\zeta^{\frac{1}{2}}. \tag{5.23}$$

Repeating the argument of Theorem 5.2 and applying Lemma 5.5 yield

$$\begin{aligned}
|\mathrm{I}| &\le ch(1 + \|\nabla P_{\mathcal{A}}q_\theta^*\|_{L^2(\Omega)}^2) \le ch\zeta,\\
|\mathrm{II}| &\le c\big(1 + \|\nabla P_{\mathcal{A}}(q_\theta^*)\|_{L^2(\Omega)}\big)\|\nabla(\widetilde{u}_h(P_{\mathcal{A}}(q_\theta^*)) - u^\dagger)\|_{L^2(\Omega)} \le c\min(h^{-1}\eta + h, 1)\zeta^{\frac{1}{2}}.
\end{aligned}$$

Next from Lemma 5.3 (with $p = 1$), the stability of $P_{\mathcal{A}}$ and the bound (5.20), we deduce

$$\begin{aligned}
|\mathrm{III}| &\le c2^{-n}h\|P_{\mathcal{A}}(\widetilde{q}_\theta^*)\|_{W^{1,\infty}(\Omega)}\|\nabla\widetilde{u}_h(P_{\mathcal{A}}(\widetilde{q}_\theta^*))\|_{L^2(\Omega)}\|\nabla P_h\varphi\|_{L^2(\Omega)}\\
&\le c2^{-n}h\zeta^{\frac{1}{2}}(\|P_{\mathcal{A}}(\widetilde{q}_\theta^*)\|_{L^\infty(\Omega)} + \|\nabla P_{\mathcal{A}}(\widetilde{q}_\theta^*)\|_{L^\infty(\Omega)})\\
&\le c2^{-n}h\zeta^{\frac{1}{2}}(1 + \|\nabla\widetilde{q}_\theta^*\|_{L^\infty(\Omega)}) \le c2^{-n}hR^LW^L\zeta^{\frac{1}{2}}.
\end{aligned}$$

The proof of the second assertion is identical with that of Theorem 5.2. □

Remark 5.3. *Theorem 5.4 indicates that the error estimate in the presence of numerical quadrature is similar to the case of exact integration, provided that the quadrature error is sufficiently small. The*

quadrature error involves a factor $R^{4L}W^{4L-1}$, which can be large for deep NNs, and hence it may require a large n to compensate its influence on the reconstruction $P_{\mathcal{A}}(\widetilde{q}_\theta^*)$. Indeed, one may take $2^{-2n}h^2R^{4L}W^{4L-4} = \mathcal{O}(1)$. This and the choice $\widetilde{\theta}^* \in \mathfrak{P}_{\infty,\epsilon}$, i.e., $L = \mathcal{O}(\log(d+2))$, $N_\theta = \mathcal{O}(\epsilon^{-\frac{d}{1-\mu}})$ and $R = \mathcal{O}(\epsilon^{-2-\frac{2+3d}{1-\mu}})$ directly imply $n = \mathcal{O}(d|\log\epsilon|)$. This estimate is a bit pessimistic. In practice, the choice $n = 0$ suffices the desired accuracy.

5.2 Parabolic inverse problem

In this section, we extend the hybrid approach to the parabolic case:

$$\begin{cases} \partial_t u - \nabla\cdot(q\nabla u) = f, & \text{in } \Omega\times(0,T), \\ u = 0, & \text{on } \partial\Omega\times(0,T), \\ u(0) = u_0, & \text{in } \Omega. \end{cases} \tag{5.24}$$

Like before, we are given the observation z^δ on the space-time domain $\Omega\times(T_0,T)$ (with $0\le T_0<T$):

$$\|u(q^\dagger) - z^\delta\|_{L^2(T_0,T;L^2(\Omega))} \le \delta,$$

with a noise level δ. We aim at recovering the coefficient $q\in\mathcal{A}$ from z^δ.

5.2.1 The regularized problem and its hybrid approximation

To recover the coefficient q in the model (5.24), we formulate a numerical scheme by

$$\min_{q\in\mathcal{A}} J_\gamma(q) = \frac{1}{2}\|u(q)(t) - z^\delta(t)\|^2_{L^2(T_0,T;L^2(\Omega))} + \frac{\gamma}{2}\|\nabla q\|^2_{L^2(\Omega)}, \tag{5.25}$$

where $u(t)\equiv u(q)(t)\in H_0^1(\Omega)$ with $u(0)=u_0$ satisfies

$$(\partial_t u(t),\varphi) + (q\nabla u(t),\nabla\varphi) = (f,\varphi), \quad \forall\varphi\in H_0^1(\Omega), \text{ a.e. } t\in(0,T). \tag{5.26}$$

Next we describe the hybrid NN-FEM discretization of problem (5.25)–(5.26). For the space discretization, we employ NNs and Galerkin FEM to approximate the diffusion coefficient q and state u, respectively. For the time discretization, we employ the backward Euler time-stepping scheme [139]: We divide the time interval $(0,T)$ into N uniform subintervals with a time step size τ and grid points $t_n = n\tau$, $n=0,\ldots,N$. Next we denote by $v^n = v(t_n)$ and define the backward difference quotient $\bar\partial_\tau$ by $\bar\partial_\tau v^n := \tau^{-1}(v^n - v^{n-1})$. Further we assume $T_0 = N_0\tau$ for some $N_0\in\mathbb{N}$. For a sequence of functions $\{v^n\}_{n=N_0}^N\subset X$, we define a discrete norm $\|(v^n)_{N_0}^N\|_{\ell^2(X)}$ by

$$\|(v^n)_{N_0}^N\|_{\ell^2(X)} = \Big(\tau\sum_{n=N_0}^N \|v^n\|_X^2\Big)^{\frac{1}{2}}.$$

With these preliminaries, the hybrid NN-FEM scheme for problem (5.25)–(5.26) reads

$$\min_{\theta\in\mathfrak{P}_{p,\epsilon}} J_{\gamma,h,\tau}(q_\theta) = \frac{1}{2}\|(U_h^n(P_{\mathcal{A}}(q_\theta)) - z_n^\delta)_{N_0}^N\|^2_{\ell^2(L^2(\Omega))} + \frac{\gamma}{2}\|\nabla q_\theta\|^2_{L^2(\Omega)}, \tag{5.27}$$

where $z_n^\delta := \tau^{-1}\int_{t_{n-1}}^{t_n} z^\delta(t)\mathrm{d}t$, and $U_h^n \equiv U_h^n(q_\theta) \in V_h^0$ with $U_h^0(q_\theta) = P_h u_0$ satisfies

$$(\bar\partial_\tau U_h^n, \varphi_h) + (P_{\mathcal{A}}(q_\theta)\nabla U_h^n, \nabla\varphi_h) = (f(t_n), \varphi_h), \quad \forall \varphi_h \in V_h^0,\ n = 1, \ldots, N. \tag{5.28}$$

For any $\gamma > 0$, a standard argument yields the well-posedness of problems (5.25)–(5.26) and (5.27)–(5.28); Let q_θ^* be the NN realization of a minimizer θ^* to problem (5.27)–(5.28). See the work [94] for relevant discussions on the pure FEM approximation. It also includes a detailed convergence analysis of the FEM approximation to a global minimizer of problem (5.25)–(5.26) as the discretization parameters $h, \tau \to 0^+$. See also [144, 84] for relevant error analysis.

5.2.2 Error analysis

Now we provide an error analysis of the approximation $P_{\mathcal{A}}(q_\theta^*)$, under the following assumption.

Assumption 5.5. *For some $p \geq \max(2, d+\mu)$ with $\mu > 0$, $q^\dagger \in W^{2,p}(\Omega)\cap\mathcal{A}$, $u_0 \in H^2(\Omega)\cap H_0^1(\Omega)\cap W^{1,\infty}(\Omega)$ and $f \in L^\infty(0,T;L^\infty(\Omega))\cap C^1([0,T];L^2(\Omega))\cap W^{2,1}(0,T;L^2(\Omega))$.*

Under Assumption 5.5, the following regularity estimates hold on $u^\dagger \equiv u(q^\dagger)$ [84, p. 128]: for any $r, q \in (1,\infty)$

$$\partial_t u^\dagger \in L^r(0,T;L^q(\Omega)), \Delta u^\dagger \in L^r(0,T;L^q(\Omega)) \text{ and } u^\dagger \in L^\infty(0,T;W^{1,\infty}(\Omega)); \tag{5.29}$$

$$\|u^\dagger(t)\|_{H^2(\Omega)} + \|\partial_t u^\dagger(t)\|_{L^2(\Omega)} + t\|\partial_{tt} u^\dagger(t)\|_{L^2(\Omega)} \leq c, \text{ a.e. } t \in (0,T]. \tag{5.30}$$

The next lemma gives the existence of an approximation in the discrete admissible set $\mathfrak{P}_{p,\epsilon}$.

Lemma 5.7. *Let Assumption 5.5 hold. Then for $\epsilon > 0$, there exists $\theta_\epsilon \in \mathfrak{P}_{p,\epsilon}$ such that*

$$\|(u^\dagger(t_n) - U_h^n(P_{\mathcal{A}}(q_{\theta_\epsilon})))_1^N\|^2_{\ell^2(L^2(\Omega))} \leq c(\tau^2 + h^4 + \epsilon^2).$$

Proof. By the argument of Lemma 5.1, we can find $\theta_\epsilon \in \mathfrak{P}_{p,\epsilon}$ such that the estimates (5.9) and (5.10) hold. Next we bound $\varrho_h^n := U_h^n(P_{\mathcal{A}}(q_{\theta_\epsilon})) - U_h^n(q^\dagger)$. It follows from the weak formulations of $U_h^n(P_{\mathcal{A}}(q_{\theta_\epsilon}))$ and $U_h^n(q^\dagger)$, cf. (5.28), that ϱ_h^n satisfies $\varrho_h^0 = 0$ and

$$(\bar\partial_\tau \varrho_h^n, \varphi_h) + (P_{\mathcal{A}}(q_{\theta_\epsilon})\nabla\varrho_h^n, \nabla\varphi_h) = \big((q^\dagger - P_{\mathcal{A}}(q_{\theta_\epsilon}))\nabla U_h^n(q^\dagger), \nabla\varphi_h\big), \quad \forall\varphi_h \in V_h^0,\ n = 1, 2, \ldots, N.$$

Setting $\varphi_h = 2\varrho_h^n$ into this identity, and then applying Hölder's inequality lead to

$$\tau^{-1}(\|\varrho_h^n\|^2_{L^2(\Omega)} - \|\varrho_h^{n-1}\|^2_{L^2(\Omega)}) + 2\underline{c}_q\|\nabla\varrho_h^n\|^2_{L^2(\Omega)} \leq 2\|q^\dagger - P_{\mathcal{A}}(q_{\theta_\epsilon})\|_{L^\infty(\Omega)}\|\nabla U_h^n(q^\dagger)\|_{L^2(\Omega)}\|\nabla\varrho_h^n\|_{L^2(\Omega)}.$$

Summing the inequality over n from 1 to N, noting $\varrho_h^0 = 0$ and applying (5.10) give

$$\begin{aligned}\|\varrho_h^N\|_{L^2(\Omega)}^2 + 2\underline{c}_q\|(\nabla\varrho_h^n)_1^N\|_{\ell^2(L^2(\Omega))}^2 &\le 2\|q^\dagger - P_{\mathcal{A}}(q_{\theta_\epsilon})\|_{L^\infty(\Omega)}\tau\sum_{n=1}^N \|\nabla U_h^n(q^\dagger)\|_{L^2(\Omega)}\|\nabla\varrho_h^n\|_{L^2(\Omega)}\\ &\le c\epsilon\|(\nabla U_h^n(q^\dagger))_1^N\|_{\ell^2(L^2(\Omega))}\|(\nabla\varrho_h^n)_1^N\|_{\ell^2(L^2(\Omega))}.\end{aligned}$$

Since $\|(\nabla U_h^n(q^\dagger))_1^N\|_{\ell^2(L^2(\Omega))} \le c$ [144, Lemma 6.2], we obtain $\|(\varrho_h^n)_1^N\|_{\ell^2(H^1(\Omega))} \le c\epsilon$. This and the estimate $\|(u^\dagger(t_n) - U_h^n(q^\dagger))_1^N\|_{\ell^2(L^2(\Omega))}^2 \le c(\tau^2 + h^4)$ [84, Lemma 4.2] complete the proof. □

The next lemma gives an important *a priori* bound.

Lemma 5.8. *Let Assumption 5.5 hold. For any $\epsilon > 0$, let $\theta^* \in \mathfrak{P}_{p,\epsilon}$ be a minimizer to problem (5.27)-(5.28) and q_θ^* its NN realization. Then the following estimate holds*

$$\|(u^\dagger(t_n) - U_h^n(P_{\mathcal{A}}(q_\theta^*)))_{N_0}^N\|_{\ell^2(L^2(\Omega))}^2 + \gamma\|\nabla P_{\mathcal{A}}(q_\theta^*)\|_{L^2(\Omega)}^2 \le c(\tau^2 + h^4 + \epsilon^2 + \delta^2 + \gamma).$$

Proof. Let q_{θ_ϵ} be the NN realization of a parameter $\theta_\epsilon \in \mathfrak{P}_{p,\epsilon}$ satisfying (5.9) and (5.10), which implies also $\|q_\epsilon\|_{H^1(\Omega)} \le c$. Under Assumption 5.5, the following estimate holds [84, Lemma 4.1]

$$\|(u^\dagger(t_n) - z_n^\delta)_{N_0}^N\|_{\ell^2(L^2(\Omega))}^2 \le c(\tau^2 + \delta^2).$$

Then by Lemma 5.7 and the minimizing property of q_θ^*, i.e., $J_{\gamma,h,\tau}(q_\theta^*) \le J_{\gamma,h,\tau}(q_{\theta_\epsilon})$, we derive

$$\begin{aligned}&\|(U_h^n(P_{\mathcal{A}}(q_\theta^*)) - z_n^\delta)_{N_0}^N\|_{\ell^2(L^2(\Omega))}^2 + \gamma\|\nabla q_\theta^*\|_{L^2(\Omega)}^2 \le \|(U_h^n(P_{\mathcal{A}}(q_{\theta_\epsilon})) - z_n^\delta)_{N_0}^N\|_{\ell^2(L^2(\Omega))}^2 + \gamma\|\nabla q_{\theta_\epsilon}\|_{L^2(\Omega)}^2\\ \le& c\big(\|(U_h^n(P_{\mathcal{A}}(q_{\theta_\epsilon})) - u^\dagger(t_n))_{N_0}^N\|_{\ell^2(L^2(\Omega))}^2 + \|(u^\dagger(t_n) - z_n^\delta)_{N_0}^N\|_{\ell^2(L^2(\Omega))}^2 + \gamma\big) \le c(\tau^2 + h^4 + \epsilon^2 + \delta^2 + \gamma),\end{aligned}$$

Then by the triangle inequality, we have

$$\begin{aligned}\|(u^\dagger(t_n) - U_h^n(P_{\mathcal{A}}(q_\theta^*)))_{N_0}^N\|_{\ell^2(L^2(\Omega))}^2 + \gamma\|\nabla q_\theta^*\|_{L^2(\Omega)}^2 &\le c\|(u^\dagger(t_n) - z_n^\delta)_{N_0}^N\|_{\ell^2(L^2(\Omega))}^2\\ &+ c\|(z_n^\delta - U_h^n(P_{\mathcal{A}}(q_\theta^*)))_{N_0}^N\|_{\ell^2(L^2(\Omega))}^2 + \gamma\|\nabla q_\theta^*\|_{L^2(\Omega)}^2 \le c(\tau^2 + h^4 + \epsilon^2 + \delta^2 + \gamma).\end{aligned}$$

Finally, the bound on $\|\nabla P_{\mathcal{A}}(q_\theta^*)\|_{L^2(\Omega)}$ follows from the stability estimate (5.5). □

Now we can state an error estimate on the NN approximation q_θ^*.

Theorem 5.6. *Let Assumption 5.5 hold. Fix any $\epsilon > 0$, and let $\theta^* \in \mathfrak{P}_{p,\epsilon}$ be a minimizer to problem (5.27)-(5.28) and q_θ^* its NN realization. Then with $\eta^2 := \tau^2 + h^4 + \epsilon^2 + \delta^2 + \gamma$, there holds*

$$\begin{aligned}&\tau^3\sum_{j=N_0+1}^N\sum_{i=N_0+1}^j\sum_{n=i}^j\int_\Omega \Big(\frac{q^\dagger - P_{\mathcal{A}}(q_\theta^*)}{q^\dagger}\Big)^2\big(q^\dagger|\nabla u^\dagger(t_n)|^2 + \big(f(t_n) - \partial_t u^\dagger(t_n)\big)u^\dagger(t_n)\big)\,\mathrm{d}x\\ \le\ & c(\min(h^{-1}\eta + h, 1) + h\gamma^{-\frac{1}{2}}\eta)\gamma^{-\frac{1}{2}}\eta.\end{aligned}$$

Proof. For any $\varphi \in H_0^1(\Omega)$, the weak formulations of $u^\dagger$ and $U_h^n(P_{\mathcal{A}}(q_\theta^*)))$ in (5.26) and (5.28) yield

$$
\begin{aligned}
&\big((q^\dagger - P_{\mathcal{A}}(q_\theta^*))\nabla u^\dagger(t_n), \nabla\varphi\big)\\
&= \big((q^\dagger - P_{\mathcal{A}}(q_\theta^*))\nabla u^\dagger(t_n), \nabla(\varphi - P_h\varphi)\big) + \big((q^\dagger - P_{\mathcal{A}}(q_\theta^*))\nabla u^\dagger(t_n), \nabla P_h\varphi\big)\\
&= \big((q^\dagger - P_{\mathcal{A}}(q_\theta^*))\nabla u^\dagger(t_n), \nabla(\varphi - P_h\varphi)\big) + \big(P_{\mathcal{A}}(q_\theta^*)\nabla(U_h^n(P_{\mathcal{A}}(q_\theta^*)) - u^\dagger(t_n)), \nabla P_h\varphi\big)\\
&\quad + \big(q^\dagger\nabla u^\dagger(t_n) - P_{\mathcal{A}}(q_\theta^*)\nabla U_h^n(P_{\mathcal{A}}(q_\theta^*)), \nabla P_h\varphi\big)\\
&= -\big(\nabla\cdot\big((q^\dagger - P_{\mathcal{A}}(q_\theta^*))\nabla u^\dagger(t_n)\big), \varphi - P_h\varphi\big) + \big(P_{\mathcal{A}}(q_\theta^*)\nabla(U_h^n(P_{\mathcal{A}}(q_\theta^*)) - u^\dagger(t_n)), \nabla P_h\varphi\big)\\
&\quad + \big(\bar\partial_\tau U_h^n(P_{\mathcal{A}}(q_\theta^*)) - \partial_t u^\dagger(t_n), P_h\varphi\big) =: \mathrm{I}^n + \mathrm{II}^n + \mathrm{III}^n.
\end{aligned}
$$

Next we set $\varphi \equiv \varphi^n = \frac{q^\dagger - P_{\mathcal{A}}(q_\theta^*)}{q^\dagger} u^\dagger(t_n)$ in the identity, and bound the three terms separately. Under Assumption 5.5, the regularity bound (5.30) and the box constraint $P_{\mathcal{A}}(q_\theta^*) \in \mathcal{A}$ imply

$$
\max_{0\le n\le N} \|\nabla\varphi^n\|_{L^2(\Omega)} \le c(1 + \|\nabla P_{\mathcal{A}}(q_\theta^*)\|_{L^2(\Omega)}). \tag{5.31}
$$

Then repeating the argument for Theorem 5.2 and applying Lemma 5.8 lead to

$$
|\mathrm{I}^n| \le ch(1 + \|\nabla P_{\mathcal{A}}(q_\theta^*)\|_{L^2(\Omega)})\|\nabla\varphi^n\|_{L^2(\Omega)} \le ch(1 + \|\nabla P_{\mathcal{A}}(q_\theta^*)\|_{L^2(\Omega)}^2) \le ch\gamma^{-1}\eta^2.
$$

Next, by the Cauchy–Schwarz inequality, the $H^1(\Omega)$-stability of P_h, the box constraint $P_{\mathcal{A}}(q_\theta^*) \in \mathcal{A}$ and the estimate (5.31), we bound the term II^n as

$$
\begin{aligned}
|\mathrm{II}^n| &\le c\|\nabla(U_h^n(P_{\mathcal{A}}(q_\theta^*)) - u^\dagger(t_n))\|_{L^2(\Omega)}\|\nabla P_h\varphi^n\|_{L^2(\Omega)}\\
&\le c\|\nabla(U_h^n(P_{\mathcal{A}}(q_\theta^*)) - u^\dagger(t_n))\|_{L^2(\Omega)}\|\nabla\varphi^n\|_{L^2(\Omega)}\\
&\le c(1 + \|\nabla P_{\mathcal{A}}(q_\theta^*)\|_{L^(\Omega)})\|\nabla(U_h^n(P_{\mathcal{A}}(q_\theta^*)) - u^\dagger(t_n))\|_{L^2(\Omega)}.
\end{aligned}
$$

Then it follows from the inverse estimate in the space V_h^0 [139, (1.12), p. 4] and (2.3) that

$$
\begin{aligned}
&\tau\sum_{n=N_0}^N |\mathrm{II}^n| \le c\gamma^{-\frac12}\eta\big\|(\nabla(U_h^n(P_{\mathcal{A}}(q_\theta^*)) - u^\dagger(t_n)))_{N_0}^N\big\|_{\ell^2(L^2(\Omega))}\\
&\le c\gamma^{-\frac12}\eta\big(\big\|(\nabla(U_h^n(P_{\mathcal{A}}(q_\theta^*)) - P_h u^\dagger(t_n)))_{N_0}^N\big\|_{\ell^2(L^2(\Omega))} + \big\|(\nabla(u^\dagger(t_n) - P_h u^\dagger(t_n)))_{N_0}^N\big\|_{\ell^2(L^2(\Omega))}\big)\\
&\le c\gamma^{-\frac12}\eta\big(h^{-1}\|(U_h^n(P_{\mathcal{A}}(q_\theta^*)) - P_h u^\dagger(t_n))_{N_0}^N\|_{\ell^2(L^2(\Omega))} + h\|(u^\dagger(t_n))_{N_0}^N\|_{\ell^2(H^2(\Omega))}\big).
\end{aligned}
$$

Now by applying the $L^2(\Omega)$-stability of P_h and Lemma 5.8, we deduce

$$
\tau\sum_{n=N_0}^N |\mathrm{II}^n| \le c\gamma^{-\frac12}\eta\big(h^{-1}\|(U_h^n(P_{\mathcal{A}}(q_\theta^*)) - u^\dagger(t_n))_{N_0}^N\|_{\ell^2(L^2(\Omega))} + h\big) \le c(h + h^{-1}\eta)\gamma^{-\frac12}\eta.
$$

Meanwhile, the box constraint $P_{\mathcal{A}}(q_\theta^*) \in \mathcal{A}$ and the standard energy argument imply

$$
\|(\nabla(U_h^n(P_{\mathcal{A}}(q_\theta^*)) - u^\dagger(t_n)))_{N_0}^N\|_{\ell^2(L^2(\Omega))} \le c. \tag{5.32}
$$

Thus we obtain

$$\tau \sum_{n=N_0}^{N} |\mathrm{II}^n| \le c\gamma^{-\frac{1}{2}}\eta \min(1, h + h^{-1}\eta).$$

For the last term III^n, we further split it into

$$\mathrm{III}^n = \big(\bar\partial_\tau U_h^n(P_{\mathcal{A}}(q_\theta^*)) - \bar\partial_\tau u^\dagger(t_n), P_h\varphi^n\big) + \big(\bar\partial_\tau u^\dagger(t_n) - \partial_t u^\dagger(t_n), P_h\varphi^n\big) =: \mathrm{III}_1^n + \mathrm{III}_2^n,$$

and then bound III_1^n and III_2^n separately. Repeating the argument in [84, Theorem 4.5] gives

$$\Big|\tau^3 \sum_{j=N_0+1}^{N} \sum_{i=N_0+1}^{j} \sum_{n=i}^{j} \mathrm{III}_2^n\Big| \le c\tau.$$

To bound the term III_1^n, by the summation by parts formula, we deduce

$$\begin{aligned}\tau \sum_{n=i}^{j} \mathrm{III}_1^n =& -\tau \sum_{n=i}^{j-1} \big(U_h^n(P_{\mathcal{A}}(q_\theta^*)) - u^\dagger(t_n), \bar\partial_\tau P_h\varphi^{n+1}\big) + \big(U_h^j(P_{\mathcal{A}}(q_\theta^*)) - u^\dagger(t_j), P_h\varphi^j\big)\\ &- \big(U_h^{i-1}(P_{\mathcal{A}}(q_\theta^*)) - u^\dagger(t_{i-1}), P_h\varphi^i\big).\end{aligned}$$

Since $\|P_h\varphi^n\|_{L^2(\Omega)} \le \|\varphi^n\|_{L^2(\Omega)} \le c$, we get

$$\Big|\tau \sum_{j=N_0+1}^{N} \big(U_h^j(P_{\mathcal{A}}(q_\theta^*)) - u^\dagger(t_j), P_h\varphi^j\big)\Big| + \Big|\tau \sum_{i=N_0+1}^{N} \big(U_h^{i-1}(P_{\mathcal{A}}(q_\theta^*)) - u^\dagger(t_{i-1}), P_h\varphi^i\big)\Big| \le c\eta.$$

Moreover, from the $L^2(\Omega)$ stability of P_h, Assumption 5.5 and the box constraint $P_{\mathcal{A}}(q_\theta^*) \in \mathcal{A}$, we deduce

$$\|\bar\partial_\tau P_h\varphi^n\|_{L^2(\Omega)} \le \tau^{-1}\Big\| \int_{t_{n-1}}^{t_n} \frac{q^\dagger - P_{\mathcal{A}}(q_\theta^*)}{q^\dagger}\partial_t u(t)\ \mathrm{d}t\Big\|_{L^2(\Omega)} \le c\|\partial_t u\|_{C([t_{n-1},t_n];L^2(\Omega))}.$$

Thus, we have

$$\Big|\tau^3 \sum_{j=N_0+1}^{N} \sum_{i=N_0+1}^{j} \sum_{n=i}^{j} \big(U_h^n(q_\theta^*) - u^\dagger(t_n), \bar\partial_\tau P_h\varphi^{n+1}\big)\Big| \le c\eta.$$

Finally, combining the preceding estimates with the identity

$$\big((q^\dagger - P_{\mathcal{A}}(q_\theta^*))\nabla u^\dagger(t_n), \nabla\varphi^n\big) = \frac{1}{2}\int_\Omega \Big(\frac{q^\dagger - P_{\mathcal{A}}(q_\theta^*)}{q^\dagger}\Big)^2 \big(q^\dagger|\nabla u^\dagger(t_n)|^2 + \big(f(t_n) - \partial_t u^\dagger(t_n)\big)u^\dagger(t_n)\big)\ \mathrm{d}x$$

completes the proof of the theorem. □

Similarly, we can impose a positivity condition: there exists some $\beta \ge 0$ such that for any $t \in [T_0, T]$

$$q^\dagger|\nabla u^\dagger(x,t)|^2 + \big(f(x,t) - \partial_t u^\dagger(x,t)\big)u^\dagger(x,t) \ge c\ \mathrm{dist}(x,\partial\Omega)^\beta, \quad \text{a.e. in } \Omega. \tag{5.33}$$

This condition holds with $\beta = 0, 2$ under suitable assumptions on the problem data [84, Propositions 4.7 and 4.8]. Under condition (5.33), the argument of Theorem 5.2 gives the following $L^2(\Omega)$ error bound.

Corollary 5.1. *Under the assumptions in Theorem 5.6 and condition* (5.33)*, there holds*

$$\|q^\dagger - q_\theta^*\|_{L^2(\Omega)} \le c\big(\min(h^{-1}\eta + h, 1) + h\gamma^{-\frac{1}{2}}\eta)\gamma^{-\frac{1}{2}}\eta\big)^{\frac{1}{2(1+\beta)}}.$$

5.2.3 Quadrature error analysis

Now we study the influence of quadrature errors on the reconstruction. Like before, we formulate a practical hybrid NN-FEM discretization scheme of problem (5.25)-(5.26) (with numerical integration) by

$$\min_{\theta\in\mathfrak{P}_{\infty,\epsilon}} \widetilde{J}_{\gamma,h,\tau}(q_\theta) = \frac{1}{2}\|(\widetilde{U}_h^n(P_{\mathcal{A}}(q_\theta)) - z_n^\delta)_{N_0}^M\|_{\ell^2(L^2(\Omega))}^2 + \frac{\gamma}{2}Q_h(|\nabla q_\theta|^2), \tag{5.34}$$

where $z_n^\delta := \tau^{-1}\int_{t_{n-1}}^{t_n} z^\delta(t)\mathrm{d}t$, and $\widetilde{U}_h^n \equiv \widetilde{U}_h^n(P_{\mathcal{A}}(q_\theta)) \in V_h^0$ with $\widetilde{U}_h^0(P_{\mathcal{A}}(q_\theta)) = P_h u_0$ satisfies

$$(\bar{\partial}_\tau \widetilde{U}_h^n, \varphi_h) + (P_{\mathcal{A}}(q_\theta)\nabla\widetilde{U}_h^n, \nabla\varphi_h)_h = (f(t_n), \varphi_h), \quad \forall\varphi_h \in V_h^0,\ n = 1,\dots,N. \tag{5.35}$$

Using the box constraint $P_{\mathcal{A}}(q_\theta) \in \mathcal{A}$ and the standard energy argument, we have

$$\|(\nabla\widetilde{U}_h^n(P_{\mathcal{A}}(q_\theta)))_1^N\|_{\ell^2(L^2(\Omega))} \le c. \tag{5.36}$$

The existence of a discrete forward map $P_{\mathcal{A}}(q_\theta) \mapsto \{U_h^n\}_{n=1}^N$ follows from the ellipticity of the broken $L^2(\Omega)$ semi-inner product $(\cdot,\cdot)_h$ over the space V_h^0, and a standard argument yields that problem (5.34)-(5.35) has at least one minimizer $\widetilde{\theta}^*$ with a continuous dependence on the data. Next we derive (weighted) $L^2(\Omega)$ error bounds of $P_{\mathcal{A}}(\widetilde{q}_\theta^*)$, with the NN realization $\widetilde{q}_\theta^*$ of the minimizer $\widetilde{\theta}^*$.

Assumption 5.7. *$q^\dagger \in W^{2,\infty}(\Omega)\cap\mathcal{A}$, $u_0 \in H^2(\Omega)\cap H_0^1(\Omega)\cap W^{1,\infty}(\Omega)$ and $f \in L^\infty(0,T;L^\infty(\Omega))\cap C^1(0,T;L^2(\Omega))\cap W^{2,1}(0,T;L^2(\Omega))$.*

The next lemma gives an analogue of Lemma 5.7 for the quadrature scheme.

Lemma 5.9. *Let Assumption 5.7 hold. Then for small $\epsilon > 0$, there exists $\theta_\epsilon \in \mathfrak{P}_{\infty,\epsilon}$ such that*

$$\|\big(u(q^\dagger)(t_n) - \widetilde{U}_h^n(P_{\mathcal{A}}(q_{\theta_\epsilon}))\big)_1^N\|_{\ell^2(L^2(\Omega))}^2 \le c(\tau^2 + h^4 + \epsilon^2).$$

Proof. It follows from Lemma 5.1 that there exists $\theta_\epsilon \in \mathfrak{P}_{\infty,\epsilon}$ such that the estimate (5.19) holds for the NN realization q_{θ_ϵ}. Let $\varrho_h^n = \widetilde{U}_h^n(q^\dagger) - \widetilde{U}_h^n(P_{\mathcal{A}}(q_{\theta_\epsilon}))$. Then it satisfies $\varrho_h^n = 0$ and for all $n = 1,2,\dots,N$

$$(\partial_\tau\varrho_h^n, \varphi_h) + (P_{\mathcal{A}}(q_{\theta_\epsilon})\nabla\varrho_h^n, \nabla\varphi_h)_h = ((P_{\mathcal{A}}(q_{\theta_\epsilon}) - q^\dagger)\nabla\widetilde{U}_h^n(q^\dagger), \nabla\varphi_h)_h, \quad \forall\varphi_h \in V_h^0.$$

Repeating the argument of Lemma 5.7 gives

$$\|(\widetilde{U}_h^n(q^\dagger) - \widetilde{U}_h^n(P_{\mathcal{A}}(q_{\theta_\epsilon})))_1^N\|_{\ell^2(L^2(\Omega))} \le c\epsilon. \tag{5.37}$$

Since $\|(u^\dagger(t_n) - U_h^n(q^\dagger))_1^N\|_{\ell^2(L^2(\Omega))} \le c(\tau + h^2)$ [84, Lemma 4.2], it suffices to show

$$\|(U_h^n(q^\dagger) - \widetilde{U}_h^n(q^\dagger))_1^N\|_{\ell^2(L^2(\Omega))} \le ch^2. \tag{5.38}$$

Let $e_h^n = U_h^n(q^\dagger) - \widetilde{U}_h^n(q^\dagger)$. Then e_h^n satisfies $e_h^n = 0$ and

$$(\partial_\tau e_h^n, \varphi_h) + (q^\dagger \nabla e_h^n, \nabla \varphi_h)_h = (q^\dagger \nabla U_h^n(q^\dagger), \nabla \varphi_h)_h - (q^\dagger \nabla U_h^n(q^\dagger), \nabla \varphi_h), \quad \forall \varphi_h \in V_h^0, n = 1, \ldots, N.$$

Now upon choosing $\varphi_h = e_h^n$ and applying Lemma 5.3 (with $p = 2$), we obtain

$$|(q^\dagger \nabla e_h^n, \nabla e_h^n)_h - (q^\dagger \nabla e_h^n, \nabla e_h^n)| \le ch^2 \|q^\dagger\|_{W^{2,\infty}(\Omega)} \|\nabla U_h^n(q^\dagger)\|_{L^2(\Omega)} \|\nabla e_h^n\|_{L^2(\Omega)}.$$

Consequently, we have

$$\tfrac{1}{2}\partial_\tau \|e_h^n\|_{L^2(\Omega)}^2 + \underline{c}_q \|\nabla e_h^n\|_{L^2(\Omega)}^2 \le ch^2 \|q^\dagger\|_{W^{2,\infty}(\Omega)} \|\nabla U_h^n(q^\dagger)\|_{L^2(\Omega)} \|\nabla e_h^n\|_{L^2(\Omega)}.$$

Then upon summing the identity over n from 1 to N, noting $e_h^0 = 0$, we arrive at

$$\|e_h^N\|_{L^2(\Omega)}^2 + \underline{c}_q \|(\nabla e_h^n)_1^N\|_{\ell^2(L^2(\Omega))}^2 \le ch^2 \|(\nabla U_h^n(q^\dagger))_1^N\|_{\ell^2(L^2(\Omega))} \|(\nabla e_h^n)_1^N\|_{\ell^2(L^2(\Omega))}.$$

Then the estimate (5.38) follows from the bound $\|(\nabla U_h^n(q^\dagger))_1^N\|_{\ell^2(L^2(\Omega))} \le c$ [144, Lemma 6.2]. □

The next lemma gives an *a priori* bound on $u(q^\dagger)(t_n) - \widetilde{U}_h^n(\widetilde{q}_\theta^*)$ and $\widetilde{q}_\theta^*$, with the quadrature approximation. The proof is identical with that for Lemma 5.8, and hence omitted.

Lemma 5.10. *Let Assumption 5.7 hold. Fix $\epsilon > 0$, and let $\theta^* \in \mathfrak{P}_{\infty,\epsilon}$ be a minimizer to problem (5.34)-(5.35) and $\widetilde{q}_\theta^*$ its NN realization. Then the following estimate holds*

$$\|(u(q^\dagger)(t_n) - \widetilde{U}_h^n(P_{\mathcal{A}}(\widetilde{q}_\theta^*)))_{N_0}^N\|_{\ell^2(L^2(\Omega))}^2 + \gamma Q_h(|\nabla P_{\mathcal{A}}(\widetilde{q}_\theta^*)|^2) \le c(\tau^2 + h^4 + \epsilon^2 + \delta^2 + \gamma).$$

Now we can present the main result of this section.

Theorem 5.8. *Let Assumption 5.7 hold. Fix $\epsilon > 0$, and let $\theta^* \in \mathfrak{P}_{\infty,\epsilon}$ be a minimizer to problem (5.34)-(5.35) and $\widetilde{q}_\theta^*$ its NN realization. Let $\eta^2 := \tau^2 + h^4 + \epsilon^2 + \delta^2 + \gamma$ and $\zeta = 1 + \gamma^{-1}\eta^2 + 2^{-2n}h^2 R^{4L} W^{4L-4}$. Then the following estimate holds*

$$\begin{aligned}
&\tau^3 \sum_{j=N_0+1}^{N} \sum_{i=N_0+1}^{j} \sum_{n=i}^{j} \int_\Omega \left(\frac{q^\dagger - P_{\mathcal{A}}(\widetilde{q}_\theta^*)}{q^\dagger}\right)^2 \big(q^\dagger |\nabla u^\dagger(t_n)|^2 + \big(f(t_n) - \partial_t u^\dagger(t_n)\big) u^\dagger(t_n)\big)\, \mathrm{d}x \\
&\le c\big(h\zeta^{\frac{1}{2}} + (\min(h^{-1}\eta + h, 1) + 2^{-n} h d^{\frac{1}{2}} R^L W^L)\zeta^{\frac{1}{2}}.
\end{aligned}$$

Proof. For any $\varphi \in H_0^1(\Omega)$, the weak formulations of $u^\dagger$ and $\widetilde{U}_h^m(\widetilde{q}_\theta^*)$, cf. (5.26) and (5.35), imply

$$\begin{aligned}
&\big((q^\dagger - P_{\mathcal{A}}(\widetilde{q}_\theta^*))\nabla u^\dagger(t_n), \nabla \varphi\big) \\
&= \big((q^\dagger - P_{\mathcal{A}}(\widetilde{q}_\theta^*))\nabla u^\dagger(t_n), \nabla(\varphi - P_h\varphi)\big) + \big((q^\dagger - P_{\mathcal{A}}(\widetilde{q}_\theta^*))\nabla u^\dagger(t_n), \nabla P_h\varphi\big) \\
&= -\big(\nabla \cdot \big((q^\dagger - P_{\mathcal{A}}(\widetilde{q}_\theta^*))\nabla u^\dagger(t_n)\big), \varphi - P_h\varphi\big) + \big(P_{\mathcal{A}}(\widetilde{q}_\theta^*)\nabla(\widetilde{U}_h^n(P_{\mathcal{A}}(\widetilde{q}_\theta^*)) - u^\dagger(t_n)), \nabla P_h\varphi\big) \\
&\quad + \big(\bar{\partial}_\tau \widetilde{U}_h^n(P_{\mathcal{A}}(\widetilde{q}_\theta^*)) - \partial_t u^\dagger(t_n), P_h\varphi\big) \\
&\quad + \Big(\big(P_{\mathcal{A}}(\widetilde{q}_\theta^*)\nabla \widetilde{U}_h^n(P_{\mathcal{A}}(\widetilde{q}_\theta^*)), \nabla P_h\varphi\big)_h - \big(P_{\mathcal{A}}(\widetilde{q}_\theta^*)\widetilde{U}_h^n(P_{\mathcal{A}}(\widetilde{q}_\theta^*)), \nabla P_h\varphi\big)\Big) =: \mathrm{I}^n + \mathrm{II}^n + \mathrm{III}^n + \mathrm{IV}^n.
\end{aligned}$$

Set $\varphi \equiv \varphi^n = \frac{q^\dagger - P_{\mathcal{A}}(\widetilde{q}_\theta^*)}{q^\dagger} u^\dagger(t_n)$ in the identity. Lemma 5.10 and the argument for (5.23) imply

$$\|\nabla\varphi\|_{L^2(\Omega)} \le c(1 + \|\nabla P_{\mathcal{A}}(\widetilde{q}_\theta^*)\|_{L^2(\Omega)}) \le c\zeta^{\frac{1}{2}}.$$

Then repeating the argument for Theorem 5.6 yields

$$|\mathrm{I}^n| \le ch\zeta, \quad \tau \sum_{m=M_0}^{M} |\mathrm{II}^n| \le c\min(h^{-1}\eta + h, 1)\zeta^{\frac{1}{2}} \quad \text{and} \quad \tau^3 \sum_{j=N_0+1}^{N} \sum_{i=N_0+1}^{j} \sum_{n=i}^{j} \mathrm{III}^n \le c\eta.$$

Then it follows from Lemma 5.3 (with $p = 1$), the stability of $P_{\mathcal{A}}$ and the bounds (5.20) and (5.36) that

$$\begin{aligned}
\tau \sum_{j=N_0}^{N} |\mathrm{IV}^n| &\le c2^{-n}h\|P_{\mathcal{A}}(\widetilde{q}_\theta^*)\|_{W^{1,\infty}(\Omega)} \Big(\max_{N_0 \le n \le N} \|\nabla P_h \varphi^n\|_{L^2(\Omega)} \Big) \big\| (\nabla \widetilde{U}_h^n(P_{\mathcal{A}}(\widetilde{q}_\theta^*)))_{N_0}^N \big\|_{\ell^2(L^2(\Omega))} \\
&\le c2^{-n}h\zeta^{\frac{1}{2}} (\|P_{\mathcal{A}}(\widetilde{q}_\theta^*)\|_{L^\infty(\Omega)} + \|\nabla P_{\mathcal{A}}(\widetilde{q}_\theta^*)\|_{L^\infty(\Omega)}) \big\| (\nabla \widetilde{U}_h^n(P_{\mathcal{A}}(\widetilde{q}_\theta^*)))_{N_0}^N \|_{\ell^2(L^2(\Omega))} \\
&\le c2^{-n}h\zeta^{\frac{1}{2}} (1 + \|\nabla \widetilde{q}_\theta^*\|_{L^\infty(\Omega)}) \big\| (\nabla \widetilde{U}_h^n(P_{\mathcal{A}}(\widetilde{q}_\theta^*)))_{N_0}^N \|_{\ell^2(L^2(\Omega))} \le c2^{-n}hd^{\frac{1}{2}}R^L W^L \zeta^{\frac{1}{2}}.
\end{aligned}$$

Combining the preceding estimates directly shows the desired assertion. □

5.3 Numerical results

First we describe the implementation of the hybrid NN-FEM approach, i.e., problems (5.7)-(5.8) and (5.27)-(5.28). We train the NNs by minimizing the losses (5.7) and (5.27) for the elliptic and parabolic cases, respectively. Traditionally, the NNs are trained using gradient type methods and the gradient is computed using back-propagation [103], which can be done in many software framework, e.g., PyTorch and Tensorflow. In the hybrid method, we employ the adjoint technique [32]. By the chain rule, the derivative of the loss J_γ to the NN parameter θ is given by $\frac{\mathrm{d}J_\gamma}{\mathrm{d}\theta} = \frac{\mathrm{d}J_\gamma}{\mathrm{d}q}\frac{\mathrm{d}q}{\mathrm{d}\theta}$. We compute $J_\gamma'(q) = \frac{\mathrm{d}J_\gamma}{\mathrm{d}q}$ using the standard adjoint technique, and $\frac{\mathrm{d}q}{\mathrm{d}\theta}$ using back-propagation.

5.3.1 Numerical experiments

Now we present numerical reconstructions $P_{\mathcal{A}}(q_\theta^*)$ and q_h^* using the hybrid NN-FEM approach and the fully FEM. Their accuracy to the exact diffusivity $q^\dagger$ is measured by the relative error:

$$e(P_{\mathcal{A}}(q_\theta^*)) := \|q^\dagger - P_{\mathcal{A}}(q_\theta^*)\|_{L^2(\Omega)}/\|q^\dagger\|_{L^2(\Omega)} \quad \text{and} \quad e(q_h^*) := \|q^\dagger - q_h^*\|_{L^2(\Omega)}/\|q^\dagger\|_{L^2(\Omega)}.$$

The exact data $u^\dagger$ is generated on a finer mesh, and in the elliptic case, the noisy data z^δ is generated by $z^\delta(x) = u^\dagger(x) + \delta\|u^\dagger\|_{L^\infty(\Omega)}\xi(x)$ for $x \in \Omega$, where $\xi(x)$ follows the standard Gaussian distribution, and $\delta > 0$ is the (relative) noise level. The parabolic case is similar. Unless otherwise stated, the NN for approximating q is taken to be d-32-32-1 (i.e., with two hidden layers, each having 32 neurons).

The mesh size h is 1/40 and 1/32 and the time step size τ is 1/1000 and 1/200, for one- and two-dimensional problems, respectively. These FEM discretization parameters are applied to both hybrid method and pure FEM. The regularization parameters γ_θ for the hybrid NN-FEM method and γ_h for the fully FEM are determined in a trail and test way. The resulting loss is minimized using ADAM [98]. All the experiments were carried out on a personal desktop (with Windows 10, with RAM 64.0GB, Intel(R) Core(TM) i9-10900 CPU, 2.80 GHz). The hybrid NN-FEM approach was implemented with Python 3.8.8 on the software framework TensorFlow using the SciKit-fem [62] package to solve the PDEs, and the pure FEM approach was implemented on MATLAB 2022a. Unless otherwise stated, the level of quadrature is fixed at $n = 0$ (i.e., no further sub-division).

Table 5.1: The relative errors for the examples at different noise levels.

	(a) Example 5.1(i)					(b) Example 5.1(ii)				
δ	10e-2	5e-2	1e-2	5e-3	1e-3	10e-2	5e-2	1e-2	5e-3	1e-3
γ_θ	1e-6	1e-6	1e-6	1e-7	1e-7	1e-7	1e-7	1e-8	1e-8	1e-8
$e(q_\theta^*)$	3.17e-2	2.25e-2	1.24e-2	1.24e-2	1.12e-2	8.92e-2	4.76e-2	3.86e-2	3.91e-2	2.67e-2
γ_h	2e-6	1e-6	1e-7	5e-8	1e-8	2e-6	1e-6	1e-7	5e-8	1e-8
$e(q_h^*)$	7.16e-2	4.76e-2	2.39e-2	2.04e-2	1.98e-2	1.23e-1	7.76e-2	3.58e-2	2.29e-2	1.54e-2
	(c) Example 5.2(i)					(d) Example 5.2(ii)				
δ	10e-2	5e-2	1e-2	5e-3	1e-3	10e-2	5e-2	1e-2	5e-3	1e-3
γ_θ	1e-6	1e-6	1e-6	1e-7	1e-7	1e-7	1e-7	1e-8	1e-8	1e-8
$e(q_\theta^*)$	3.30e-2	3.13e-2	1.48e-2	1.47e-2	1.08e-2	6.21e-2	4.62e-2	2.85e-2	2.63e-2	2.68e-2
γ_h	2e-6	1e-6	1e-7	5e-8	1e-8	2e-7	1e-7	1e-8	5e-9	1e-9
$e(q_h)$	5.63e-2	4.97e-2	1.58e-2	1.53e-2	1.21e-2	7.18e-2	4.70e-2	2.08e-2	1.81e-2	1.80e-2
	(e) Example 5.3									
δ	10e-2	5e-2	1e-2	5e-3	1e-3					
γ_θ	1e-6	1e-6	1e-6	1e-6	1e-6					
$e(q_\theta^*)$	2.92e-2	2.25e-2	1.43e-2	1.92e-2	1.36e-2					
γ_h	2e-6	1e-6	1e-7	5e-8	1e-8					
$e(q_h)$	6.15e-2	4.09e-2	3.01e-2	2.20e-2	1.52e-2					

The first two examples are about the inverse problem in the elliptic case.

Example 5.1. *(i)* $\Omega = (0, 1)$, $q^\dagger(x) = 2 + \sin(2\pi x)$ *and* $f \equiv 10$.

(ii) $\Omega = (0,1)^2$, $q^\dagger(x_1, x_2) = 2 + \sin(2\pi x_1)\sin(2\pi x_2)$, $u_0(x_1, x_2) = 4x_1(1 - x_2)$ *and* $f \equiv 10$.

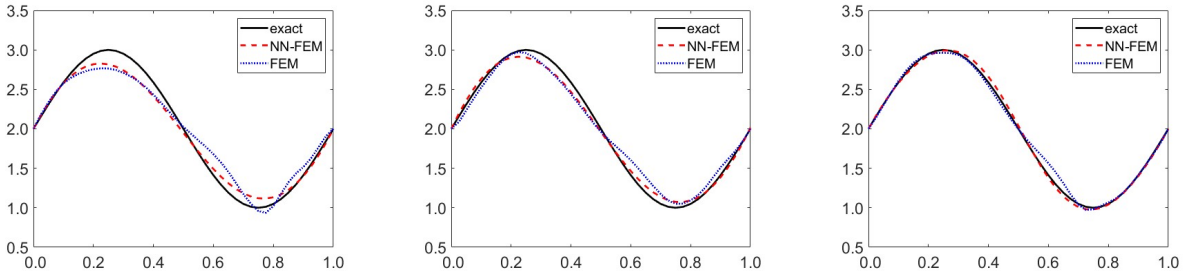

(a) $\delta = 10e\text{-}2$ (b) $\delta = 5e\text{-}2$ (c) $\delta = 1e\text{-}2$

Figure 5.1: The reconstructions for Example 5.1(i) at three noise levels by the hybrid approach and pure FEM.

In the ADAM optimizer, the hybrid scheme employs a learning rate 1e-3 and 1e-2 for cases (i) and (ii), respectively. The reconstructions for case (i) in Fig. 5.1 show that the hybrid approach is more accurate than the pure FEM, although visually they are largely comparable, consistent with the prior observation [19]. This is also confirmed by the relative errors in Table 5.1(a). These results clearly show the influence of the discretization scheme on numerical inversion. The excellent performance of the hybrid method might be attributed to the strong implicit smoothness prior imposed by NNs, which strongly favors smooth solutions [125], when compared with that by the FEM basis.

To gain further insights, we examine the change of the loss during the training process in Fig. 5.2. The plots are for two cases: the 1-32-32-1 architecture with different noise levels to study the impact of data noise, and three architectures: i.e., 1-16-16-1, 1-32-32-1 and 1-32-32-32-1 (at a noise level 5%) to study the impact of the architectural choice. During the training, the loss J first decreases only slowly, exhibiting a plateau phenomenon, and then it experiences a rapid decreasing period, after which it almost stagnates and oscillates a little bit. This pattern is consistently observed for all the considered noise levels. The origin of the plateau remains elusive; see [3] for an interesting investigation of the phenomenon for gradient descent on ReLU networks. The evolution of the relative error shows a similar behavior: it first decreases slowly, then enjoys a fast decay and finally tends to be nearly steady.

Now we examine the influence of quadrature error, by varying the quadrature level n over the set $\{0, 1, \cdots, 5\}$. This is carried out on two settings with 1% noise: (i) the standard setting as before, and (ii) the setting with the architecture 1-128-128-128-1, a mesh size $h = 1/40$, $\gamma =$ 1e-6, and a learning rate 1e-3. The architecture in the latter is far bigger, and hence, according to the error estimate in Theorem 5.4, the problem becomes more challenging and may require more quadrature points to deliver quality reconstructions. The numerical results are given in Fig. 5.3. It is observed that the

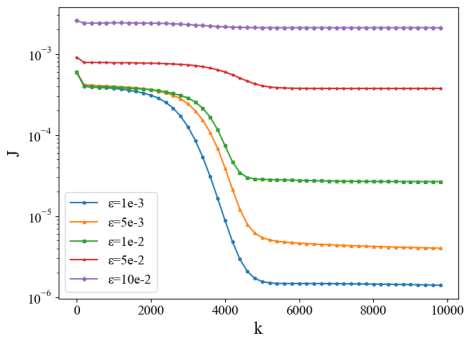

(a) loss v.s. noise level

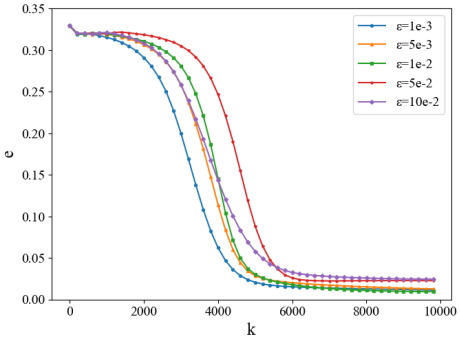

(b) relative error v.s. noise level

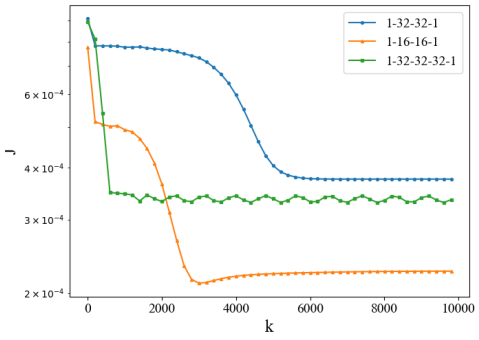

(c) loss v.s. NN architecture

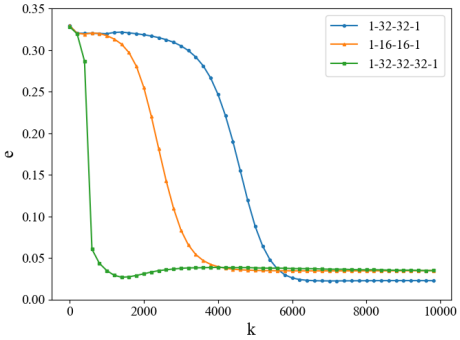

(d) relative error v.s. NN architecture

Figure 5.2: The variation of the loss J and error e during the training for Example 5.1(i) at different noise levels and NN architectures.

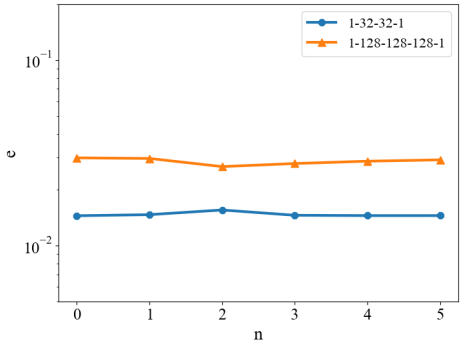

(a) Example 5.1(i)

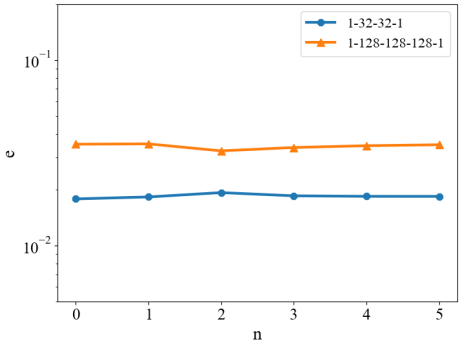

(b) Example 5.2(i)

Figure 5.3: The relative errors for Examples 5.1(i) and 5.2(i) versus quadrature level and NN architectures, at a noise level 1%.

relative error e does decay slightly when using more quadrature points but the influence is very minor. Hence, the error bound in Theorem 5.4 might be overly pessimistic in terms of the quadrature error. In the rest of the experiments, we do not increase the quadrature level.

In case (ii), the reconstructions by the hybrid approach is slightly more accurate than that by the pure FEM, when the data is highly noisy; see Fig. 5.4 and Table 5.1(b). When the data is very accurate, the hybrid approach is actually slightly less accurate. This is attributed to the complex optimization issue: the loss is highly nonconvex in the NN parameters, and its landscape is very complicated, which may prevent the ADAM optimizer from finding a global minimizer. Fig. 5.5 shows the evolution of the loss J and relative error e in the two settings during the training process: (i) the 2-32-32-1 architecture with noise level varying form 0.1% to 10% and (ii) with a fixed 1% noise level, on three NNs, i.e., 2-16-16-1, 2-32-32-1, and 2-32-32-32-1. The results show a similar behavior as for case (i): the convergence curve shows fast convergence only after an initial plateau (of length about 5000 iterations). This may indicate the need of a better initialization strategy for the NN parameters in order to shorten the plateau length (and thus faster convergence).

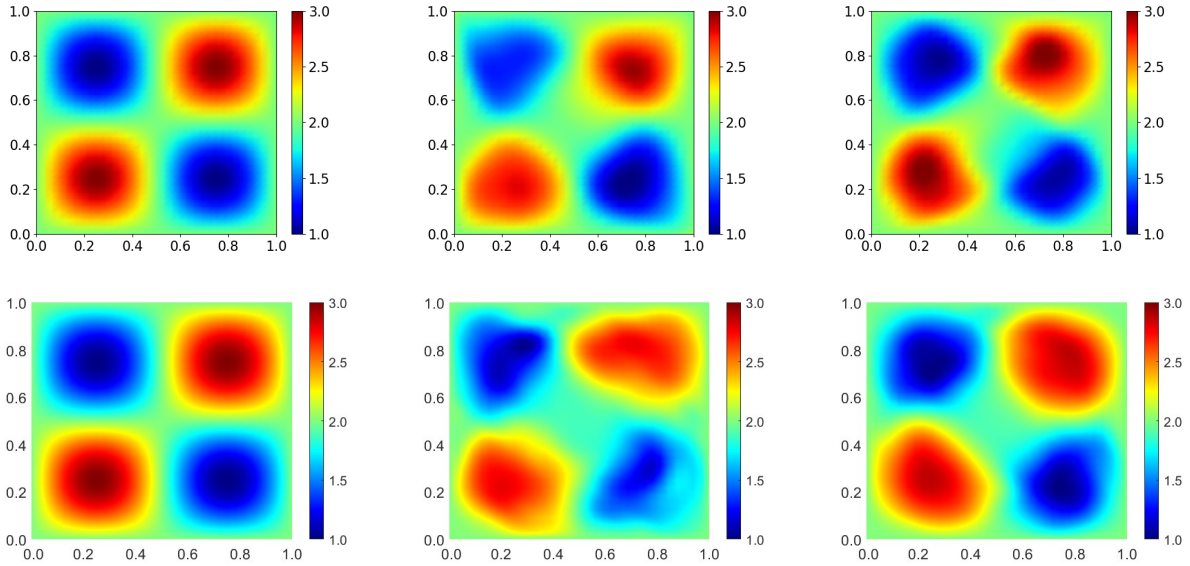

(a) exact (b) $\delta = 5e\text{-}2$ (c) $\delta = 1e\text{-}2$

Figure 5.4: The reconstructions for Example 5.1(ii) at two noise levels with the hybrid method (top) and the pure FEM (bottom).

The second set of experiments is for the inverse diffusivity problem in the parabolic case.

Example 5.2. *(i)* $\Omega = (0,1)$, $q^\dagger(x) = 2 + \sin(2\pi x)$ *and* $f(x,t) = 10t$, $T_0 = 0.9$, *and* $T = 1$.

(ii) $\Omega = (0,1)^2$, $q^\dagger(x_1,x_2) = 2 + \sin(2\pi x_1)\sin(2\pi x_2)$, $u_0(x_1,x_2) = 4x_1(1-x_1)$ *and* $f(x_1,x_2,t) = 10t$, $T_0 = 0.9$ *and* $T = 1$.

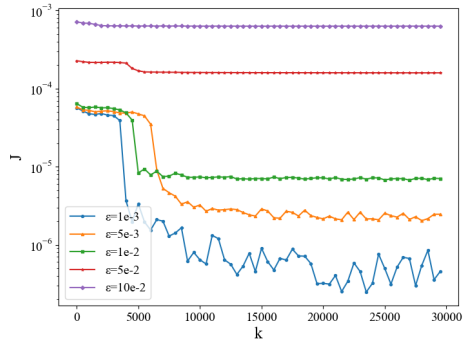

(a) loss v.s. noise level

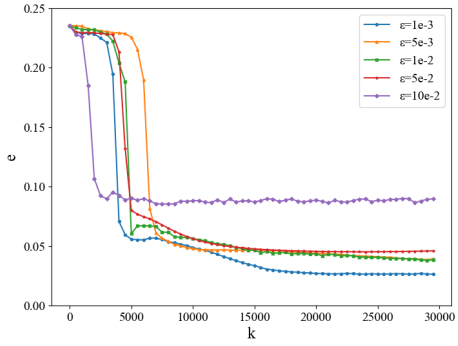

(b) relative error v.s. noise level

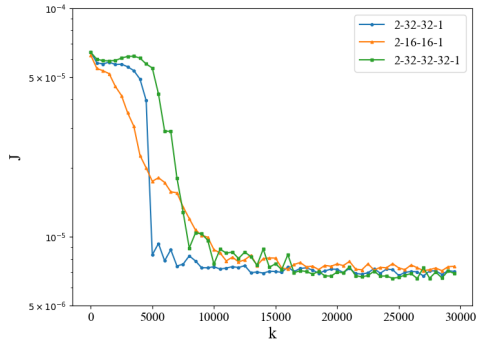

(c) loss v.s. NN architecture

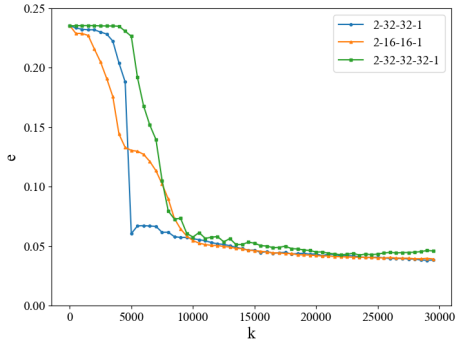

(d) relative error v.s. NN architecture

Figure 5.5: The variation of the loss J and error e during the training for Example 5.1(ii) at different noise levels and NN architectures.

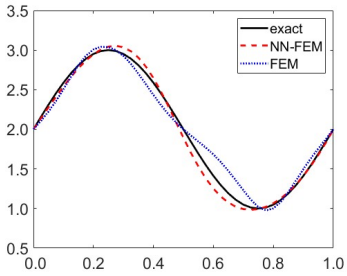

(a) $\delta = 10e\text{-}2$

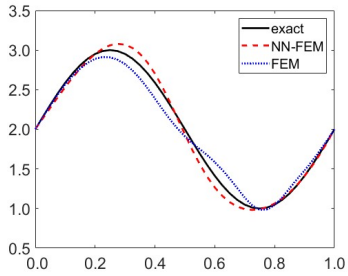

(b) $\delta = 5e\text{-}2$

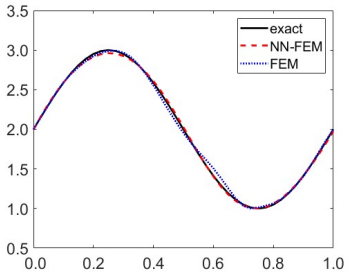

(c) $\delta = 1e\text{-}2$

Figure 5.6: The reconstructions for Example 5.2(i) with three noise levels, obtained by the hybrid method and the pure FEM.

In the ADAM optimizer, the hybrid scheme employs a learning rate 1e-3 and 1e-2 for cases (i) and (ii), respectively. The numerical results in Figs. 5.6 and 5.7 (also Tables 5.1(c)–(d)) show similar observations as for the elliptic case: the hybrid approach appears to more accurate for highly noisy data. Likewise, the influence of the quadrature error on the reconstruction eerror e is again very mild, cf. Fig. 5.3(b).

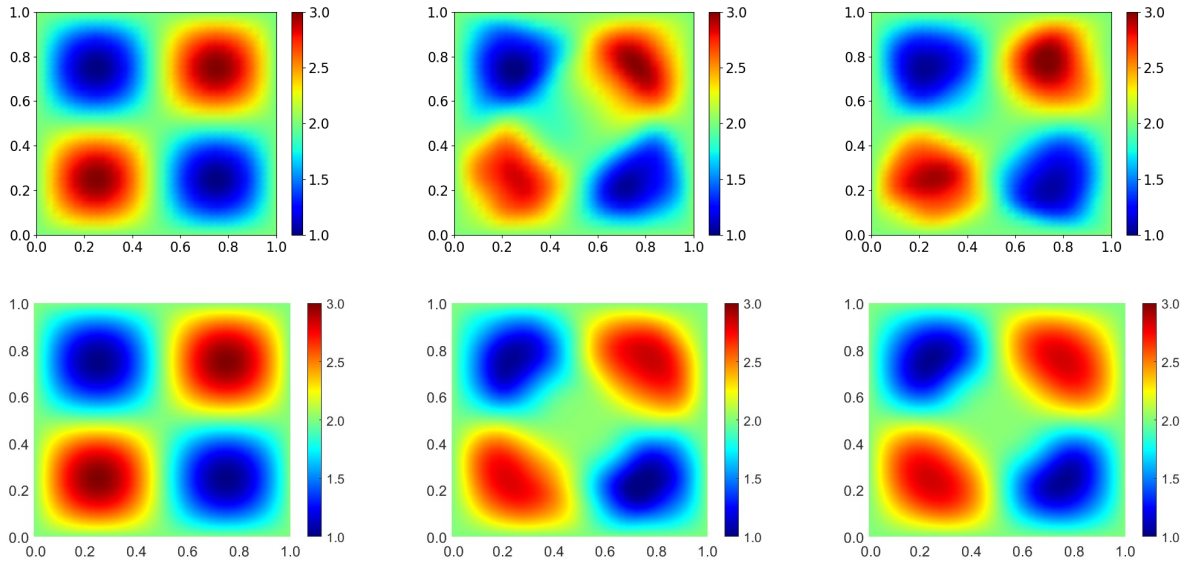

(a) exact (b) $\delta = 5e\text{-}2$ (c) $\delta = 1e\text{-}2$

Figure 5.7: The reconstructions for Example 5.2(ii) at two noise levels, by the hybrid method (top) and the pure FEM (bottom).

The last example is about partial interior data (on a subdomain $\Omega' \subset \Omega$).

Example 5.3. $\Omega = (0,1)$, $q^\dagger(x) = 2 + 10(1-x)x^2$ *and* $f \equiv 10$, $\Omega' = (0.3, 0.7)$.

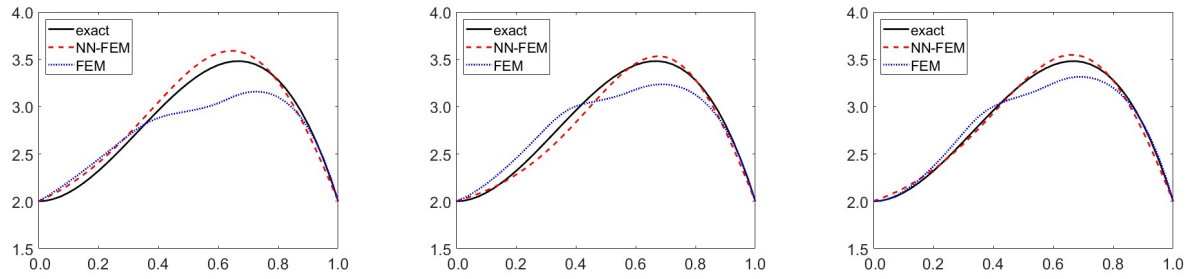

(a) $\delta = 10e\text{-}2$ (b) $\delta = 5e\text{-}2$ (c) $\delta = 1e\text{-}2$

Figure 5.8: The numerical reconstructions for Example 5.3 at three noise levels, obtained with the hybrid method and the pure FEM.

For the hybrid inversion, we employ a learning rate 1e-3. The numerical results are presented in

Fig. 5.8; see also Table 5.1(e) for the relative errors. Due to the availability of the only partial interior data, the problem is far more ill-posed. It is observed that the reconstructions by the hybrid approach is more accurate than that by the pure FEM, indicating the high robustness of the hybrid approach for more challenging inverse problems.

CHAPTER 6.

Recovery of Multiple Parameters in Subdiffusion from One Lateral Boundary Measurement

This work is concerned with an inverse problem of simultaneously recovering multiple parameters in a subdiffusion model from one single lateral boundary measurement in a partly unknown medium.

Let $\Omega \subset \mathbb{R}^d$ $(d = 2, 3)$ be an open bounded domain with a Lipschitz and piecewise $C^{1,1}$ boundary and $T > 0$ be a fixed final time. Consider the following subdiffusion problem for the function u:

$$\begin{cases} \partial_t^\alpha u - \nabla \cdot (q(x)\nabla u(x)) = f & \text{in } \Omega \times (0, T], \\ q\partial_\nu u = g & \text{on } \partial\Omega \times (0, T], \\ u(0) = u_0 & \text{in } \Omega, \end{cases} \tag{6.1}$$

where ∂_t^α, $\alpha \in (0, 1)$ is the fractional derivative defined in (1.11), $u_0 \in L^2(\Omega)$ and (time-independent) $f \in L^2(\Omega)$ are unknown initial and source data, and ν denotes the unit outward normal vector to the boundary $\partial\Omega$.

In this chapter, we study mathematical and numerical aspects of an inverse problem of recovering the diffusion coefficient q and fractional order α from a single lateral boundary measurement of the solution,

$$H(x, t) = u(x, t), \quad x \in \Gamma_0 \subset \partial\Omega, t \in (0, T],$$

without the knowledge of the initial data u_0 and source f. In particular, we assume the diffusion coefficient q is piecewise constant:

$$q(x) = 1 + \mu\, \chi_\omega(x), \tag{6.2}$$

where $\mu > -1$ is a nonzero unknown constant, ω is an unknown convex polyhedron in Ω satisfying $\operatorname{diam}(\omega) < \operatorname{dist}(\omega, \partial\Omega)$ and χ_ω denotes the characteristic function of ω.

We design a special excitation g, which is separable:

$$g(x, t) = \psi(t)\eta(x), \tag{6.3}$$

[1]Chapter 6 is reprinted with permission from "Recovery of Multiple Parameters in Subdiffusion from One Lateral Boundary Measurement", Siyu Cen, Bangti Jin, Yikan Liu, Zhi Zhou, Inverse Problems, 39 (10) (2023), 104001. The candidate mainly works on the research methodology discussion and the coding and data collection in numerical experiments.

where $0 \not\equiv \eta \in H^{\frac{1}{2}}(\partial\Omega)$ satisfies the compatibility condition $\int_{\partial\Omega} \eta \mathrm{d}S = 0$ and $\psi \in C^1(\mathbb{R}_+)$ satisfies

$$\psi(t) = \begin{cases} 0, & t < T_0, \\ 1, & t > T_1, \end{cases} \tag{6.4}$$

with $0 < T_0 < T_1 < T$. Note that the inverse problem involves missing data (u_0 and f), whereas the available data is only on a partial boundary. Thus, it is both mathematically and numerically very challenging, due to not only the severe ill-posed nature and high degree of nonlinearity but also the unknown forward map from the parameters to the data.

The rest of the paper is organized as follows. In Section 6.1 we describe preliminary results on the model, especially time analyticity of the data. Then in Section 6.2 we give the uniqueness result in case of piecewise constant q, and in Section 6.3 we develop a recovery algorithm based on the level set method. We present extensive numerical experiments to illustrate the feasibility of recovering multiple parameters in Section 6.4.

6.1 Time analyticity of solutions

In this section, we present preliminary analytical results. Let A be the $L^2(\Omega)$ realization of the elliptic operator $-\nabla \cdot (q\nabla)$, with a domain $\mathrm{Dom}(A) := \{v \in L^2(\Omega) : -\nabla \cdot (q\nabla v) \in L^2(\Omega), \partial_\nu v|_{\partial\Omega} = 0\}$. Let $\{\lambda_\ell\}_{\ell \geq 1}$ be a strictly increasing sequence of eigenvalues of A, and denote the multiplicity of λ_ℓ by m_ℓ and $\{\varphi_{\ell,k}\}_{k=1}^{m_\ell}$ an $L^2(\Omega)$ orthonormal basis of $\ker(A - \lambda_\ell)$. That is, for any $\ell \in \mathbb{N}$, $k = 1, \ldots, m_\ell$:

$$\begin{cases} -\nabla \cdot (q\nabla\varphi_{\ell,k}) = \lambda_\ell \varphi_{\ell,k} & \text{in } \Omega, \\ q\partial_\nu \varphi_{\ell,k} = 0 & \text{on } \partial\Omega. \end{cases} \tag{6.5}$$

The eigenvalues $\{\lambda_\ell\}_{\ell=1}^\infty$ are nonnegative, and the eigenfunctions $\{\varphi_{\ell,k} : k = 1, \ldots, m_\ell\}_{\ell=1}^\infty$ form a complete orthonormal basis of $L^2(\Omega)$. Note that $\lambda_1 = 0$ (and has multiplicity 1) and the corresponding eigenfunction $\varphi_1 = |\Omega|^{-\frac{1}{2}}$ is constant valued, where $|E|$ denotes the Lebesgue measure of a set E. Due to the piecewise constancy of the coefficient q, $\varphi_{\ell,k}$ is smooth in ω and $\Omega \setminus \overline{\omega}$. Moreover, it satisfies the following transmission condition on the interface $\partial\omega$:

$$\varphi_{\ell,k}|_- = \varphi_{\ell,k}|_+ \quad \text{and} \quad \partial_n \varphi_{\ell,k}|_- = (1+\mu)\partial_n \varphi_{\ell,k}|_+ \quad \text{on } \partial\omega, \tag{6.6}$$

where $\varphi_{\ell,k}|_+$ and $\varphi_{\ell,k}|_-$ denote the limits from ω and $\Omega \setminus \overline{\omega}$ to the interface $\partial\omega$, respectively, and $\partial_n \varphi_{\ell,k}|_\pm$ denotes the derivative with respect to the unit outer normal vector n on $\partial\omega$. Then we define the fractional power A^s ($s \geq 0$) via functional calculus by

$$A^s v := \sum_{\ell=1}^\infty \lambda_\ell^s \sum_{k=1}^{m_\ell} (v, \varphi_{\ell,k})\varphi_{\ell,k},$$

with a domain $\mathrm{Dom}(A^s) = \{v \in L^2(\Omega) : A^s v \in L^2(\Omega)\}$, and the associated graph norm

$$\|v\|_{\mathrm{Dom}(A^s)} = \Big(\sum_{\ell=1}^{\infty} \lambda_\ell^{2s} \sum_{k=1}^{m_\ell} (v, \varphi_{\ell,k})^2 \Big)^{\frac{1}{2}}.$$

By linearity, we may split the solution u of problem (6.1) into $u = u_i + u_b$, with u_i and u_b solving

$$\begin{cases} \partial_t^\alpha u_i - \nabla \cdot (q \nabla u_i) = f & \text{in } \Omega \times (0,T], \\ q \partial_\nu u_i = 0 & \text{on } \partial\Omega \times (0,T], \\ u_i(0) = u_0 & \text{in } \Omega \end{cases} \quad \text{and} \quad \begin{cases} \partial_t^\alpha u_b - \nabla \cdot (q \nabla u_b) = 0 & \text{in } \Omega \times (0,T], \\ q \partial_\nu u_b = g & \text{on } \partial\Omega \times (0,T], \\ u_b(0) = 0 & \text{in } \Omega, \end{cases} \tag{6.7}$$

respectively. The following result gives the representations of u_i and u_b, where $E_{\alpha,\beta}$ denotes the Mittag-Leffler function defined in (2.5).

Proposition 6.1. *Let $u_0, f \in L^2(\Omega)$. Then there exist unique solutions $u_i, u_b \in L^2(0,T;H^1(\Omega))$ that can be respectively represented by*

$$\begin{aligned} u_i(t) &= (u_0, \varphi_1)\varphi_1 + \frac{(f,\varphi_1)\varphi_1 t^\alpha}{\Gamma(1+\alpha)} \\ &\quad + \sum_{\ell=2}^{\infty} \sum_{k=1}^{m_\ell} \big(\big[(u_0, \varphi_{\ell,k}) - \lambda_\ell^{-1} (f, \varphi_{\ell,k}) \big] E_{\alpha,1}(-\lambda_\ell t^\alpha) + \lambda_\ell^{-1} (f, \varphi_{\ell,k}) \big) \varphi_{\ell,k}, \\ u_b(t) &= \sum_{\ell=1}^{\infty} \sum_{k=1}^{m_\ell} \int_0^t (t-s)^{\alpha-1} E_{\alpha,\alpha}(-\lambda_{\ell,k}(t-s)^\alpha)(g(s), \varphi_{\ell,k})_{\partial\Omega} \, \mathrm{d}s \, \varphi_{\ell,k}. \end{aligned}$$

Hence, the solution u to problem (6.1) *can be represented as*

$$u(t) = \rho_0 + \rho_1 t^\alpha + \sum_{\ell=2}^{\infty} E_{\alpha,1}(-\lambda_\ell t^\alpha)\rho_\ell + \sum_{\ell=1}^{\infty} \int_0^t (t-s)^{\alpha-1} E_{\alpha,\alpha}(-\lambda_\ell (t-s)^\alpha) \sum_{k=1}^{m_\ell} (g(s), \varphi_{\ell,k})_{\partial\Omega} \, \mathrm{d}s \, \varphi_{\ell,k},$$

with ρ_ℓ given by

$$\rho_\ell := \begin{cases} (u_0, \varphi_1)\varphi_1 + \displaystyle\sum_{\ell=2}^{\infty} \sum_{k=1}^{m_\ell} \lambda_\ell^{-1} (f, \varphi_{\ell,k}) \varphi_{\ell,k}, & \ell = 0, \\ \dfrac{(f,\varphi_1)}{\Gamma(1+\alpha)} \varphi_1, & \ell = 1, \\ \displaystyle\sum_{k=1}^{m_\ell} \big[(u_0, \varphi_{\ell,k}) - \lambda_\ell^{-1} (f, \varphi_{\ell,k}) \big] \varphi_{\ell,k}, & \ell = 2, 3, \ldots. \end{cases} \tag{6.8}$$

Proof. The representations follow from the standard separation of variables technique ([134], [76, Section 6.2]). The piecewise constancy of the diffusivity q requires special care due to a lack of global regularity. By multiplying the governing equation of u_i by $\varphi_{\ell,k}$ and then integrating over Ω, we get

$$\partial_t^\alpha (u_i(t), \varphi_{\ell,k}) + (\mathcal{A} u_i(t), \varphi_{\ell,k}) = (f, \varphi_{\ell,k}).$$

Integrating by parts twice and using the transmission condition (6.6) for $\varphi_{\ell,k}$ (and u_i) on $\partial\omega$ gives

$$\begin{aligned}
(-\nabla\cdot(q\nabla u_i),\varphi_{\ell,k}) &= -\int_{\Omega\setminus\overline{\omega}} \nabla\cdot(\nabla u_i)\,\varphi_{\ell,k}\,\mathrm{d}x - \int_{\omega}\nabla\cdot((1+\mu)\nabla u_i)\,\varphi_{\ell,k}\,\mathrm{d}x\\
&= -\int_{\partial\Omega}(\nabla u_i\cdot\nu)\,\varphi_{\ell,k}\,\mathrm{d}S - \int_{\partial\omega}(\nabla u_i\cdot n_-)\,\varphi_{\ell,k}|_-\,\mathrm{d}S + \int_{\Omega\setminus\overline{\omega}}\nabla u_i\cdot\nabla\varphi_{\ell,k}\,\mathrm{d}x\\
&\quad -\int_{\partial\omega}(1+\mu)(\nabla u_i\cdot n_+)\,\varphi_{\ell,k}|_+\,\mathrm{d}S + \int_{\omega}(1+\mu)\nabla u_i\cdot\nabla\varphi_{\ell,k}\,\mathrm{d}x\\
&= \int_{\Omega\setminus\overline{\omega}}\nabla u_i\cdot\nabla\varphi_{\ell,k}\,\mathrm{d}x + \int_{\omega}(1+\mu)\nabla u_i\cdot\nabla\varphi_{\ell,k}\,\mathrm{d}x\\
&= \int_{\partial\Omega}(\nabla\varphi_{\ell,k}\cdot\nu)\,u_i\,\mathrm{d}S + \int_{\partial\omega}(\nabla\varphi_{\ell,k}\cdot n_-)\,u_i|_-\,\mathrm{d}S - \int_{\Omega\setminus\overline{\omega}}\nabla\cdot(\nabla\varphi_{\ell,k})\,u_i\,\mathrm{d}x\\
&\quad +\int_{\partial\omega}(1+\mu)(\nabla\varphi_{\ell,k}\cdot n_+)\,u_i|_+\,\mathrm{d}S - \int_{\omega}\nabla\cdot((1+\mu)\nabla\varphi_{\ell,k})\,u_i\,\mathrm{d}x\\
&= (u_i,-\nabla\cdot(\nabla\varphi_{\ell,k})) = \lambda_\ell(u_i,\varphi_{\ell,k}).
\end{aligned}$$

Hence

$$(\partial_t^\alpha+\lambda_\ell)u_i^{\ell,k}(t) = f_{\ell,k} := (f,\varphi_{\ell,k}) \qquad \text{for } 0<t\le T, \quad \text{with } u_i^{\ell,k}(0) = u_0^{\ell,k} := (u_0,\varphi_{\ell,k}).$$

Then $u_i^{\ell,k}(t)$ is given by [76, Proposition 4.5]

$$u_i^{\ell,k}(t) = u_0^{\ell,k}E_{\alpha,1}(-\lambda_\ell t^\alpha) + f_{\ell,k}\int_0^t s^{\alpha-1}E_{\alpha,\alpha}(-\lambda_\ell s^\alpha)\,\mathrm{d}s.$$

Note that $u_i^1 = u_0^1 + \frac{1}{\Gamma(1+\alpha)}f_1 t^\alpha$. Now using the identity

$$\frac{\mathrm{d}}{\mathrm{d}t}E_{\alpha,1}(-\lambda t^\alpha) = -\lambda\, t^{\alpha-1}E_{\alpha,\alpha}(-\lambda t^\alpha), \tag{6.9}$$

we have for $\ell\ge 2$ and $k=1,\ldots,m_\ell$ that

$$\begin{aligned}
u_i^{\ell,k}(t) &= u_0^{\ell,k}E_{\alpha,1}(-\lambda_\ell t^\alpha) + \lambda_\ell^{-1}\left[1-E_{\alpha,1}(-\lambda_\ell t^\alpha)\right]f_{\ell,k}\\
&= \left(u_0^{\ell,k}-\lambda_\ell^{-1}f_{\ell,k}\right)E_{\alpha,1}(-\lambda_\ell t^\alpha) + \lambda_\ell^{-1}f_{\ell,k}.
\end{aligned}$$

This gives the representation of u_i. Similarly, multiplying the governing equation for u_b by $\varphi_{\ell,k}$ and repeating the argument yields that $u_b^{\ell,k}(t) := (u_b(t),\varphi_{\ell,k})$ satisfies

$$(\partial_t^\alpha+\lambda_\ell)u_b^{\ell,k}(t) = (g(t),\varphi_{\ell,k})_{\partial\Omega} \quad \text{for } 0<t\le T, \qquad \text{with } \; u_b^{\ell,k}(0)=0.$$

The solution $u_b^{\ell,k}(t)$ is given by [76, Proposition 4.5]

$$u_b^{\ell,k}(t) = \int_0^t (t-s)^{\alpha-1}E_{\alpha,\alpha}(-\lambda_\ell(t-s)^\alpha)(g(s),\varphi_{\ell,k})_{\partial\Omega}\,\mathrm{d}s\,\varphi_{\ell,k}.$$

Thus the desired assertion follows. The representation of the solution u to problem (6.1) follows directly from that of u_b and u_i, and the identity (6.9). □

Next we show properties of the boundary data H. This is achieved by first proving related properties of u and then applying the trace theorem. Below we study the analyticity of

$$u_i(t) = \rho_0 + \rho_1 t^\alpha + \sum_{\ell=2}^{\infty} E_{\alpha,1}(-\lambda_\ell t^\alpha)\rho_\ell,$$
$$u_b(t) = \sum_{\ell=1}^{\infty}\sum_{k=1}^{m_\ell} \int_0^t (t-s)^{\alpha-1} E_{\alpha,\alpha}(-\lambda_\ell (t-s)^\alpha)(g(s), \varphi_{\ell,k})_{\partial\Omega}\, \mathrm{d}s\, \varphi_{\ell,k}.$$

Since our focus is the trace on $\partial\Omega$, we only study u on the subdomain $\Omega \setminus \overline{\omega}$. Let $\omega' \supset \omega$ be a small neighborhood of ω with a smooth boundary and denote $\Omega' = \Omega \setminus \overline{\omega'}$. Recall that for a Banach space B, the notation $C^\omega(T, \infty; B)$ denotes the set of functions valued in B and analytic in $t \in (T, \infty)$.

Proposition 6.2. *For $u_0 \in L^2(\Omega)$, $f \in L^2(\Omega)$ and g as in (6.3), the following statements hold.*

(i) $u_i \in C^\omega(0, \infty; H^2(\Omega'))$ and $u_b \in C^\omega(T_1 + \varepsilon, \infty; H^2(\Omega'))$ for arbitrarily fixed $\varepsilon > 0$.

(ii) The Laplace transforms $\widehat{u_i}(z)$ and $\widehat{u_b}(z)$ of u_i and u_b in t exist for all $\Re(z) > 0$ and are respectively given by

$$\widehat{u_i}(z) = z^{-1}\rho_0 + \Gamma(\alpha+1) z^{-\alpha-1}\rho_1 + \sum_{\ell=2}^{\infty} \frac{\rho_\ell z^{\alpha-1}}{z^\alpha + \lambda_\ell} \quad \text{and} \quad \widehat{u_b}(z) = \sum_{\ell=1}^{\infty}\sum_{k=1}^{m_\ell} \frac{(\widehat{g}(z), \varphi_{\ell,k})_{\partial\Omega}\varphi_{\ell,k}}{z^\alpha + \lambda_\ell}.$$

Proof. Throughout this proof, let $\varepsilon > 0$ be arbitrarily fixed. Since $\lambda_1 = 0$, by Lemma 2.3, there exist constants $c > 0$ and $\theta \in (0, \frac{\pi}{2})$ such that for any $z \in \Sigma_\theta := \{z \in \mathbb{C} \setminus \{0\} : |\arg(z)| \le \theta\}$, we have

$$\begin{aligned}
\|u_i(z)\|^2_{\mathrm{Dom}(A)} &= \sum_{n=1}^{\infty} \lambda_n^2 \sum_{j=1}^{m_n} \left(\varphi_{n,j}, \rho_0 + \rho_1 z^\alpha + \sum_{\ell=2}^{\infty} E_{\alpha,1}(-\lambda_\ell z^\alpha)\rho_\ell \right)^2 \\
&= \sum_{n=2}^{\infty} \lambda_n^2 \sum_{j=1}^{m_n} \left(\varphi_{n,j}, \sum_{\ell=2}^{\infty}\sum_{k=1}^{m_\ell} \left\{ E_{\alpha,1}(-\lambda_\ell z^\alpha)\left[(u_0, \varphi_{\ell,k}) - \lambda_\ell^{-1}(f, \varphi_{\ell,k})\right] + \lambda_\ell^{-1}(f, \varphi_{\ell,k}) \right\} \varphi_{\ell,k} \right)^2 \\
&\le c \sum_{n=2}^{\infty} \lambda_n^2 E_{\alpha,1}(-\lambda_n z^\alpha)^2 \sum_{j=1}^{m_n} \left\{ (u_0, \varphi_{n,j})^2 + \lambda_n^{-2}(f, \varphi_{n,j})^2 \right\} + c \sum_{n=1}^{\infty}\sum_{j=1}^{m_n} (f, \varphi_{n,j})^2 \\
&\le c|z|^{-2\alpha} \sum_{n=2}^{\infty}\sum_{j=1}^{m_n} \left\{ (u_0, \varphi_{n,j})^2 + \lambda_n^{-2}(f, \varphi_{n,j})^2 \right\} + c\|f\|^2_{L^2(\Omega)} \\
&\le c|z|^{-2\alpha} \big(\|u_0\|^2_{L^2(\Omega)} + \|f\|^2_{L^2(\Omega)} \big) + c\|f\|^2_{L^2(\Omega)}.
\end{aligned}$$

Since $u_0, f \in L^2(\Omega)$, $\|u_i(z)\|^2_{\mathrm{Dom}(A)}$ is uniformly bounded for $z \in \Sigma_\theta$. Since $E_{\alpha,1}(-\lambda_n z^\alpha)$ is analytic in $z \in \Sigma_\theta$ and the series converges uniformly in any compact subset of Σ_θ, $u_i(t)$ is analytic in $t \in (0, \infty)$ as a $\mathrm{Dom}(A)$-valued function, i.e., $u_i \in C^\omega(0, \infty; \mathrm{Dom}(A))$. By Sobolev embedding, $u_i \in C^\omega(0, \infty; H^2(\Omega'))$.

Next we prove the analyticity of u_b. By the choice $g(x,t) = \eta(x)\psi(t)$ in (6.3) and integration by

parts, for $t > T_1$, $u_b^1(t) := (u_b(t), \varphi_1)$ is given by

$$\begin{aligned} u_b^1(t) &= \frac{1}{\Gamma(\alpha)} \int_0^t (t-s)^{\alpha-1} (g(s), \varphi_1)_{\partial\Omega} \, \mathrm{d}s = \frac{(\eta, \varphi_1)_{\partial\Omega}}{\Gamma(\alpha)} \int_0^t (t-s)^{\alpha-1} \psi(s) \, \mathrm{d}s \\ &= \frac{(\eta, \varphi_1)_{\partial\Omega}}{\alpha \, \Gamma(\alpha)} \left[-(t-s)^{\alpha} \psi(s) |_{s=0}^{s=t} + \int_0^t (t-s)^{\alpha} \psi'(s) \, \mathrm{d}s \right] \\ &= \frac{(\eta, \varphi_1)_{\partial\Omega}}{\Gamma(\alpha+1)} \int_{T_0}^{T_1} (t-s)^{\alpha} \psi'(s) \, \mathrm{d}s, \end{aligned}$$

where the last step follows from the condition on ψ in (6.4). Thus the time-analyticity of $u_b^1(t)\varphi_1$ for $t \in (T_1 + \varepsilon, \infty)$ follows. Next, again by integration by parts, (6.3)–(6.4) and the identity (6.9), for $t > T_1$, $u_b^{\ell,k}(t) := (u_b(t), \varphi_{\ell,k})$ with $\ell \geq 2$, $k = 1, \ldots, m_\ell$ can be written as

$$\begin{aligned} u_b^{\ell,k}(t) &= \int_0^t (t-s)^{\alpha-1} E_{\alpha,\alpha}(-\lambda_\ell (t-s)^{\alpha}) (g(s), \varphi_{\ell,k})_{\partial\Omega} \, \mathrm{d}s \\ &= \int_0^t \frac{(g(s), \varphi_{\ell,k})_{\partial\Omega}}{\lambda_\ell} \frac{\mathrm{d}}{\mathrm{d}s} E_{\alpha,1}(-\lambda_\ell (t-s)^{\alpha}) \, \mathrm{d}s \\ &= \lambda_\ell^{-1} \Big[(g(s), \varphi_{\ell,k})_{\partial\Omega} E_{\alpha,1}(-\lambda_\ell (t-s)^{\alpha}) \Big]_{s=0}^{s=t} - \frac{(\eta, \varphi_{\ell,k})_{\partial\Omega}}{\lambda_\ell} \int_0^t E_{\alpha,1}(-\lambda_\ell (t-s)^{\alpha}) \psi'(s) \, \mathrm{d}s \\ &= \frac{(\eta, \varphi_{\ell,k})_{\partial\Omega}}{\lambda_\ell} \psi(t) - \frac{(\eta, \varphi_{\ell,k})_{\partial\Omega}}{\lambda_\ell} \int_{T_0}^{T_1} E_{\alpha,1}(-\lambda_\ell (t-s)^{\alpha}) \psi'(s) \, \mathrm{d}s =: u_{b,1}^{\ell,k}(t) + u_{b,2}^{\ell,k}(t). \end{aligned}$$

Since $\psi(t) = 1$ for $t > T_1$, we see that $u_{b,1}^{\ell,k}(t)$ is a constant for $t > T_1$. Next we consider the following boundary value problem

$$-\nabla \cdot (q \nabla U) = 0 \ \text{ in } \Omega, \quad \text{with} \quad q \partial_\nu U = \eta \ \text{ on } \partial\Omega. \tag{6.10}$$

The compatibility condition $(\eta, 1)_{\partial\Omega} = 0$ implies that there exist solutions to problem (6.10). We take an arbitrary solution U. Since q is piecewise constant and $\eta \in H^{\frac{1}{2}}(\partial\Omega)$, we know that $U \in H^1(\Omega)$ and its restriction $U|_{\Omega'} \in H^2(\Omega')$. Integrating by parts twice yields

$$(\eta, \varphi_{\ell,k})_{\partial\Omega} = \lambda_\ell (U, \varphi_{\ell,k}).$$

Similar to the argument for Proposition 6.1, from the transmission condition (6.6), we deduce

$$\sum_{\ell=2}^{\infty} \sum_{k=1}^{m_\ell} u_{b,1}^{\ell,k}(t) \varphi_{\ell,k} = \sum_{\ell=2}^{\infty} \sum_{k=1}^{m_\ell} \psi(t) (U, \varphi_{\ell,k}) \varphi_{\ell,k},$$

which is analytic in $t \in (T_1 + \varepsilon, \infty)$ since it is constant in time and $U \in L^2(\Omega)$. Moreover, by the standard elliptic regularity theory,

$$\sum_{\ell=2}^{\infty} \sum_{k=1}^{m_\ell} u_{b,1}^{\ell,k} \varphi_{\ell,k} \in C^{\omega}(T_1 + \varepsilon, \infty; H^2(\Omega')).$$

Recall Young's inequality for convolution, i.e., $\|f * g\|_{L^r(\mathbb{R})} \leq \|f\|_{L^p(\mathbb{R})} \|g\|_{L^q(\mathbb{R})}$ for $p, q, r \geq 1$ with $p^{-1} + q^{-1} = r^{-1} + 1$ and any $f \in L^p(\mathbb{R})$ and $g \in L^q(\mathbb{R})$. Then by Young's inequality, Lemma 2.3 and

the regularity estimate $\sum_{\ell=2}^{\infty}\lambda_\ell^{-2}\sum_{k=1}^{m_\ell}(\eta,\varphi_{\ell,k})_{\partial\Omega}^2\le\|U\|_{L^2(\Omega)}<\infty$, we deduce

$$\begin{aligned}\left\|\sum_{\ell=2}^{\infty}\sum_{k=1}^{m_\ell}u_{b,2}^{\ell,k}(z)\varphi_{\ell,k}\right\|_{\mathrm{Dom}(A)}^2&=\sum_{n=1}^{\infty}\lambda_n^2\sum_{j=1}^{m_n}\left(\varphi_{n,j},\sum_{\ell=2}^{\infty}\sum_{k=1}^{m_\ell}u_{b,2}^{\ell,k}(z)\varphi_{\ell,k}\right)^2\\&=\sum_{n=2}^{\infty}\lambda_n^2\sum_{j=1}^{m_n}\left(\frac{(\eta,\varphi_{n,j})_{\partial\Omega}}{\lambda_n}\int_{T_0}^{T_1}E_{\alpha,1}(-\lambda_n(z-s)^\alpha)\psi'(s)\,\mathrm{d}s\right)^2\\&\le\sum_{n=2}^{\infty}\sum_{j=1}^{m_n}(\eta,\varphi_{n,j})_{\partial\Omega}^2\left(\frac{c}{\lambda_n|z-T_1|^\alpha}\int_{T_0}^{T_1}|\psi'(s)|\,\mathrm{d}s\right)^2\\&\le\left(\frac{c\|\psi\|_{W^{1,\infty}(\mathbb{R}_+)}}{|z-T_1|^\alpha}\right)^2\sum_{n=2}^{\infty}\lambda_n^{-2}\sum_{j=1}^{m_n}|(\eta,\varphi_{n,j})_{\partial\Omega}|^2\le\frac{c}{|z-T_1|^{2\alpha}}.\end{aligned}$$

Since $u_{b,2}^{\ell,k}(t)$ is analytic in $(T_1+\varepsilon,\infty)$ and the series $\sum_{\ell=2}^{\infty}\sum_{k=1}^{m_\ell}u_{b,2}^{\ell,k}(z)\varphi_{\ell,k}$ converges uniformly in $\mathrm{Dom}(A)$ for $z\in T_1+\varepsilon+\Sigma_\theta$, it belongs to $C^\omega(T_1+\varepsilon,\infty;\mathrm{Dom}(A))$, and hence $u_b\in C^\omega(T_1+\varepsilon,\infty;H^2(\Omega'))$. This proves part (i).

The argument for part (i) implies that the series converges uniformly in $\mathrm{Dom}(A)$ for $t\in(0,\infty)$, and

$$\|\mathrm{e}^{-tz}u_i(t)\|_{\mathrm{Dom}(A)}\le c\,\mathrm{e}^{-t\,\Re(z)}(t^{-\alpha}+1),\quad t>0.$$

The function $\mathrm{e}^{-t\,\Re(z)}(t^{-\alpha}+1)$ is integrable in t over $(0,\infty)$ for any fixed z with $\Re(z)>0$. By Lebesgue's dominated convergence theorem and taking Laplace transform termwise, we obtain

$$\widehat{u_i}(z)=z^{-1}\rho_0+\Gamma(\alpha+1)z^{-\alpha-1}\rho_1+\sum_{\ell=2}^{\infty}\frac{\rho_\ell z^{\alpha-1}}{z^\alpha+\lambda_\ell},\quad\forall\,\Re(z)>0.$$

The argument for part (i) also implies

$$\|\mathrm{e}^{-tz}u_b(t)\|_{\mathrm{Dom}(A)}\le c\,\mathrm{e}^{-t\,\Re(z)}|t-T_1|^{-\alpha},\quad t>0.$$

Then termwise Laplace transform and Lebesgue's dominated convergence theorem complete the proof of the proposition. □

Thus, u_i and u_b are analytic in time and have $H^2(\Omega')$ regularity. Since $\partial\Omega$ is Lipschitz and piecewise $C^{1,1}$, their traces on $\partial\Omega$ are well defined. The next result is direct from the trace theorem and Sobolev embedding theorem.

Corollary 6.1. *Let the assumptions in Proposition 6.2 hold. Then the data $H=u|_{\Gamma_0\times(0,T)}$ to problem* (6.1) *can be represented by*

$$\begin{aligned}H(t)=&\underbrace{\rho_0+\rho_1t^\alpha+\sum_{\ell=2}^{\infty}E_{\alpha,1}(-\lambda_\ell t^\alpha)\rho_\ell}_{=:H_i(t)}\\&+\underbrace{\sum_{\ell=1}^{\infty}\sum_{k=1}^{m_\ell}\int_0^t(t-s)^{\alpha-1}E_{\alpha,\alpha}(-\lambda_\ell(t-s)^\alpha)(g(s),\varphi_{\ell,k})_{\partial\Omega}\,\mathrm{d}s\,\varphi_{\ell,k}}_{=:H_b(t)}.\end{aligned}$$

Moreover, H_i and H_b satisfy the following properties.

(i) $H_i \in C^\omega(0,\infty;L^2(\Gamma_0))$ and $H_b \in C^\omega(T_1+\varepsilon,\infty;L^2(\Gamma_0))$ for arbitrarily fixed $\varepsilon>0$.

(ii) The Laplace transforms $\widehat{H_i}(z)$ and $\widehat{H_b}(z)$ of H_i and H_b in t exist for all $\Re(z)>0$ and are given by

$$\widehat{H_i}(z) = z^{-1}\rho_0 + \Gamma(\alpha+1)z^{-\alpha-1}\rho_1 + \sum_{\ell=2}^{\infty}\frac{\rho_\ell z^{\alpha-1}}{z^\alpha+\lambda_\ell},$$
$$\widehat{H_b}(z) = \sum_{\ell=1}^{\infty}\sum_{k=1}^{m_\ell}\frac{(\widehat{g}(z),\varphi_{\ell,k})_{\partial\Omega}\varphi_{\ell,k}}{z^\alpha+\lambda_\ell}.$$

Remark 6.1. *The analysis of Theorem 6.1 crucially exploits the analyticity of the measurement $H_i(t)$ in time, which relies on condition (6.4), i.e., $\psi(t)\equiv 0$ for $t\in[0,T_0]$. The condition $\psi(t)\equiv 1$ for $t\geq T_1$ for some $T_1<T$ from (6.4) ensures the time analyticity of $H_b(t)$ for $t>T_1+\varepsilon$, which is needed for Theorem 6.2. It should be interpreted as analytically extending the observation $H_b(t)$ by analytically extending $\psi(t)$, both from (T_1,T) to (T_1,∞). Alternative conditions on $\psi(t)$ ensuring the time analyticity of $H_b(t)$ for $t>T_1+\varepsilon$, e.g., $\psi(t)$ vanishes identically on (T_1,T), would also be sufficient for Theorem 6.2.*

6.2 Uniqueness

Now we establish a uniqueness result for recovering the fractional order α and piecewise constant q. The proof proceeds in two steps: First we show the uniqueness of the order α from the observation, despite that the initial condition u_0 and source f are unknown. Then we show the uniqueness of q. The key observation is that the contributions from u_0 and f can be extracted explicitly. Since the Dirichlet data is only available on a sub-boundary Γ_0, we view ρ_k as a $L^2(\Gamma_0)$-valued function. The notation $\mathbb{K}$ denotes the set $\{k\in\mathbb{N}:\rho_k\not\equiv 0 \text{ in } L^2(\Gamma_0)\}$, i.e., the support of the sequence $(\rho_0,\rho_1,\dots)$ in $L^2(\Gamma_0)$ sense, similarly, $\widetilde{\mathbb{K}}=\{k\in\mathbb{N}:\widetilde{\rho}_k\not\equiv 0 \text{ in } L^2(\Gamma_0)\}$, and $\mathbb{N}^*=\mathbb{N}\setminus\{1\}$. Below we denote by $\mathcal{A}$ the admissible set of conductivities, i.e.,

$$\mathcal{A}=\{1+\mu\chi_\omega(x):\mu>-1 \text{ and } \omega\subset\Omega \text{ is a convex polygon}\}.$$

Theorem 6.1. *Let $\alpha,\widetilde{\alpha}\in(0,1)$, $(q,f,u_0),(\widetilde{q},\widetilde{f},\widetilde{u}_0)\in\mathcal{A}\times L^2(\Omega)\times L^2(\Omega)$, and fix g as (6.3) with $\psi(t)$ satisfying condition (6.4). Let H and $\widetilde{H}$ be the corresponding Dirichlet observations. Then for some $\theta>0$, the condition $h=\widetilde{H}$ on $\Gamma_0\times[T_0-\theta,T_0]$ implies $\alpha=\widetilde{\alpha}$, $\rho_0=\widetilde{\rho}_0$ and $\{(\rho_k,\lambda_k)\}_{k\in\mathbb{K}}=\{(\widetilde{\rho}_k,\widetilde{\lambda}_k)\}_{k\in\widetilde{\mathbb{K}}}$ if $\mathbb{K},\widetilde{\mathbb{K}}\neq\emptyset$.*

Proof. By the definition of g, we have $g(y,t) \equiv 0$ for $y \in \partial\Omega$, $t \in [0, T_0]$. Then by Corollary 6.1, $H(y,t)$ admits a Dirichlet representation

$$H(y,t) = \rho_0(y) + \rho_1(y)t^\alpha + \sum_{k\in\mathbb{K}\cap\mathbb{N}^*} \rho_k(y) E_{\alpha,1}(-\lambda_k t^\alpha).$$

By Corollary 6.1(i), $H(t)$ is analytic as an $L^2(\partial\Omega)$-valued function in $t > 0$. By analytic continuation, the condition $H(t) = \widetilde{H}(t)$ for $t \in [T_0 - \theta, T_0]$ implies that $H(t) = \widetilde{H}(t)$ in $L^2(\Gamma_0)$ for all $t > 0$, i.e.,

$$\rho_0(y) + \rho_1(y)t^\alpha + \sum_{k\in\mathbb{K}\cap\mathbb{N}^*} \rho_k(y) E_{\alpha,1}(-\lambda_k t^\alpha) = \widetilde{\rho}_0(y) + \widetilde{\rho}_1(y)t^{\widetilde{\alpha}} + \sum_{k\in\widetilde{\mathbb{K}}\cap\mathbb{N}^*} \widetilde{\rho}_k(y) E_{\widetilde{\alpha},1}(-\widetilde{\lambda}_k t^{\widetilde{\alpha}}).$$

From the decay property of $E_{\alpha,1}(-\eta)$ (see Lemma 2.3), we derive $\rho_0(y) + \rho_1(y)t^\alpha = \widetilde{\rho}_0(y) + \widetilde{\rho}_1(y)t^{\widetilde{\alpha}}$, indicating $\rho_0 = \widetilde{\rho}_0$ and $\rho_1 = \widetilde{\rho}_1$. Moreover, we have $\alpha = \widetilde{\alpha}$ if $1 \in \mathbb{K}$. If $1 \notin \mathbb{K}$ and $1 \notin \widetilde{\mathbb{K}}$, i.e., $\rho_1 = \widetilde{\rho}_1 = 0$, then

$$\sum_{k\in\mathbb{K}\cap\mathbb{N}^*} \rho_k(y) E_{\alpha,1}(-\lambda_k t^\alpha) = \sum_{k\in\widetilde{\mathbb{K}}\cap\mathbb{N}^*} \widetilde{\rho}_k(y) E_{\widetilde{\alpha},1}(-\widetilde{\lambda}_k t^{\widetilde{\alpha}}) \quad \text{on } \Gamma_0 \times (0,\infty).$$

Proposition 6.1(ii) and Laplace transform give

$$\sum_{k\in\mathbb{K}\cap\mathbb{N}^*} \frac{\rho_k(y) z^{\alpha-1}}{z^\alpha + \lambda_k} = \sum_{k\in\widetilde{\mathbb{K}}\cap\mathbb{N}^*} \frac{\widetilde{\rho}_k(y) z^{\widetilde{\alpha}-1}}{z^{\widetilde{\alpha}} + \widetilde{\lambda}_k}.$$

Assuming that $\alpha > \widetilde{\alpha}$, dividing both sides by $z^{\widetilde{\alpha}-1}$ and setting $\zeta := z^\alpha$, we have

$$\sum_{k\in\mathbb{K}\cap\mathbb{N}^*} \frac{\rho_k(y)\zeta^{1-\frac{\widetilde{\alpha}}{\alpha}}}{\zeta + \lambda_k} = \sum_{k\in\widetilde{\mathbb{K}}\cap\mathbb{N}^*} \frac{\widetilde{\rho}_k(y)}{\zeta^{\frac{\widetilde{\alpha}}{\alpha}} + \widetilde{\lambda}_k}.$$

Upon noting $\mathbb{K} \neq \emptyset$, choosing an arbitrary $k_0 \in \mathbb{K}$ and rearranging terms, we derive

$$\rho_{k_0}(y)\zeta^{1-\frac{\widetilde{\alpha}}{\alpha}} = \left(\sum_{k\in\widetilde{\mathbb{K}}\cap\mathbb{N}^*} \frac{\widetilde{\rho}_k(y)}{\zeta^{\frac{\widetilde{\alpha}}{\alpha}} + \widetilde{\lambda}_k} - \sum_{k\in\mathbb{K}\cap\mathbb{N}^*\setminus\{k_0\}} \frac{\rho_k(y)\zeta^{1-\frac{\widetilde{\alpha}}{\alpha}}}{\zeta + \lambda_k} \right) (\zeta + \lambda_{k_0}).$$

Letting $\zeta \to -\lambda_{k_0}$ and noting $\alpha > \widetilde{\alpha}$, the right hand side tends to zero (since all $\widetilde{\lambda}_k$ are positive, and $\arg((-\lambda_{k_0})^{\frac{\widetilde{\alpha}}{\alpha}}) = \frac{\widetilde{\alpha}\pi}{\alpha} \in (0,\pi)$) and hence $\rho_{k_0} \equiv 0$ in $L^2(\Gamma_0)$, which contradicts the assumption $k_0 \in \mathbb{K}$. Thus, we deduce $\alpha \leq \widetilde{\alpha}$. The same argument yields $\alpha \geq \widetilde{\alpha}$, so $\alpha = \widetilde{\alpha}$. These discussions thus yield

$$\sum_{k\in\mathbb{K}\cap\mathbb{N}^*} \frac{\rho_k(y)}{\zeta + \lambda_k} = \sum_{k\in\widetilde{\mathbb{K}}\cap\mathbb{N}^*} \frac{\widetilde{\rho}_k(y)}{\zeta + \widetilde{\lambda}_k}. \tag{6.11}$$

Note that both sides of the identity (6.11) are $L^2(\Gamma_0)$-valued functions in ζ. Next we show both converge uniformly in any compact subset in $\mathbb{C} \setminus (\{-\lambda_k\}_{k\in\mathbb{K}\cap\mathbb{N}^*} \cup \{-\widetilde{\lambda}_k\}_{k\in\widetilde{\mathbb{K}}\cap\mathbb{N}^*})$ and are analytic in $\mathbb{C} \setminus (\{-\lambda_k\}_{k\in\mathbb{K}\cap\mathbb{N}^*} \cup \{-\widetilde{\lambda}_k\}_{k\in\widetilde{\mathbb{K}}\cap\mathbb{N}^*})$. Indeed, since $u_0, f \in L^2(\Omega)$, for all ζ in any compact subset of $\mathbb{C} \setminus (\{-\lambda_k\}_{k\in\mathbb{K}\cap\mathbb{N}^*} \cup \{-\widetilde{\lambda}_k\}_{k\in\widetilde{\mathbb{K}}\cap\mathbb{N}^*})$, we have

$$\begin{aligned}
&\left\| \sum_{k\in\mathbb{K}\cap\mathbb{N}^*} \frac{\rho_k}{\zeta + \lambda_k} \right\|^2_{\mathrm{Dom}(A)} \leq c \sum_{\ell\in\mathbb{N}^*} \lambda_\ell^2 \frac{|(u_0,\varphi_\ell)|^2 + \lambda_\ell^{-2}|(f,\varphi_\ell)|^2}{|\zeta + \lambda_\ell|^2} \\
\leq & c \sum_{\ell\in\mathbb{N}^*} \left(|(u_0,\varphi_\ell)|^2 + \lambda_\ell^{-2}|(f,\varphi_\ell)|^2 \right) < \infty.
\end{aligned}$$

Hence, by the trace theorem, the identity (6.11) holds for all $\zeta \in \mathbb{C} \setminus (\{-\lambda_k\}_{k\in\mathbb{K}\cap\mathbb{N}^*} \cup \{-\widetilde{\lambda}_k\}_{k\in\widetilde{\mathbb{K}}\cap\mathbb{N}^*})$. Assume that $\lambda_j \notin \{\widetilde{\lambda}_k\}_{k\in\widetilde{\mathbb{K}}\cap\mathbb{N}^*}$ for some $j \in \mathbb{K}\cap\mathbb{N}^*$. Then we can choose a small circle C_j centered at $-\lambda_j$ which does not contain $\{-\widetilde{\lambda}_k\}_{k\in\widetilde{\mathbb{K}}\cap\mathbb{N}^*}$. Integrating on C_j and applying the Cauchy theorem give $2\pi\sqrt{-1}\,\rho_j/\lambda_j = 0$, which contradicts the assumption $\rho_j \not\equiv 0$ in $L^2(\Gamma_0)$. Hence, $\lambda_j \in \{\widetilde{\lambda}_k\}_{k\in\widetilde{\mathbb{K}}\cap\mathbb{N}^*}$ for every $j \in \mathbb{K}\cap\mathbb{N}^*$. Likewise, $\widetilde{\lambda}_j \in \{\lambda_k\}_{k\in\mathbb{K}\cap\mathbb{N}^*}$ for every $j \in \widetilde{\mathbb{K}}\cap\mathbb{N}^*$, and hence $\{\lambda_k\}_{k\in\mathbb{K}\cap\mathbb{N}^*} = \{\widetilde{\lambda}_k\}_{k\in\widetilde{\mathbb{K}}\cap\mathbb{N}^*}$. From (6.11), we obtain

$$\sum_{k\in\mathbb{K}\cap\mathbb{N}^*} \frac{\rho_k(y) - \widetilde{\rho}_k(y)}{\zeta + \lambda_k} = 0, \quad \forall \zeta \in \mathbb{C} \setminus \{-\lambda_k\}_{k\in\mathbb{K}\cap\mathbb{N}^*}.$$

Varying $j \in \mathbb{K}\cap\mathbb{N}^*$ and integrating over C_j, we obtain $2\pi\sqrt{-1}\,(\rho_j - \widetilde{\rho}_j)/\lambda_j = 0$, which directly implies $\rho_j = \widetilde{\rho}_j$ in $L^2(\Gamma_0)$. This completes the proof of the theorem. □

Remark 6.2. *The condition $\mathbb{K} \neq \emptyset$ holds whenever the following condition is valid $(f, \varphi_1) \neq 0$ or $(u_0, \varphi_{\ell,k}) - \lambda_\ell^{-1}(f, \varphi_{\ell,k}) \neq 0$, $k = 1, \ldots, m_\ell$, $\ell = 2, 3, \ldots$. Note that the condition $(f, \varphi_1) \neq 0$ does not rely on the unknown parameter q, and can be easily guaranteed.*

The next result gives the uniqueness of recovering the diffusion coefficient q from the lateral boundary observation.

Theorem 6.2. *Let condition* (6.4) *be fulfilled, and let (q, f, u_0), $(\widetilde{q}, \widetilde{f}, \widetilde{u}_0) \in \mathcal{A}\times L^2(\Omega)\times L^2(\Omega)$, and fix g as* (6.3). *Let H and $\widetilde{H}$ be the corresponding Dirichlet data. Then for any $\theta \in (0, T_0]$, the condition $H = \widetilde{H}$ on $\Gamma_0 \times [T_0 - \theta, T]$ implies $q = \widetilde{q}$.*

Proof. In view of the linearity of problem (6.1), we can decompose the data $H(t)$ into

$$H(t) = H_i(t) + H_b(t), \quad t \in (0, T],$$

with $H_i(t)$ and $H_b(t)$ given by

$$\begin{aligned} H_i(t) &= \rho_0 + \rho_1 t^\alpha + \sum_{k\in\mathbb{K}\cap\mathbb{N}^*} \rho_k E_{\alpha,1}(-\lambda_k t^\alpha), \\ H_b(t) &= \sum_{\ell=1}^{\infty} \int_0^t (t-s)^{\alpha-1} E_{\alpha,\alpha}(-\lambda_\ell (t-s)^\alpha) \sum_{k=1}^{m_\ell} (g(s), \varphi_{\ell,k})_{\partial\Omega}\, \mathrm{d}s\, \varphi_{\ell,k}, \end{aligned}$$

which solve problem (6.1) with $g \equiv 0$ and $f = u_0 \equiv 0$, respectively. By the choice of g in (6.3), the interval $[0, T]$ can be divided into two subintervals: $(0, T_0]$ and $[T_0, T]$. For $t \in (0, T_0)$, $\psi(t) \equiv 0$, Theorem 6.1 implies that $\{(\rho_k, \lambda_k)\}_{k\in\mathbb{K}} = \{(\widetilde{\rho}_k, \widetilde{\lambda}_k)\}_{k\in\widetilde{\mathbb{K}}}$ and $\alpha = \widetilde{\alpha}$, from which we deduce $H_i(t) = \widetilde{H}_i(t)$ for all $t > 0$. For $t \in [T_0, T]$, this and the condition $H(t) = \widetilde{H}(t)$ imply $H_b(t) = \widetilde{H}_b(t)$ in $L^2(\Gamma_0)$, and hence

$$\begin{aligned} &\sum_{\ell=1}^{\infty} \int_{T_0}^t (t-s)^{\alpha-1} E_{\alpha,\alpha}(-\lambda_\ell (t-s)^\alpha) \sum_{k=1}^{m_\ell} (g(s), \varphi_{\ell,k})_{\partial\Omega}\, \mathrm{d}s\, \varphi_{\ell,k} \\ =&\sum_{\ell=1}^{\infty} \int_{T_0}^t (t-s)^{\alpha-1} E_{\alpha,\alpha}(-\widetilde{\lambda}_\ell (t-s)^\alpha) \sum_{k=1}^{\widetilde{m}_\ell} (g(s), \widetilde{\varphi}_{\ell,k})_{\partial\Omega}\, \mathrm{d}s\, \widetilde{\varphi}_{\ell,k}, \quad t \in [T_0, T]. \end{aligned}$$

By the analyticity in Corollary 6.1, the above identity holds for $t \in [T_0, \infty)$. Thus applying Laplace transform on both side gives

$$\sum_{\ell=2}^{\infty} \frac{\sum_{k=1}^{m_\ell} (\widehat{g}(z), \varphi_{\ell,k})_{\partial\Omega} \varphi_{\ell,k}}{z^\alpha + \lambda_\ell} = \sum_{\ell=2}^{\infty} \frac{\sum_{k=1}^{\widetilde{m}_\ell} (\widehat{g}(z), \widetilde{\varphi}_{\ell,k})_{\partial\Omega} \widetilde{\varphi}_{\ell,k}}{z^\alpha + \widetilde{\lambda}_\ell}, \quad \forall\, \Re(z) > 0. \tag{6.12}$$

Since $\lambda_1 = \widetilde{\lambda}_1 = 0$ and $\varphi_1 = \widetilde{\varphi}_1 = |\Omega|^{-\frac{1}{2}}$, the index in (6.12) starts with $\ell = 2$. Below we repeat the argument for Theorem 6.1. First we show that both sides of (6.12) are analytic with $\zeta = z^\alpha$ in any compact subset of $\mathbb{C} \setminus \{-\lambda_\ell, -\widetilde{\lambda}_\ell\}_{\ell \geq 2}$. Let $U \in \mathrm{Dom}(A^{\frac{1}{4}+\varepsilon})$ be a solution of problem (6.10), for all ζ in a compact subset of $\mathbb{C} \setminus \{-\lambda_\ell, -\widetilde{\lambda}_\ell\}_{\ell \geq 2}$, we have

$$\begin{aligned} &\left\| \sum_{\ell=2}^{\infty} \frac{\sum_{k=1}^{m_\ell} (\widehat{g}(\zeta^{\frac{1}{\alpha}}), \varphi_{\ell,k})_{\partial\Omega} \varphi_{\ell,k}}{\zeta + \lambda_\ell} \right\|^2_{\mathrm{Dom}(A^{\frac{1}{4}+\varepsilon})} \leq c \sum_{\ell=2}^{\infty} \lambda_\ell^{\frac{1}{2}+2\varepsilon} \sum_{k=1}^{m_\ell} \left| \frac{(\eta, \varphi_{\ell,k})_{\partial\Omega}}{\zeta + \lambda_\ell} \right|^2 \\ =& c \sum_{\ell=1}^{\infty} \lambda_\ell^{\frac{1}{2}+2\varepsilon} \sum_{k=1}^{m_\ell} \left| \frac{\lambda_\ell (U, \varphi_{\ell,k})}{\zeta + \lambda_\ell} \right|^2 \leq c \|U\|^2_{\mathrm{Dom}(A^{\frac{1}{4}+\varepsilon})} < \infty. \end{aligned}$$

Since each term of the series is a $\mathrm{Dom}(A^{\frac{1}{4}+\varepsilon})$-valued function analytic in ζ and converges uniformly in ζ, by the trace theorem, we obtain that both sides of (6.12) are $L^2(\partial\Omega)$-valued functions analytic in $\zeta \in \mathbb{C} \setminus \{-\lambda_\ell, -\widetilde{\lambda}_\ell\}_{\ell \geq 2}$. Since $\lambda_\ell, \widetilde{\lambda}_\ell > 0$ for $\ell \geq 2$, we may take $\zeta \to 0$ in (6.12) and obtain

$$\sum_{\ell=2}^{\infty} \frac{\sum_{k=1}^{m_\ell} (\widehat{g}(0), \varphi_{\ell,k})_{\partial\Omega} \varphi_{\ell,k}}{\lambda_\ell} = \sum_{\ell=2}^{\infty} \frac{\sum_{k=1}^{\widetilde{m}_\ell} (\widehat{g}(0), \widetilde{\varphi}_{\ell,k})_{\partial\Omega} \widetilde{\varphi}_{\ell,k}}{\widetilde{\lambda}_\ell}. \tag{6.13}$$

Hence, $w = \widetilde{w}$ on Γ_0, where w and $\widetilde{w}$ are the Dirichlet boundary data with q and $\widetilde{q}$ in the elliptic problem

$$\begin{cases} -\nabla \cdot (q \nabla w) = 0 & \text{in } \Omega, \\ q \partial_\nu w = \widehat{g}(0) & \text{on } \partial\Omega \end{cases} \tag{6.14}$$

with the compatibility condition $\int_\Omega w \, \mathrm{d}x = 0$. Indeed, the solution w of (6.14) can be represented as

$$w = \sum_{\ell=2}^{\infty} \sum_{k=1}^{m_\ell} (w, \varphi_{\ell,k}) \varphi_{\ell,k} = \sum_{\ell=2}^{\infty} \sum_{k=1}^{m_\ell} \lambda_\ell^{-1} (\widehat{g}(0), \varphi_{\ell,k})_{\partial\Omega} \varphi_{\ell,k},$$

where the first equality follows from the compatibility condition $\int_\Omega w \, \mathrm{d}x = 0$ and the second is due to integration by part. By the choice of g in (6.3), the elliptic problem (6.14) is uniquely solvable. Then from [55, Theorem 1.1], we deduce that $\omega = \widetilde{\omega}$ is uniquely determined by the input $\widehat{g}(0) = \widehat{\psi}(0)\eta$. Indeed, Friedman and Isakov [55] proved the unique determination of the convex polygon ω for the case $\mu \equiv 1$, based on extending the solution w harmonically across a vertex of ω and leading a contradiction. The proof does not depend on the knowledge of the parameter μ and hence it is also applicable here. Once ω is determined, it suffices to show the uniqueness of the scalar μ. Suppose $\mu \leq \widetilde{\mu}$, i.e., $q \leq \widetilde{q}$ in ω and $q \equiv \widetilde{q} \equiv 1$ outside ω. Thus w and $\widetilde{w}$ are harmonic functions near $\partial\Omega$ with

identical Cauchy data on Γ_0, we conclude $w = \widetilde{w}$ near $\partial\Omega$. By multiplying both sides of the governing equation in (6.14) with w, integrating over the domain Ω and applying Green's formula, we have

$$0 = \int_\Omega -\nabla \cdot (q\nabla w) w \,\mathrm{d}x = \int_\Omega q|\nabla w|^2 \,\mathrm{d}x - \int_{\partial\Omega} w\, \partial_\nu w \,\mathrm{d}S,$$

i.e.,

$$\int_\Omega q|\nabla w|^2 \,\mathrm{d}x = \int_{\partial\Omega} w\, \partial_\nu w \,\mathrm{d}S.$$

Now since w and $\widetilde{w}$ have identical Cauchy data on the boundary $\partial\Omega$, we have $\int_{\partial\Omega} w\, \partial_\nu w \,\mathrm{d}S = \int_{\partial\Omega} \widetilde{w}\, \partial_\nu \widetilde{w} \,\mathrm{d}S$, and consequently

$$\int_\Omega q|\nabla w|^2 \,\mathrm{d}x = \int_\Omega \widetilde{q}|\nabla \widetilde{w}|^2 \,\mathrm{d}x.$$

This identity and the inequality $\widetilde{q} \geq q$ a.e. in Ω imply

$$\int_\Omega q|\nabla w|^2 \,\mathrm{d}x \geq \int_\Omega q|\nabla \widetilde{w}|^2 \,\mathrm{d}x,$$

which immediately implies

$$\frac{1}{2}\int_\Omega q|\nabla w|^2 \mathrm{d}x - \int_{\partial\Omega} w\widehat{g}(0) \,\mathrm{d}S \geq \frac{1}{2}\int_\Omega q|\nabla \widetilde{w}|^2 \,\mathrm{d}x - \int_{\partial\Omega} \widetilde{w}\widehat{g}(0) \,\mathrm{d}S.$$

By the Dirichlet principle [42], w is the minimizer of the energy integral, and hence $w = \widetilde{w}$ and $q = \widetilde{q}$. □

Remark 6.3. *Note that the uniqueness of the inclusion ω in [55] relies on the assumption ω being a convex polygon with* $\mathrm{diam}(\omega) < \mathrm{dist}(\omega, \partial\Omega)$. *Alessandrini [10] removed the diameter assumption for a specialized choice of the boundary data. The works [136, 93] proved the unique determination of ω when ω is a disc or ball. For general shapes, even for ellipses or ellipsoids, this inverse problem appears still open. Note that in the uniqueness proof, the key is the reduction of the problem to the elliptic case, with a nonzero Neumann boundary condition. In particular, the result will not hold if the temporal component ψ vanishes identically over the interval $[0, T]$, i.e., condition* (6.4) *does not hold.*

Remark 6.4. *If the diffusion coefficient q is not piecewise constant, it is also possible to show the unique recovery if the boundary excitation data g is specially designed. For example, consider problem* (6.1) *with a more general elliptic operator*

$$\mathcal{L}u(x) := -\nabla \cdot (D(x)\nabla u(x)) + \sigma(x)u(x), \quad x \in \overline{\Omega}. \tag{6.15}$$

Here $D \in C^2(\overline{\Omega})$ and $\sigma \in L^\infty(\Omega)$ with $0 < \underline{c}_D \leq D \leq \overline{c}_D$ in $\overline{\Omega}$ and $0 \leq \sigma \leq \overline{c}_\sigma$ in Ω, and the Neumann data g is constructed as follows. First, we choose sub-boundaries Γ_1 and Γ_2 such that $\Gamma_1 \cup \Gamma_2 = \partial\Omega$ and $\Gamma_1 \cap \Gamma_2 \neq \emptyset$. Let $\chi \in C^\infty(\partial\Omega)$ be a cut-off function with $\mathrm{supp}(\chi) = \Gamma_1$ *and $\chi \equiv 1$ on Γ_1', with $\Gamma_1' \subset \Gamma_1$*

such that $\Gamma_1' \cup \Gamma_2 = \partial\Omega$, $\Gamma_1' \cap \Gamma_2 \neq \emptyset$. *Now we fix* $0 \leq T_0 < T_1 < T$ *and choose a strictly increasing sequence* $\{t_k\}_{k=0}^{\infty}$ *such that* $t_0 = T_0$ *and* $\lim_{k\to\infty} t_k = T_1$. *Consider a sequence* $\{p_k\}_{k=1}^{\infty} \subset \mathbb{R}_+$ *and a sequence* $\{\psi_k\}_{k=1}^{\infty} \subset C^{\infty}([0,\infty); \overline{\mathbb{R}_+})$ *such that*

$$\psi_k = \begin{cases} 0 & \text{on } [0, t_{2k-1}], \\ p_k & \text{on } [t_{2k}, \infty). \end{cases}$$

Then we fix $\{b_k\}_{k=0}^{\infty} \subset \mathbb{R}_+$ *such that* $\sum_{k=1}^{\infty} b_k \|\psi_k\|_{W^{2,\infty}(\mathbb{R}_+)} < \infty$, *and define the Neumann data* g *by*

$$g(y,t) := \sum_{k=1}^{\infty} g_k(y,t) = \chi \sum_{k=1}^{\infty} b_k \psi_k(t) \eta_k(y), \tag{6.16}$$

where the set $\{\eta_k\}_{k=1}^{\infty}$ *is chosen to be dense in* $H^{\frac{1}{2}}(\partial\Omega)$ *and* $\|\eta_k\|_{H^{\frac{1}{2}}(\partial\Omega)} = 1$. *Note that the Neumann data* g *defined in* (6.16) *plays the role of infinity measurements [29, 30], and hence the unique recovery of the fractional order* α *and both* a *and* q *from one boundary measurement. See also some related discussions in [96, 95] with different problem settings. However, this choice of* g *is impossible to numerically realize in practice, due to the need to numerically represent infinitesimally small quantities.*

6.3 Reconstruction algorithm

In this section, we derive an algorithm for recovering the fractional order α and the coefficient q, directly inspired by the uniqueness proof. We divide the recovery procedure into three steps:

(i) use the asymptotic behavior of the solution of problem (6.1) near $t = 0$ to recover α;

(ii) use analytic extension to extract the solution of problem (6.1) with zero f and u_0;

(iii) use the level set method [123] to recover the shape of the unknown medium $\omega \subset \Omega$.

First, we give an asymptotics of the Dirichlet data $H(t)$ of problem (6.1). The result is direct from the representation and properties of $E_{\alpha,1}(z)$ near $z = 0$ and the trace theorem.

Proposition 6.3. *If* $u_0 \in \mathrm{Dom}(A^{1+\frac{s}{2}})$ *and* $f \in \mathrm{Dom}(A^{\frac{s}{2}})$ *with* $s > 1$. *Let* $H = u|_{\partial\Omega\times(0,T)}$ *be the Dirichlet trace of the solution to problem* (6.1) *with* g *given as* (6.3), *then the following asymptotic holds:*

$$H(y,t) = u_0(y) + (\mathcal{A}u_0 - f)(y)t^{\alpha} + O(t^{2\alpha}) \quad \text{as } t \to 0^+.$$

In view of Proposition 6.3, for any fixed $y_0 \in \partial\Omega$, the asymptotic behavior of $H(y_0,t)$ as $t \to 0^+$ allows recovering the order α. This can be achieved by minimizing the following objective in α, c_0 and c_1:

$$J(\alpha, c_0, c_1) = \|c_0 + c_1 t^{\alpha} - H(y_0,t)\|^2_{L^2(0,t_0)}, \tag{6.17}$$

for some small $t_0 > 0$. Note that it is important to take t_0 sufficiently small so that higher-order terms can indeed be neglected. The idea of using asymptotics for order recovery was employed in [67, 77, 78].

When recovering the diffusion coefficient q, we need to deal with the unknown functions u_0 and f. This poses significant computational challenges since standard regularized reconstruction procedures [50] require a fully known forward operator. To overcome the challenge, we appeal to Theorem 6.2: u_0 and f only contribute to $H_i(t)$ which is fully determined by $\{\lambda_\ell, \rho_\ell\}_{\ell\in\mathbb{K}}$. Indeed, by Theorem 6.1, $\{\lambda_\ell, \rho_\ell\}_{\ell\in\mathbb{K}}$ can be uniquely determined by $H(t)$, $t \in [0, T_0]$. Hence in theory we can extend $H(t) = H_i(t)$ from $t \in [0, T_0]$ to $t \in [0, T]$, by means of analytic continuation, to approximate the Dirichlet data of (6.1) with $g \equiv 0$ and given u_0 and f. In practice, we look for approximations of the form

$$H(t) \approx \frac{p_0 + p_1 t + \cdots + p_r t^r}{q_0 + q_1 t + \cdots + q_r t^r} := H_r(t), \quad t \in [0, T],$$

where $r \in \mathbb{N}$ is the polynomial order. This choice is motivated by the observation that Mittag-Leffler functions can be well approximated by rational polynomials [12, 115, 48]. The approximation H_r can be constructed efficiently by the AAA algorithm [121]. Now, we can get the Dirichlet data of problem (6.1) with a given g and $u_0 = f \equiv 0$, by defining the reduced data

$$\overline{H}(t) := \begin{cases} 0, & t \in [0, T_0], \\ H(t) - H_r(t), & t \in [T_0, T]. \end{cases}$$

Below we use the reduced data $\overline{H}$ to recover a piecewise constant q. Parameter identification for the subdiffusion model is commonly carried out by minimizing a suitable penalized objective. Since q is piecewise constant, it suffices to recover the interface between different media. The level set method can effectively capture the interface in an elliptic problem [135, 74, 26, 38], which we extend to the time-fractional model (6.1) below. Specifically, we consider a slightly more general setting where the inclusion $\omega \subset \Omega$ has a diffusivity value q_1 and the background $\Omega \setminus \omega$ has a diffusivity value q_2, with possibly unknown q_1 and q_2. That is, the diffusion coefficient q is represented as

$$a(x) = q_1 \sigma(\phi(x)) + q_2(1 - \sigma(\phi(x))) \quad \text{in } \Omega, \tag{6.18}$$

where $\sigma(x)$ and $\phi(x)$ denote the Heaviside function and level set function (a signed distance function):

$$\sigma(x) := \begin{cases} 1, & x \geq 0, \\ 0, & x < 0, \end{cases} \quad \text{and} \quad \phi(x) := \begin{cases} d(x, \partial\omega), & x \in \omega, \\ -d(x, \partial\omega), & x \in \Omega \setminus \overline{\omega}, \end{cases}$$

respectively. Then ϕ satisfies $\omega = \{x \in \Omega : \phi(x) > 0\}$, $\Omega \setminus \overline{\omega} = \{x \in \Omega : \phi(x) < 0\}$ and $\partial\omega = \{x \in \Omega : \phi(x) = 0\}$. To find the values q_1 and q_2 and the interface $\partial\omega$, we minimize the following functional

$$J(\phi, q_1, q_2) = \frac{1}{2}\|u(q) - \overline{H}\|^2_{L^2(0,T;L^2(\Gamma_0))} + \gamma \int_\Omega |\nabla q|, \tag{6.19}$$

where $u(q)$ is the solution to problem (6.7), and $\gamma > 0$ is the penalty parameter. The total variation term $\int_\Omega |\nabla q|$ is to stabilize the inverse problem, which is defined by

$$\int_\Omega |\nabla q| := \sup_{\varphi \in (C_0(\overline{\Omega}))^d, |\varphi| \le 1} \int_\Omega q \nabla \cdot \varphi \, \mathrm{d}x,$$

where $|\cdot|$ denotes the Euclidean norm. Then we apply the standard gradient descent method to minimize problem (6.19). The next result gives the gradient of J. The notations $J_{T-}^{1-\alpha}$ and D_{T-}^{α} denote the backward Riemann-Liouville integral and derivative, defined respectively by [76, Sections 2.2 and 2.3]

$$J_{T-}^{1-\alpha} v(t) := \frac{1}{\Gamma(1-\alpha)} \int_t^T (s-t)^{-\alpha} v(s) \, \mathrm{d}s,$$
$$D_{T-}^{\alpha} v(t) := -\frac{1}{\Gamma(1-\alpha)} \frac{\mathrm{d}}{\mathrm{d}t} \int_t^T (s-t)^{-\alpha} v(s) \, \mathrm{d}s.$$

Proposition 6.4. *The derivative $\frac{\mathrm{d}}{\mathrm{d}q} J$ is formally given by*

$$\frac{\mathrm{d}}{\mathrm{d}q} J(q) = -\int_0^T \nabla u \cdot \nabla v \, \mathrm{d}t - \gamma \nabla \cdot \left(\frac{\nabla q}{|\nabla q|} \right),$$

where $v = v(x, t; q)$ solves the adjoint problem

$$\begin{cases} D_{T-}^{\alpha} v - \nabla \cdot (q \nabla v) = 0 & \text{in } \Omega \times [0, T), \\ q \partial_\nu v = (u - \overline{h}) \chi_{\Gamma_0} & \text{on } \partial\Omega \times [0, T), \\ J_{T-}^{1-\alpha} v(\cdot, T) = 0 & \text{in } \Omega. \end{cases} \tag{6.20}$$

By the chain rule, the derivatives of J with respect to q_1, q_2 and ϕ are given by

$$\frac{\partial J}{\partial \phi} = \frac{\mathrm{d}J}{\mathrm{d}q} \frac{\partial q}{\partial \phi} = \frac{\mathrm{d}J}{\mathrm{d}q} (q_1 - q_2) \delta(\phi),$$
$$\frac{\partial J}{\partial q_1} = \int_\Omega \frac{\mathrm{d}J}{\mathrm{d}q} \frac{\partial q}{\partial q_1} \, \mathrm{d}x = \int_\Omega \frac{\mathrm{d}J}{\mathrm{d}q} \sigma(\phi) \, \mathrm{d}x,$$
$$\frac{\partial J}{\partial q_2} = \int_\Omega \frac{\mathrm{d}J}{\mathrm{d}q} \frac{\partial q}{\partial q_2} \, \mathrm{d}x = \int_\Omega \frac{\mathrm{d}J}{\mathrm{d}q} (1 - \sigma(\phi)) \, \mathrm{d}x,$$

where δ is the Dirac delta function. Hence the iterative scheme for updating q_1, q_2 and ϕ reads

$$\phi^{k+1} = \phi^k - r^k \frac{\partial J}{\partial \phi}(\phi^k, q_1^k, q_2^k) \quad \text{and} \quad q_j^{k+1} = q_j^k - r_j^k \frac{\partial J}{\partial q_j}(\phi^{k+1}, q_1^k, q_2^k), \quad j = 1, 2.$$

The step sizes r^k and r_j^k can be either fixed or obtained by means of line search. The implementation of the method requires some care. First, we approximate the delta function $\delta(x)$ and Heaviside function $\sigma(x)$ by

$$\delta_\varepsilon(x) = \frac{\varepsilon}{\pi(x^2 + \varepsilon^2)} \quad \text{and} \quad \sigma_\varepsilon(x) = \frac{1}{\pi} \arctan\left(\frac{x}{\varepsilon}\right) + \frac{1}{2},$$

respectively, with $\varepsilon > 0$ of order of the mesh size [33, 38]. Second, during the iteration, the new iterate of ϕ may fail to be a signed distance function. Although one is only interested in $\operatorname{sign}(\phi)$, it is

undesirable for $|\phi|$ to get too large near the interface. Thus we reset ϕ to a signed distance function whenever ϕ changes by more than 10% in the relative $L^2(\Omega)$-norm. The resetting procedure is to find the steady solution of the following equation [123, 38]:

$$\partial_t d + \operatorname{sign}(d)(|\nabla d| - 1) = 0, \quad \text{with } d(0) = \phi.$$

6.4 Numerical result

Now we present numerical results for reconstructing the fractional order α and piecewise constant diffusion coefficient q, with unknown u_0 and f. In all experiments, the domain Ω is taken to be the unit square $\Omega = (0,1)^2$, and the final time $T = 1$. We divide the domain Ω into uniform squares with a length $h = 1/50$ and then divide along the diagonals of each square. We discretize the time interval $[0, T]$ into uniform subintervals with a time step size $\tau = 1/100$. All direct and adjoint problems are solved by standard continuous piecewise linear Galerkin finite element method in space and backward Euler convolution quadrature in time (see e.g.,[79] and [88, Chapters 2 and 3]). Below we investigate the following four cases:

(i) ω is a disc with radius $\frac{1}{3}$, centered at $(\frac{1}{2}, \frac{1}{2})$,

(ii) ω is a square with length $\frac{1}{2}$, centered at $(\frac{1}{2}, \frac{1}{2})$,

(iii) ω is a concave polygon, and

(iv) ω are two discs with radius $\frac{1}{5}$, centered at $(\frac{1}{4}, \frac{1}{2})$ and $(\frac{3}{4}, \frac{1}{2})$, respectively.

Throughout, the unknown initial condition u_0 and source f are fixed as

$$u_0(x_1, x_2) = x_1^2 x_2^2 (1 - x_1)^2 (1 - x_2)^2 \quad \text{and} \quad f(x_1, x_2) = 1 + x_1 + z_2,$$

respectively. Meanwhile, we fix the exact fractional order $\alpha^\dagger = 0.8$ and the diffusion coefficient $q^\dagger = 10 - 9\chi_\omega$, i.e. $q_1 = 1$, $q_2 = 10$. Unless otherwise stated, the Neumann excitation g is taken as $g(y,t) = \eta(y)\chi_{[0.5,1]}(t)$, where η is the cosine function with a frequency 2π on each edge for cases (i)–(iii) and is constant 1 for case (iv). We set g on $\partial\Omega \times [0,T]$, and take the measurement H on $\partial\Omega \times [0,T]$.

First, we show the numerical recovery of the fractional order α for three different values, i.e., 0.3, 0.5 and 0.8. In view of Proposition 6.3, it suffices to fix one point $y_0 \in \partial\Omega$ (which is fixed at the origin $y_0 = (0,0)$ below) and to minimize problem (6.17), for which we use the L-BFGS-B with constraint $\alpha \in [0,1]$ [27]. The recovered orders are presented in Table 6.1. Note that the least-squares functional has many local minima. Hence, the algorithm requires a good initial guess to get a correct value for

Table 6.1: The recovered order α based on least-squares fitting.

(a) case (i)				(b) case (ii)			
$t_0\backslash\alpha$	0.3000	0.5000	0.8000	$t_0\backslash\alpha$	0.3000	0.5000	0.8000
1e-3	0.2402	0.5289	0.8353	1e-3	0.2380	0.5243	0.8350
1e-4	0.2516	0.5244	0.8795	1e-4	0.2479	0.5239	0.8797
1e-5	0.2649	0.4994	0.8006	1e-5	0.2612	0.5022	0.7803
1e-6	0.2712	0.4637	0.7978	1e-6	0.2695	0.5182	0.7977
1e-7	0.2665	0.5267	0.8019	1e-7	0.2662	0.5279	0.8019
1e-8	0.2558	0.4913	0.7989	1e-8	0.2562	0.4914	0.7989
1e-9	0.2744	0.4925	0.7999	1e-9	0.2741	0.4925	0.7999
(c) case (iii)				(d) case (iv)			
$t_0\backslash\alpha$	0.3000	0.5000	0.8000	$t_0\backslash\alpha$	0.3000	0.5000	0.8000
1e-3	0.2383	0.5214	0.8485	1e-3	0.2384	0.5247	0.8436
1e-4	0.2480	0.5198	0.8821	1e-4	0.2486	0.5221	0.8816
1e-5	0.2600	0.5098	0.8005	1e-5	0.2617	0.5033	0.8005
1e-6	0.2667	0.5213	0.7977	1e-6	0.2692	0.5178	0.7977
1e-7	0.2634	0.5273	0.8019	1e-7	0.2650	0.5273	0.8019
1e-8	0.2654	0.4913	0.7990	1e-8	0.2703	0.4913	0.7989
1e-9	0.2718	0.4925	0.7999	1e-9	0.2740	0.4925	0.7999

α. It is observed that the reconstruction is more accurate when $t_0 \to 0^+$, since the high order terms are then indeed negligible. Also, for a fixed interval $(0, t_0)$, due to the asymptotic behavior, we have slightly better approximations when the true order α is large. However, this does not influence much the reconstruction results for cases (i)–(iv), since the coefficient q is constant near origin.

Now we apply analytic continuation to extend the observed data H by a rational function H_r from the interval $[0, 0.5]$ to $[0, 1]$, using the AAA algorithm [121] with degree $r = 4$. This step is essential for dealing with missing data u_0 and f: subtracting H_r from H yields the reduced data $\overline{H}$ for a given g and $u_0 = f \equiv 0$, which is then used in recovering q. Fig. 6.1 shows the $L^2(\partial\Omega)$ error between H_r and the exact data H_0 which is obtained by solving (6.1) with given g and vanishing u_0 and f. Note that higher order rational approximations can reduce the error over the interval $[0, 0.5]$, but it tends to lead to larger errors in the interval $[0.5, 1]$. The approach is numerically sensitive to the presence of data noise, reflecting the well-known severe ill-posed nature of analytic continuation.

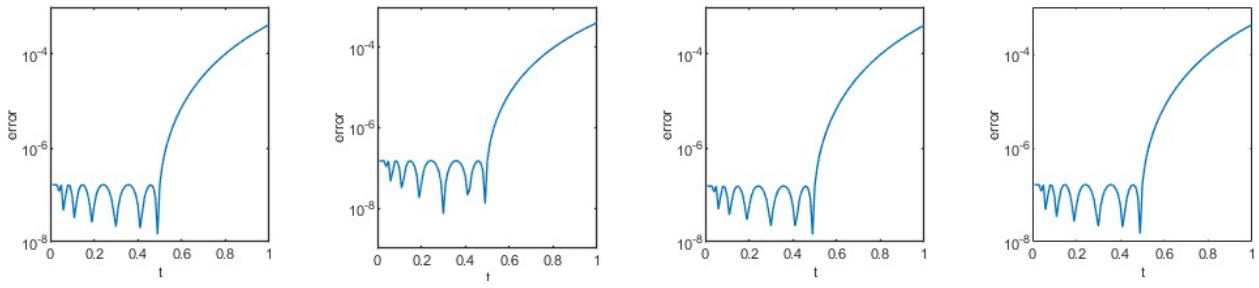

Figure 6.1: The $L^2(\partial\Omega)$-error between the analytic continuation H_r and true data H_0 for cases (i)–(iv).

Finally, we present recovery results for the piecewise constant coefficient q, or equivalently, the shape ω. The exact value is 1 inside the inclusion ω and 10 outside, unless otherwise stated. We use the standard gradient descent method to minimize problem (6.19). Unless otherwise stated, we fix the step sizes $r^k \equiv 1$, $r_1^k \equiv 0$, $r_2^k \equiv 0$, i.e., fixing the values inside and outside the inclusion ω. The regularization parameter γ is chosen to be 1e-8, and the coefficients q_1 and q_2 are set to $q_1 = 0.9$ and $q_2 = 10$. The results are summarized in Figs. 6.2-6.8, where dashed lines denote the recovered interfaces.

Fig. 6.2 shows the result for case (i), when the initial guesses are a small circle but with two different centers. In either case, the algorithm can successfully reconstruct the exact circle after 10000 iterations. For case (ii), the exact interface is a square, again with the initial guess being small circles inside the square, cf. Fig. 6.3. The algorithm accurately recovers the four edges of the square. However, due to the non-smoothness, the corners are much more challenging to reconstruct and hence less accurately resolved. These results indicate that the method does converge with a reasonable initial guess, but it may take many iterations to yield satisfactory reconstructions. Fig. 6.4

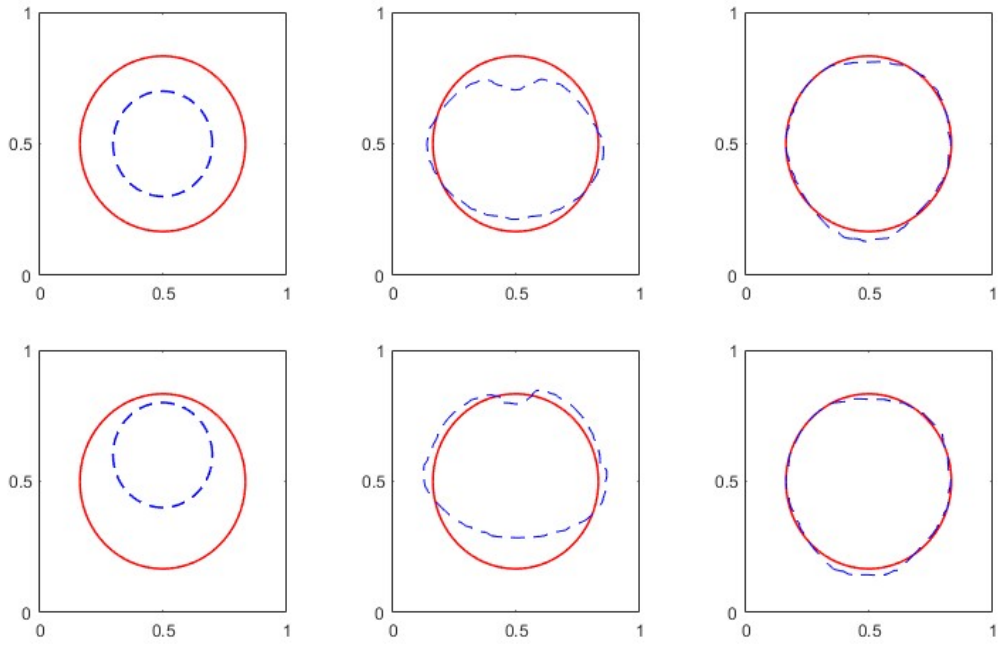

Figure 6.2: The reconstructions of the interface for case (i) at iteration 0, 100 and 10000 from left to right, with two different initial guesses.

shows the results for case (iii) for which the exact interface is a concave polygon, which is much more challenging to resolve. Nonetheless, the algorithm can still recover the overall shape of the interface. The reconstruction around the concave part has lower accuracy. To the best of our knowledge, the unique determination of a concave polygonal inclusion (in an elliptic equation) is still open. Fig. 6.5 shows the results for case (iv) which contains two discs as the exact interface. The initial guess is two small discs near the boundary $\partial\Omega$. Note that in this case, we choose the boundary data $\eta \equiv 1$ in order to strengthen the effect of inhomogeneity. The final reconstruction is very satisfactory.

Fig. 6.6 shows a variant of case (ii), with the initial interface being two disjoint discs. It is observed that the two discs first merge into one concave contour, and then it evolves slowly to resolve the square. This shows one distinct feature of the level set method, i.e., it allows topological changes. Due to the complex evolution, the algorithm takes many more iterations to reach convergence (i.e., 30000 iterations versus 8000 iterations in case (ii)).

Fig. 6.7 shows a case which aims at simultaneously recovering the interface and the diffusivity value inside the inclusion, for which the exact interface is a square and the exact values of q_1 and q_2 are 1 and 10, respectively. In the experiment, we take two different initial guesses. The initial value of q_1 for both cases is $q_1 = 1.2$, and we take the step sizes $r^k \equiv 1$, $r_1^k \equiv 10$ and $r_2^k \equiv 0$. The recovered value q_1 is 0.92 for the first row and 0.89 for the second row. It is observed that for both cases, one can roughly recover the interface. These experiments clearly indicate that the level set method can

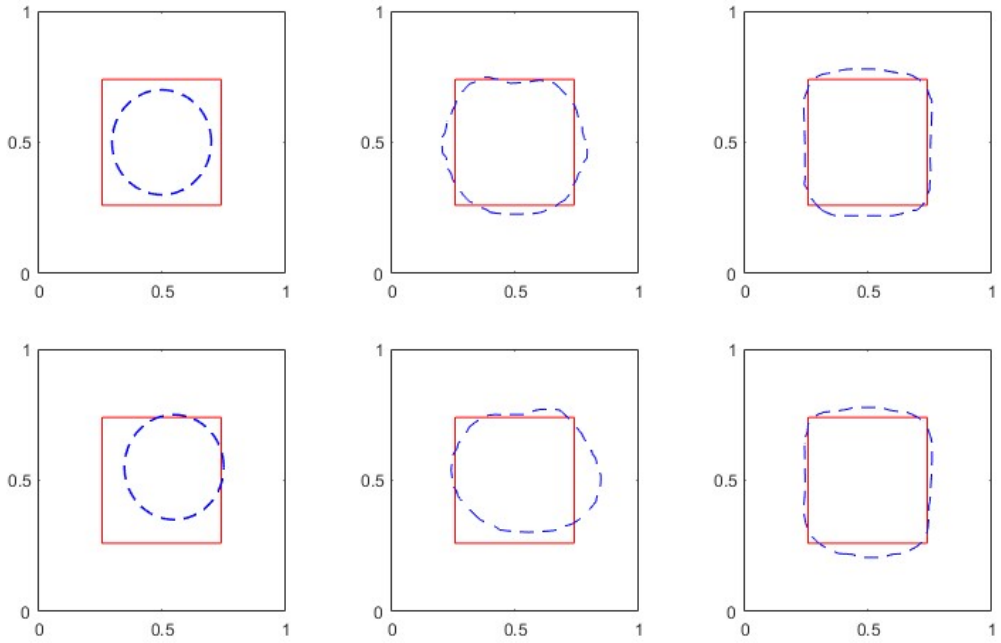

Figure 6.3: The reconstructions of the interface for case (ii) with different initial guesses at iteration 0, 100 and 8000 from left to right.

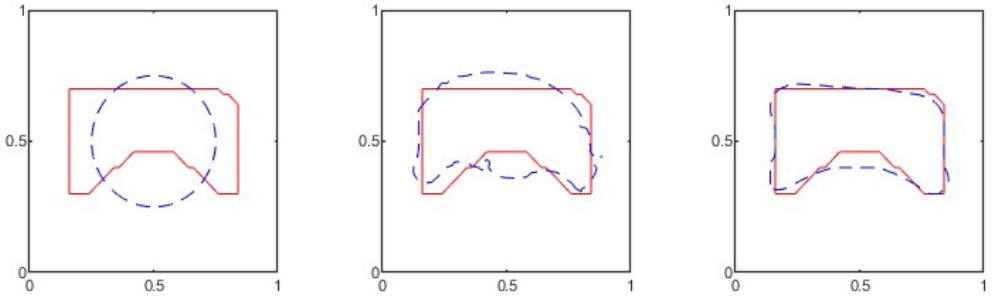

Figure 6.4: The reconstructions of the interface for case (iii) at iteration 0, 100 and 8000 from left to right.

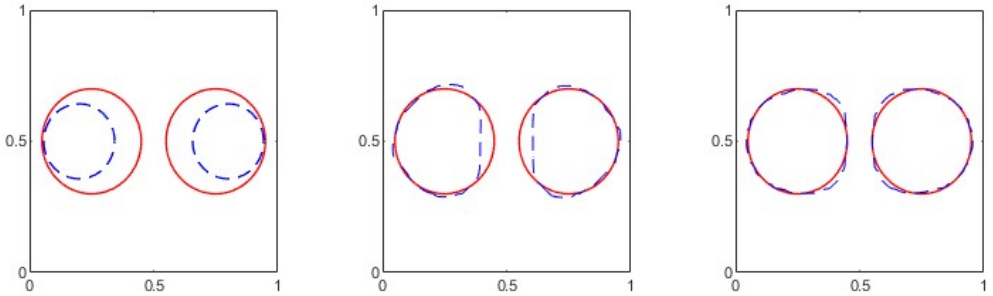

Figure 6.5: The reconstructions of the interface for case (iii) at iteration 0, 1000 and 15000 from left to right.

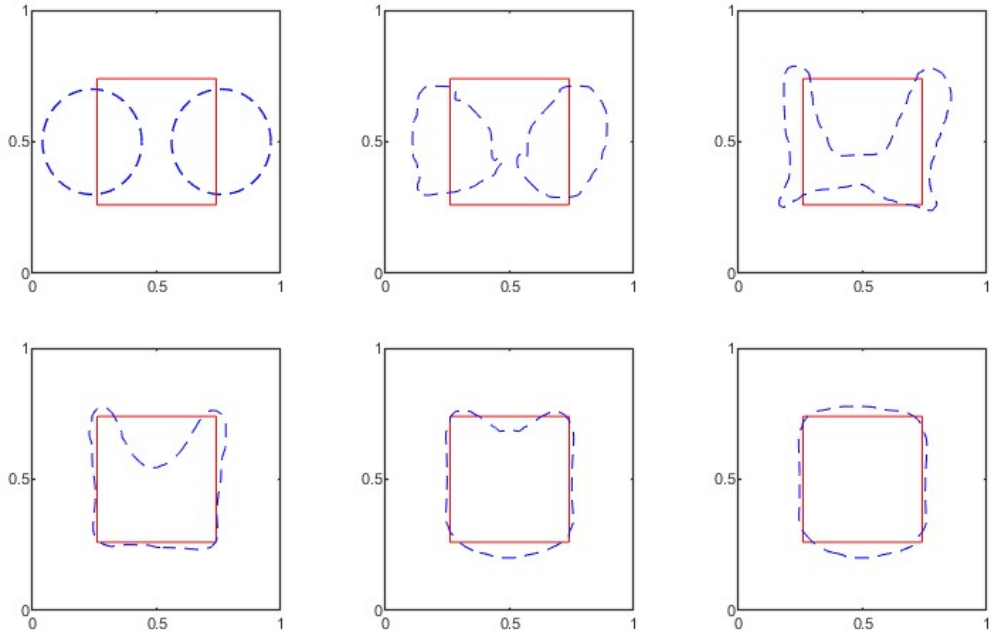

Figure 6.6: The reconstruction of the interface for case (ii) with a different initial guess, at different iterations 0, 100, 1000, 10000, 20000 and 30000 (from left to right).

accurately recover the interface ω. However, it generally takes many iterations to obtain satisfactory results. This is attributed partly to topological changes and the presence of nonsmooth points, and partly to the direct gradient flow formulation. Indeed, one observes from Proposition 6.4 that the gradient field for updating the level set function is actually not very smooth, which hinders the rapid evolution of the interface. Hence, there is an imperative need to accelerate the method, especially via suitable preconditioning and post-processing [74].

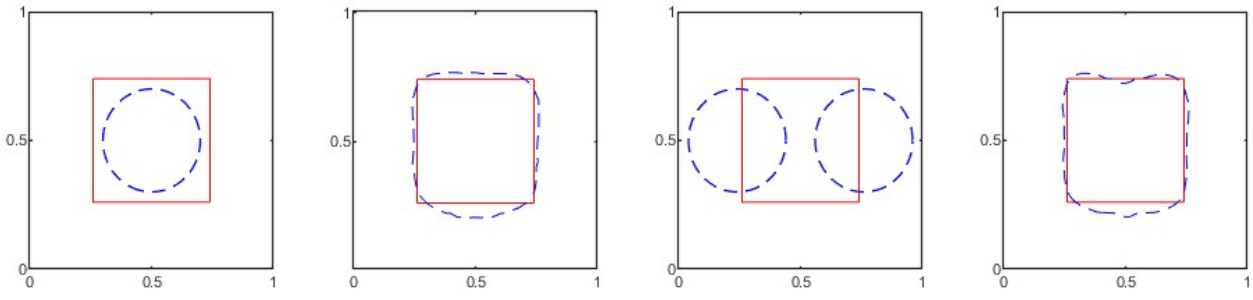

Figure 6.7: Initial guesses and reconstructions for case (ii) with a non-fixed diffusivity value q_1.

Last, Fig. 6.8 shows reconstruction results with noisy data. Due to the instability of analytic continuation for noisy data, we use boundary data corresponding to zero u_0, f as our measurement and only focus on reconstructing q. That is, we denote $H^\dagger$ the solution of problem (6.1) with $u_0 \equiv 0$

and $f \equiv 0$ which plays the role of $\overline{H}$. The noisy measurement H^δ is generated by

$$H^\delta(y,t) = H^\dagger(y,t) + \delta \|H^\dagger\|_{L^\infty(\partial\Omega\times[0,1])}\xi(y,t),$$

where $\delta > 0$ denotes the relative noise level, and ξ follows the standard Gaussian distribution. We take the exact interface as a concave polygon and the initial guess is a circle; see the left panel in Fig. 6.4. We consider two different noise levels and three different input boundary data. The first and second rows in Fig. 6.8 are for 1% and 5% noise, obtained with a regularization parameter $\gamma =$ 1e-7 and $\gamma =$ 5e-7, respectively. We consider three input Neumann data g_1, g_2 and g_3: $g_1 = g$ (i.e., identical as before), and g_2 and g_3 are given by

$$g_2(x,t) = \eta_1(x)\chi_{[0.25,1]}(t) + \eta_2(x)\chi_{[0.5,1]}(t) + \eta_3(x)\chi_{[0.75,1]}(t),$$
$$g_3(x,t) = \eta_1(x)\chi_{[1/6,1]}(t) + \eta_2(x)\chi_{[2/6,1]}(t) + \eta_3(x)\chi_{[3/6,1]}(t) + \eta_4(x)\chi_{[4/6,1]}(t) + \eta_5(x)\chi_{[5/6,1]}(t),$$

where η_n $(n = 1, \ldots, 5)$ is a cosine function with frequency $2n\pi$ on each edge. The inputs g_2 and g_3 contain higher frequency information and are designed to examine the influence of boundary excitation on the reconstruction. Fig. 6.8 shows that with the knowledge of $H^\dagger$, the method for recovering the interface is largely stable with respect to the presence of data noise. With more frequencies in the input excitation, the reconstruction results would improve slightly. This agrees with the observation that the concave shape contains more high-frequency information.

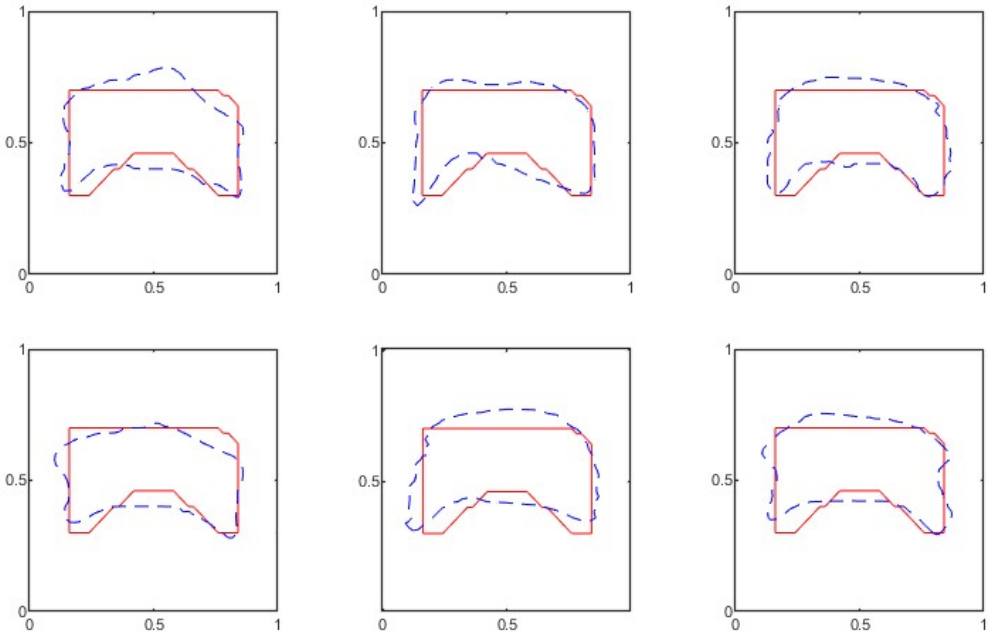

Figure 6.8: The reconstruction for case (iii) with noisy data and different boundary excitations g_1, g_2 and g_3 (from left to right). The top and bottom rows are for noise levels 1% and 5%.

CHAPTER 7.

Conclusion and future works

In this thesis, we investigate the numerical algorithms and their analysis for the parameter identification problem in PDEs. Our focus is on numerical schemes with error analysis that align with conditional stability results. We present our work through a model problem: the inverse diffusivity problem. We study two derivations of this model problem: the diffusion-reaction model and the QPAT model. Additionally, We propose a numerical scheme for the inverse diffusivity problem combining the theoretical foundations of FEMs and computational innovations of NNs. Finally, we investigate a severely ill-posed inverse problem in a subdiffusion model with partial data. We develop a reliable numerical inversion algorithm based on the uniqueness analysis.

In Chapter 3, we investigated the simultaneous reconstruction of the diffusion and reaction coefficients inherent in elliptic/parabolic equations. This is achieved through the utilization of two internal measurements of the solutions. We proposed a decoupled algorithm capable of sequentially recovering these two parameters. The approach begins with a straightforward reformulation leading to a standard problem of identifying the diffusion coefficient. This coefficient is numerically recovered, without any requirement for knowledge of the potential, by employing an output least-square method in conjunction with finite element discretization. In the subsequent step, the previously recovered diffusion coefficient becomes instrumental in the reconstruction of the potential coefficient. The approach is inspired by a constructive conditional stability, and we have provided rigorous *a priori* error estimates in $L^2(\Omega)$ for the recovered diffusion and potential coefficients. The derivation of these estimates necessitated the development of a weighted energy argument and suitable positivity conditions. These estimates serve as a helpful guide to choose appropriate regularization parameters and discretization mesh sizes, aligned with the noise level.

In Chapter 4, we investigated the reconstruction of the diffusion and absorption coefficients in QPAT model. This is achieved by using multiple internal measurements illuminated by random boundary data. The reconstruction method starts with a straightforward reformulation, leading to an inverse diffusivity problem. A Hölder type stability is established by using energy estimates with special test function as well as the non-zero condition, guaranteed by the use of random boundary illuminations. The diffusivity coefficient is numerically recovered by employing a least-square formulation with a finite element discretization. The stability estimate motivates the approximation error analysis. With appropriate choices of the discretization mesh size and of the regularization parameters in relation with the noise level, the convergence rate of the approximation error is comparable to the

stability result. In the subsequent step, we solve a direct problem involving the reconstructed diffusivity and optical energy measurement. The diffusion and absorption coefficients can be recovered by an algebraic relation using the solution of the direct problem and the reconstructed diffusivity in the previous stage.

In Chapter 5, we developed and analyzed the FEM-NN hybrid scheme for reconstructing the diffusivity in elliptic/parabolic equations. The approach combines neural networks for approximating the unknown coefficient with finite element methods for discretizing the solution. We established rigorous $L^2(\Omega)$ error estimates that explicitly depend on the discretization parameter, noise level, regularization parameter, neural network approximation accuracy, and network architecture. The proofs leverage the smoothness properties of neural networks and the structural characteristics of finite element spaces. Extensive numerical experiments demonstrate the efficiency and accuracy of the proposed hybrid method.

In Chapter 6, we studied a challenging inverse problem of recovering multiple coefficients from one single boundary measurement, in a partially unknown medium, due to the formal under-determined nature of the problem. We have presented two uniqueness results, i.e., recovering the order and the piecewise constant diffusion coefficient from a fairly general Neumann input data and recovering the order and two distributed parameters from a fairly specialized Neumann input data (Remark 6.4). For the former, we have also developed a practical reconstruction algorithm based on asymptotic expansion, analytic continuation and level set method, which is inspired by the uniqueness proof, and have presented extensive numerical experiments to showcase the feasibility of the approach.

Despite the detailed discussion, there are still many interesting issues that deserve further investigation, which we briefly discuss below.

In Section 3.4 and Section 4.3, our numerical experiments indicated that the empirical rates surpassed the theoretical ones. Future work will focus on investigating the reasons behind this discrepancy and improving the error estimate. It is worthwhile to explore the stability results of inverse problems from numerical perspective. In particular, the error analysis for the inverse diffusion problem relies on the conditional stability presented in [22]. This stability result utilizes the weak formulations of PDEs and a weighted energy argument, which are frequently employed in numerical analysis. Consequently, the error estimation can be derived by mimicking the proof of stability in numerical aspect and the convergence rate would align with the condition stability. From this perspective, it is crucial to establish the stability in continuous level, which can then be applied to numerical analysis. We highlight this issue with the following example. For many inverse problems, the Carleman estimate [72, 148] plays a essential role in continuous stability estimation. This type of estimation is based on an exponential type weighted function and integration by parts. However, the derivation of Carleman

estimates at discrete level is a challenging problem. In fact, in the proof of such estimates, the Carleman large parameter s must be connected to the mesh size h through the relation: $sh \leq \epsilon$ [100, 23]. Thus the discrete Carleman estimate requires restrictive condition for the mesh size h, which leads to challenges for related error analysis.

As the use of DNNs for solving forward and inverse problems for PDEs has been explored only recently, the theoretical foundation of DNNs still requires further investigation. For instance, the neural network approximation error presented in Lemma 2.1 may not be optimal. Indeed, the proof of Lemma 2.1 is constructive, involving the design of neural networks to approximate polynomials. Interestingly, numerical experiments have shown that the empirical rates surpassed the theoretical ones. Even very shallow and small neural networks exhibit excellent expressivity. Besides, the presented hybrid scheme cannot overcome the curse of dimensionality, which is one of the main motivations using neural network for solving PDEs. Since the numerical algorithm requires to solve the equation with FEMs, it cannot be implemented in high dimensional space. In the future, we aim to develop an inversion algorithm with pure neural network approximation and provide rigorous error estimate which aligns with the stability result. In this framework, high-dimensional integrals are computed via a Monte Carlo method, whose error contribution requires further investigation.

In addition, it is also interesting to derive the error estimation for inverse problems with poor stability. In Chapter 6, we only examined the uniqueness and numerical inversion of the identification. It would be intriguing to investigate the stability estimate when observation is taken on the boundary or subdomain. In practical scenario, the measurement data are typically not available on the entire domain, which deteriorates the stability of the inverse problem. Therefore, it is crucial to study the conditional stability of these highly ill-posed identification problems and derive rigorous error estimates that align with the stability. Liu et al [151] derived Hölder stability for inverse diffusion problem with measurements on a subdomain, but they assumed the diffusion coefficient is analytic to propose analytic extension. For problem data satisfying weaker assumptions, Carleman estimates can be utilized to derive stability results. However, the design of robust numerical algorithms based on this technical tool requires further investigation.

Bibliography

[1] Assyr Abdulle and Gilles Vilmart. A priori error estimates for finite element methods with numerical quadrature for nonmonotone nonlinear elliptic problems. *Numer. Math.*, 121(3):397–431, 2012.

[2] Robert A. Adams and John J. F. Fournier. *Sobolev Spaces*. Elsevier/Academic Press, Amsterdam, 2nd edition, 2003.

[3] Mark Ainsworth and Yeonjong Shin. Plateau phenomenon in gradient descent training of ReLU networks: explanation, quantification, and avoidance. *SIAM J. Sci. Comput.*, 43(5):A3438–A3468, 2021.

[4] Giovanni S. Alberti. Non-zero constraints in elliptic PDE with random boundary values and applications to hybrid inverse problems. *Inverse Problems*, 38(12):Paper No. 124005, 26, 2022.

[5] Giovanni S. Alberti, Guillaume Bal, and Michele Di Cristo. Critical points for elliptic equations with prescribed boundary conditions. *Arch. Ration. Mech. Anal.*, 226(1):117–141, 2017.

[6] Giovanni S. Alberti and Yves Capdeboscq. Combining the Runge approximation and the Whitney embedding theorem in hybrid imaging. *Int. Math. Res. Not. IMRN*, 2022(6):4387–4406, 2020.

[7] G. Alessandrini and R. Magnanini. Elliptic equations in divergence form, geometric critical points of solutions, and Stekloff eigenfunctions. *SIAM J. Math. Anal.*, 25(5):1259–1268, 1994.

[8] Giovanni Alessandrini. An identification problem for an elliptic equation in two variables. *Ann. Mat. Pura Appl. (4)*, 145:265–295, 1986.

[9] Giovanni Alessandrini, Michele Di Cristo, Elisa Francini, and Sergio Vessella. Stability for quantitative photoacoustic tomography with well-chosen illuminations. *Ann. Mat. Pura Appl. (4)*, 196(2):395–406, 2017.

[10] Giovanni Alessandrini and Victor Isakov. Analyticity and uniqueness for the inverse conductivity problem. *Rend. Istit. Mat. Univ. Trieste*, 28(1-2):351–369 (1997), 1996.

[11] S. R. Arridge. Optical tomography in medical imaging. *Inverse Problems*, 15(2):R41–R93, 1999.

[12] Colin Atkinson and Adel Osseiran. Rational solutions for the time-fractional diffusion equation. *SIAM J. Appl. Math.*, 71(1):92–106, 2011.

[13] Nikolai Yu. Bakaev. Maximum norm resolvent estimates for elliptic finite element operators. *BIT*, 41(2):215–239, 2001.

[14] Nikolai Yu. Bakaev, Vidar Thomée, and Lars B. Wahlbin. Maximum-norm estimates for resolvents of elliptic finite element operators. *Math. Comp.*, 72(244):1597–1610, 2003.

[15] Guillaume Bal and Kui Ren. Multi-source quantitative photoacoustic tomography in a diffusive regime. *Inverse Problems*, 27(7):075003, 20, 2011.

[16] Guillaume Bal and Gunther Uhlmann. Inverse diffusion theory of photoacoustics. *Inverse Problems*, 26(8):085010, 20, 2010.

[17] Guillaume Bal and Gunther Uhlmann. Reconstruction of coefficients in scalar second-order elliptic equations from knowledge of their solutions. *Comm. Pure Appl. Math.*, 66(10):1629–1652, 2013.

[18] Andrew R Barron. Approximation and estimation bounds for artificial neural networks. *Machine learning*, 14:115–133, 1994.

[19] Jens Berg and Kaj Nyström. Neural networks as smooth priors for inverse problems for pdes. *J. Comput. Math. Data Sci.*, 1:100008, 2021.

[20] Stefano Berrone, Claudio Canuto, and Moreno Pintore. Variational physics informed neural networks: the role of quadratures and test functions. *J. Sci. Comput.*, 92(3):100, 27, 2022.

[21] Radu Ioan Boţ and Bernd Hofmann. Conditional stability versus ill-posedness for operator equations with monotone operators in Hilbert space. *Inverse Problems*, 32(12):125003, 23 pp., 2016.

[22] Andrea Bonito, Albert Cohen, Ronald DeVore, Guergana Petrova, and Gerrit Welper. Diffusion coefficients estimation for elliptic partial differential equations. *SIAM J. Math. Anal.*, 49(2):1570–1592, 2017.

[23] Franck Boyer, Florence Hubert, and Jérôme Le Rousseau. Discrete Carleman estimates for elliptic operators and uniform controllability of semi-discretized parabolic equations. *J. Math. Pures Appl. (9)*, 93(3):240–276, 2010.

[24] Susanne C. Brenner and L. Ridgway Scott. *The mathematical theory of finite element methods*, volume 15 of *Texts in Applied Mathematics*. Springer, New York, third edition, 2008.

[25] Haïm Brezis and Petru Mironescu. Gagliardo-Nirenberg inequalities and non-inequalities: the full story. *Ann. Inst. H. Poincaré C Anal. Non Linéaire*, 35(5):1355–1376, 2018.

[26] Martin Burger. A level set method for inverse problems. *Inverse Problems*, 17(5):1327–1355, 2001.

[27] Richard H. Byrd, Peihuang Lu, Jorge Nocedal, and Ci You Zhu. A limited memory algorithm for bound constrained optimization. *SIAM J. Sci. Comput.*, 16(5):1190–1208, 1995.

[28] Alberto-P. Calderón. On an inverse boundary value problem. In *Seminar on Numerical Analysis and its Applications to Continuum Physics (Rio de Janeiro, 1980)*, pages 65–73. Soc. Brasil. Mat., Rio de Janeiro, 1980.

[29] B. Canuto and O. Kavian. Determining coefficients in a class of heat equations via boundary measurements. *SIAM J. Math. Anal.*, 32(5):963–986, 2001.

[30] Bruno Canuto and Otared Kavian. Determining two coefficients in elliptic operators via boundary spectral data: a uniqueness result. *Boll. Unione Mat. Ital. Sez. B Artic. Ric. Mat. (8)*, 7(1):207–230, 2004.

[31] Kenneth M. Case and Paul F. Zweifel. *Linear transport theory.* Addison-Wesley Publishing Co., Reading, Mass.-London-Don Mills, Ont., 1967.

[32] Jean Céa. Conception optimale ou identification de formes: calcul rapide de la dérivée directionnelle de la fonction coût. *RAIRO Modél. Math. Anal. Numér.*, 20(3):371–402, 1986.

[33] Tony F. Chan and Xue-Cheng Tai. Level set and total variation regularization for elliptic inverse problems with discontinuous coefficients. *J. Comput. Phys.*, 193(1):40–66, 2004.

[34] J. Cheng and M. Yamamoto. One new strategy for a priori choice of regularizing parameters in Tikhonov's regularization. *Inverse Problems*, 16(4):L31–L38, 2000.

[35] Jin Cheng, Junichi Nakagawa, Masahiro Yamamoto, and Tomohiro Yamazaki. Uniqueness in an inverse problem for a one-dimensional fractional diffusion equation. *Inverse Problems*, 25(11):115002, 16, 2009.

[36] Mourad Choulli and Masahiro Yamamoto. Generic well-posedness of an inverse parabolic problem—the Hölder-space approach. *Inverse Problems*, 12(3):195–205, 1996.

[37] Mourad Choulli and Masahiro Yamamoto. An inverse parabolic problem with non-zero initial condition. *Inverse Problems*, 13(1):19–27, 1997.

[38] Eric T. Chung, Tony F. Chan, and Xue-Cheng Tai. Electrical impedance tomography using level set representation and total variational regularization. *J. Comput. Phys.*, 205(1):357–372, 2005.

[39] P. G. Ciarlet. Basic error estimates for elliptic problems. In *Handbook of Numerical Analysis, Vol. II*, Handb. Numer. Anal., II, pages 17–351. North-Holland, Amsterdam, 1991.

[40] P. G. Ciarlet and P.-A. Raviart. Interpolation theory over curved elements, with applications to finite element methods. *Comput. Methods Appl. Mech. Engrg.*, 1:217–249, 1972.

[41] Philippe G. Ciarlet. *The Finite Element Method for Elliptic Problems*. SIAM, Philadelphia, PA, 2002.

[42] Richard Courant. *Dirichlet's Principle, Conformal Mapping, and Minimal Surfaces*. Interscience Publishers, Inc., New York, N.Y., 1950. Appendix by M. Schiffer.

[43] M. Crouzeix and V. Thomée. The stability in L_p and W_p^1 of the L_2-projection onto finite element function spaces. *Math. Comp.*, 48(178):521–532, 1987.

[44] George Cybenko. Approximation by superpositions of a sigmoidal function. *Mathematics of control, signals and systems*, 2(4):303–314, 1989.

[45] Maarten V. de Hoop, Lingyun Qiu, and Otmar Scherzer. Local analysis of inverse problems: Hölder stability and iterative reconstruction. *Inverse Problems*, 28(4):045001, 16, 2012.

[46] Klaus Deckelnick and Michael Hinze. Convergence and error analysis of a numerical method for the identification of matrix parameters in elliptic PDEs. *Inverse Problems*, 28(11):115015, 15, 2012.

[47] Hamid Dehghani, Brian W. Pogue, Jiang Shudong, Ben Brooksby, and Keith D. Paulsen. Three-dimensional optical tomography: resolution in small-object imaging. *Appl. Opt.*, 42(16):3117–3128, Jun 2003.

[48] Beiping Duan and Zhimin Zhang. A rational approximation scheme for computing Mittag-Leffler function with discrete elliptic operator as input. *J. Sci. Comput.*, 87(3):75, 20, 2021.

[49] Herbert Egger and Bernd Hofmann. Tikhonov regularization in Hilbert scales under conditional stability assumptions. *Inverse Problems*, 34(11):115015, 17, 2018.

[50] Heinz W. Engl, Martin Hanke, and Andreas Neubauer. *Regularization of Inverse Problems*. Kluwer, Dordrecht, 1996.

[51] Heinz W. Engl, Karl Kunisch, and Andreas Neubauer. Convergence rates for Tikhonov regularisation of nonlinear ill-posed problems. *Inverse Problems*, 5(4):523–540, 1989.

[52] Alexandre Ern and Jean-Luc Guermond. *Theory and practice of finite elements*, volume 159 of *Applied Mathematical Sciences*. Springer-Verlag, New York, 2004.

[53] Lawrence C Evans. *Partial differential equations*, volume 19. American Mathematical Society, 2022.

[54] Richard S. Falk. Error estimates for the numerical identification of a variable coefficient. *Math. Comp.*, 40(162):537–546, 1983.

[55] Avner Friedman and Victor Isakov. On the uniqueness in the inverse conductivity problem with one measurement. *Indiana Univ. Math. J.*, 38(3):563–579, 1989.

[56] Emil O Frind and George F Pinder. Galerkin solution of the inverse problem for aquifer transmissivity. *Water Resources Res.*, 9(5):1397–1410, 1973.

[57] Mariano Giaquinta and Luca Martinazzi. *An introduction to the regularity theory for elliptic systems, harmonic maps and minimal graphs*, volume 11 of *Appunti. Scuola Normale Superiore di Pisa (Nuova Serie) [Lecture Notes. Scuola Normale Superiore di Pisa (New Series)]*. Edizioni della Normale, Pisa, second edition, 2012.

[58] David Gilbarg and Neil S. Trudinger. *Elliptic partial differential equations of second order*, volume 224 of *Grundlehren der mathematischen Wissenschaften [Fundamental Principles of Mathematical Sciences]*. Springer-Verlag, Berlin, second edition, 1983.

[59] I Golding and E Cox. Physical nature of bacterial cytoplasm. *Phys. Rev. Lett.*, 96(9):098102, 2006.

[60] P. Grisvard. *Elliptic problems in nonsmooth domains*, volume 24 of *Monographs and Studies in Mathematics*. Pitman (Advanced Publishing Program), Boston, MA, 1985.

[61] Ingo Gühring and Mones Raslan. Approximation rates for neural networks with encodable weights in smoothness spaces. *Neural Networks*, 134:107–130, 2021.

[62] Tom Gustafsson and G. D. McBain. scikit-fem: A Python package for finite element assembly. *J. Open Source Software*, 5(52):2369, 2020.

[63] Johnny Guzmán, Dmitriy Leykekhman, Jürgen Rossmann, and Alfred H Schatz. Hölder estimates for green's functions on convex polyhedral domains and their applications to finite element methods. *Numerische Mathematik*, 112(2):221–243, 2009.

[64] Ingo Gühring and Mones Raslan. Approximation rates for neural networks with encodable weights in smoothness spaces. *Neural Networks*, 134:107–130, 2021.

[65] Dinh Nho Hào and Tran Nhan Tam Quyen. Convergence rates for total variation regularization of coefficient identification problems in elliptic equations I. *Inverse Problems*, 27(7):075008, 28, 2011.

[66] Yuko Hatano and Naomichi Hatano. Dispersive transport of ions in column experiments: An explanation of long-tailed profiles. *Water Res. Research*, 34(5):1027–1033, 1998.

[67] Yuko Hatano, Junichi Nakagawa, Shengzhang Wang, and Masahiro Yamamoto. Determination of order in fractional diffusion equation. *J. Math-for-Ind.*, 5A:51–57, 2013.

[68] Tapio Helin, Matti Lassas, Lauri Ylinen, and Zhidong Zhang. Inverse problems for heat equation and space-time fractional diffusion equation with one measurement. *J. Differential Equations*, 269(9):7498–7528, 2020.

[69] Michael Hinze, Barbara Kaltenbacher, and Tran Nhan Tam Quyen. Identifying conductivity in electrical impedance tomography with total variation regularization. *Numer. Math.*, 138(3):723–765, 2018.

[70] Kurt Hornik. Approximation capabilities of multilayer feedforward networks. *Neural Networks*, 4(2):251–257, 1991.

[71] Victor Isakov. Inverse parabolic problems with the final overdetermination. *Comm. Pure Appl. Math.*, 44(2):185–209, 1991.

[72] Victor Isakov. *Inverse Problems for Partial Differential Equations*. Springer, New York, second edition, 2006.

[73] Kazufumi Ito and Bangti Jin. *Inverse Problems: Tikhonov Theory and Algorithms*. World Scientific Publishing Co. Pte. Ltd., Hackensack, NJ, 2015.

[74] Kazufumi Ito, Karl Kunisch, and Zhilin Li. Level-set function approach to an inverse interface problem. *Inverse Problems*, 17(5):1225–1242, 2001.

[75] Huabei Jiang, Yong Xu, N. Iftimia, J. Eggert, K. Klove, L. Baron, and L. Fajardo. Three-dimensional optical tomographic imaging of breast in a human subject. *IEEE Transactions on Medical Imaging*, 20(12):1334–1340, 2001.

[76] Bangti Jin. *Fractional differential equations—an approach via fractional derivatives*, volume 206 of *Applied Mathematical Sciences*. Springer, Cham, [2021] ©2021.

[77] Bangti Jin and Yavar Kian. Recovering multiple fractional orders in time-fractional diffusion in an unknown medium. *Proc. A.*, 477(2253):20210468, 21, 2021.

[78] Bangti Jin and Yavar Kian. Recovery of the order of derivation for fractional diffusion equations in an unknown medium. *SIAM J. Appl. Math.*, 82(3):1045–1067, 2022.

[79] Bangti Jin, Raytcho Lazarov, and Zhi Zhou. Numerical methods for time-fractional evolution equations with nonsmooth data: a concise overview. *Comput. Methods Appl. Mech. Engrg.*, 346:332–358, 2019.

[80] Bangti Jin, Xiyao Li, and Xiliang Lu. Imaging conductivity from current density magnitude using neural networks. *Inverse Problems*, 38(7):075003, 36, 2022.

[81] Bangti Jin, Xiliang Lu, Qimeng Quan, and Zhi Zhou. Convergence rate analysis of Galerkin approximation of inverse potential problem. *Inverse Problems*, 39(1):Paper No. 015008, 26, 2023.

[82] Bangti Jin and William Rundell. A tutorial on inverse problems for anomalous diffusion processes. *Inverse Problems*, 31(3):035003, 40, 2015.

[83] Bangti Jin and Zhi Zhou. An inverse potential problem for subdiffusion: Stability and reconstruction. *Inverse Problems, DOI:10.1088/1361-6420/abb61e*, 2020.

[84] Bangti Jin and Zhi Zhou. Error analysis of finite element approximations of diffusion coefficient identification for elliptic and parabolic problems. *SIAM J. Numer. Anal.*, 59(1):119–142, 2021.

[85] Bangti Jin and Zhi Zhou. Numerical estimation of a diffusion coefficient in subdiffusion. *SIAM J. Control Optim.*, 59(2):1466–1496, 2021.

[86] Bangti Jin and Zhi Zhou. Recovering the potential and order in one-dimensional time-fractional diffusion with unknown initial condition and source. *Inverse Problems*, 37(10):105009, 28, 2021.

[87] Bangti Jin and Zhi Zhou. Recovery of a space-time-dependent diffusion coefficient in subdiffusion: stability, approximation and error analysis. *IMA Journal of Numerical Analysis*, 43(4):2496–2531, 09 2022.

[88] Bangti Jin and Zhi Zhou. *Numerical treatment and analysis of time-fractional evolution equations*, volume 214 of *Applied Mathematical Sciences*. Springer, Cham, [2023] ©2023.

[89] Xiaohua Jing and Jigen Peng. Simultaneous uniqueness for an inverse problem in a time-fractional diffusion equation. *Appl. Math. Lett.*, 109:106558, 7, 2020.

[90] Xiaohua Jing and Masahiro Yamamoto. Simultaneous uniqueness for multiple parameters identification in a fractional diffusion-wave equation. *Inverse Probl. Imaging*, 16(5):1199–1217, 2022.

[91] Josep Jordana, Manel Gasulla, and Ramon Pallàs-Areny. Electrical resistance tomography to detect leaks from buried pipes. *Measurement Science and Technology*, 12(8):1061, aug 2001.

[92] Barbara Kaltenbacher and William Rundell. Recovery of multiple coefficients in a reaction-diffusion equation. *J. Math. Anal. Appl.*, 481(1):123475, 23, 2020.

[93] Hyeonbae Kang and Jin Keun Seo. A note on uniqueness and stability for the inverse conductivity problem with one measurement. *J. Korean Math. Soc.*, 38(4):781–791, 2001.

[94] Yee Lo Keung and Jun Zou. Numerical identifications of parameters in parabolic systems. *Inverse Problems*, 14(1):83–100, 1998.

[95] Yavar Kian. Simultaneous determination of different class of parameters for a diffusion equation from a single measurement. *Inverse Problems*, 38(7):075008, 29, 2022.

[96] Yavar Kian, Zhiyuan Li, Yikan Liu, and Masahiro Yamamoto. The uniqueness of inverse problems for a fractional equation with a single measurement. *Math. Ann.*, 380(3):1465–1495, 2021.

[97] Anatoly A. Kilbas, Hari M. Srivastava, and Juan J. Trujillo. *Theory and Applications of Fractional Differential Equations*, volume 204 of *North-Holland Mathematics Studies*. Elsevier Science B.V., Amsterdam, 2006.

[98] Diederik P. Kingma and Jimmy Ba. Adam: A method for stochastic optimization. In *3rd International Conference for Learning Representations*, San Diego, CA, 2015. ICLR.

[99] J Kirchner, X Feng, and C Neal. Fractal stream chemistry and its implications for contaminant transport in catchments. *Nature*, 403(6769)(6769):524, 2000.

[100] Michael V. Klibanov and Fadil Santosa. A computational quasi-reversibility method for Cauchy problems for Laplace's equation. *SIAM J. Appl. Math.*, 51(6):1653–1675, 1991.

[101] Robert V. Kohn and Bruce D. Lowe. A variational method for parameter identification. *RAIRO Modél. Math. Anal. Numér.*, 22(1):119–158, 1988.

[102] Adam Kubica, Katarzyna Ryszewska, and Masahiro Yamamoto. *Time-Fractional Differential Equations — A Theoretical Introduction*. Springer, Singapore, 2020.

[103] Yann LeCun. A theoretical framework for back-propagation. In D Touretzky, G Hinton, and T Sejnowski, editors, *Proceedings of the 1988 Connectionist Models Summer School*, pages 21–28, CMU, Pittsburg, PA, 1988. Morgan Kaufmann.

[104] M. Lenoir. Optimal isoparametric finite elements and error estimates for domains involving curved boundaries. *SIAM J. Numer. Anal.*, 23(3):562–580, 1986.

[105] Buyang Li and Shu Ma. Exponential convolution quadrature for nonlinear subdiffusion equations with nonsmooth initial data. *SIAM J. Numer. Anal.*, 60(2):503–528, 2022.

[106] Buyang Li and Weiwei Sun. Maximal L^p analysis of finite element solutions for parabolic equations with nonsmooth coefficients in convex polyhedra. *Math. Comp.*, 86(305):1071–1102, 2017.

[107] Changhui Li and Lihong V Wang. Photoacoustic tomography and sensing in biomedicine. *Physics in Medicine & Biology*, 54(19):R59, 2009.

[108] Zhiyuan Li, Oleg Yu. Imanuvilov, and Masahiro Yamamoto. Uniqueness in inverse boundary value problems for fractional diffusion equations. *Inverse Problems*, 32(1):015004, 16, 2016.

[109] Zhiyuan Li, Yikan Liu, and Masahiro Yamamoto. Inverse problems of determining parameters of the fractional partial differential equations. In *Handbook of fractional calculus with applications. Vol. 2*, pages 431–442. De Gruyter, Berlin, 2019.

[110] Zhiyuan Li and Masahiro Yamamoto. Inverse problems of determining coefficients of the fractional partial differential equations. In *Handbook of Fractional Calculus with Applications. Vol. 2*, pages 443–464. De Gruyter, Berlin, 2019.

[111] J.-L. Lions and E. Magenes. *Non-homogeneous boundary value problems and applications. Vol. I*, volume Band 181 of *Die Grundlehren der mathematischen Wissenschaften*. Springer-Verlag, New York-Heidelberg, 1972. Translated from the French by P. Kenneth.

[112] Huan Liu, Bangti Jin, and Xiliang Lu. Imaging anisotropic conductivities from current densities. *SIAM J. Imaging Sci.*, 15(2):860–891, 2022.

[113] J.J. Liu and M. Yamamoto. A backward problem for the time-fractional diffusion equation. *Applicable Analysis*, 89(11):1769–1788, nov 2010.

[114] Yikan Liu, Zhiyuan Li, and Masahiro Yamamoto. Inverse problems of determining sources of the fractional partial differential equations. In *Handbook of fractional calculus with applications. Vol. 2*, pages 411–429. De Gruyter, Berlin, 2019.

[115] Francesco Mainardi. On some properties of the Mittag-Leffler function $E_\alpha(-t^\alpha)$, completely monotone for $t > 0$ with $0 < \alpha < 1$. *Discrete Contin. Dyn. Syst. Ser. B*, 19(7):2267–2278, 2014.

[116] R Metzler, J H Jeon, A G Cherstvy, and E Barkai. Anomalous diffusion models and their properties: non-stationarity, non-ergodicity, and ageing at the centenary of single particle tracking. *Phys. Chem. Chem. Phys.*, 16(44):24128–24164, 2014.

[117] Ralf Metzler and Joseph Klafter. The random walk's guide to anomalous diffusion: a fractional dynamics approach. *Phys. Rep.*, 339(1):77, 2000.

[118] Hrushikesh N Mhaskar. Neural networks for optimal approximation of smooth and analytic functions. *Neural computation*, 8(1):164–177, 1996.

[119] S. Minakshisundaram and Å. Pleijel. Some properties of the eigenfunctions of the Laplace-operator on Riemannian manifolds. *Canad. J. Math.*, 1:242–256, 1949.

[120] Sebastian K. Mitusch, Simon W. Funke, and Miroslav Kuchta. Hybrid FEM-NN models: combining artificial neural networks with the finite element method. *J. Comput. Phys.*, 446:110651, 21, 2021.

[121] Yuji Nakatsukasa, Olivier Sète, and Lloyd N. Trefethen. The AAA algorithm for rational approximation. *SIAM J. Sci. Comput.*, 40(3):A1494–A1522, 2018.

[122] Maria Elizabeth G. Ong. Uniform refinement of a tetrahedron. *SIAM J. Sci. Comput.*, 15(5):1134–1144, 1994.

[123] Stanley Osher and Ronald P. Fedkiw. Level set methods: an overview and some recent results. *J. Comput. Phys.*, 169(2):463–502, 2001.

[124] R. Prakash, M. Hrizi, and A. A. Novotny. A noniterative reconstruction method for solving a time-fractional inverse source problem from partial boundary measurements. *Inverse Problems*, 38(1):015002, 27, 2022.

[125] Nasim Rahaman, Aristide Baratin, Devansh Arpit, Felix Draxler, Min Lin, Fred Hamprecht, Yoshua Bengio, and Aaron Courville. On the spectral bias of neural networks. In *Proceedings of the 36th International Conference on Machine Learning, PMLR 97*, pages 5301–5310, Long Beach, CA, 2019. JMLR.

[126] M. Raissi, P. Perdikaris, and G. E. Karniadakis. Physics-informed neural networks: a deep learning framework for solving forward and inverse problems involving nonlinear partial differential equations. *J. Comput. Phys.*, 378:686–707, 2019.

[127] Rolf Rannacher and Ridgway Scott. Some optimal error estimates for piecewise linear finite element approximations. *mathematics of computation*, 38(158):437–445, 1982.

[128] Gerard R. Richter. An inverse problem for the steady state diffusion equation. *SIAM J. Appl. Math.*, 41(2):210–221, 1981.

[129] Gerard R. Richter. Numerical identification of a spatially varying diffusion coefficient. *Math. Comp.*, 36(154):375–386, 1981.

[130] Jon A. Rivera, Jamie M. Taylor, Ángel J. Omella, and David Pardo. On quadrature rules for solving partial differential equations using neural networks. *Comput. Methods Appl. Mech. Engrg.*, 393:114710, 21, 2022.

[131] William Rundell and Masahiro Yamamoto. Recovery of a potential in a fractional diffusion equation. Preprint, arXiv:1811.05971, 2018.

[132] William Rundell and Masahiro Yamamoto. Uniqueness for an inverse coefficient problem for a one-dimensional time-fractional diffusion equation with non-zero boundary conditions. *Appl. Anal.*, 102(3):815–829, 2023.

[133] William Rundell and Zhidong Zhang. Recovering an unknown source in a fractional diffusion problem. *J. Comput. Phys.*, 368:299–314, 2018.

[134] Kenichi Sakamoto and Masahiro Yamamoto. Initial value/boundary value problems for fractional diffusion-wave equations and applications to some inverse problems. *J. Math. Anal. Appl.*, 382(1):426–447, 2011.

[135] Fadil Santosa. A level-set approach for inverse problems involving obstacles. *ESAIM Contrôle Optim. Calc. Var.*, 1:17–33, 1995/96.

[136] Jin Keun Seo. On the uniqueness in the inverse conductivity problem. *J. Fourier Anal. Appl.*, 2(3):227–235, 1996.

[137] H. Bruce Stewart. Generation of analytic semigroups by strongly elliptic operators. *Trans. Amer. Math. Soc.*, 199:141–162, 1974.

[138] Derick Nganyu Tanyu, Jianfeng Ning, Tom Freudenberg, Nick Heilenkötter, Andreas Rademacher, Uwe Iben, and Peter Maass. Deep learning methods for partial differential equations and related parameter identification problems. Preprint, arXiv:2212.03130, 2022.

[139] Vidar Thomée. *Galerkin Finite Element Methods for Parabolic Problems*. Springer-Verlag, Berlin, second edition, 2006.

[140] G. Uhlmann. Electrical impedance tomography and Calderón's problem. *Inverse Problems*, 25(12):123011, 39, 2009.

[141] J. L. Vázquez. A strong maximum principle for some quasilinear elliptic equations. *Appl. Math. Optim.*, 12(3):191–202, 1984.

[142] Roman Vershynin. *High-dimensional probability*, volume 47 of *Cambridge Series in Statistical and Probabilistic Mathematics*. Cambridge University Press, Cambridge, 2018. An introduction with applications in data science, With a foreword by Sara van de Geer.

[143] Lihong V Wang. Multiscale photoacoustic microscopy and computed tomography. *Nature photonics*, 3(9):503–509, 2009.

[144] Lijuan Wang and Jun Zou. Error estimates of finite element methods for parameter identifications in elliptic and parabolic systems. *Discrete Contin. Dyn. Syst. Ser. B*, 14(4):1641–1670, 2010.

[145] Ting Wei and Xiong-Bin Yan. Uniqueness for identifying a space-dependent zeroth-order coefficient in a time-fractional diffusion-wave equation from a single boundary point measurement. *Appl. Math. Lett.*, 112:106814, 7, 2021.

[146] Ting Wei, Yun Zhang, and Dingqian Gao. Identification of the zeroth-order coefficient and fractional order in a time-fractional reaction-diffusion-wave equation. *Math. Methods Appl. Sci.*, 46(1):142–166, 2023.

[147] Frank Werner and Bernd Hofmann. Convergence analysis of (statistical) inverse problems under conditional stability estimates. *Inverse Problems*, 36(1):015004, 23, 2020.

[148] Masahiro Yamamoto. Carleman estimates for parabolic equations and applications. *Inverse Problems*, 25(12):123013, 75 pp., 2009.

[149] Dmitry Yarotsky. Error bounds for approximations with deep relu networks. *Neural Networks*, 94:103–114, 2017.

[150] William W G Yeh. Review of parameter identification procedures in groundwater hydrology: The inverse problem. *Water Resources Res.*, 22(2):95–108, 1986.

[151] Qian Zhang and Jijun Liu. On the reconstruction of medium conductivity by integral equation method based on the levi function. *Inverse Problems and Imaging*, 18(5):1096–1120, 2024.

[152] Zhengqi Zhang, Zhidong Zhang, and Zhi Zhou. Identification of Potential in Diffusion Equations from Terminal Observation: Analysis and Discrete Approximation. *SIAM J. Numer. Anal.*, 60(5):2834–2865, 2022.

[153] Zhengqi Zhang and Zhi Zhou. Numerical analysis of backward subdiffusion problems. *Inverse Problems*, 36(10):105006, 2020.

[154] M.S. Zhdanov. *Geophysical Inverse Theory and Regularization Problems.* Methods in Geochemistry and Geophysics. Elsevier Science, 2002.

[155] William P. Ziemer. *Weakly Differentiable Functions.* Springer-Verlag, New York, 1989.

[156] Miloš Zlámal. Curved elements in the finite element method. I. *SIAM J. Numer. Anal.*, 10:229–240, 1973.

[157] Miloš Zlámal. Curved elements in the finite element method. II. *SIAM J. Numer. Anal.*, 11:347–362, 1974.

[158] Jun Zou. Numerical methods for elliptic inverse problems. *Int. J. Comput. Math.*, 70(2):211–232, 1998.